

Brookhaven National Laboratory's
Annual Report of
Laboratory Directed
Research & Development
Program Activities
For FY 2002

Director's Office

BROOKHAVEN NATIONAL LABORATORY
BROOKHAVEN SCIENCE ASSOCIATES
UPTON, NEW YORK 11973-5000
UNDER CONTRACT NO. DE-AC02-98CH10886
UNITED STATES DEPARTMENT OF ENERGY

December 2002

Acknowledgments

The Laboratory Directed Research and Development (LDRD) Program is managed by Leonard Newman, who serves as the Scientific Director, and by Kevin Fox, Special Assistant to the Assistant Laboratory Director for Finance & Administration (ALDFA). Preparation of the FY 2002 report was coordinated and edited by Leonard Newman and Kevin Fox, who wish to thank D.J. Greco and Regina Paquette for their assistance in organizing, typing, and proofing the document. A special thank you is also extended to the Photography and Graphic Arts Division for their help in publishing. Of course, a very special acknowledgement is extended to all of the authors of the project annual reports and to their assistants.

Table of Contents

Introduction	1
Management Process	3
Peer Review.....	7
Self Assessment	9
Relatedness of LDRD to Laboratory Programs and Initiatives	11
Summary of Metric Data	15
Projects Funding Table.....	17
 Project Summaries	
Rapid Real-Time Measurement of Aerosol Chemical Composition.....	25
Novel Techniques to Measure Aerosols and Aerosol Precursors: Multiple Humidity Tandem Differential Mobility Analyzer (TDMA)	29
Microvascular Endothelial Cells as Targets of Ionizing Radiation.....	31
The Structure of Membrane Proteins: Monolayers and Thin Films.....	35
Understanding the Pathways of Ubiquitin Dependent Proteolysis.....	37
New Protein Expression Tools for Proteomics	39
Development of Superconducting Accelerator Magnets Capable of High dB/dt.....	43
Combination of Magnetic Fields and 20 keV Synchrotron X-Rays to Produce Microbeams for Cell Culture Experiments	45
Gene Expression Profiling of Methamphetamine-Induced Toxicity in Neurons in Culture Using DNA Microarrays	47
"Functional Spectral Signature" (FSS) Method for Signal to Noise-Enhancement of Brain Patterns in PET Images.....	51

Table of Contents

Exploration and Development of Ultrafast Single Shot Detection Methods for Use with Pulse Radiolysis Experiments at LEAF	55
Metal NanoClusters and Electron Transfer in One, Two, and Three Dimensions.....	59
Molecular Wires for Energy Conversion and Nono-Electronics.....	63
Nanoscale Catalysts: Preparation, Structure and Reactivity.....	67
Experimental and Theoretical Studies of the Formation of Titanium-Carbon Nanoclusters.....	69
Development of a UV-Raman, Near-Field Scanning Optical Microscope for <i>in-situ</i> Studies of Chemical Intermediates on Metal Nanoparticles	73
Development of New Techniques for Improvements in PET Imaging of Small Animals and Other Applications.....	75
Development of CZT Array Detector Technology for Synchrotron Radiation Applications	77
New Applications of Circular Polarized VUV-Light.....	83
Soft X-Ray Magnetic Speckle	85
Prototype Approaches Toward Infrared Nanospectroscopy.....	87
Pressure-Induced Protein Folding Monitored by Small Angle X-Ray Scattering and Fourier Transform Infrared Microspectroscopy	89
Soft Condensed Matter Probed by Low-Energy Resonant Scattering.....	91
Femto-Seconds Electron Microscope Based on the Photocathode RF Gun.....	95
First-Principles Theory of the Magnetic and Electronic Properties of Nanostructures.....	97
Cryo-EM for Solving Membrane Proteins	99
Human DNA Damage Responses: DNA-PK and p53	103
Molecular Mechanisms Underlying Structural Changes in the Adult Brain: A Genetic Analyses	107

Table of Contents

Catalytic Microcombustion Systems	109
Mapping Electron Densities in Porphyrin Radical Crystals Using the NSLS	111
High Sensitivity Mass Spectrometer	115
Development and Application of Cavity Ringdown Spectroscopy to the Detection and Monitoring of Trace Chemical Species in the Atmosphere	117
Development of a High Field Magnet for Neutrino Factory Storage Rings.....	121
DNA-Nano Wires that AutoConnect in 3 Dimensions	123
Carbon Nanotube Chemical Probes for Biological Membrane Attachment Quantification	129
Self-Organized Nanoparticles for Probing Charge Transfer at Metallic/Organic Interfaces	133
Charge Transfer on the Nano Scale: Theory	135
Charge Transport Through Dye-Sensitized Nanocrystalline Semiconductor Films	137
Magnetic Nanodispersions	141
High Resolution Magneto-optical Study of Magnetic Nanostructures, Nanocomposite Functional and Superconducting Materials	145
Size Selected Quantum-Dots Under Environmentally Controlled Conditions	149
Crystallization and X-Ray Analysis of Membrane Proteins.....	153
<i>In Vitro</i> Investigation of the DNA Double Strand Break Repair Mechanism by Non-Homologous End-Joining in the Context of Chromatin	155
Creating a MicroMRI Facility for Research and Development.....	159
Targeting Tin-117m to Estrogen Receptors for Breast Cancer Therapy	161
Biom mineralization of Actinides: A Mechanistic Study of the Genesis of Novel and Stable Compounds.....	163
Using Mini-LIDAR for Verification and Long-Term Monitoring of Cover Systems.....	167

Table of Contents

Electrical Systems Reliability.....	171
Liquid Fuel Gasifier for Combustion and Fuel Cells	173
Study of a Power Source for Nano-Devices.....	175
Ultrafast Nonlinear Spectroscopic Studies of Model Catalytic Surfaces	177
Combined Use of Radiotracers and Positron Emission Imaging in Understanding the Integrated Response of Plants to Environmental Stress	181
Arranging Nanoparticles into Arbitrary Patterns with Optical Trapping	185
Advanced Multidimensional Techniques to Explore the Biochemical and Behavioral Consequences of VOC Exposure	187
Project to Detect pp and ⁷ Be Solar Neutrinos in Real Time: LENS, the Low-Energy Neutrino Spectrometer.....	191
Combined Theoretical and Experimental Study of Crystal Lattice Defects in Complex Transition Metal Oxides	195
Chemical Sensors: Immobilization of Organometallic Complexes into Sol-gel Matrices.....	197
Size Dependence of Catalytic Reactivity of Iron Oxide Nanocrystals	199
Femtosecond Synchronization for Ultra-Short Pulse DUV-FEL Radiation	201
Rapid Wavelength Tunability for the DUV-FEL	203
High-Gain Harmonic-Generation at the DUV/FEL	207
Biom mineralization: A Route to Advanced Materials	209
Theory of Electronic Transport in Nanostructures and Low-Dimensional Systems	213
Pressure in Nanopores	215
Genomic SELEX to Study Protein DNA/RNA Interactions in <i>Ralstonia Metallidurans</i> CH34 Regulating Heavy Metal Homeostasis and Resistance.....	217

Table of Contents

Lead Resistance in <i>Ralstonia Metallidurans</i> CH34.....	219
Design of a <i>Ralstonia Metallidurans</i> Two-Hybrid Protein System for Studying Signaling Pathways Regulating Heavy Metal Homeostasis and Resistance	221
Ultrafast X-Ray Science	223
X-Ray Photon Correlation Spectroscopy Studies of Nanostructured Block Copolymers.....	225
Fine Grain Gas and Silicon Detectors for Future Experiments in Nuclear Physics at High Energies	227
Appendix A - 2003 Project Summaries.....	229
Exhibit A - Call for Proposals for FY 2004	241
Exhibit B - LDRD Proposal Questionnaire.....	243
Exhibit C - LDRD Data Collection Form	251

Introduction

Brookhaven National (BNL) Laboratory is a multidisciplinary laboratory that carries out basic and applied research in the physical, biomedical, and environmental sciences, and in selected energy technologies. It is managed by Brookhaven Science Associates, LLC, under contract with the U. S. Department of Energy. BNL's total annual budget has averaged about \$450 million. There are about 3,000 employees, and another 4,500 guest scientists and students who come each year to use the Laboratory's facilities and work with the staff.

The BNL Laboratory Directed Research and Development (LDRD) Program reports its status to the U.S. Department of Energy (DOE) annually in March, as required by DOE Order 413.2A, "Laboratory Directed Research and Development," January 8, 2001, and the LDRD Annual Report guidance, updated February 12, 1999. The LDRD Program obtains its funds through the Laboratory overhead pool and operates under the authority of DOE Order 413.2A.

The goals and objectives of BNL's LDRD Program can be inferred from the Program's stated purposes. These are to (1) encourage and support the development of new ideas and technology, (2) promote the early exploration and exploitation of creative and innovative concepts, and (3) develop new "fundable" R&D projects and programs. The emphasis is clearly articulated by BNL to be on supporting exploratory research "which could lead to new programs, projects, and directions" for the Laboratory.

As one of the premier scientific laboratories of the DOE, BNL must continuously foster

groundbreaking scientific research. At Brookhaven National Laboratory one such method is through its LDRD Program. This discretionary research and development tool is critical in maintaining the scientific excellence and long-term vitality of the Laboratory. Additionally, it is a means to stimulate the scientific community and foster new science and technology ideas, which becomes a major factor in achieving and maintaining staff excellence and a means to address national needs within the overall mission of the DOE and BNL.

The LDRD Annual Report contains summaries of all research activities funded during Fiscal Year 2002. The Project Summaries with their accomplishments described in this report reflect the above. Aside from leading to new fundable or promising programs and producing especially noteworthy research, the LDRD activities have resulted in numerous publications in various professional and scientific journals and presentations at meetings and forums.

All FY 2002 projects are listed and tabulated in the Project Funding Table. Also included in this Annual Report in Appendix A is a summary of the proposed projects for FY 2003. The BNL LDRD budget authority by DOE in FY 2002 was \$7 million. The actual allocation totaled \$6.7 million.

The following sections in this report contain the management processes, peer review, and the portfolio's relatedness to BNL's mission, initiatives and strategic plans. Also included is a metric of success indicators.

Management Process

PROGRAM ADMINISTRATION:

Overall Coordination: Overall responsibility for coordination, oversight, and administration of BNL's LDRD Program resides with the Laboratory's Director. Day-to-day responsibilities regarding funding, oversight, proposal evaluation, and report preparation have been delegated to the dedicated Scientific Director (SD) for the LDRD Program. The Office of the Assistant Laboratory Director for Finance & Administration (ALDF&A) continues to assist in the administration of the program. This includes administering the program budget, establishment of project accounts, maintaining summary reports, and providing reports of Program activities to the DOE through the Brookhaven Area Manager.

Responsibility for the allocation of resources and the review and selection of proposals lies with a management-level group called the Laboratory Directed Research & Development Program Committee. For Fiscal Year 2002, the Program Committee--which selected the 2003 programs--consisted of eight members. The Scientific Director of the LDRD Program chaired the Committee, and the other members were the Interim Laboratory Director (LD), four Associate Laboratory Directors (ALDs), and two members from the scientific departments and divisions.

2002 LDRD PROGRAM COMMITTEE

Leonard Newman	Chairperson (SD)
Peter Paul	Interim Laboratory Director (LD)
Ralph James	Energy, Environment & National Security (ALD)

Thomas Kirk	High Energy & Nuclear Physics (ALD)
Nora Volkow	Life Sciences (ALD)
Richard Osgood	Basic Energy Sciences (ALD)
Yu Shin Ding	Chemistry (S)
Stephen Shapiro	Physics (S)

Allocating Funds: There are two types of decisions to be made each year concerning the allocation of funds for the LDRD Program. These are: (1) the amount of money that should be budgeted overall for the Program; and (2) of this, how much, if any, should go to each competing project or proposal. Both of these decisions are made by high-level management.

For each upcoming fiscal year the Laboratory Director, on recommendation by the SD for LDRD and in consultation with the ALDF&A, develops an overall level of funding for the LDRD Program. The budgeted amount is incorporated into the Laboratory's LDRD Plan, which formally requests authorization from the DOE to expend funds for the LDRD Program up to this ceiling amount.

The majority of projects are authorized for funding at the start of the fiscal year. However, projects can be authorized throughout the fiscal year, as long as funds are available and the approved ceiling for the LDRD Program is not exceeded.

The actual level, which may be less, is determined during the course of the year and is affected by several considerations including: the specific merits of the various project proposals, as determined by Laboratory management and the members of the LDRD Program Committee; the overall financial health of the Laboratory; and a number of budgetary tradeoffs between LDRD

and other overhead expenses. At BNL the LDRD Program has historically amounted to a much smaller portion of the total budget than at comparable National Laboratories. This prevented the Laboratory from preparing itself for work in emerging areas of research. Accordingly, the LDRD budget has been increased over the past ten years from \$2.0 million to \$8.5 million, or from less than 1% to almost 2% of the laboratory budget. The target level is to go to about 4%, which would still be significantly less than the DOE mandated maximum of 6%.

Request for Proposals: The availability of special funds for research under the LDRD Program is well publicized throughout the Laboratory. This is done using two methods - one occurring at yearly intervals, the other occurring irregularly. Each year a call letter is sent by the SD for LDRD to the Scientific Staff and as a separate memorandum to all the Associate Laboratory Directors and Department Chairpersons. The FY 2004 call issued in February 2003 is attached as Exhibit A. This early schedule better facilitated the recruitment of post-doctorate candidates to support LDRD projects. In addition, in FY 02 we initiated a process that permits the deferral of expending the budget allocation into a third year to permit the full funding of post doctorates for two years, as they might not arrive at the onset of the LDRD project. The call references the BNL LDRD Standards-Based Management System (SBMS) Subject Area, which is available to all employees on the web at <https://sbms.bnl.gov/ld/ld03/ld03d011.htm>. The other method is through a feature article in The Bulletin, the Laboratory's weekly newspaper.

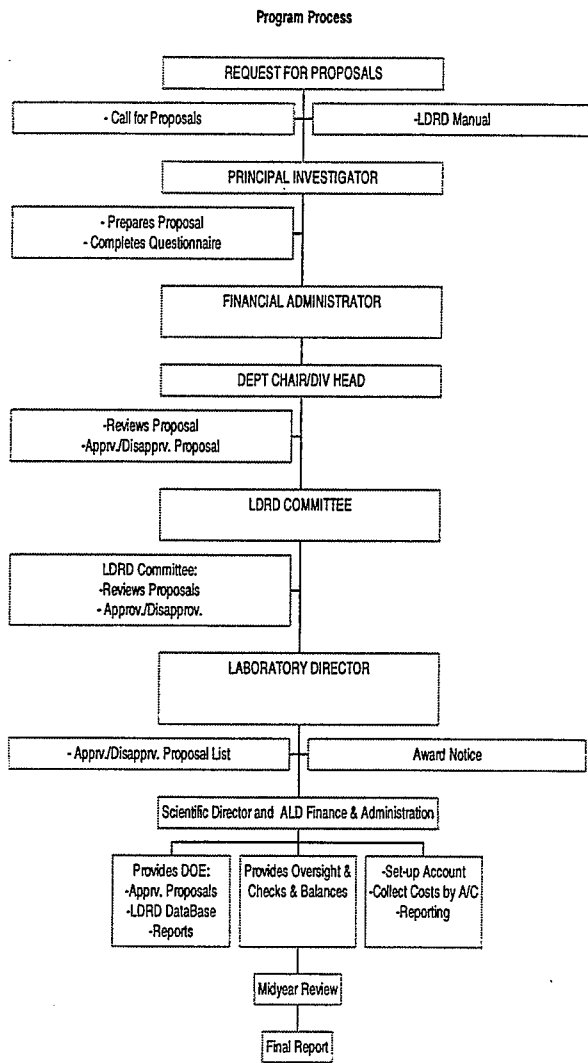
The LDRD SBMS Subject Area specifies the requirements necessary for participation in the program. It states the program's purpose, general characteristics, procedures for applying, and restrictions. An application for funding, i.e., a project proposal, takes the form

of a completed "Proposal Information Questionnaire," Exhibit B. An application must be approved up the chain-of-command which includes the initiator's Department or Division Budget Administrator and the Department Chairperson or Division Head. Plans to ensure the satisfactory continuation of the principal investigator's regularly funded programs must also be approved. The applications are then forwarded to the LDRD Program Committee for full review and consideration for funding.

The process that solicits and encourages the development of proposals has evolved into two modes of operation. Specifically, the ideas for proposal development may originate among the scientific staff in response to the general call for proposals. Alternatively, they may be initiated by Laboratory science management. Eventually, both follow the standard procedures for proposal approval up the chain-of-command to the same decision makers. The fact that all proposals must be approved up the chain-of-command permits BNL managers to consider all ideas together when designing the mix of projects for the LDRD Program.

An initiative from management typically takes the form of a broad topical area or item of special interest such as nanoscale science. Then these "areas of interest" are communicated broadly to the scientific staff and in particular to staff members who are known to be in a position to pursue and develop their ideas in the form of a more formal proposal.

Proposal Review: Once the cognizant line managers approve the proposals, they are forwarded to the Chairperson of the Committee (SD for LDRD) who transmits a copy of all proposals received to the Committee for review. The Committee considers all proposals that have met certain



minimum requirements pertaining to the Department's and BNL's LDRD policies.

Lead proponent responsibility of a proposal is assigned to that Associate Laboratory Director of the Committee who oversees and directs the technical area from which the proposal originated. Two other members of the committee serve as second proponents and the LD serves as a third proponent. A description of the process is outlined in the Figure above. All members have several weeks to review the proposals and prepare for a full debate on each proposal.

Selection Criteria: Minimum requirements for each proposal are: (1) consistency with

program purpose; (2) consistency with missions of BNL, DOE, and NRC; (3) approval by Department Chairperson and/or Division Head, and cognizant Associate/Assistant Director; (4) assurance of satisfactory continuation of principal investigator's regularly funded programs; (5) modest size and generally scheduled for 2 years but limited to no more than 3 years; (6) will not substitute for, supplement, or extend funding for tasks normally funded by DOE, NRC, or other users of the Laboratory; (7) will not require the acquisition of permanent staff; (8) will not create a commitment of future multi-year funding to reach a useful stage of completion; and (9) will not fund construction line-item projects, facility maintenance, or general purpose capital equipment.

The selection criteria used to evaluate and rank individual proposals are stated in broad terms. While the LDRD SBMS Subject Area clearly states that selection is based on (1) scientific or technological merit, (2) innovativeness, (3) compliance with minimum requirements, (4) proposal cost as compared to the amount of available funding, and (5) its potential for follow-on funding. The requirements of DOE Order 413.2A are also carefully considered during the selection process to ensure that proposals are consistent with DOE criteria.

Project Approval: After all proposals are discussed, the Committee selects the highest priority proposals by concurrence. Differences, if any, are resolved by the Chairperson. Some funding may be held in reserve during the earlier meetings of the fiscal year so that funds remain available for proposals submitted at later dates. The funding amount requested in any one specific proposal may be changed or adjusted during the approval process. The Committee's recommendation is then submitted to the Laboratory Director for approval. After approval by the Lab Director all new projects are submitted to the DOE-

Brookhaven Area Office (DOE-BAO) for concurrence prior to start. The ALDF&A then sets up a separate laboratory overhead account to budget and collect the costs for the project.

Project Supervision: The SD for LDRD carries out overall supervision of the projects. Supervision over the actual performance of LDRD projects is carried out in the same way as other research projects at the Laboratory. Each principal investigator is assigned to an organizational unit (Department, Division), that is supervised by a chairperson or manager.

Each chairperson or manager is responsible for seeing that the obligations of the principal investigator are satisfactorily fulfilled and that the research itself is carried out according to standard expectations of professionalism and scientific method. The SD for LDRD monitors the project's status, schedule, and progress and coordinates with the chairperson or manager as necessary.

The SD for LDRD organizes a mid-year review of all projects. Each PI presents a progress report on the status of their project. In attendance will be the SD for LDRD, the LD, the cognizant ALD and Department Chair, and a representative from the ALDF&A and DOE-BAO. This review checks on the progress of the projects including its funding schedule. This allows the SD for LDRD to ensure that the work is being completed in a timely manner.

In addition, the SD for LDRD conducts a monthly meeting with the DOE LDRD Project Manager to update the progress of the program and to solicit assistance to verify that the BNL LDRD Program is meeting the overall LDRD requirements. This includes providing the DOE-BAO with copies of all funded proposals, an LDRD Program database, and a project funding and schedules summary report.

Project Reporting: Routine documentation of each project funded under the LDRD Program consists of a file containing: (1) a copy of the written proposal; (2) all interim status reports; (3) notifications of changes in research direction, if any; and (4) reports on costs incurred. Also, a formal LDRD Plan and the Annual Report on the LDRD Program (this Report) are submitted to BNL management and the DOE summarizing work progress, accomplishments, and project status on all projects.

Documentation for the overall Program consists of (1) various program history files, (2) a running list of all proposals with their acceptance/rejection status, (3) funding schedule and summary reports for all approved projects, (4) permanent records on cost accounting, and a database containing information on each funded project (description, funding by fiscal year, status and accomplishments, follow-on funding, publications, etc.). This year we established a Data Collection Form (Exhibit C) so that we can more formally collect information on the impacts of the projects. Each project will be tracked for two years after its completion so as to gather a complete set of information on the impact of the project. Also, this year BNL has begun inputting LDRD data into the DOE-Chief Financial Officer's Laboratory/Plant Directed Research and Development Web Site (<https://ldrdrpt.doe.gov>) to support DOE reporting of LDRD to Congress.

Some of the projects may involve animals or humans. Those projects will have received approval from the Laboratory's appropriate review committees. The projects which involve animals or humans are identified in this report as follows:

Note: This project involves animal vertebrates or human subjects.

This is noted on the summary sheet and also at the end of each report.

Peer Review

LDRD projects have peer reviews performed in several different ways. Primarily, LDRD research is managed and reviewed by the cognizant Department and Division manager. These projects are a part of the activities of their respective Department and Divisions in which they reside. The BNL LDRD Program itself does not solicit formal peer reviews, consisting of written comments by experts outside the normal lines of supervision. Instead, advisory committees that consist of subject matter experts from academia and industry conduct peer reviews of LDRD projects as part of a department's program review. One such group is the Brookhaven Science Associates' Science Advisory Committee, which performs peer reviews of different Laboratory programs on a rotating basis. There are also periodic reviews of the science at the Laboratory performed by various offices of DOE.

In addition to these outside peer reviews of the BNL program, the members of the LDRD Committee are considered to have sufficient technical knowledge to perform peer reviews of projects during the initial selection process and annual renewal. Also, all LDRD projects go through a formal mid-year review (described in the previous section under project supervision) conducted by the SD of the LDRD Program that includes the cognizant Department Chair and Associate Laboratory Director.

Self Assessment

BNL supports the concept of continued improvement as part of its management of the Laboratory. To achieve this goal every year BNL performs self assessments on various functions at the Laboratory. In FY 2002, BNL updated last year's self assessment on the LDRD Program administration. This self assessment of BNL's LDRD Program administration was based on the Malcolm Baldrige National Quality Award Criteria for 1998. The assessment detailed the LDRD's administration strengths and opportunities for improvement (OFI) for each criterion identified.

The overall summary of the assessment's strengths and opportunities for improvement are as follows:

Summary of Strengths:

The LDRD Program has a good customer satisfaction rating. Last year's customer survey revealed that on average 65% of those that responded gave a favorable review of the administration of the LDRD Program. Whereas only 16% gave a Disagree or Tend to Disagree rating.

The FY 2003 LDRD Plan was submitted to DOE in August of 2002 for review. In October of 2002 the 2003 Plan was approved, and DOE-HQ informed the DOE-BAO that the plan was an excellent document.

The favorable customer satisfaction is a result of the SD of the LDRD and ALDF&A staff being knowledgeable and making themselves readily available and responding promptly to customer inquiries. Communication within the group is very good. Every effort is made

to update and streamline processes and procedures.

Summary of Opportunities for Improvements:

The areas identified below as opportunities for improvement will only enhance current operations. None are considered major.

1. Maintain the legacy LDRD policy within the correct Standard Based Management System format
2. Establish a Data Collection Form to collect data on the impact of each project for a period of two years after its completion.
3. Continue the increase awareness of the LDRD Program to the Laboratory scientific community

The FY 2002 self assessment contained meaningful recommendations and will continue to be utilized to improve the LDRD Program at Brookhaven.

Relatedness of LDRD to Laboratory Programs and Initiatives

BNL's mission is to produce excellent science in a safe, environmentally benign manner with the cooperation, support, and appropriate involvement of our many communities. Brookhaven was founded as a laboratory which would provide specialized research facilities that could not be designed, built, and operated at a university or industrial complex, and provides a scientific core effort for these facilities. This still remains a basic mission of the Laboratory.

BNL is committed to cultivating programs (including the LDRD) of the highest quality. These programs address DOE's Strategic Mission which is to conduct programs relating to energy resources, national nuclear security, environmental quality, and science.

Brookhaven National Laboratory has the following four elements in its mission which support the four DOE programmatic business lines.

<p style="text-align: center;"><u>RESEARCH FACILITIES</u></p> <p>Conceive, design, construct, and operate complex, leading-edge, user-oriented facilities in responsive to the needs of the DOE, and the needs of the international community users.</p>
<p style="text-align: center;"><u>SCIENTIFIC RESEARCH</u></p> <p>Carry out basic and applied research in long-term high risk programs at the frontier of science.</p>

<p style="text-align: center;"><u>TECHNOLOGY DEVELOPMENT</u></p> <p>Develop advanced technologies that address national needs and to transfer them to other organizations and to the commercial sector.</p>
<p style="text-align: center;"><u>KNOWLEDGE TRANSFER</u></p> <p>Disseminate technical knowledge to educate new generations of scientists and engineers, to maintain technical capabilities in the nation's workforce, and to encourage scientific awareness in the general public.</p>

Research Facilities and Scientific Research have a synergistic relationship. To maintain and constantly improve a research facility and to keep it at the cutting edge, it is essential that the Laboratory have a significant research staff of excellent stature. The staff drives the performance of the facility. Having several complementary facilities at one location, such as the National Synchrotron Light Source (NSLS) and now the Relativistic Heavy Ion Collider (RHIC), allows unique research capabilities. The other two elements of the Laboratory's mission-- Technology Development and Knowledge Transfer-- bridge all of the research facilities and research programs.

The four elements of Brookhaven's mission support and cut across the four central activities of the Department of Energy as defined in its Strategic Plan.

The Laboratory's breadth of expertise as delineated in Tables 1 and 2 provides the basis for its contributions to the DOE's missions and focuses on providing extraordinary tools for the pursuit of basic science and technology.

Table 1 - Expertise Derived from Brookhaven's Core Competencies – Science

High Energy and Nuclear Physics:

- Rare kaon decays
- Muon anomalous magnetic moment
- Exotics and glueball spectroscopy
- Strange matter
- Solar neutrinos
- Nuclear matter in extremes of temperature and density
- QCD phase transitions

Advanced Accelerator Concepts:

- Short wavelength accelerating structures
- Production of coherent radiation free electron laser
- Muon collider and storage ring
- Neutron Sources
- Interlaboratory collaboration on the design and construction of the Spallation Neutron Source

Materials Sciences:

- High T_c superconductivity
- Magnetism
- Surface studies-catalysis, corrosion and adhesion
- Condensed matter theory: metallic alloys and correlated electron systems
- Materials synthesis and characterization with neutron- and X-ray diffraction
- Structure and dynamics
- Defect structure

Chemical Sciences:

- Dynamics, energetics, reaction kinetics on the pico-second time scale
- Thermal-, photo- and radiation-reactions
- Catalysis and interfacial chemistry
- Homogeneous catalysis with metal hydrides
- Porphyrin chemistry

- Electrochemistry

Environmental Sciences:

- Global change
- Atmospheric chemistry
- Marine science
- Soil chemistry
- Cycling of pollutants
- Environmental remediation
- Counter Terrorism

Medical Science:

- Medical imaging: PET, MRI, SPECT, Coronary Angiography
- Nuclear medicine
- Radionuclides, radiopharmaceuticals, synthesis and application
- Advanced cancer therapies: neutron capture, microbeam radiation, proton radiation, photon-activation therapy
- Mechanisms of oncogenesis

Molecular Biology and Biotechnology:

- Genome structure, gene expression, molecular genetics
- DNA replication, damage and repair
- Structure and function of enzymes, protein engineering
- Plant genomics, biochemistry and energetics
- Solution structure, kinetics and interaction of biomolecules
- Biostructure determination by X-ray and Neutron scattering
- Biostructure determination and mass measurements by electron microscopy

Advanced Scientific Computing and Systems Analysis:

- Atmospheric Transport Modeling
- Infrastructure assessment
- Energy modeling
- Groundwater modeling
- Intelligent sensor and security systems

Table 2 - Expertise Derived from Brookhaven's Core Competencies - Technology

Physical, Chemical and Materials Science:

- Advanced instrumentation and devices for precision electronics, optics and microelectronics
- Superconducting and magnetic materials
- Micromachining
- Battery technology
- Permanent magnets
- "Designer" polymers

Accelerator Technology:

- High-field, high-quality superconducting magnets
- High-power radio-frequency systems
- Ultrahigh vacuum systems
- Advanced accelerator designs
- Accelerator/spallation source applications
- Insertion device development: wigglers and undulators
- High-power, short-pulse lasers

Medical Technologies:

- Biomedical applications of nuclear technology
- Development and production of radio-nuclides/radiopharmaceuticals
- Development of particle and X-ray radiation therapies for cancer
- Medical imaging
- X-ray microbeam therapy

Biotechnology:

- Neutron and synchrotron x-ray scattering
- Large scale genome sequencing
- High resolution scanning and cryogenic electron microscopy

- Cloning, expressing and engineering genes
- Metal cluster compounds for electron microscope labels
- Phage displays for probing specific interactions
- Biocatalytic treatment of heavy oils

Environmental and Conservation Technologies:

- Ultra sensitive detection and characterization
- Environmental remediation and mitigation
- Waste treatment
- Disposal of nuclear materials
- Energy-efficiency technologies
- Fuel cell technologies
- Infrastructure modernization
- Transportation: Intelligent transportation systems, MAGLEV, RAPTOR
- Radiation protection
- Bioremediation technologies

Safety, Safeguards, and Risk Assessment:

- Safeguards, non-proliferation and arms control
- Design and development of non-proliferation reactors and fuel cycles
- Material and component survivability testing
- Remote sensing of chemical signatures
- Technical support for U. S. policy
- Safety analysis of complex systems
- Probabilistic risk assessment and management
- Human factors
- Energy-system modeling
- Structural, thermal hydraulics and nuclear design
- Integrated Safety Management

The following is a list of themes that are derived from the breadth and expertise expressed in Tables 1 and 2. The number of LDRD projects as related to these BNL themes is shown in Table 3.

Table 3 - THEMES

THEMES	Number of LDRD Projects
1 Scientific Facilities Operations <ul style="list-style-type: none"> • RHIC • NSLS • ATF • LEAF • STEM • Tandem • BMRR 	0
2 Nuclear Physics <ul style="list-style-type: none"> • Quark/gluon plasma • Spin Physics 	0
3 High Energy Physics <ul style="list-style-type: none"> • Standard Model • Rare Particles & Processes 	1
4 Advanced Accelerator & Detector Concept and Designs - Advanced Instrumentation <ul style="list-style-type: none"> • Muon Collider • DUV-FEL • LHC • SNS 	12
5 The Physics & Chemistry of Materials <ul style="list-style-type: none"> • Superconductivity • Magnetism • Surfaces • Nanostructure 	26
6 Energy Sciences <ul style="list-style-type: none"> • Combustion • Catalysis • Bio-fuels • Batteries • Geothermal • Buildings 	8
7 Environmental Sciences <ul style="list-style-type: none"> • Atmospheric • Terrestrial • Bio-remedial • Waste Technologies 	6
8 Medical and Imaging Sciences & Technology	1
9 Advanced Computation	0
10 Biological Sciences	15
11 Critical Infrastructure	1
Totals	70

Overall, the LDRD portfolio supports all of the BNL themes and strategic objectives which in turn supports the DOE strategic initiatives.

Summary of Metric Data

Statistical data is collected on all projects for the annual report. Since the LDRD Program is intended to promote high-risk research, the data collected has nominal value on a project-by-project basis. It does provide a general overall picture of the productivity of the LDRD Program.

Some of the more common indicators/measures of success are: 1) the number of proposed, received and approved projects, 2) amount of follow-on funding, 3) the number of patents applied for, and 4) the number of articles published in peer-reviewed journals.

Historically, statistics on the number of projects approved, compared to those rejected, show an overall approval rate of about 30 percent for new starts. Thirteen scientific departments were represented in the FY 2002 LDRD Program. From inception of the program through September 2002 (for FY 2002), 1071 project proposals were considered and 337 were approved. These show and demonstrate that the LDRD Program at BNL is expanding and is generating interest from across the entire Laboratory population.

In FY 2002, the BNL LDRD Program funded 70 projects, 29 of which were new starts, at a total cost of \$6,731,882. Included in this report is the Project Funding Table, which lists all of the FY 2002 funded projects and gives a history of funding for each by year.

FISCAL YEAR	AUTH K\$	COSTED K\$	NO. REC'D	NEW STARTS
1985	1,842	1,819	39	13
1986	2,552	2,515	22	15
1987	1,451	1,443	29	8
1988	1,545	1,510	46	14
1989	2,676	2,666	42	21
1990	2,008	1,941	47	9
1991	1,353	1,321	23	14
1992	1,892	1,865	30	14
1993	2,073	2,006	35	14
1994	2,334	2,323	44	15
1995	2,486	2,478	46	13
1996	3,500	3,050	47	17
1997	4,500	3,459	71	10
1998	4,000	2,564	53	4
1999	4,612	4,526	67	25
2000	6,000	5,534	93	21
2001	6,000	5,345	97	38
2002	7,000	6,732	87	29
2003	8,482		153	43
TOTALS	65,528	53,145	1,071	337

An analysis of the FY 2002 projects shows that many of the projects were reported to have submitted proposals for grants or follow-on funding (several received funding), and a multitude of articles or reports were reported to be in publication or submitted for publication. Several of these projects have already experienced varying degrees of success, as indicated in the individual Project Program Summaries that follow. The complete summary of success indicators is as follows:

SUCCESS INDICATORS	QTY
Total number of refereed publications based on the work supported by LDRD funds and done during the active period of this project.	100
Total number of formal presentations originating in whole or in part from this LDRD, including those that have been accepted for presentation but not yet presented.	196
Total number of reports originating in whole or in part from this LDRD.	12
Total number of patent licenses and copyrights either applied for or granted that were either derived from this LDRD project directly or from any follow-on efforts to date.	5
Total number of invention disclosures submitted to the Laboratory's Office of Intellectual Property & Industrial Partnership that were derived either from this LDRD project directly or from any follow-on efforts to date.	8
Total number of review presentations that pertain to this work.	24
Total number of students and postdocs (combined total as FTEs) directly supported by this LDRD project while this project was active.	51
Total number of new, permanent, full-time staff hired as a direct result of this LDRD Project.	24
Total number of proposals submitted for follow-on funding (other than LDRD).	70

In conclusion, the overall LDRD Program has been successful. In FY 2002, the LDRD Program has improved on the level established in FY 2001 which already was at a historically high level. This increase in size is a consequence of the identification of the LDRD Program by Laboratory Management to be an important part of its future. The LDRD Program is a key component for developing new areas of science for the Laboratory. In FY 2002 the Laboratory continues to experience a significant scientific gain by the achievements of the LDRD Projects.

NOTE: Total number means sum total for all years of the project

FUNDING TABLE OF LDRD PROJECTS APPROVED FY 2002

					Actual	Actual	Actual	Approved Budget	Requested Budget	Total
LDRD Proj. No.	Project Title	P.I.	Dept./Bldg.	Theme	FY 00\$	FY 01\$	FY 02\$	FY 03 \$	FY 04 \$	
00-25A	Rapid Real-time Measurement of Aerosol Chemical Composition	Lee, Y.-N.	ESD/815E	7		\$118,156	\$120,892			\$239,048
00-25B	Novel Techniques to Measure Aerosols and Aerosol Precursors: Multiple Humidity Tandem Differential Mobility Analyzer(TDMA)	Brechtel, F.	ESD/815E	7		\$117,080	\$120,777			\$237,857
00-32	Microvascular Endothelial Cells as Targets of Ionizing Radiation	Pena, L.	MED/490	10	\$82,633	\$100,622	\$63,874			\$247,129
00-40	The Structure of Membrane Proteins: Monolayers and Thin Films	Ocko, B.	PHYS/510B	5	\$16,566	\$636	\$16,126			\$33,328
00-43	Understanding the Pathways of Ubiquitin Dependent Proteolysis	Bewley, M.	BIO/463	10	\$244,247	\$216,260	\$214,827			\$675,334
00-45	New Protein Expression Tools for Proteomics	Freimuth, P. L.	BIO/463	10	\$41,698	\$109,754	\$110,919			\$262,371
01-07	Development of Superconducting Accelerator Magnets Capable of High dB/dt	Ghosh, A.	SUPERCONDUCT MAGNET DIV/ 902A	4		\$143,588	\$145,950			\$289,538
01-11	Combination of Magnetic Fields and 20 keV Synchrotron X-rays to produce Microbeams for Cell Culture Experiments	Pena, L.	MED/490	10		\$11,169	\$11,697			\$22,866
01-12	Gene Expression Profiling of Methamphetamine-Induced Toxicity in Neurons in Culture Using DNA Microarrays	Vazquez, M.	MED/490	10		\$105,192	\$99,642			\$204,834
01-13	"Functional Spectral Signature" (FSS) Method for Signal to Noise-Enhancement of Brain Patterns in PET Images	Felder, C.	MED/490	10		\$85,941	\$45,085	\$53,000		\$184,026
01-18	Exploration and Development of Ultrafast Single Shot Detection Methods for Use with Pulse Radiolysis Experiments at LEAF	Cook, A. R.	CHEM/555A	4		\$62,401	\$64,870			\$127,271
01-19	Metal NanoClusters and Electron Transfer in One, Two, and Three Dimensions (NANO III)	Creutz, C.	CHEM/555A	5		\$81,202	\$144,617			\$225,819
01-20	Molecular Wires for Energy Conversion and Nano-Electronics	Miller, J. R.	CHEM/555A	5		\$47,655	\$49,784			\$97,439
01-21	Nanoscale Catalysts: Preparation, Structure and Reactivity (NANO II)	Hrbek, J.	CHEM/555A	6		\$76,395	\$79,880			\$156,275
01-23	Experimental and Theoretical Studies of the Formation of Titanium-Carbon Nanoclusters (NANO II)	Sears, T.	CHEM/555A	5		\$103,067	\$106,912			\$209,979

FUNDING TABLE OF LDRD PROJECTS APPROVED FY 2002

LDRD Proj. No.	Project Title	P.I.	Dept./Bldg.	Theme	Actual	Actual	Actual	Approved Budget	Requested Budget	Total
					FY 00\$	FY 01\$	FY 02\$	FY 03 \$	FY 04 \$	
01-24	Development of a UV-Raman, Near-field Scanning Optical Microscope for <i>in-situ</i> Studies of Chemical Intermediates on Metal Nanoparticles (NANO II)	White, M. G.	CHEM/555A	5		\$96,203	\$99,850			\$196,053
01-28	Development of New Techniques for Improvements in PET Imaging of Small Animals and Other Applications	Schlyer, D.	CHEM/555A	8		\$86,322	\$89,885			\$176,207
01-30	Development of CZT Array Detector Technology for Synchrotron Radiation Applications	Siddons, D. P.	NSLS/725D	4		\$106,592	\$68,399	\$50,000		\$224,991
01-31	New Applications of Circular Polarized VUV-light (NANO IV)	Vescovo, E.	NSLS/725D	5		\$23,860	\$52,904	\$50,000		\$126,764
01-32	Soft X-Ray Magnetic Speckle (NANO IV)	Sanchez-Hanke, C.	NSLS/725D	5		\$41,173	\$40,942			\$82,115
01-35	Prototype Approaches Toward Infrared Nanospectroscopy	Carr, G. L.	NSLS/725D	5		\$33,689	\$64,030	\$65,000		\$162,719
01-36	Pressure-Induced Protein Folding Monitored by Small Angle X-Ray Scattering and Fourier Transform Infrared Microspectroscopy	Miller, Lisa	NSLS/725D	10		\$43,499	\$43,511	\$50,000		\$137,010
01-38	Soft Condensed Matter Probed by Low-Energy Resonant Scattering	Caliebe, W.	NSLS/725D	5		\$32,873	\$50,401	\$50,000		\$133,274
01-39	Femto-Seconds Electron Microscope Based on the Photocathode RF Gun	Wang, X. J.	NSLS/725C	4		\$145,593	\$62,119	\$65,000		\$272,712
01-45	First-Principles Theory of the Magnetic and Electronic Properties of Nanostructures (NANO IV)	Weinert, M.	PHYS/510A	5		\$88,387	\$89,928			\$178,315
01-50	Cryo-EM for Solving Membrane Proteins	Hainfeld, J.F.	BIO/463	4		\$115,949	\$119,346			\$235,295
01-51	Human DNA Damage Responses: DNA-PK and p53	Anderson, C. W.	BIO/463	10		\$167,158	\$124,613	\$105,000		\$396,771
01-52A	Molecular Mechanisms Underlying Structural Changes in the Adult Brain: A Genetic Analyses	Dunn, J. J.	BIO/463	10		\$117,218	\$117,111			\$234,329
01-58A	Catalytic Microcombustion Systems	Krishna, C. R.	ES&T/526	6		\$93,108	\$95,677			\$188,785
01-62	Mapping Electron Densities in Porphyrin Radical Crystals Using the NSLS	Barkigia, K. M.	MSD/555	6		\$29,102	\$69,694			\$98,796
01-67	High Sensitivity Mass Spectrometer	Vanier, P. E.	NNS/197C	4		\$117,574	\$120,988			\$238,562

FUNDING TABLE OF LDRD PROJECTS APPROVED FY 2002

LDRD Proj. No.	Project Title	P.I.	Dept./Bldg.	Theme	Actual	Actual	Actual	Approved Budget	Requested Budget	Total
					FY 00\$	FY 01\$	FY 02\$	FY 03 \$	FY 04 \$	
01-78	Development and Application of Cavity Ringdown Spectroscopy to the Detection and Monitoring of Trace Chemical Species in the Atmosphere	Sedlacek, A. J.	ESD/703	7		\$86,743	\$89,625			\$176,368
01-79	Development of a High Field Magnet for Neutrino Factory Storage Rings	Gupta, R.	SUPERCONDUCTM AGNET DIV/ 902A	4		\$98,066	\$100,659			\$198,725
01-82	DNA-Nano Wires that AutoConnect in 3 Dimensions (NANO III)	Hainfeld, J. F.	BIO/463	5		\$58,814	\$60,337			\$119,151
01-85	Carbon Nanotube Chemical Probes for Biological Membrane Attachment Quantification (NANO III)	Panessa-Warren, B.	INST/ 535B	5		\$48,378	\$50,113			\$98,491
01-86	Self-Organized Nanoparticles for Probing Charge Transfer at Metallic/Organic Interfaces (NANO III)	Strongin, M.	PHYS/510B	5		\$46,504	\$49,321			\$95,825
01-87	Charge Transfer on the Nano Scale: Theory (NANO III)	Newton, M. D.	CHEM/555A	5		\$43,063	\$54,429	\$18,000		\$115,492
01-88	Charge Transport through Dye-Sensitized Nanocrystalline Semiconductor Films (NANO III)	Brunschwig, B.	CHEM/555A	5		\$52,555	\$54,740			\$107,295
01-91	Magnetic Nanodispersions (NANO IV)	Lewis, L. H.	MSD/480	5		\$71,175	\$72,892			\$144,067
01-93	High Resolution Magneto-optical Study of Magnetic Nanostructures, Nanocomposite Functional and Superconducting Materials (NANO IV)	Li, Qiang	MSD/480	5		\$32,748	\$45,797	\$26,000		\$104,545
01-97	Size Selected Quantum Dots Under Environmentally Controlled Conditions	Imre, D.	ESD/815E	5		\$87,349	\$89,705			\$177,054
02-02	Crystallization and X-ray Analysis of Membrane Proteins	Fu, D.	BIO/463	10			\$380,454	\$396,000	\$414,400	\$1,190,854
02-03	<i>In Vitro</i> Investigation of the DNA Double Strand Break Repair Mechanism by Non-Homologous End-Joining in the context of Chromatin	Lymar, E.	BIO/463	10			\$63,659	\$62,600	\$65,400	\$191,659
02-08	Creating a MicroMRI Facility for Research and Development	Benveniste, H.	MED/490	4			\$94,494	\$196,000	\$180,000	\$470,494
02-09	Targeting Tin-117m to Estrogen Receptors for Breast Cancer Therapy	Kolsky, K.	MED/801	10			\$48,242	\$100,000	\$50,000	\$198,242
02-16	Biominerallization of Actinides: A Mechanistic Study of the Genesis of Novel and Stable Compounds	Francis, A. J.	ESD/490A	7			\$88,871	\$93,000		\$181,871

FUNDING TABLE OF LDRD PROJECTS APPROVED FY 2002

LDRD Proj. No.	Project Title	P.I.	Dept./Bldg.	Theme	Actual	Actual	Actual	Approved Budget	Requested Budget	Total
					FY 00\$	FY 01\$	FY 02\$	FY 03 \$	FY 04 \$	
02-17	Using Mini-LIDAR for Verification and Long-Term Monitoring of Cover Systems	Heiser, J.	ESD/830	6			\$124,610	\$125,080		\$249,690
02-22	Electrical Systems Reliability	Bari, R.	ES&T/475B	11			\$83,965	\$100,000	\$157,000	\$340,965
02-24	Liquid Fuel Gasifier for Combustion and Fuel Cells	Butcher, T.	ES&T/526	6			\$72,993	\$109,000		\$181,993
02-31	Study of a Power Source for Nano-Devices	Lin, M.	ES&T/815	5			\$99,920	\$100,000	\$165,000	\$364,920
02-42	Ultrafast Nonlinear Spectroscopic Studies of Model Catalytic Surfaces	Camillone, N.	CHEM/555	6			\$184,847	\$185,000		\$369,847
02-45	Combined Use of Radiotracers and Positron Emission Imaging in Understanding the Integrated Response of Plants to Environmental Stress	Ferrieri, R.	CHEM/901	7			\$99,220	\$100,000		\$199,220
02-46	Arranging Nanoparticles into Arbitrary Patterns with Optical Trapping	Fockenber, C.	CHEM/555A	5			\$119,860	\$120,000		\$239,860
02-48	Advanced Multidimensional Techniques to Explore the Biochemical and Behavioral Consequences of VOC Exposure	Gerasimov, M. R.	CHEM/555A	7			\$119,827	\$95,000		\$214,827
02-49	Project to Detect pp and 7Be Solar Neutrinos in Real Time: LENS, the Low-Energy Neutrino Spectrometer	Hahn, R.	CHEM/555A	3			\$70,248	\$70,000		\$140,248
02-53	Combined Theoretical and Experimental Study of Crystal Lattice Defects in Complex Transition Metal Oxides	Davenport, J.	DA/463B	5			\$39,678	\$66,825		\$106,503
02-55	Chemical Sensors: Immobilization of Organometallic Complexes into Sol-gel Matrices	Renner, M.	MSD/555	6			\$81,940	\$86,000		\$167,940
02-56	Size Dependence of Catalytic Reactivity of Iron Oxide Nanocrystals	Wong, S.	MSD/480	6			\$84,575	\$104,000		\$188,575
02-58	Femtosecond Synchronization for Ultra-Short Pulse DUV-FEL Radiation	Graves, W.	NSLS/725D	4			\$134,883	\$135,000	\$135,000	\$404,883
02-62	Rapid Wavelength Tunability for the DUV-FEL	Sheehy, B.	NSLS/725D	4			\$135,269	\$135,000	\$135,000	\$405,269
02-66	High-Gain Harmonic-Generation at the DUV/FEL	Yu, L. H.	NSLS/725C	4			\$134,947	\$135,000		\$269,947
02-67	Biom mineralization: A Route to Advanced Materials	DiMasi, E.	Condensed Matter Physics/510B	5			\$99,935	\$105,400	\$111,000	\$316,335
02-70	Theory of Electronic Transport in Nanostructures and Low-Dimensional Systems	Tsvelik, A.	Condensed Matter Physics/510A	5			\$134,268	\$139,900	\$145,500	\$419,668

FUNDING TABLE OF LDRD PROJECTS APPROVED FY 2002

LDRD Proj. No.	Project Title	P.I.	Dept./Bldg.	Theme	Actual	Actual	Actual	Approved Budget	Requested Budget	Total
					FY 00\$	FY 01\$	FY 02\$	FY 03 \$	FY 04 \$	
02-71	Pressure in Nanopores	Vogt, T.	Condensed Matter Physics/510B	5			\$79,000	\$82,600	\$86,700	\$248,300
02-84a	Genomic SELEX to study Protein DNA/RNA Interactions in <i>Ralstonia Metallidurans</i> CH34 Regulating Heavy Metal Homeostasis and Resistance	van der Lelie, D.	BIO/463	10			\$163,972	\$170,900	\$49,900	\$384,772
02-84b	Lead Resistance in <i>Ralstonia Metallidurans</i> CH34	van der Lelie, D.	BIO/463	10			\$161,408	\$170,100		\$331,508
02-85	Design of a <i>Ralstonia Metallidurans</i> Two-Hybrid Protein System for Studying Signaling Pathways Regulating Heavy Metal Homeostasis and Resistance	Taghavi, S.	BIO/463	10			\$168,188	\$173,900	\$51,200	\$393,288
02-86	Ultrafast X-Ray Science	Dierker, S.	NLSL/725B	5			\$100,018	\$105,000		\$205,018
02-88	X-Ray Photon Correlation Spectroscopy Studies of Nanostructured Block Copolymers	Dierker, S.	NLSL/725B	5			\$90,212	\$105,000		\$195,212
02-91	Fine Grain Gas and Silicon Detectors for Future Experiments in Nuclear Physics at High Energies	Woody, C.	PHYS/510C	4			\$99,511	\$100,000		\$199,511
					385,144	3,342,814	6,731,882	\$ 4,198,305	\$ 1,746,100	16,404,245

LABORATORY DIRECTED RESEARCH AND DEVELOPMENT
2002 PROJECT PROGRAM SUMMARIES

Rapid Real-time Measurement of Aerosol Chemical Composition

Yin-Nan Lee

00-25A

PURPOSE:

The main objective of this research project is to develop a fast in-situ real-time analytical technique to quantitatively determine the chemical composition of ambient aerosol particles. The chemicals to be measured include inorganic and organic ions and total organic carbon (TOC). The fast data acquired (time resolution < 10 min on the ground and 3 min on aircraft) are to provide crucial information needed to understand the sources and chemical evolution of aerosol particles and their properties that impact the environment and human health.

APPROACH:

Ambient aerosols were collected using a newly developed technique, particle-into-liquid-sampler (PILS) which grows submicron size particles into supermicron droplets under supersaturated conditions. The resulting droplets are collected using a single orifice impactor. The liquid sample is washed off from the impactor and transported to the analytical instruments using a constant carrier liquid flow. Two ion chromatographs (IC) are used to determine cations (Na^+ , NH_4^+ , K^+ , Mg^{2+} , Ca^{2+}) and anions (NO_3^- , SO_4^{2-} , formate, oxalate). Total organic carbon was determined using a TOC instrument (Ionics, Inc., model 800 Turbo). Organic compounds are oxidized to CO_2 using UV oxidation aided by an oxidizing agent, ammonium persulfate. The resulting CO_2 was detected conductometrically. A PILS-IC-TOC instrument suitable for aircraft deployment was constructed and tested on the DOE G1 aircraft during the New

England Aerosol and Oxidant Study (NEAOS) between July 13 and August 12, 2002. Dr. Xiaoying Yu, a postdoctoral associate, was working on this project during the period April 2001 to September 2002.

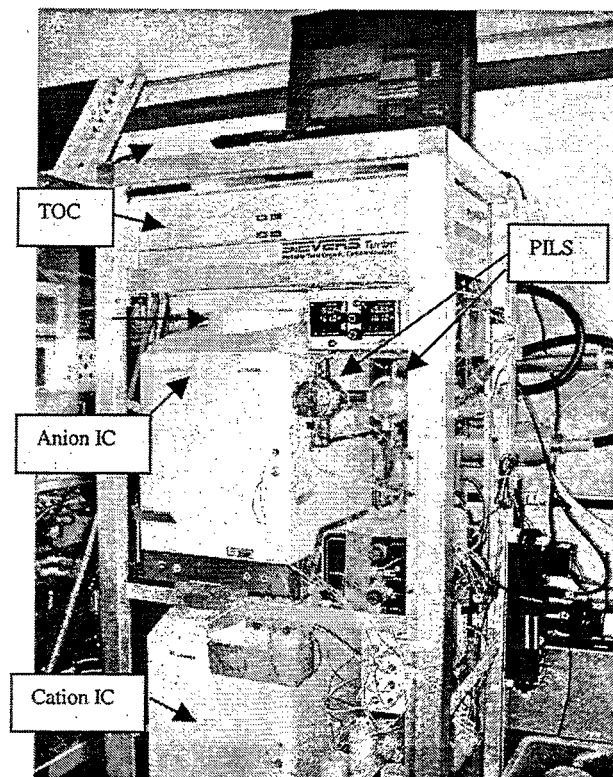


Figure 1. The PILS-IC-TOC system deployed on the DOE G1 aircraft during the 2002 NEAOS study in Worcester, MA.

TECHNICAL PROGRESS AND RESULTS:

The main objective of this LDRD project in its 2nd year was the development of an airborne capability of the PILS-IC-TOC instrument with an emphasis on the detection of TOC contained in aerosol particles. The ability to detect inorganic ionic components of aerosol particles has been established and reported in the previous annual report. This new system was first tested in the laboratory to insure proper operation in terms of flow condition, sensitivity, and time response. The laboratory setup involved the use of a

Tapered Element Oscillating Microbalance (TEOM) to determine the total aerosol mass loading in real time, providing baseline information the PILS measurements can be compared and constrained to (see presentation on Laboratory setup). An example of the data collected during this lab characterization is shown in presentation on proof of concept. These results showed that TOC comprised a major portion of the aerosol mass and that the sensitivity and time response of the TOC measurement is $\sim 0.2 \mu\text{g m}^{-3}$ and 70 s, respectively. Also tested during this laboratory study was the effectiveness of a carbon impregnated denuder (purchased from Prof. Eatough of Brigham Young University, Utah) for removing gaseous organic compounds upstream of the PILS. This filter was found to work properly in the laboratory environment.

In the NEAOS field study based in Worcester, MA, the performance of the TOC was found to be affected by the large temperature change in the aircraft cabin and subsequently a warm up period up to two hours was necessary to insure the proper operation of this instrument. The data collected during a night flight on 7/31/02 over the Boston metropolitan area are shown in Figure 2.

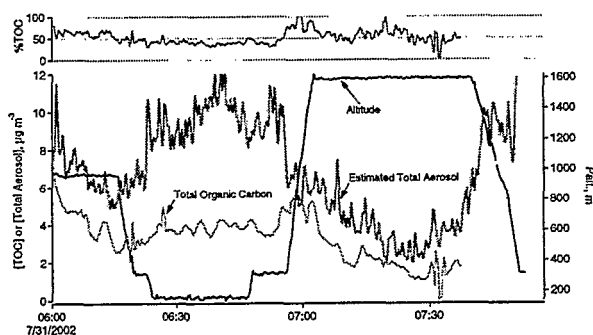


Figure 2. Aerosol total organic carbon content measured during a night flight on 7/31/02 showing that organic components accounted for a significant fraction of the total aerosol mass.

The level of TOC varied between $1\text{-}6 \mu\text{g m}^{-3}$, and accounted for a significant fraction of the total aerosol mass which was estimated from the particle size/number distribution measured using a passive cavity aerosol spectrometer probe (PCASP, PMS). This result demonstrated the feasibility of the PILS-IC-TOC instrument for making fast and quantitative TOC measurements of aerosol particles on aircraft platforms as well as on the ground.

The TOC content of aerosol particles was measured at a high time resolution (~ 1 min), representing an order of magnitude improvement over a filter-base technique using programmed thermal analysis for elemental and organic carbon.

SPECIFIC ACCOMPLISHMENTS:

The Continuation-in-Part (CIP) application entitled, "An Apparatus for Rapid Measurement of Aerosol Bulk Chemical Composition" with the formal papers was submitted to U.S. Patent and Trademark Office on 10/24/02 after having received Notice of Allowance from the U.S. Patent Office.

Publications:

A particle-into-liquid collector for rapid measurement of aerosol bulk chemical composition, R.J. Weber, D. Orsini, Y. Duan, Y.-N. Lee, P. J. Klotz, and F. Brechtel. *Aerosol Sci. Technol.*, 35, 718-727, 2001.

A manuscript describing the improvements made on the PILS-IC system used in the NASA Transport and Chemical Evolution-Pacific (TRACE-P) and the NSF ACE-Asia field measurements in 2001 (for which the PI has participated) was submitted to *Atmospheric Environment: Refinements to the particle-into-liquid sampler (pils) for ground and airborne measurements of water soluble aerosol chemistry*, Y. Ma, D. Orsini,

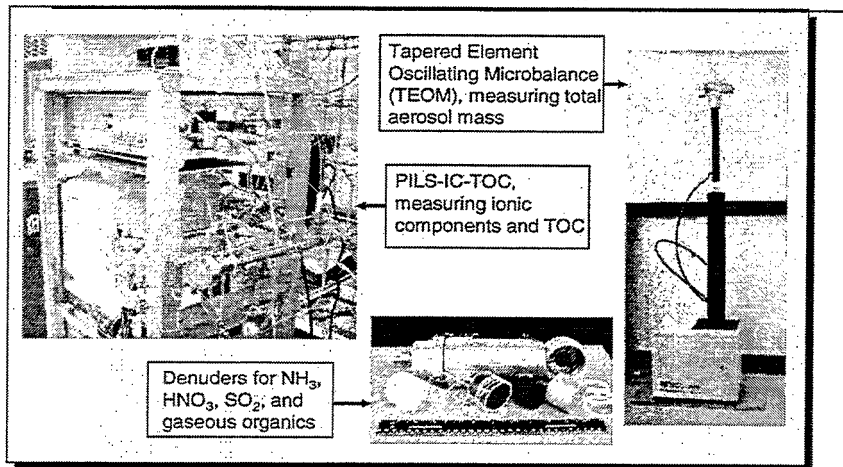
K. Maxwell, Y.-N. Lee, K. Moore, V.N. Kapustin, A. D. Clarke, R. Weber.

LDRD FUNDING:

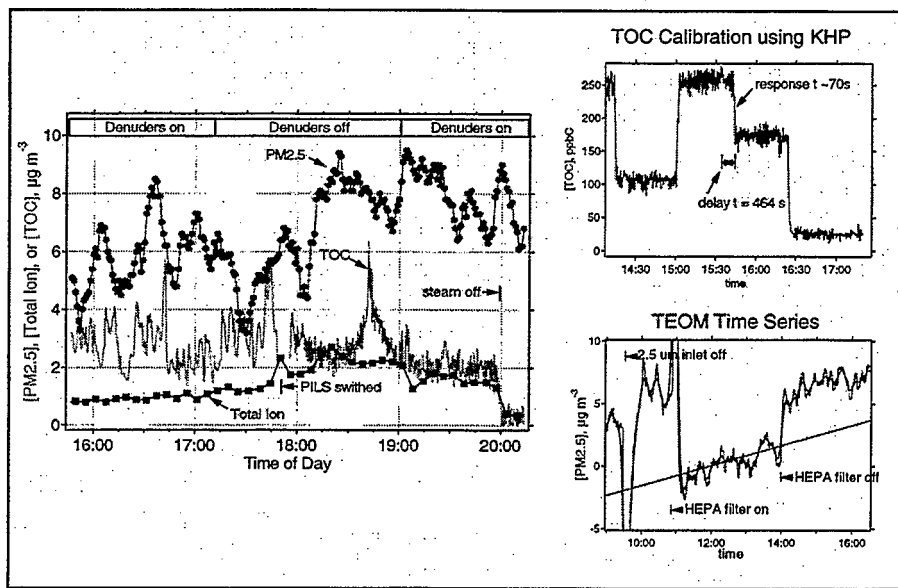
FY 2001
FY 2002

\$118,156
\$120,892

Laboratory Setup



Proof of Concept



Novel Techniques to Measure Aerosols and Aerosol Precursors: Multiple Humidity Tandem Differential Mobility Analyzer

Fredrick J. Brechtel

00-25B

PURPOSE:

The response of ambient aerosols to relative humidity plays a critical role in determining their visibility, health, and climate impacts. Current techniques do not have sufficient time response and cannot reveal how chemical composition influences the water uptake properties of aerosols. The objective of this project is to develop a new instrument capable of rapid, size-resolved measurements of aerosol water uptake that can be deployed on-board research aircraft during missions over heavily polluted urban areas. Successful implementation of the new measurement system will provide unique future funding opportunities and position BNL at the forefront of integrated studies of aerosol physical, thermodynamic and chemical properties.

APPROACH:

Over the past several decades traditional Tandem Differential Mobility Analyzer (TDMA) techniques have been used to measure the size-resolved water uptake properties (hygroscopicity) of ambient aerosols. Previous studies in urban areas have demonstrated that at any given size, particles typically contain multiple chemical compounds leading to complex hygroscopic properties. The TDMA requires multiple hours to obtain water uptake information on several different particle size classes at different relative humidities (RH); this time scale is much too long for aircraft

observations where changes in aerosol properties are often observed over minute time scales.

To address the need for rapid aircraft measurements of particle hygroscopic growth, a new method is proposed to study multiple particle sizes in parallel at several different RHs. The technique involves scanning multiple particle mobility spectrometers in parallel to simultaneously select different size particles that are exposed to a coordinated time-varying RH within humidifiers placed between the sets of spectrometers. The first set of spectrometers select the various dry particle sizes, the exiting particles are then humidified, and the grown droplets are then sized using the second set of spectrometers. A post-doctoral researcher, Gintautas Buzorius, is a key collaborator on the project.

TECHNICAL PROGRESS AND RESULTS:

The prototype instrument design and initial construction began in FY 2000, with testing of traditional TDMA, humidification techniques and new data acquisition software and hardware. The prototype involved a scanning RH system with only two mobility spectrometers. During FY 2001, the sizing capability of the second spectrometer of the prototype was improved by employing a scanning voltage system, increasing the time resolution of hygroscopic growth measurements by more than one order of magnitude. New data acquisition software was completed, control algorithms for RH and spectrometer control were revamped and optimized, and the system was tested with calibration aerosols having known chemical composition and hygroscopic properties. The prototype was deployed at a surface site during the Aerosol Characterization Experiment-Asia (ACE-

Asia) on Cheju Island, Republic of Korea. This system has the capability for simultaneous determination of individual particle size, hygroscopicity, and composition of internally and externally mixed aerosols. A humidity(H)TDMA is used to select particles according to their size and hygroscopicity for compositional analysis by a single particle mass spectrometer. The capability of the system was demonstrated using a laboratory aerosol consisting of polystyrene latex spheres coated with a layer of ammonium nitrate to represent an internally mixed aerosol with controllable hygroscopicity that is externally mixed with pure ammonium nitrate particles. The instrument was applied to the study of ambient aerosols. The results demonstrate that this system is clearly capable of providing information linking individual particle composition with their hygroscopic properties. The ambient data showed that sulfate was present in most of the particles of the more hygroscopic growth mode, while the less hygroscopic mode was mostly of crustal origin.

SPECIFIC ACCOMPLISHMENTS:

Publications:

Buzorius, G.; Zelenyuk, A.; Brechtel, F.; and Imre, D. Simultaneous determination of individual ambient particle size, hygroscopicity and composition. *Geophys. Res. Lett.* 29,1974,doi:1029/2001GL014221(2002).

Presentations:

F. J. Brechtel, A. Zelenyuk, D. Imre, and G. Buzorius, First Simultaneous Particle Size, Hygroscopicity and Composition Measurements by Coupled HTDMA-MS. Paper presented at the AAAR conference, Portland, OR, Oct. 2001.

F. J. Brechtel, G. Buzorius, C.-H. Jung, J.-Y. Kim, S.-N. Oh, A. Zelenyuk, D. Imre, P. Chuang, and H. Swan, Aerosol Physical and Chemical Properties at Cheju Island, Korea During ACE-Asia. Poster presented at the ACE-Asia data workshop, Pasadena, CA, Oct. 2001.

New Developments and needs in the hygroscopicity measurements of ambient aerosol. F. Brechtel, A. Maasling, S. Leinert, A. Nowak, A. Wiedensohler, G. Buzorius, D. Covert, D. Imre, A. Zelenyuk. *Eos. Trans. AGU*, 83(47), Fall Meet. Suppl. Abstract, 2002.

J-H. Han, T. Onasch, S. Oatis, F. Brechtel, D. Imre. Thermodynamics of common atmospheric particles on the nano-scale. American Association for Aerosol Research Annual Conference, Charlotte, NC, Oct 7-11, 2002.

LDRD FUNDING:

FY 2001	\$117,080
FY 2002	\$120,777

Microvascular Endothelial Cells as Targets of Ionizing Radiation

Louis A. Peña

00-32

PURPOSE:

This LDRD supported the establishment of *in vitro* models of brain microvascular endothelial cells (EC) for radiobiology studies. A significant amount of pilot work was necessary to adapt published protocols and local resources to establish model systems of two types (i) pure EC cultures capable of differentiation, and (ii) EC-astrocyte co-cultures which serve as a model for the blood brain barrier (BBB). Finally, this LDRD also supported studies of the microvascular endothelium *in vivo* in rodent brain. Development of EC models allowed the initiation of a new program of basic and applied research of relevance to Radiobiology and Radiation Oncology, using modern cell- and molecular biology techniques. These model systems are not only important for this project but has promoted collaborations with other investigators/projects at BNL (e.g., neuro-imaging drug development [S.J. Gatley], neuro-imaging and the BBB [W. Rooney], microbeam radiation therapy [F.A. Dilmanian], radiation-induced cell death of CNS glial cells [L.A. Peña]).

APPROACH:

A significant portion of radiation injury arising from the therapeutic use of ionizing radiation is attributable to damage of blood vessels. Microvascular endothelial cells are the cells of which capillaries are composed, and are the cells which line the inner lumen of large blood vessels (e.g., arteries and veins). With respect to the central nervous system, there is one added level of

complexity. Capillaries in the brain and spinal cord consist of ECs possessing intracellular tight junctions that confer a chemical permeability barrier known as the blood brain barrier (BBB).

First, EC monolayer cultures with cells from various sources were grown under various conditions and configurations and evaluated for radiation tolerance. The ECs evaluated were (i) BAEC (bovine aortic endothelial cells), (ii) BAEC that were induced to differentiate into a *microvascular* phenotype, (iii) HAEC (human aortic endothelial cells), (iv) HUVEC (human umbilical vein endothelial cells), and (v) RMEC (rat kidney microvascular endothelial cells). The first four are primary cell cultures, and the fifth is a cell line. The parameters of interest were cell growth, cell proliferation, cell death (radiation-induced apoptosis and radiation-induced cell toxicity), cell differentiation into tube-like structures that resemble normal capillaries, and *de novo* expression of biochemical markers typical of a differentiated state (e.g., alkaline phosphatase, gamma-glutamyl-transferase). The culture variables of interest were the requirements for certain growth factors (e.g., VEGF, bFGF), plastic substrates, microporous membrane substrate, Matrigel® coating.

Second, co-culture of ECs with glial cells of the astrocytic type (e.g., primary astrocytes, glioma cell lines), were similarly subjected to the systematic optimization outlined above, with additional parameters. EC-astrocyte co-cultures can form a patent "BBB" *in vitro*, thus two additional assays were employed to confirm this: diffusion of HRP (horseradish peroxidase) from one chamber of the co-culture to the other chamber, and electrophysiological measurement of the voltage potential between chambers. Two alternate methods for producing a BBB culture system were

evaluated (i) co-cultured cells grown as a bilayer (astrocytes or C6 glioma cells seeded on top a monolayer of BAEC), or (ii) BAEC grown as a confluent monolayer on one surface of a sterile microporous membrane and C6 glioma cells monolayers on the other surface (the membrane contains 3 μm pores permitting limited cell-cell contact in addition to solutes passing from one side to the other).

EC culture systems of different configurations were irradiated by x-ray or by gamma-ray in a dose range of 5 to 500 cGy using ionizing radiation sources in both the Medical Department and the Biology Department. In addition, some EC culture systems were subjected to x-ray microbeams (3-100 μm in width) at the X15B and X17B beamlines at the NSLS. After various timepoints, cultures were assayed for the parameters listed above. In addition, we performed DNA microarray analysis of HAEC monolayer cultures. Supplementary, extramural funding was obtained from the Stony Brook Research Foundation (State University of New York at Stony Brook), in collaboration with Hong Lau, MD, PhD, of the Department of Radiation Oncology, School of Medicine, SUNY Stony Brook. HAEC cultures in a proliferating versus a quiescent state were irradiated at BNL, mRNA harvested, and then transported to the SUNY Stony Brook Biotechnology Center DNA Microarray Core Facility. The proliferating HAEC were a model for angiogenic EC, as in tumor growth, for example. The quiescent HAEC were a model for normal, resting EC. Following conversion of mRNA to cDNA, the sample were hybridized to Affymetrix® DNA Chips, and the up- and down- regulation of ~12,000 genes were quantitated.

Finally, a class of novel, synthetic cytokine analogs were developed which confer a significant degree of radioprotection to ECs.

The first two lead compounds (F2A3 and F2A4) are analogs of natural bFGF (basic fibroblast growth factor, a.k.a. FGF-2). Thus, following optimization, EC cultures were subjected to ionizing radiation with or without F2A3, F2A4, or bFGF at various doses up to 500 ng/ml. All of these experiments gave positive results, thus we advanced to *in vivo* rodent models.

Two type of rodent models were set-up and optimized, (i) x-ray irradiation to the cervical spinal cord of adult rats, and (ii) whole body gamma irradiation to adult mice. The radioprotective compounds F2A3 and F2A4 were compared to natural bFGF in each of these models, each applied by i.v. route of administration. Histological endpoints were employed in the rat spinal cord studies. Survival from radiation-induced Gastrointestinal Syndrome was employed in the mouse studies. The latter was not directly relevant to EC responses, however, it was a more efficient *in vivo* assay to study the novel radioprotective drugs.

TECHNICAL PROGRESS AND RESULTS:

Development and optimization of the *in vitro* EC culture systems was completed.

Development and optimization of the *in vitro* BBB co-culture model was completed. Parameter described above is nearly complete.

Growth, survival, and differentiation data have been collected on normal and irradiated EC model systems.

The DNA microarray analysis has resulted in anticipated and unanticipated findings. For example, many genes involved responses to oxidative stress were upregulated, as expected. However, we

unexpectedly found that EC releases two secreted death-inducing ligands (soluble “death signals”) in response to irradiation (e.g., TRAIL). The unexpected releases of death factors may contribute to a novel mechanism responsible for the so-called bystander effect. Ongoing studies are being done to address this issue.

Synthetic cytokine analogs F2A3 and F2A4 have been shown to be biologically equivalent to bFGF in all respects, in both in vitro and in rodent model systems.

This project involves mice and rats and is done under IACUC-approved Protocols #198, 200 and 231.

SPECIFIC ACCOMPLISHMENTS:

A patent filed on the subject of synthetic cytokine analogs. [Peña, L.A.; Zamora, P.O.; Glass, J.; Lin, X.; Synthetic Heparin-Binding Growth Factor Analogs; BSA-02-07/BSA02-08].

Brookhaven Science Associates offered an exclusive license to BioSET, Inc. (College Park, MD) to develop this technology. Dr. Paul Zamora of BioSET was a collaborator on this project.

Pending Grant Applications:

“Modulation of Radiation Tolerance by FGF-like Peptides” (submitted to NIH).

“HZE Radiation Effects of Oligodendrocytes and Progenitors *In Vivo*” (submitted to NASA).

“Effects of Low-dose/Low-fluence Radiation on Differentiation of Bone Progenitor cells” (submitted to DOE).

LDRD FUNDING:

FY 2000	\$ 82,633
FY 2001	\$100,622
FY 2002	\$ 63,874

The Structure of Membrane Proteins: Monolayers and Thin Films

Ben Ocko

00-40

PURPOSE:

To investigate the structure, oligomeric state, and interactions of membrane integral proteins by surface x-ray scattering techniques with the twin goals of developing new methods for obtaining structural information and to obtain fundamental information on the nature of protein membrane interactions. By varying the protein to membrane component concentration, detailed information can be obtained on the structure and on the protein-membrane interactions. An important aspect of our studies is to map out the phase behavior of membrane proteins as a function of multiple environmental parameters including temperature, vapor pressure, surface pressure, solution phase conditions (salt, pH, etc.), and lipid terminal group interactions. These environmental conditions will provide for control of the internal protein conformations, and we will try to correlate these internal conformations with biological activity. In the initial phase of the program, studies will be limited to membranes themselves. Due to advances in the use of liquid mercury as a substrate, studies were extended to membranes of this subphase.

APPROACH:

The Physics Department X-ray Scattering Group has a significant effort devoted to understanding the structure of liquid/vapor interfaces and maintains a Liquid Spectrometer at the NSLS and APS to carry

out these studies. Langmuir monolayers (monolayer film on a liquid subphase) provide an ideal environment for studying biological membranes. The molecular area and surface pressure can be accurately controlled which provides a degree of freedom not available in the bulk. In addition, the surface provides preferential alignment. Our approach is to use x-ray reflectivity and grazing angle diffraction to study the adsorption of integral membrane proteins.

TECHNICAL PROGRESS AND RESULTS:

In FY 2001, we received the specialized x-ray Langmuir trough that was ordered in the previous year. This allowed us to resume investigations which were on hold since August 2000 when our previous x-ray trough (on loan) was returned. We were unable to hire a qualified post-doc to the very tight labor market in biophysics. This search was curtailed when most of the funds for this project were withdrawn.

Over the past few years we have studied artificial Alpha-helical bundles and VPU. In addition, studies of Langmuir monolayers of saturated and unsaturated fatty acids, both single component and mixtures were completed, and the paper was published in Langmuir this fall. Studies of the adsorption of poly-L-lysine, first carried out on a phospholipid monolayer were extended to fatty acids. Studies on Sphigomyelin with David Vaknin (Iowa) were completed, leading to a publication in the Journal of Biophysics. Studies of protein adsorption on metal chelating liquids were initiated with Michael Kent (Sandia Laboratory) and a paper was published in Langmuir. Finally, the first studies of the structure of a Langmuir monolayer on a mercury surface were carried out with Moshe Deutsch (Bar

Ilan). This work was published in Science this year. Initial studies of protein adsorption on the mercury surface were not successful. Finally structural studies of lipopolysaccharides at the air water interface were initiated over the summer at the NSLS in collaboration with Ivan Kuzmenko. Grazing incident diffraction (GID) studies showed a single peak at 1.46\AA^{-1} , corresponding to hexagonal packing of untilted chains. According to preliminary structure factor calculations, the sugar moieties do not play a noticeable role in the structural organization of the film. Further, the presence of calcium ions do not affect the structure as suggested by less direct methods.

B.M. Ocko, and P.S. Pershan, Science 298 (5597): 1404-1407 NOV 15 2002

2. *Segment Concentration Profile of Myoglobin Adsorbed to Metal Ion Chelating Lipid Monolayers at the Air-Water Interface by Neutron Reflection*, M.S. Kent, H. Yim, D.Y. Sasaki, J. Majewski, G.S. Smith, K. Shin, S. Satija, B.M. Ocko, Langmuir 18, 3754 (2002).
3. Structure and phase behavior of mixed *monolayers* of saturated and unsaturated fatty acids, B.M. Ocko, M Kelley, A.T. Nikova and D. K. Schwartz, Langmuir 2002; 18(25); 9810-9815

SPECIFIC ACCOMPLISHMENTS:

1. *Structure of a Langmuir film on a liquid metal surface*, H. Kraack, M. Deutsch,

LDRD FUNDING

FY 2000	\$16,566
FY 2001	\$ 636
FY 2002	\$16,126

Understanding the Pathways of Ubiquitin Dependent Proteolysis

Maria C. Bewley

00-43

PURPOSE:

A biological cell is a complex set of machines that work in harmony, yet little is understood about its inner workings. A key first step in addressing this problem is to study simpler multi-component biological systems and this is the overall goal of this research. Current understanding of the simpler systems is often incomplete because, typically, individual proteins are studied in isolation rather than in the context of their biologically relevant complex. In order to address this problem, structural studies must be made on a system as a whole. Two examples of such systems that have been chosen for further study are the pathway by which DNA double strand break (DSB) repair occurs in mammalian cells and the secondary system is the electron transfer pathway of fatty acid biosynthesis and nitrate reductase (NR). The first pathway is important because unrepaired DNA damage leads to chromosomal errors and cell death. The second pathway is important in understanding a basic principle in cellular function.

APPROACH:

Addressing the question of DSB repair is a huge undertaking that can only be successful if a large number of approaches are tried. Therefore, in a collaborative effort with Carl Anderson, Paul Freimuth, and John Flanagan, we are each addressing a distinct aspect of this pathway. This LDRD is using a "divide and conquer" strategy to obtain structural information about the proteins

involved. Briefly, domains of DNA-Protein Kinase will be identified using a combined bio-informatics and controlled proteolysis approach. Domains identified in this way will be overexpressed initially in *Escherichia coli* using commercially available expression vectors that incorporate a purification tag and any soluble products purified utilizing the tag. Pure protein will then be crystallized and its structure determined using the Multiple Anomalous Dispersion (MAD) technique. It is not uncommon that mammalian protein domains do not express as a soluble entity. In such cases, either attempts to refold the protein or alternative expression systems such as insect cell lines will be investigated.

Addressing the question of electron transfer, by comparison to DSB repair, is a more modest undertaking. The reduction of nitrate to nitrite is catalyzed by the enzyme nitrate reductase (NR). It contains three domains, a flavinadenininedinucleotide (FAD)-binding domain, a cytochrome and a molybdopterin. The electron flow during catalysis follows the scheme substrate \rightarrow FAD \rightarrow cytochrome \rightarrow Mo \rightarrow nitrate. In a different system, fatty acid desaturation, involves the transfer of electrons from b_5 reductase (B5R)-bound substrate to cytochrome b_5 . Clearly, communication between the domains and thus protein:protein interactions will play a key role. In collaboration with Dr. M. Barber at the University of South Florida, who provides the protein samples, permits the use of protein crystallography to understand this transfer process.

TECHNICAL PROGRESS AND RESULTS:

DSB-repair: During FY 2002, in collaboration with Dr. Freimuth, alternative vectors developed in house for over

expression in *E. coli* were used to attempt to produce soluble protein. In addition, in collaboration with Dr. Flanagan, other expression systems were tried. Only very small quantities of protein could be obtained and these were insufficient for crystallization.

Electron transfer: My collaborator has overexpressed and purified fusion proteins that contain an active complex of the FAD and cytochrome domains of rat b₅r and b₅.

In FY 2002, three mutants of b₅r that give rise to the two forms of methemoglobinemia were crystallized and their structures determined. A fourth mutant was crystallized but its structure has not been determined due possibly to a conformational change. Semnomethionine-labeled protein is now being prepared and these crystals will be phased using the MAD technique. In addition, conditions that allow for stability of the b₅:b₅r complex were obtained and crystals grown. They have yet to be characterized.

SPECIFIC ACCOMPLISHMENTS:

Publications:

Bewley, M. C.; Marohnic, C. C.; and Barber, M. J. The structure and biochemistry of NADH-dependent cytochrome b₅ reductase are now consistent. *Biochemistry* 40, 13574-13582 (2001).

Two manuscripts have been submitted to peer-reviewed journals: "Structural plasticity in the FAD of nitrate reductase suggests a mechanism for the first stages of electron transfer" and "The structure of the S127P mutant of cytochrome b₅ reductase that causes methemoglobinemia shows AMP moiety of the flavin occupying the substrate-binding site." These structures show different conformations for the FAD domains and suggest a model for substrate binding.

LDRD FUNDING:

FY 2000	\$244,247
FY 2001	\$216,260
FY 2002	\$214,827

New Protein Expression Tools for Proteomics

Paul I. Freimuth

00-45

PURPOSE:

Our technical objective is to optimize the folding of recombinant proteins into their native, biologically active conformations in *Escherichia coli*, a bacterium which can synthesize proteins in large quantities sufficient for biophysical analyses such as X-ray crystallography. The folding of most proteins *in vivo* is assisted by chaperones, *trans*-acting factors which associate with nascent polypeptides to prevent them from aggregating during the folding process. Methods have been developed to divert most of the cell's protein synthesis machinery (ribosomes) to the production of a single protein species. Under these conditions, synthesis of the normal complement of cell proteins, including chaperones, is reduced. Deficits in chaperone activity may cause mis-folding of many proteins that are over-expressed using high yielding methods (e.g. the bacteriophage T7-based system). Other groups have attempted to solve this problem by increasing chaperone levels in bacterial cells during protein over-expression, but this approach has met with only limited success. In our method, proteins are directly modified to promote their own folding. About half of the proteins in an initial test set could fold properly when expressed by our method. If this trend holds, then this innovative approach will enable the production of large quantities of many proteins that are refractory to over-expression using existing methods. This technical advance would benefit applications such as the BNL Proteomics Initiative that seeks to determine X-ray crystal structures of many different proteins, and it would

further lead to an understanding of the basic mechanisms of protein folding *in vivo*.

APPROACH:

Background: In studies leading to this LDRD project, we observed that a human membrane protein (CAR) which usually misfolds in *E. coli* could fold properly if the protein carboxy-terminal end was fused to a particular short peptide derived from the carboxyl-terminal end of the bacteriophage T7 gene 10B protein. This effect is specific, since folding of the protein was not rescued by fusion to other peptides of similar length but with a different sequence. We formulated the hypothesis that this C-terminal peptide mediates folding either by compensating for the deficit in chaperone activity that results from conditions of protein over-expression (e.g. that the peptide acts synergistically with residual chaperones to assist protein folding), or alternatively, that the peptide mediates folding by a novel, chaperone-independent pathway.

Scope: The scope of our project is (1) to characterize features of this C-terminal peptide that are necessary for its protein folding activity within bacterial cells, (2) to determine the generality of this folding activity and the rules governing what types of proteins can or cannot be folded by this peptide, and (3) to determine whether this peptide can promote renaturation of misfolded proteins *in vitro*.

Methods: To characterize features of the peptide necessary for its protein folding activity, we first analyzed the peptide sequence using computer programs to predict its secondary structure and its similarity to other known peptide sequences. Then, mutations were designed to disrupt specific features suggested by the computer analyses. To assess the generality

(universality) of this peptide-mediated folding approach, we fused the peptide to a set of yeast proteins selected in the BNL Proteomics Initiative as targets for X-ray crystallographic analysis. In the absence of the peptide all of these proteins misfold and precipitate during synthesis in *E. coli*. Proteins with or without C-terminal peptide extensions were denatured and then subjected to *in vitro* refolding conditions in parallel to assess whether the peptide extension can increase the yield of a soluble, properly folded protein.

TECHNICAL PROGRESS AND RESULTS:

Peptide Features: To determine the mechanism by which the T7 gene 10B-derived peptide promotes folding of proteins, the peptide sequence was varied by site-directed mutagenesis and the effects of these changes on folding of a test protein (CAR D1) were assessed. Folding of CAR D1 was quantitative when the variant peptides had net negative charges greater than -4. Extension of the analysis to other test proteins also showed that protein solubility increased with the magnitude of the net negative charge of the variant peptides. Based on these results, we propose that extension of a protein C-terminus with peptides that carry large net negative charges can promote protein folding by limiting aggregation of the nascent polypeptide chains immediately after protein synthesis *in vivo*. Electrostatic repulsion between the highly charged C-terminal extensions is the most probable basis for this effect. Thus, the peptides serve the same function as molecular chaperones—to block aggregation of nascent polypeptide chains during the protein folding process. Importantly, C-terminal extensions do not become limiting during protein overexpression, since they are

an integral part of the polypeptide chain. Molecular chaperones, on the other hand, are not abundant cellular proteins and thus may become limiting during overexpression of substrate proteins.

Universality of Approach: We observed that folding of different test proteins was promoted to different extents by C-terminal peptide extensions. To explore these differential effects in more detail, we have extended our investigation to other sets of test proteins that have closely related homologues in other species. A literature search revealed a number of proteins which have 3-dimension structures similar to CAR D1 and which fold in *E. coli* with widely different efficiencies. Several of these proteins were acquired, and the effect of C-terminal extensions on folding of the proteins was investigated. Remarkably, one human protein folded with about 50% yield whereas folding of the homologous mouse protein, which is over 95% identical in amino acid sequence, was negligible. Folding of both proteins was increased significantly after extension of the protein C-termini with negatively charged peptides. In future studies, investigation of additional pairs of proteins that also have high degrees of sequence homology but widely different folding efficiencies should provide insights into intrinsic properties of protein folding. In the above-cited case, for example, the high degree of sequence homology between the mouse and human proteins will allow us to construct mouse/human hybrid proteins and thus identify regions of the polypeptide chains that govern folding efficiency.

***In Vitro* Refolding:** Refolding reactions were conducted on a set of test proteins with or without the standard C-terminal peptide extension. In most cases, C-terminal extensions significantly increased protein solubility after renaturation, but upon further

analysis several of the proteins were found to be misfolded and microaggregated. Analysis of the renatured proteins by scanning transmission electron microscopy showed that the microaggregates were distributed in a size range between 1-20 MDa. Although these soluble proteins clearly did not fold into their native conformations and thus are not useful for functional studies, nonetheless their microaggregated state could be useful for biotechnology applications. For example, controlled aggregation and dis-aggregation of bioactive proteins might have medical applications in drug delivery or vaccine development. In future studies we plan to examine whether animals can mount effective immune responses to protein microaggregates in the absence of adjuvants.

SPECIFIC ACCOMPLISHMENTS:

A patent application on the C-terminal peptide extensions has been filed ("Facilitating Protein Folding and Solubility by Use of Peptide Extensions," Filed U.S. Patent Office, January 4, 2002, Serial Number 10/037,243, Inventors: P. Freimuth, J. Howitt, and Y.-B. Zhang). A manuscript describing the use of C-terminal extensions to promote protein folding is in preparation.

Publication:

Zhang, Y.-B.; Howitt, J.; McCorkle, S.; Lawrence, P.; Springer, K.; and Freimuth, P. Negatively charged C-terminal extensions limit aggregation and may promote folding of overexpressed proteins. *Science* (2002, submitted).

LDRD FUNDING:

FY 2000	\$ 41,698
FY 2001	\$109,754
FY 2002	\$110,919

Development of Super-conducting Accelerator Magnets Capable of High dB/dt

Arup K. Ghosh

01-07

PURPOSE:

The goal of this project is to design, fabricate, and test a prototype *super-conducting* dipole magnet, which can be cyclically ramped to 4T in a few seconds with reasonable losses per cycle. When developed, this technology will enable the construction of future rapid-cycling synchrotrons using superconducting magnets such as the one being proposed by the GSI Laboratory in Darmstadt, Germany.

APPROACH:

Using the design of the RHIC dipole magnet as a starting point, we have examined the various components of the magnet that contribute to the losses when operating at a dB/dt of $\sim 2T/s$. These losses occur in several places: inside the superconducting wire, between the wires of the cable, the iron yoke, and the bore tube. The losses are due to both hysteresis and eddy-currents. Initial work was done to quantify these losses for a RHIC type dipole and subsequently research focussed on developing low-loss superconducting wire and cable for a prototype magnet. Collaborators in this study include the following: P. Wanderer, M. Anerella, R. Thomas, and A. Jain (BNL), G. Moritz (GSI), M. Wilson and W. Hassenzahl (GSI- consultants).

TECHNICAL PROGRESS AND RESULTS:

Conductor R&D

During FY 2001 considerable progress was made in the development of a low-loss cable similar in dimension to the RHIC cable, which makes it easier to build a prototype magnet with minor modification to existing tooling. This was achieved by 1) reducing the twist pitch of RHIC type strand from 13mm to 4mm, and 2) by introducing a $25\mu m$ core within the Rutherford cable. With this approach, the losses in the cable have been reduced by more than an order of magnitude as compared to the RHIC cable. 16 km of tightly twisted strands of 6mm and 4mm twist was produced by industry. Measurements showed that the critical current and mechanical properties were minimally affected.

To reduce inter-strand ac losses in the cable, prototype 30-strand cable lengths were fabricated with several different core materials like stainless steel, anodized titanium, kapton and Nomex. The core raises the inter-strand resistance, R_c , between the upper and lower layers of the cable, which thereby reduces the eddy-currents induced in the cable in the rapidly changing magnetic field. Inter-strand resistance measurements showed that cables made with Sn-4%Ag solder-coated strands with a stainless steel core had the best properties of low loss and good electrical stability. However, in fabricating a long length of cable, perforations in the core were observed. In FY 2002, this problem was analyzed and eliminated with the use of two strips of stainless-steel foil. The first prototype magnet coil was wound from cable made with the modified core.

In FY 2002, significant advances were made in the measurement and understanding of R_c in core-cables. A new technique was developed to directly measure this quantity in the cable. Experiments were also done which showed the highly localized nature of the adjacent resistance, R_a . These results

have improved the theoretical understanding of the nature of the losses in these cables.

Magnet Construction

Surplus RHIC tooling was modified for coil fabrication and magnet assembly. The design work for these modifications was completed in FY 2001, with tooling fabrication completed during FY 2002. Using this tooling, the first coils have been made with the low-loss cable.

Alternate cable insulation schemes were also studied. This is an important feature as the heat generated in the cable has to be conducted away rapidly into the helium. After studying two different schemes, a technique using a laser to cut holes in the kapton at the cable edge was adopted. Fixtures to test the turn-to-turn voltage integrity of cable made with insulation open along the edge were built and test procedures established. Cooling slots in the kapton insulation at the cable edge of 300 m of the final core-cable was successfully done at a company in Germany, and tests showed that it met the insulation integrity requirements for the magnet coils.

In FY 2003, the first prototype magnet with core-cable will be assembled and tested. Testing methods at high ramp rates will be established and schemes to measure the field quality at high ramp rates will be explored.

SPECIFIC ACCOMPLISHMENTS:

Publications:

“Towards Fast Pulsed Superconducting Synchrotron Magnets” in the proceedings of the Particle Accelerator Conference, 2001, p211-213, 2001 (pre-FY 2001)

“Design Studies on Superconducting $\cos\theta$ Magnets for a Fast Pulsed Synchrotron,” in the *IEEE transactions on Applied Superconductivity*, 12, No.1, p313-316, (2002) (FY2001 work).

Following are two papers accepted for publication in the journal of to be published in *IEEE transactions on Applied Superconductivity Vol. 13(2003)*:

“Cored Rutherford Cables for the GSI Fast Ramping Synchrotron,” (FY 2002-work)

In preparation is a paper, which is to be submitted to Cryogenics for publication. This will contain details of the Inter-strand Resistance measurements that were developed for cored-cables and an in-depth analysis of the results.

LDRD FUNDING:

FY 2001	\$143,588
FY 2002	\$145,950

Combination of Magnetic Fields and 20 keV Synchrotron X-rays to Produce Microbeams for Cell Culture Experiments

Louis A. Peña

01-11

PURPOSE:

There had been an ongoing effort to utilize the NSLS to generate x-ray microbeams for radiobiology studies. The 50-150 keV range has proved suitable for tissue and small animals, and 8-20 keV for cell cultures. At the latter, however, scattering of secondary emitted electrons threatens the sharpness of the microbeam edges. It is known that ionized particle microbeams can have their path deflected by magnetic fields, but this has not been evaluated for x-rays to date. We hypothesized that a magnetic field could control the direction of secondary electrons. This project, therefore, was set up with the limited aim of performing proof-of-principle experiments to test the effectiveness of combining magnetic fields with 8-20 keV x-rays to minimize the blurring of x-ray microbeams, (i) in simulations, (ii) with physical, and (iii) in live cell cultures utilizing capillary endothelial cell cultures.

APPROACH:

This project was done at the X15B beamline of the National Synchrotron Light Source (NSLS) and the BNL Medical Department. It was a collaboration with Dr. Itzhak Orion, Department of Nuclear Engineering, Ben Gurion University, Israel, and with Dr. Zhong Zhong of the NSLS, BNL.

An electromagnet with magnetic flux (0, 1, or 2T) perpendicular to the direction of the photoelectron was used to effect the electron transport of x-rays shaped into a planar

microbeam (1-100 μm thick) by a set of collimators, filters, and shutters. Two kinds of samples were irradiated for these studies: (i) MOSFET devices for physical microdosimetry measurements, and (ii) capillary endothelial cell cultures grown with specially modified plastic microscope "chamber slides."

The EGS4 Monte Carlo code system was used to simulate physical parameters of microbeams, particularly low energy polarized photon transport. Additionally, this code permitted control of the photoelectron angular distribution in the simulation. User modifications were designed in order to parameterize the microbeam array size and spacing and to compare the absorbed dose profile with experimental MOSFET measurements.

The primary biological endpoint was identification of radiation-induced apoptosis *in situ* by morphological criteria. Secondary endpoints include specific histochemical stains to visualize the cytoskeleton of neighboring non-irradiated cells, and measurements of observable cellular changes versus microbeam with and/or deposited dose (0 - 100 Gy).

TECHNICAL PROGRESS AND RESULTS:

The utility of combining magnetic fields with 8-20 keV x-ray microbeams was confirmed. Microdosimetry MOSFET measurements compared very well with Monte Carlo simulations, and demonstrated that application of 2T magnetic fields had the effect of sharpening the microbeam dose distribution. Moreover, beam sharpness was reflected in width of the zone of apoptotic cells in irradiated cell cultures.

SPECIFIC ACCOMPLISHMENTS:

Submitted grant proposal to NIH ("UV & X-ray Microbeams for Cell Stress Signaling Studies)

LDRD FUNDING:

FY 2001	\$11,169
FY 2002	\$11,697

Gene Expression Profiling of Methamphetamine-Induced Toxicity in Neurons in Culture Using DNA Microarrays

Marcelo E. Vazquez

01-12

PURPOSE:

This project has two purposes: **First**, a new emphasis on the neuronal neurotoxicity is proposed which utilizes micro-array DNA chip technology to identify a specific set of genes in neuronal culture systems that respond to methamphetamine exposure. This study will enhance our current research projects in the field allowing us to understand the molecular mechanisms of drug addiction and toxicity. **Second**, in addition to providing state-of-the-art information on the application of DNA microarrays, high-resolution x-ray microscopy and image analysis technology for neurotoxicology studies. Several collaborations will be established between BNL, SUNY Stony Brook, and LBNL using their unique scientific resources.

Goals: Propose to study the patterns of gene expression and its correlated cellular responses induced by methamphetamine in cell culture model systems. Identification of the key regulatory genes that activate or repress or in some way regulate cascades or major circuits is our focus of interest. Any major cellular process is likely to involve major gene expression changes. Thus, the goal is to identify: 1) **which set of genes is a key regulator of the cellular response**, and 2) **whether modulation of the gene is possible**, and 3) **if it will result in an amelioration of the neurotoxic process**.

APPROACH:

Background. Amphetamines and analogs such as methamphetamine (METH) are misused as psychostimulants and have become popular recreational drugs of abuse over the last decade. METH's addictive potential is thought to occur through activation of the mesolimbic

dopaminergic system. In addition to its effects on dopaminergic systems, METH can also affect the biochemistry of glutamatergic and serotonergic pathways. There is also abundant evidence demonstrating the neurotoxic effects of METH. The cellular and molecular mechanisms involved in METH-induced neurotoxicity are not completely understood. The converging evidence indicates that METH redistributes DA from the reducing environment within synaptic vesicles to extravesicular oxidizing environments, thus generating oxygen radicals and reactive metabolites within DA neurons that may trigger selective terminal loss and cell death. The observation that neuronal cell death and neuroplasticity involves an activation of gene expression and new protein synthesis, coupled with recent reports indicating that amphetamines are capable of inducing immediately early genes such as *c-fos*, *Zif268* and *p53*, offers a possible clue as to their neurotoxic mechanism of action. Thus, it is important to understand the patterns of oxidative stress-induced gene expression, which can provide valuable insight with respect to how free radicals-oxidative stress influences neuronal functional integrity. In addition, such information may provide new molecular targets for the development of countermeasures to ameliorate the toxic response.

Methods:

Neuronal cells (NT-2 and hNT-dopaminergic type) were cultured on multi-well plates; slide chambers-flasks or silicon windows, all pre-coated with attachment factors. Cultures were treated with graded doses of METH (0 to 500 mM/ml) and cells were harvested and/or processed at subsequent intervals for various biochemical, functional and structural studies. Samples were processed to measure cell viability (Live and Death kit) using fluorescence microscopy, cell phenotyping (immunofluorescence microscopy and western blot), structural integrity using soft x-ray microscopy and live images were recorded for neurite outgrowth quantification using a image analysis algorithm developed for this project.

For gene expression studies, mRNA was isolated with the Micro-FastTrack 2.0 mRNA isolation

kit (Invitrogen Corp.), following lysis of the cells directly on the dishes. Subsequent steps were performed according to the kit manufacturer's protocols. Total isolated RNA from cultures was frozen down for shipment to SUNYSB. One microgram of mRNA will be used for making fluorescent-labeled cDNA probes for hybridizing to the 5K or 40K microarrays on glass slides. Hybridization, washes, and fluorescent scans will be performed at SUNYSB.

TECHNICAL PROGRESS AND RESULTS:

The primary focus of this project during 2001-2002 has been aimed to:

- Define the cellular toxicity of METH using hNT human post-mitotic neurons.
- Profile genes differentially expressed by exposure to METH in vitro.

METH-induced toxicity:

The goal of this experiment is to establish and characterize the cellular effects of METH exposures on dopaminergic-like cells in culture. These experiments provided the necessary "ranging" data to determine in vitro cellular and molecular effects of METH.

Specific aims:

- Determine cell toxicity and phenotypic changes for hNT cells exposed to METH as a function of dose, and time post-treatment;

The Live-Dead assay (Molecular Probes, Inc.) was used to determine cell toxicity of attached neural cells. Utilizing ethidium hemodimer and calcein-AM, we were able to achieve good discrimination between dead (red) and viable cells (green) after 15-min incubation at 37°C.

Results in Fig. 1 show that METH induced a dose- and time-dependant toxic response on hNT-dopaminergic cells. Doses as low as 0.5 to 1 mM/ml and as early as 48 hours produced apoptotic cell death as well as morphological effects such as membrane blebbing, neurite degeneration and vacuolization (Fig. 2). Previous experiments showed comparable

results using neural precursor cells (NT-2) exposed to similar doses of METH.

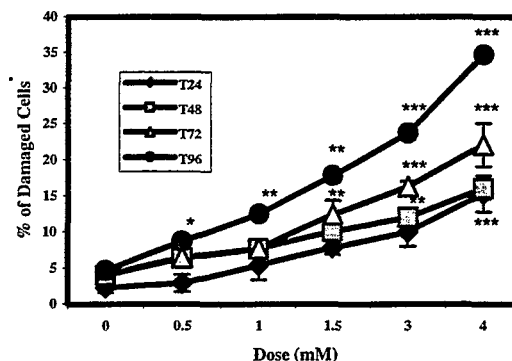


Figure 1: Dose-response of METH-mediated cell death in hNT-dopaminergic cells at different times in culture. Cell cultures were exposed to acute doses of 0 to 4 mM/ml of METH. Cell damage was detected using the Live Cell/Dead kit and visualized by fluorescence microscopy analysis. Values represent means \pm SEM.

• Quantification of neurite outgrowth using image analysis algorithms:

In order to quantify the effect of METH on neuronal terminals or neurites (neuronal processes), images from experimental series were captured and analyzed. The aims of this study were to observe the neurite outgrowth from neurons treated with METH in culture, and quantify the extent of growth as a marker of functional integrity. We were able to adapt algorithms for dissociated cells such as hNT cells. The algorithm uses digital images that are processed to enhance contrast and resolution using several masking and filter techniques. In a second step, the algorithm recognizes cell bodies and neural processes (neurites) in order to differentially capture and quantitate neurite outgrowth. The final result is the measure of cell body or neurite total mass expressed as pixel count (Figure 3). This method allows us to monitor an important marker of functional integrity, neurite outgrowth, as a function of dose and time after treatment. The results correlate very well with the toxicity assay (Figure 1) and phenotypic changes observed in digital images (Figure 2). In conclusion, doses as low as 1 mM of METH were able to induce apoptotic cell death and decrease of functional

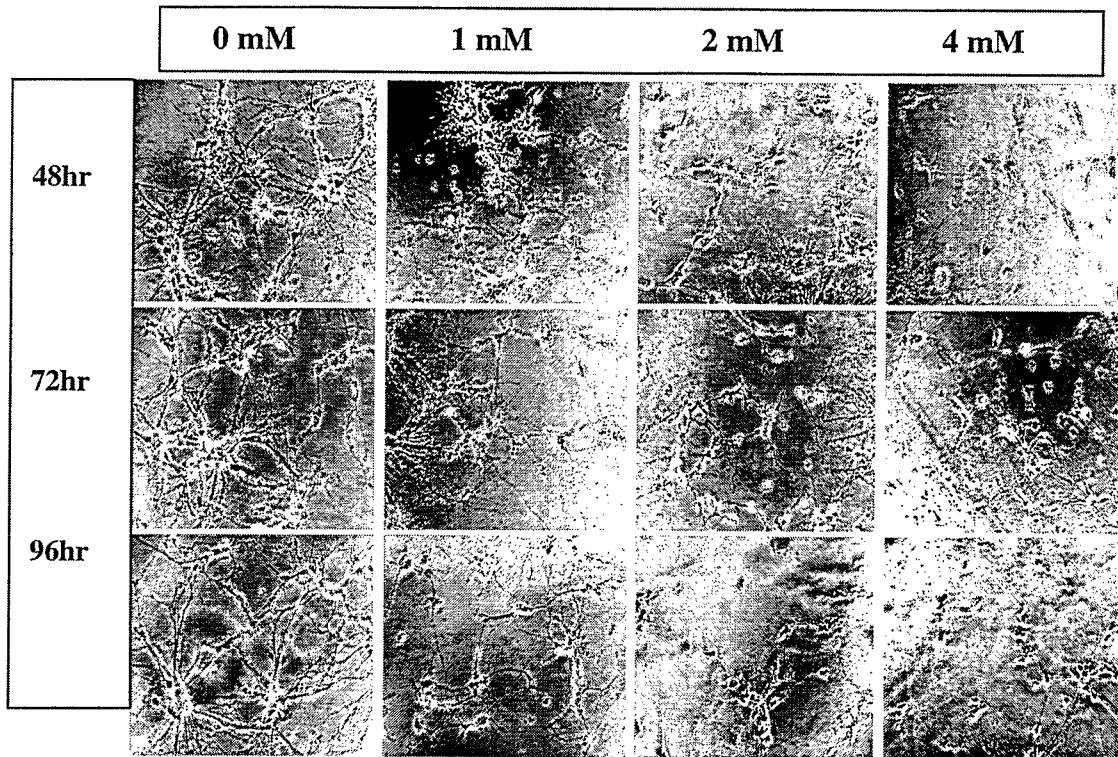


Figure 2: Dose-response of METH-mediated cell death in hNT-dopaminergic cells at different times in culture. Phase-contrast images of hNT cells plated onto polyp-L-lysine coated slides. Observe the dose- and time-dependent decrease of neurite network and cell number.

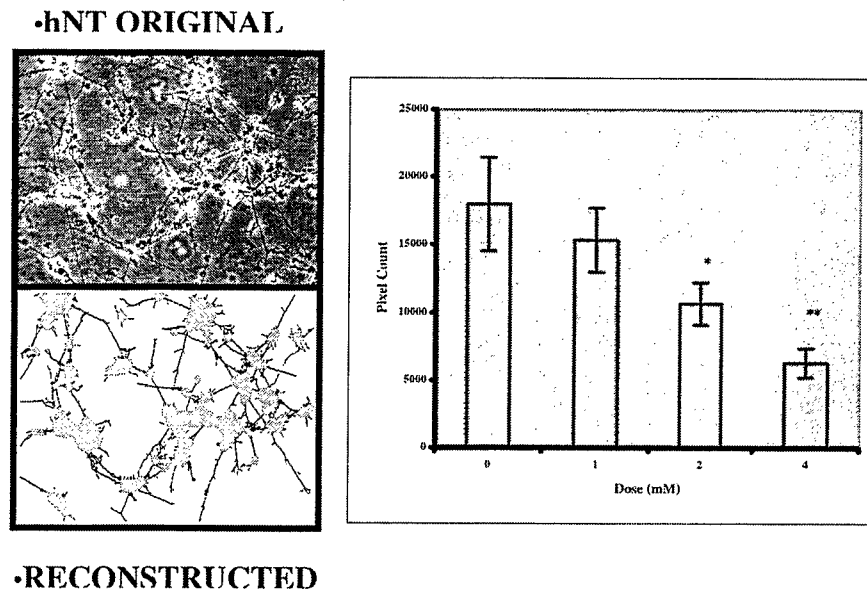


Figure 3: Neurite outgrowth of hNT cells exposed to graded doses of METH at 96 hours in vitro. Quantitation of neurite mass was carried out using the automatic image analysis software developed for this project. Left panel: images of hNT cells before (top panel) and after reconstruction and image analysis (bottom panel, black lines represent reconstructed neurites). Right Panel: dose-response curves for pixel count (neurite mass) vs. dose of METH.

integrity (expressed as a decrease of neurite outgrowth and/or synapgenesis in vitro) in cultures after 96 hours in vitro.

These results are consistent with literature on the in vitro effects of METH on primary striatal dopaminergic cultures and other human cell systems validating the use of NT2-hNT cell systems for METH-induced neurotoxicity.

b) Select a specific dose and time point for microarray sampling.

- **Microarray sample processing**

Samples of treated NT2 and hNT cells (0, and 1 mM) at 48 hrs post-treatment were obtained and processed for DNA microarrays, WB and RT-PCR. mRNA samples were isolated with the Micro-FastTrack 2.0 mRNA isolation kit (Invitrogen Corp.), following lysis of the cells directly on the flask chambers for DNA microarray processing. Total isolated RNA. from cultures was frozen down for storage at -80°C. Unfortunately, the quality of the initial set of samples for microarray analysis was poor preventing the completion of the studies. Therefore, we are finishing a second set of hNT and NT-2 cells to be treated with METH and processed for mRNA extraction.

- **Soft x-ray microscopy experiment at LBNL-ALS.**

Our first experiment was successfully completed at LBNL validating our protocols for hNT cells cultured on poly-L-lysine coated silicon windows. Several images were taken from untreated cultures chemically fixed, demonstrating that high-resolution images can be obtained for structural analysis.

Collaborators:

Core Project:

- Marcelo E. Vazquez, PI, Peter Guida, Luis Estevez and Jeanine Thomas

DNA Microarrays

- Anilkumar Dhundale, Center for Biotechnology at SUNYSB.

Soft X-ray Imaging

- Carolyn Larabell, Advanced Light Source at Lawrence Berkeley National Laboratory.

Image Analysis

- Christina Wilson, Applied Mathematics and Statistics at SUNY Stony Brook, and BNL CDIC and Brent Lindquist, Applied Mathematics and Statistics at SUNY Stony Brook.

SPECIFIC ACOMPLISHMENTS:

PAPER:

Weaver C., Pinezich J., Lindquist B., Vazquez M., An Algorithm for Reconstruction of Neurite Outgrowth, (submitted to *Journal of Neuroscience Methods*, Sept. 2002)

POSTER:

An Algorithm for Neurite Outgrowth Reconstruction <http://www.ams.sunysb.edu/~cweaver/poster.html>, presentation at SIAM Life Sciences Conference, Boston. March 2002.

LDRD FUNDING:

FY 2001	\$105,192
FY 2002	\$ 99,642

Functional Spectral Signature (FSS) Method for Signal to Noise-Enhancement of Brain Patterns in PET Images

Christoph Felder
Y. Ma

01-13

PURPOSE:

Our goal is to significantly improve the current brain image analysis tools and technologies from the following aspects: (1) to develop a software to automate the voxel-level brain image analysis; (2) to develop a software to automatically extract brain regions of interest; (3) to develop a novel measure for brain functional homogeneity/heterogeneity analysis and to build the corresponding software.

By accomplishing the above three goals, we would (1) greatly reduce time and manpower lost to the tedious and intensive manual operation of regions of interest (ROI) extraction and voxel-wise image analysis; (2) significantly reduce the errors either systematic or non-systematic in brain image processing and analysis; (3) enable the medical researchers to examine not only the mean level of brain functional changes but also changes in brain functional patterns due to disease or drug addiction.

The product of this project will be a suite of versatile bioinformatics tools, which will benefit not only medical researchers inside BNL, but also the entire mental health research society and especially patients with mental disease. It would bring recognition to the Lab in the field of bioinformatics and gain future funding in this increasingly important field from NIH, NSF, and DOE.

APPROACH:

Automated voxel-wise PET analysis. A new trend in brain functional image analysis is to perform the statistical test at each voxel. The advantage of this approach is that one could examine the entire brain instead of the selected brain regions of interest which would usually cover only a moderate portion of the brain. A public domain software - statistical parametric mapping (SPM)

<http://www.fil.ion.ucl.ac.uk/spm/>)

was developed for this purpose, however, the software is not automated and thus for each analysis, researchers must click the buttons and enter the strings manually which is tedious, labor-intensive and extremely error-prone. Since the software is open source and entirely written in Matlab, our plan was to download the entire code and subsequently establish a graphical user interface, also written in Matlab, with built-in analysis routine such that for each subsequent analysis, one could key in a few major parameters and submit the job in batch mode. We have one graduate student volunteer, Manlong Rao (SUNY Stony Brook) working on this project with us. In addition, we receive advice on the medical aspects from Drs. Nora Volkow, Gene-Jack Wang, and Joanna Fowler at BNL life sciences.

Automated anatomical ROI extraction.

Traditionally, the brain regions of interest are mostly manually traced by highly trained domain experts for each study. Not only is this a very labor-intensive task, the outcome is also rather observer-dependent. Therefore, we proposed to fully automate this task. The human brains vary in size, aspect ratio, and even in the spatial relationships of their features. In addition, brain scans of different patients are rarely taken at an identical

orientation. To eliminate these variations, we first map all brains into a common, normalized brain space – the Talairach brain using SPM. Next we obtain the precise location of common anatomical regions in the Talairach brain from the NIH supported public domain Talairach Daemon (TD) database,
<http://ric.uthscsa.edu/projects/talairachdaemon.html>.

The TD database includes major anatomical structures from the entire cortex to the Brodman areas. However, TD functions as a uni-directional server only: the user can obtain the anatomical information for a given Talairach coordinate but not vice versa. Our task was to find the inverse mapping, i.e. to extract the Talairach coordinates of all voxels belonging to each anatomical region and therefore achieve the automatic extraction of each major anatomical region.

Brain functional heterogeneity study via coefficient of variation (CV). Traditionally, researchers only examine the average activity level of each brain region of interest (ROI mean). However, some disease or drug would render similar changes in brain regional mean but rather different activation patterns. For this we proposed to develop the analysis of brain functional homogeneity and heterogeneity using the CV as the measure of functional variability. The analysis is to be done at both ROI and voxel level and all corresponding algorithms will be compiled into software with graphical user interface for dissemination of our results.

TECHNICAL PROGRESS AND RESULTS:

Accomplished Task 1 – software for automated voxel level analysis. We have successfully developed the batch mode

voxel analysis software for routine PET image analysis. Figure 1 is a screen shot of the user interface. To date we have performed the analysis of 2 PET studies using this software.

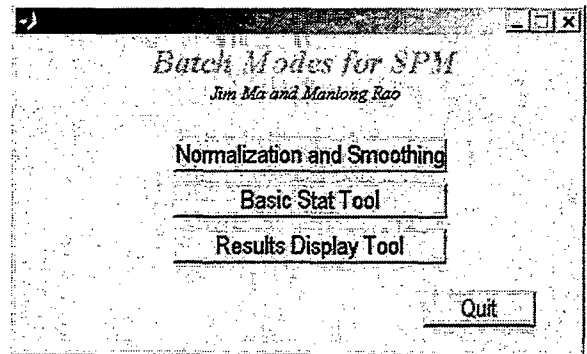


Figure 1.

Accomplished Task 2 – tool for automated anatomical ROI extraction.

Most recently we have completed the automatic extraction of 5 levels of anatomical ROIs from the TD database. These ROIs include all major brain anatomical regions of various sizes from the entire cortex to the Brodman areas. We have also developed a software such that researcher can locate and visualize the position and shape of each anatomical region from the name of each region and vice versa. Figure 2 shows part of the extracted cortex displayed on our software.

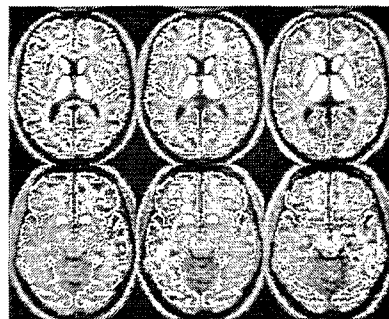


Figure 2.

Accomplished Task 3 – analysis tool for functional heterogeneity study. In FY 2001, we accomplished task 3(a): the analysis of brain functional heterogeneity at

the ROI level. In FY 2002, we have accomplished task 3(b): the analysis of the functional heterogeneity at the voxel-level and the software for doing this type of analysis. Figure 3 is a screen shot of the original PET image and its corresponding functional heterogeneity image from our newly developed software "BrainCV."

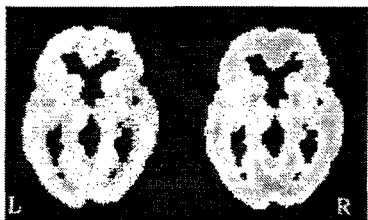


Figure 3.

SPECIFIC ACCOMPLISHMENTS:

Refereed journal publication

Non-MAO A binding of clorgyline in white matter in human brain. Fowler, J.S.; Logan, J.; Ding, Y.S.; Franceschi, D.; Wang, G.-J.; Volkow, N.D.; Pappas, N.; Schlyer, D.; Gatley, S.J.; Alexoff, D.; Felder, C.; Biegon, A.; Zhu, W. *J Neurochem.*, 79(5), 1039-1046 (2001).

Alcohol Increases Brain Functional Homogeneity. Volkow, N.D.; Ma, Y.; Zhu, W.; Li, J.; Mueller, K.; Rao, M.; Wang, G.-J.; Wong, C.; Fowler, J.S. Submitted to *Psychiatry Research*.

Enhanced resting activity of the oral somatosensory cortex in obese subjects. Wang, G.-J.; Volkow, N.D.; Felder, C.; Fowler, J.S.; Levy, A.V.; Pappas, N.R.; Wong, C.T.; Zhu, W.; Netusil, N. *Neuroreport.*, 13(9), 1151-1155 (2002).

Changes in brain functional homogeneity in subjects with Alzheimer's disease. Volkow, N.D.; Zhu, W.; Felder, C.; Mueller, K.; Welsh, T.F.; Wang, G.-J.; de Leon, M.J. *Psychiatry Res.*, 114(1), 39-50 (2002).

Grant application

"Imaging the Mind" NIH P20 proposal to be submitted on November 27, 2002. PI Dr. Arie Kaufman, co-PI Dr. Nora Volkow.

LDRD FUNDING:

FY 2001	\$85,941
FY 2002	\$45,085
FY 2003 (budgeted)	\$53,000

Exploration and Development of Ultrafast Single Shot Detection Methods For Use with Pulse Radiolysis Experiments at LEAF

Andrew R. Cook
J. Miller

01-18

PURPOSE:

This project was established to explore new detection methods that can be used to study chemical problems at the Laser Electron Accelerator Facility (LEAF) in the Chemistry Department's Center for Radiation Chemistry (CRCR). While pulse radiolysis is a very powerful tool for the study of many chemical systems, there are two main problems that we hope to solve. These include the large amount of time that can be required to collect transient data in repetitive variably delayed electron pulse - (laser pump) - laser probe experiments where as many as 10^4 shots are needed per probe wavelength, and the fact that radiation chemistry techniques often cause the degradation of samples and buildup of ionization products. As photocathode accelerators have opened new fields of chemical studies, the development of single shot detection methods for fast timescales have the potential to not only accelerate current studies, but enable whole new areas of study where synthetic samples of often the greatest interest are available only in very small quantities. Success would lead to dramatic contributions to DOE programs in diverse areas such as photochemical energy conversion and molecular electronics/nanotechnology, would help propel LEAF to the status as the world's premier facility for accelerator based chemistry, and consequently help us to maintain and expand

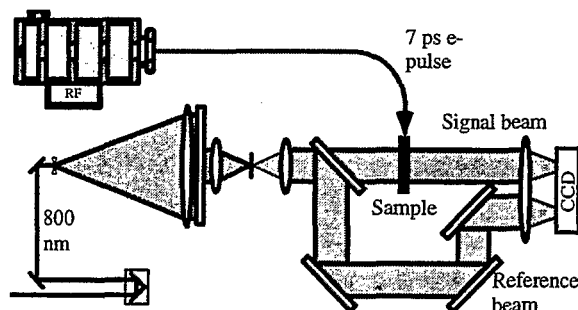
existing DOE/BES core funding as well as compete for new external funding.

APPROACH:

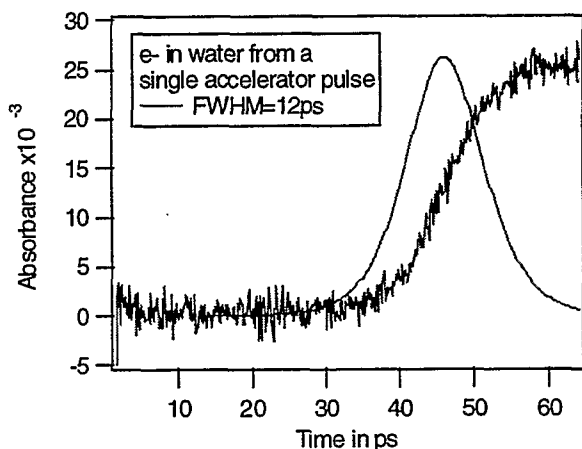
The basis for ultrafast single shot detection is spatial encoding of temporal information. Related methods are currently used for the measurement of ultrafast laser pulse widths and were recently applied for the first time at MIT to ultrafast time resolved spectroscopy for the study of irreversible reactions in solids. Such methods have never been applied to accelerator based chemistry problems. Temporal information can be encoded in a variety of ways across a laser beam, and be read out by collecting a snapshot of the transverse profile of the beam on a charge coupled device (CCD) camera. The goals for this second year's work were: 1) improve existing experiment and make first pulse radiolysis tests to demonstrate the feasibility of the concept at LEAF; 2) begin exploring more powerful alternative techniques.

TECHNICAL PROGRESS AND RESULTS:

Building on last year's efforts, an improved ultrafast single shot (UFSS) experimental system consisting of shaped signal and reference beams crossing the electron beam in the sample at 90° , and recorded by a CCD camera was constructed as seen schematically below:



Time information is encoded on the signal beam due to differing relative arrival time of the electron pulse and laser pulse across the sample width. The experiment is optically complicated, and required considerable care to eliminate interference effects, maintain time registration between the probe and reference, and required careful imaging of the shaped beams from the sample to the detector.



The first data collected using this new apparatus, seen in the figure below, recorded the absorption rise of the aqueous solvated electron at 800 nm following pulse radiolysis. This is a very exciting result for two main reasons. First, the data shown was collected in 1-2 minutes using a “single” electron pulse. Comparable data collected with the standard pulse-probe experiment requires many thousands of shots and ~1 hour to collect. While the point spacing shown is not needed for this exact experiment, it becomes critical in others utilizing additional optical excitation to gain sub-picosecond time resolution. The second exciting feature of this data is the apparent noise level, which is only perhaps a factor of 2 worse than data collected in pulse-probe experiments. This is due primarily to elimination of noise sources from laser shot to shot energy and mode fluctuations, careful correction for spatial mode variation

by using a reference beam, and signal averaging of CCD pixels that all carry the same time information. The rise time of 12 ps is driven by both the 7 ps electron pulse width, and the 2 mm thickness of the sample. Better time resolution will only be obtained in experiments where 100 fs optical excitation follows the electron pulse and samples become very thin making signals very small. The total time window of the experiment is determined by the length of the sample, in this case 2 cm. Larger time windows will be difficult due to limited penetration power of the electron beam and its scattering as it travels through the sample. Despite these limitations, however, this apparatus clearly demonstrates the feasibility of UFSS techniques for pulse radiolysis experiments.

In order to overcome these limitations, work began to explore two alternate methods of encoding temporal information on the probe beam. The first is designed to extend the available temporal window out to many nanoseconds, and possibly longer, while maintaining 5-7 ps time resolution. It uses bundles of differing length optical fibers inserted in the probe beam. A custom-made test bundle with 100 fibers where each is different in length by 5 ps was purchased, and the first tests of imaging the end of the bundle successfully completed. Significant additional technical work is needed to image the end of the bundle successively onto both the sample and CCD detector, and to develop image analysis software for data collection. While the ultimate time resolution possible with such fiber bundles is unclear, if proven this method has the exciting possibility to generally replace the use of optical delay lines for collecting transient data not only at LEAF, but also in many other labs outside BNL.

The second alternative UFSS method under consideration provides ~100 fs time

resolution in experiments where 100 fs optical excitation of radical species formed by the electron pulse is used. In this case, spatial delay variations in the probe beam are introduced by inserting custom-made transmissive stair-stepped optical echelons. It is possible to make such components with steps as small as ~10 femtoseconds. Two such 20 step echelons were purchased to be used with steps at 90° to each other, giving a total of 400 square regions with a net 40 fs step size and 16 ps total time window. Optical imaging requirements are somewhat more complicated than those of fiber bundles, but it is expected that both fibers and echelons will be able to share similar optical setups and data collection software.

SPECIFIC ACCOMPLISHMENTS:

Results of this work were presented as part of an on-site programmatic DOE review & proposal, October 28-29, 2002. Increases in base funding were requested based on new scientific projects possible due to UFSS developments described in this report.

LDRD FUNDING:

FY 2001	\$62,401
FY 2002	\$64,870

Metal Nanoclusters and Electron Transfer in One, Two, and Three Dimensions

Carol Creutz

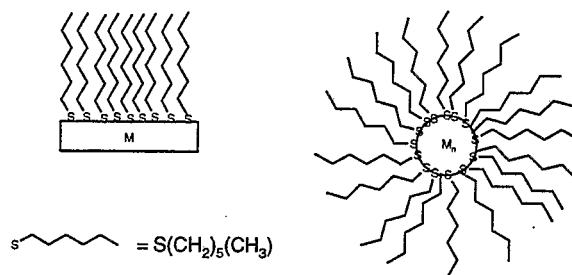
01-19

PURPOSE:

The purpose of this work is to initiate a new program in the reactivity and properties of nanoscale metal clusters, which are of great interest for their novel properties and possible applications. The nanoclusters will be used to characterize, model and control electron-transfer reactions involving molecular and nanoparticle partners in order to advance the design and construction of "molecularly wired," nanoscale devices. An initial goal is to explore and understand the interaction of excited states of transition-metal complexes with metal nanoclusters as a function of cluster size. This project is a component of the BNL nanoscience initiative and the proposed *Brookhaven Center for Functional Nanomaterials*.

APPROACH:

Monolayer Protected Cluster Molecules ("MPCs," e.g. $\text{Au}_{145}(\text{S}(\text{CH}_2)_5(\text{CH}_3)_{50})$) are isolable, alkanethiolate-protected gold clusters of 5-nm core diameter.¹ Since 1994, with the publication of a new synthetic method inspired by recent work on self-assembled monolayers on surfaces,² research exploiting the novel properties of these nanometer-scale metal clusters/crystals enveloped by a structured layer of organic molecules has exploded. Phosphine-capped gold clusters in the 0.5 to 3.0 nm range,^{3,4} e.g. $\text{Au}_{101}[\text{P}(\text{C}_6\text{H}_5)_3]_{21}\text{Cl}_3$ exhibit similar properties and provide useful starting materials for construction of clusters of specific size. Larger clusters from citrate-based colloidal gold preparations are also of interest.⁵



Left: Self-assembled monolayer (SAM) of 6-carbon thiolate, $\text{S}(\text{CH}_2)_5(\text{CH}_3)$, on (bulk) metal M surface

Right: Monolayer protected cluster (MPC) of the same thiolate on M_n , a nanocluster of metal M

Electron donors and acceptors will be covalently or electrostatically attached to the same or to different clusters and the effect of the size, charge state, and nature of the clusters and tethers on thermal and photo-induced charge-transfer processes will be examined. Dr. Janet Petroski who started experimental work in March 2001 is responsible for the results reported here.

TECHNICAL PROGRESS AND RESULTS:

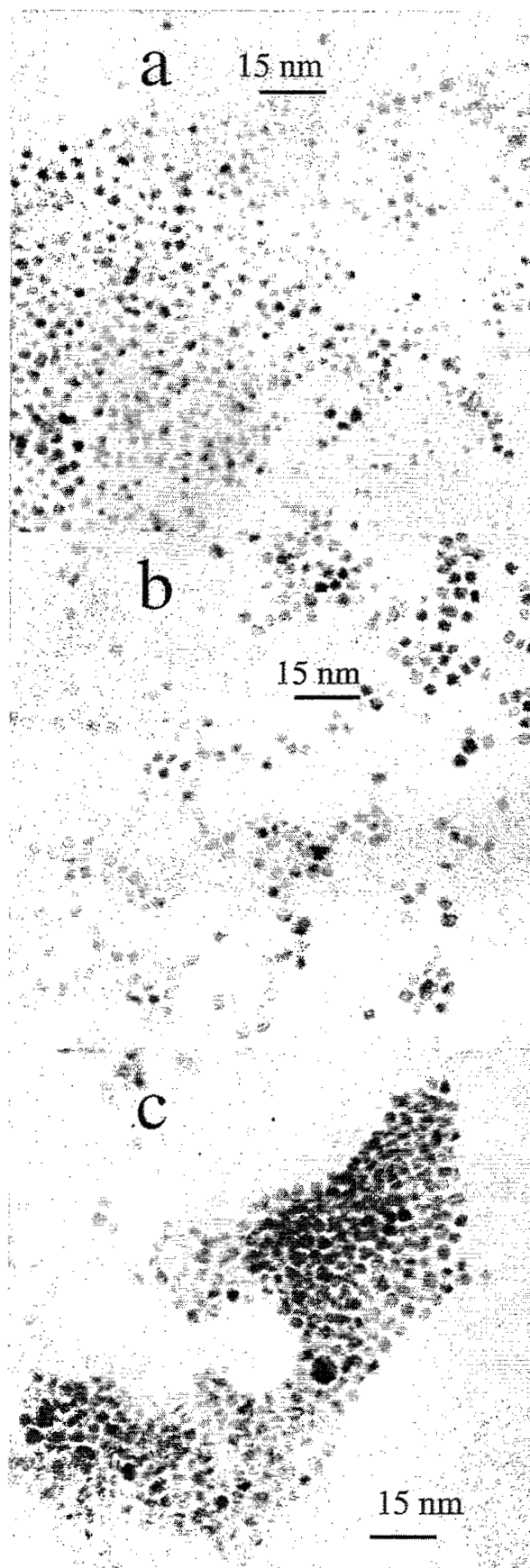
Both "colloidal" and molecule-like gold clusters were synthesized and characterized by nuclear magnetic resonance (NMR) (^1H and ^{31}P) to verify incorporation of the desired organic cap and by electronic absorption spectroscopy. Verification of particle sizes and size distributions was essentially impossible until 11/01 because of lack of access to transmission electron microscopy (TEM). The JEOL 100CXII located in Bldg. 830 has been rebuilt and is providing highly needed TEM characterizations; a charge coupled device (CCD) is to be installed in 12/02 to eliminate the need for conventional photographic methods.

In FY02, evidence for interactions of gold clusters with the excited states of transition

metal complexes such as $\text{Ru}(\text{bpy})_2(\text{NCS})_2$ was sought. Methods for narrowing the size distribution of the cluster solution were tried with limited success. Dialysis, ultrafiltration, syringe filters have been tried, with dialysis and ultrafiltration tending to either precipitate the particles or make it difficult to redissolve them. Size-Exclusion Chromatography remains under consideration.

To characterize electron-transfer reactions of the clusters, a water-soluble cluster capped with triethylene oxide thiol (EO3) was synthesized and pulse radiolysis experiments were begun in collaboration with D. Cabelli. In these experiments, an electron is captured by methyl viologen MV^{2+} and the MV^+ produced transfers the electron to the gold cluster at a nearly diffusion-controlled rate. TEM images taken for samples before and after addition of methyl viologen MV^{2+} and the reaction are presented in Figure 1 and reveal remarkable, but problematic, features. Changes in the clusters are evident in the “after” images, not only in size but the shape of the clusters, as well. It may be that small particles fuse under reductive conditions. The changes in sizes under these conditions could limit the utility of the particles for solution applications. This issue is being pursued with DOE nanoscience funding.

Figure 1. TEM images of clusters used in pulse radiolysis experiments showing the AuEO3 clusters a) before and b) after the addition of MV^{2+} and pulse radiolysis and c) after 2 min in the cobalt-60 source. The average size of the particles in a) is ~ 3 nm with a wide size distribution (between 1 and 7 nm) and predominately spherically shaped particles. The average size in b) increases to 4 nm with a much narrower size distribution and a large concentration of cubic and rod-shaped nanoparticles (the rods average 6 nm in size). The sample in c) also shows a narrow size distribution with an average size of 4 nm. Though the regular prismatic shapes can be detected (cubes, rods), it is not to the same extent as that of b).



We gratefully acknowledge the assistance and cooperation of B. Panessa-Warren and C. Czjakowski in making the TEM measurements possible and thank M. Chou for her help with synthesis and characterization.

References:

- (1) Templeton, A. C.; Wuelfing, W. P.; Murray, R. W. *Acc. Chem. Res.* **2000**, *33*, 27-36.
- (2) Brust, M.; Walker, M.; Bethell, D.; Schiffrin, D. J.; Whyman, R. *J. Chem. Soc., Chem. Commun.* **1994**, 801-802.
- (3) Hainfeld, J. F.; Powell, R. D. *J. Histochem Cytochem.* **2000**, *48*, 471-480.
- (4) Weare, W. W.; Reed, S. M.; Warner, M. G.; Hutchison, J. E. *J. Am. Chem. Soc.* **2000**, *122*, 12890-12891.

- (5) Enustun, B. V.; Turkevich, J. *J. Am. Chem. Soc.* **1963**, *85*, 3317-3328.

SPECIFIC ACCOMPLISHMENTS:

BES-Chemical Sciences Nanoscience and Technology Award FY01 – 04 \$650K/year.

This LDRD award made possible the start up of a new program in metal nanoclusters. It also made possible the development of TEM infrastructure so critical for nanoscience at BNL. The CCD to be added to the TEM was purchased with a combination of pollution prevention funds and BES equipment funds.

LDRD FUNDING:

FY 2001	\$ 81,202
FY 2002	\$144,617

Molecular Wires for Energy Conversion and Nano-Electronics

John Miller

01-20

PURPOSE:

To examine molecules that may act as molecular wires to learn about their 1) energy levels, 2) changes in optical spectra upon addition of an electron or a hole, 3) transport properties for movement of electrons and holes, and 4) effect of stray charges (e.g. Na⁺) on the transport and spectra.

A beginning goal is to determine applicability of the new techniques proposed to obtain answers to the questions above.

APPROACH:

Interest in molecular electronics has led to an explosion of interest in "molecular wires," molecules of nanoscale lengths that are capable of transporting electronic charge. The premises of our approach are that such wires would have applications to energy capture and storage as well as to electronics, and that special insight could be gained from the use of BNL's new Laser-Electron Accelerator Facility (LEAF).

Much information about transport properties can be gained from spectra. While there are many chemical methods to obtain such spectra, LEAF can obtain them in situations where they cannot be produced chemically. These situations include production in media incompatible with strong redox reagents necessary to add charges to the wires, or in weakly or non-polar media or in such media in the presence of inert counter-ions that may trap the electronic charge.

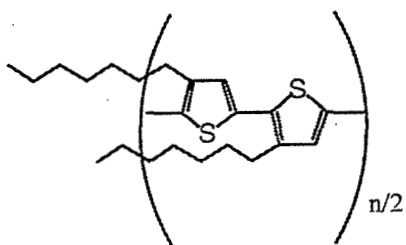
The second advantage to LEAF experiments is the potential for high-time resolution. Investigators in other laboratories have attached molecules to electrodes and measured current-voltage characteristics. Such experiments are rich in information but have very low time resolution. Further attachment of the wires to the electrodes is difficult to accomplish, and it is more difficult to know what has been attached - how many wires, and in what configuration. At LEAF it may be possible to observe the movement of charge in molecular wires in a direct, time-resolved way.

The LEAF experiments have their own difficulties to be overcome. One of these is getting sufficient material into solution to enable it to capture charges quickly. It is necessary to obtain appropriate materials and find appropriate solvents. We recently received an interesting material from Tianbo Liu (BNL Physics) that may be helpful in this regard.

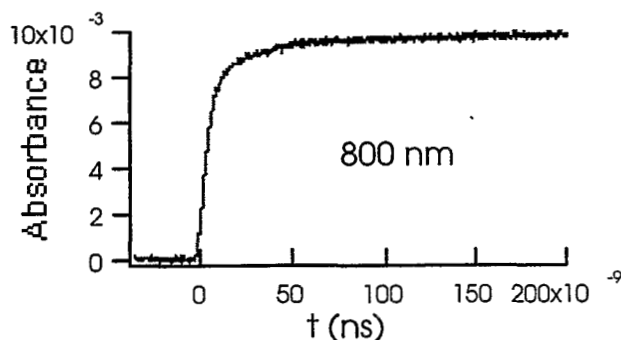
TECHNICAL PROGRESS AND RESULTS:

FY2001

- LDRD funding was received for a postdoc and after a search, an excellent person, Dr. Norihiko Takeda, joined us in April. Dr. Takeda has become familiar with use of the LEAF accelerator and begun experiments. Because one of the principal hurdles is getting material into solution, he has performed tests on solubilities of materials in several solvents. Satisfactory results were obtained in only a few cases.
- Transient absorption was observed after electron attachment to alkylated (for solubility) polythiophene:



A transient spectrum was observed showing a broad band in the near infrared and a much stronger one at 800 nm, both of which had a long lifetime after creation by a pulse from LEAF. A kinetic trace at 800 nm is shown below, which represents an electron within the "wire."



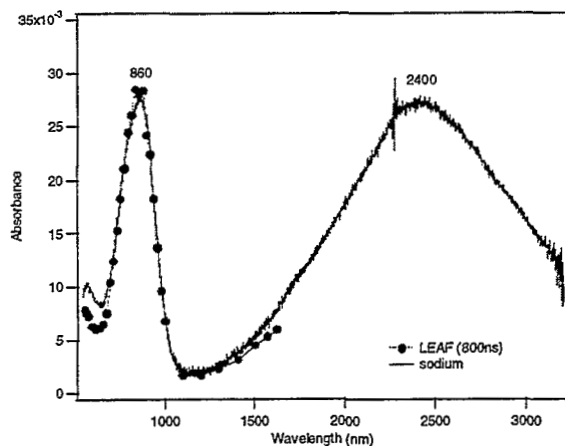
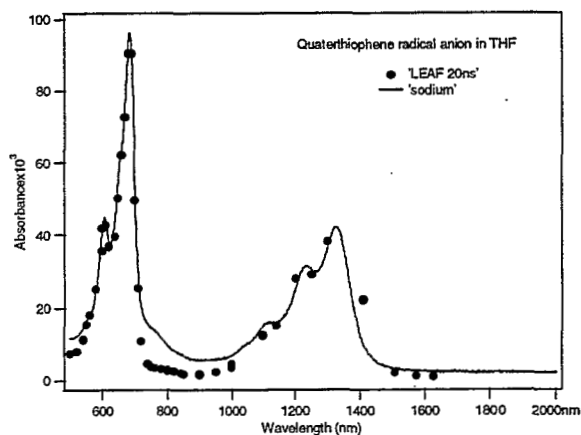
- In the coming year spectral data from this and other molecules will be compared to seek information about relationships between the spectra and transport properties. A strategy has been developed to "dope" the wires with charge traps at low densities (e.g. 1 dopant/100 repeat units). Experiments will seek conditions in which the doping strategy can successfully determine transport within the wire.

FY 2002

- Spectroscopy was obtained for addition of a single negative charge to a small molecule tetrathiophene (4T) and a long polydecylthiophene (P3DT) having ~ 150 units. In both cases chemical reduction by Na metal was compared with reduction at LEAF. In the chemical

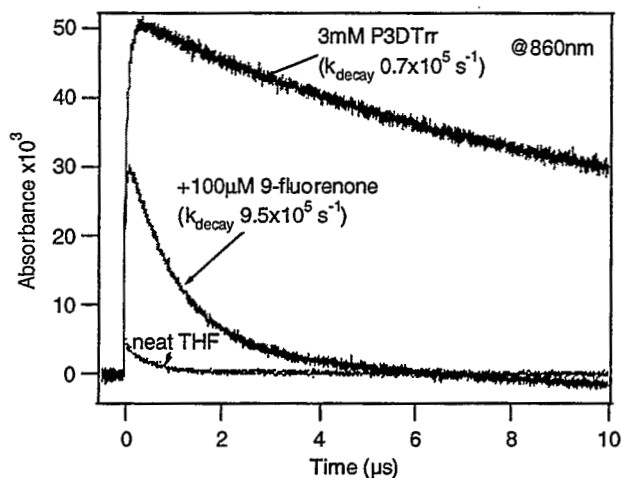
reductions negative ions are likely to be paired with Na^+ ions; at LEAF negative ions are produced without ion pairing. The similarity of the spectra suggests that the Na^+ counter ions are not able to localize the electrons in either the short or long molecules.

Optical Absorption Spectra of Negative Ions of tetrathiophene and poly octylthiophene in tetrahydrofuran (THF). Points: free ions at LEAF; Lines: Ions prepared by reduction with Na.



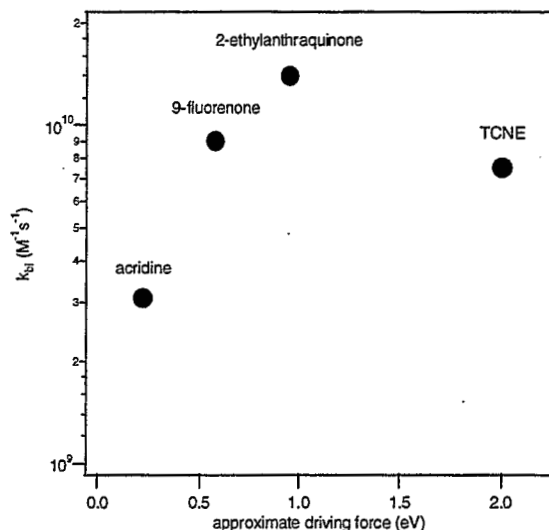
These negative ion molecules also transfer their electrons to molecules having higher electron affinities (more positive reduction potentials). Rates for these bimolecular electron transfer reactions are measured at

LEAF (see example below for reaction of the several nm long molecule P3DT with the small molecule 9-fluorenone in THF.



The following hypothesis is being explored: Charges injected into long, conjugated molecules such as P3DT are delocalized over several units of the polymer. They will, therefore, have smaller electronic interactions (also called transfer integrals or tunneling integrals) with small molecules. Such bimolecular electron transfer reactions of delocalized electrons will therefore have slower electron transfer rates for each diffusional encounter with a molecule such as the 9-fluorenone in the example above. The hypothesized weaker electronic couplings would make the reactions less sensitive to the diffusion-controlled limit and therefore more energy-selective than reactions between two small molecules.

Specifically, it may be possible to observe the “inverted region” in which electron transfer rates slow because the reaction is too exoergic.



- The data above suggest that this is indeed the case and that the highly delocalized nature of electronic states in these multi- nm sized molecules impacts the behavior of simple bimolecular electron transfer reactions.

SPECIFIC ACCOMPLISHMENTS:

The project has received DOE Nanoscience funding (\$650 K/yr split between this and projects of Creutz and Newton) and will continue under that funding. The author is grateful for the LDRD support that led to the DOE grant.

LDRD FUNDING:

FY 2001	\$47,655
FY 2002	\$49,784

Nanoscale Catalysis: Preparation, Structure and Reactivity

Jan Hrbek

01-21

J.A. Rodriguez

PURPOSE:

Investigate and explore the use of dislocation arrays existing on the Au(111) surface as a template for self-organized and tailored growth of molybdenum and molybdenum compounds nanoclusters. Correlate the structure and morphology of nanoclusters with their chemical reactivity.

APPROACH:

The clean Au(111) surface exhibits a long range reconstruction (herringbone). It has been shown that this surface can be used as a template for adsorption and direct growth of metal nanoclusters that have a narrow size distribution. Our approach involves the use of the Au(111) surface as a template for growing MoS_x, MoO_x and MoC_x clusters using Mo(CO)₆ molecular precursor. The structure and morphology of the formed nanoparticles will be examined by means of scanning tunneling microscopy (STM), whereas photoemission at the NSLS will be the main tool for characterizing the chemical properties.

TECHNICAL PROGRESS AND RESULTS:

The project was successfully completed in September 2002. We have demonstrated that Mo, MoO₃ and MoS_x clusters can be prepared by the reactions of Mo(CO)₆, NO₂, and S₂ on a Au(111) substrate. A novel growth mode of Mo nanoclusters was identified and described in a recently submitted paper. At low coverages

nanoscale Mo clusters grow at the elbow sites and in the fcc regions of the reconstructed Au surface. With increasing coverage the Mo clusters aggregate without coalescence forming ramified cluster islands. The differences observed for chemical vapor deposition of Mo are related to the mobility of the clusters in the presence of CO from the precursor molecule. Oxidation of Mo clusters leads to formation of 2-dimensional clusters of disordered oxide that spread and cover substantially larger fraction of Au surface than the original 3-dimensional Mo cluster islands. The MoS_x nanoparticles were more reactive towards thiophene than extended MoS₂(0002) surfaces, MoS_x films or MoS_x/Al₂O₃ catalysts.

SPECIFIC ACCOMPLISHMENTS:

Early results of this work were used in a proposal "Catalysis on the Nanoscale" submitted to the DOE Office of Basic Energy Sciences in response to the NSET solicitation and funded in July 2002.

Publications:

Formation of Mo and MoS_x Nanoparticles on Au(111) from Mo(CO)₆ and S₂ Precursors: Electronic and Chemical Properties, J.A. Rodriguez, J. Dvorak, T. Jirsak and J. Hrbek, *Surf. Sci.*, **490**, 315-326(2001).

Synthesis, Electronic and Chemical Properties of MoO_x Clusters on Au(111), Z. Chang, Z. Song, G. Liu, J.A. Rodriguez and J.Hrbek, *Surf. Sci.* **512**, L353-360(2002)

A Novel Growth Mode of Mo on Au(111) from a Mo(CO)₆ Precursor: An STM Study, Z. Song, T. Cai, J.A. Rodriguez, J. Hrbek, A.S.Y. Chan and C.M. Friend, *J. Phys. Chem. B* **107**, 1036-1043(2003)

Presentations:

Strained Metallic Layers as Templates for Growth of Nanoparticles (invited), J. Hrbek, Z. Song and J.A. Rodriguez, American Chemical Society, Orlando, FL, April 7-10, 2002 Chemistry Department, BNL.

A Novel Growth Mode of Mo on Au(111) from a Mo(CO)₆ Precursor: An STM Study (oral), Z. Song, T. Cai, J.A. Rodriguez, J. Hrbek, A.S.Y. Chan and C.M. Friend, American Vacuum Society, Denver, CO, Nov 2-7, 2002.

LDRD FUNDING:

FY 2001	\$76,395
FY 2002	\$79,880

Experimental and Theoretical Studies of the Formation of Titanium-Carbon Nanoclusters

Trevor J. Sears

01-23

G. E. Hall

J. T. Muckerman

PURPOSE:

This research focuses on a fundamental understanding of the structure, formation, and reactivity of small metal-containing cluster species. These are precursors to nanocrystalline materials that have many potential applications, including highly specific and efficient catalysts for industry. The effort incorporates both experimental and theoretical approaches with the former directed towards high precision measurements of cluster properties that will validate high-level *ab initio* calculations of the properties of small cluster compounds. These in turn will serve as benchmarks for future semi-empirical approaches to calculations on larger nano-crystalline materials where rigorous methods are not applicable. The work forms part of the nanocatalysis initiative within the Chemistry Department and BNL.

APPROACH:

There has recently been much interest in the properties and reactivity of metallo-carbohedrene or met-car clusters which were originally discovered in 1992 in the form of positive ions of the type $M_8C_{12}^+$, where M is a transition metal atom. Initially, interest centered on the unusual stability of these species and, by analogy to fullerenes, this is assumed to be related to a highly symmetric cage-like structure. However, there is more than academic interest in such species because many have been shown to possess chemical or physical properties that have

important industrial and economic consequences.

During the past year, we have not only focused on carbides, but also early transition metal chalcogenides, specifically oxygen and sulfur complexes and clusters. Several of these species show great potential as new catalysts with highly specific and efficient properties. For example, molybdenum sulfide is already used in the oil industry for hydrodesulfurization. It has also been found that nano-clusters of nominal composition MoS_2 exhibit structured visible absorption and photoluminescence spectra that tune as a function of cluster size. These properties have been used in a demonstration of catalytic photoremediation of aqueous solutions polluted by chlorinated organics using MoS_2 as the active catalyst, with catalytic activity correlated with cluster size distributions.

The rational design of future materials depends upon a fundamental knowledge of the basic principles that underlie correlations between the electronic and geometrical structure of the nanoparticles and their physical and chemical properties. Understanding the reactivity and stability of a coordinatively unsaturated metal atom in an active catalytic site, for example, must necessarily involve a *molecular* description of the chemical bonding and electronic wavefunctions.

In this program, we have designed and constructed an experimental apparatus for the production of small metal-containing species that are subsequently studied using high-resolution optical probes. Samples of the molecular clusters can be deposited downstream of the gas phase spectroscopic experiments and subsequently characterized by microscopic and X-ray techniques. These experiments yield very precise information on the electronic structures of the molecular

clusters and correlate specific gas phase chemistry with resultant film or bulk crystalline structures.

In parallel, we have developed computational techniques that can accurately reproduce the measured electronic and structural properties of the molecular species. The aim is to understand and validate the approximations that can be made to increase computational efficiency without compromising the accuracy of the calculation. Such knowledge is essential for future application of numerical methods to larger or bulk crystalline materials where high level *ab initio* calculations are impractical.

TECHNICAL PROGRESS AND RESULTS:

As detailed in last year's report, we have designed and constructed a new experimental apparatus for the production of molecular beams of metal-containing species. In the past year, we have finished constructing the time-of-flight mass spectrometer detector for the apparatus. We have also investigated the chemistry of other ablation sources and gas mixtures as a prelude to species characterization using the various laser spectroscopic techniques at our disposal. Figure 1 shows the mass spectrum of Mo_xS_y clusters formed in the ablation source, skimmed and ionized at 193 nm.

We have similar results for the Mo-C, Mo-O and Mo-N systems. The mass distributions are interesting and one often sees "magic numbers" in cluster stoichiometries where intense peaks at certain masses stand out above smoothly varying distributions, implying unusual stability for a particular cluster size. In Fig. 1, for example, the Mo_6S_4 cluster appears particularly stable. These mass spectra provide the information needed for future spectroscopic studies on

each of the cluster masses that appear in them. The computational work described below suggests that all the small clusters will possess extremely low-lying excited electronic states at energies corresponding to the absorption of infrared and near infrared photons. Figure 2 shows the calculated D_{2d} symmetry-constrained structure of the Mo_6S_4 species obtained in a DFT calculation with a minimal basis set.

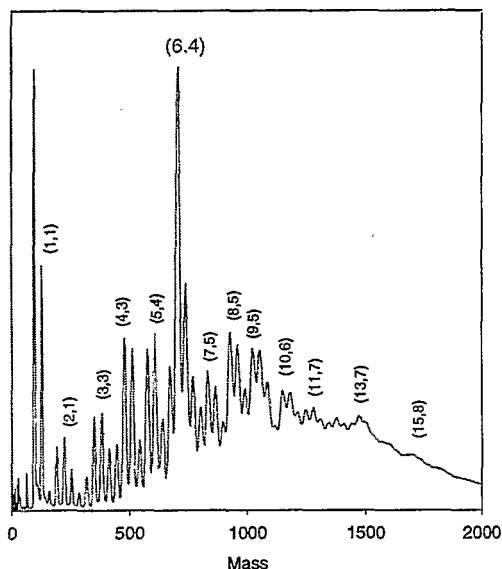


Figure 1: Mo_xS_y mass distribution from Mo ablation source and 5% H_2S in He.

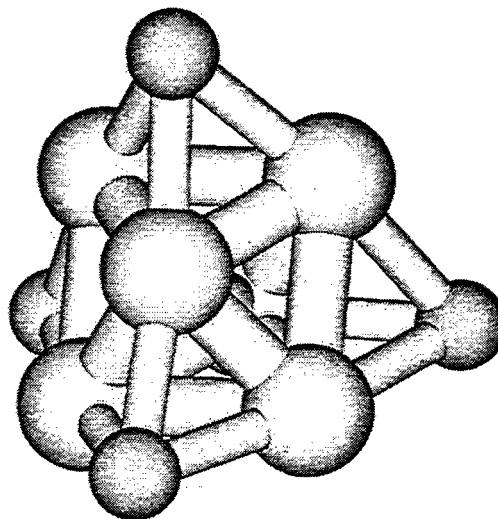


Figure 2: Calculated D_{2d} symmetry-constrained structure of the Mo_6S_4 species using the DFT mPW1PW91 method with a STO-3G basis.

At Stony Brook, we have constructed a new laser system designed to produce pulsed infrared and near-IR light with sufficient intensity to promote resonantly enhanced ionization of the clusters. This will permit spectroscopic characterization of mass-selected clusters and provide information on their structure and potential surface that can then be compared to computational results such as those described below. There is presently very little or no experimental information on the structure or electronic properties of even the simplest Mo-S molecules or clusters, so any information derived from our measurements will be of great interest.

The computational aspect of this project has moved much faster than the experimental one, and we have results on a number of prototypical systems. These await experimental verification or testing. For titanium carbide, we have devoted considerable computational resources to the Ti_8C_{12} system, and smaller fragments that may be the building blocks for these larger cage-like clusters. Figure 3 shows our optimized structure for the 8-12 Ti met-car, and Fig. 4 shows a simulated vibrational spectrum at roughly experimental resolution 24 cm^{-1} . This is one of the very few clusters of this type for which experimental information is available and our calculated frequencies are in excellent agreement where the experimental data exist. The optimized structure is not completely symmetrical and one can recognize two kinds of T-C₂ bonding in the cluster. This implies the TiC_2 building block would be of interest in itself, and we have spent considerable time computing the electronic structure for this molecule. Figure 5 shows the optimized structure for the TiC_2 molecule.

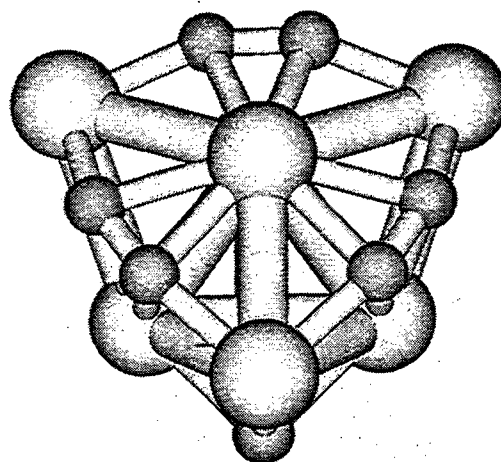


Figure 3: Optimized D_{2d} structure of Ti_8C_{12} from MP2 calculation with a large basis set [Wachters(sp) + Bauschlicher(f), Ti; Dunning cc-pVTZ(sp), C].

We previously described computational results for TiC and found more than 10 electronic states below 1 eV (8065 cm^{-1}). Amazingly, TiC_2 is calculated to possess several excited electronic states at energies as low as a few hundred wavenumbers, i.e., below the vibrational fundamental energies. The bonding in TiC_2 is found to be strongly ionic with Ti^{2+} and C_2^{2-} -like moieties. The low-lying states all arise from the lowest Ti^{2+} d^2 -like lowest energy configuration and the number of low-lying states derives from the various ways of arranging the two highest energy electrons among the available orbitals.

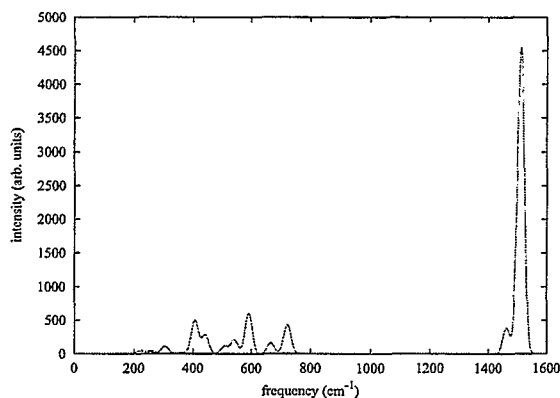


Figure 4: Calculated infrared spectrum of Ti_8C_{12} , shown at roughly the same experimental resolution as in ref. 7, from scaled RHF harmonic frequencies obtained using the same basis as in Fig. 3.

Molybdenum carbide is another material that has recently been reported as a potential replacement for noble metal catalysts in industrial processes. We have performed similar calculations on the low-lying states of MoC and MoC₂. For the latter, and in contrast to TiC₂, we find the lowest energy excited states lie at 4,696, 6,624 and 15,383 cm⁻¹ above the ground state. The difference arises because the bonding in MoC₂ is more covalent than in TiC₂. These calculations will guide experimental searches using the new spectrometer at Stony Brook, which is designed to access the infrared and near-IR spectral regions corresponding to the energy of the lowest excited states of these species.

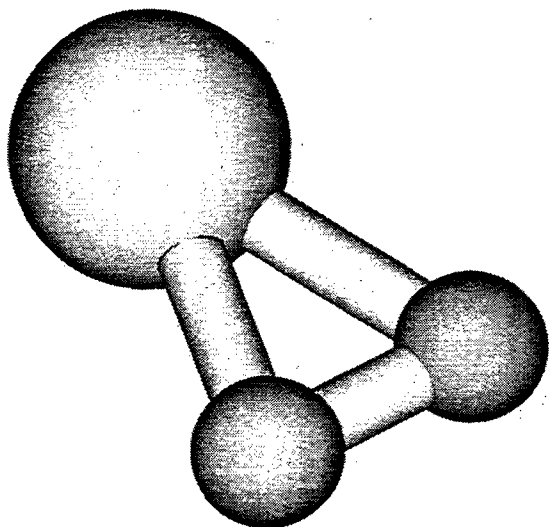


Figure 5: Calculated equilibrium structure of the ground ³B₂ state of TiC₂ with the RCCSD(T) method and the same basis as in Figs. 3 and 4. The excited states ³B₁, ³A₂ and ³A₁ are calculated to lie just 40, 1520 and 3762 cm⁻¹, respectively, above the ground state, and have very similar structures. Note the similarity of the TiC₂ structure to an inner-Ti—C₂ moiety in Ti₈C₁₂.

SPECIFIC ACCOMPLISHMENTS:

K. Kobayashi, G. E. Hall, J. T. Muckerman, T. J. Sears and A. J. Merer, *The E-X*

transition of jet-cooled TiO observed in absorption paper published in *J. Molec. Spectrosc.* **212**, 133-141, 2002.

Nicolas Poulin, James T. Muckerman and Trevor J. Sears, *Calculating rovibronic spectra of transition metal carbides*, poster presentation, XVIIIth Conference on the Dynamics of Molecular Collisions, Copper Mountain, CO, July 15-20, 2001.

James T. Muckerman and Hua Hou, *Ab initio calculations of the geometry and electronic properties of the met-car Ti₈C₁₂*, poster presentation, Nanocenter Workshop, Brookhaven National Laboratory, 2002.

K. Kobayashi, G. E. Hall, J. T. Muckerman, T. J. Sears, and A. J. Merer, *J. Molec. Spectrosc.* **212**, 133 (2002).

James T. Muckerman and Hua Hou, *Ab initio calculations of the geometry and electronic properties of the met-car Ti₈C₁₂*, poster presentation, International Workshop on Electron-Phonon Effects in Nanosystems, Montauk, NY, Sept. 23-25, 2002.

Prepared and submitted proposal to the National Science Foundation: *Spectroscopic and theoretical studies of potential catalytic materials based on group VIB chalcogenides*, for \$602,323 over 36 months. (for continuation of this research at SUNY Stony Brook.) The proposal is currently under review at NSF.

LDRD FUNDING:

FY 2002	\$103,067
FY 2003 (budgeted)	\$106,912

Development of a UV-Raman, Near-field Scanning Optical Microscope for *in-situ* Studies of Chemical Intermediates on Metal Nanoparticles

Michael White

01-24

M. Wu

PURPOSE:

In this project, we propose to establish the feasibility of using UV Raman spectroscopy as a basis for near-field scanning microscopy (NSOM) with chemical information. The project involves (1) the demonstration of the high sensitivity of UV resonance-enhanced Raman spectroscopy for detecting chemical species at very low surface concentrations; (2) feasibility studies for using UV Raman scattering for chemical imaging microscopy near the diffraction limit. The long-term goal of this effort is to combine optical spectroscopy (e.g., UV-Raman) with scanning probe techniques to develop apertureless approaches to near-field microscopy with high spatial resolution ($\leq 1\text{nm}$) and chemical sensitivity. Such *ultraspectromicroscopy* would find applications to current research on the structure and reactivity of nanoparticles used for catalysis, and in soft-matter research involving bio-macromolecules, polymers, and organic thin films.

APPROACH:

The main issues for spectromicroscopy with NSOM are the conflicting requirements imposed by the use of hollow fiber tips typically used to transmit light to the tip-surface interaction point. On the one-hand, the small exit apertures required for lateral spatial resolution are currently fairly large,

30-50 nm, however, the light transmission of such tapered tips is extremely small, ranging from 10^{-3} to 2×10^{-12} as the diameter of the fiber core is reduced from 100nm to 20nm. In addition, the hollow fiber tips must be coated with a reflective metal (typically Al) to enhance transmission and prevent light leakage outside the tip. Such coatings, however, are easily damaged and thereby place constraints on the input laser power. As a result, NSOM has been limited to light scattering, transmission or fluorescence detection of nanometric features or substrate materials. In this work, we want to explore the use of Raman scattering of UV light as the basis for spectroscopic microscopy. This choice is based on (1) the general applicability of VIS-UV Raman to a wide variety of chemical environments (vacuum, ambient, liquids); (2) ν^4 Raman scattering enhancements using deep UV excitation wavelengths (220 - 260 nm); (3) the use of well-known surface enhanced Raman scattering (SERS) and resonance enhancement processes which can significantly improve the surface sensitivity of Raman scattering. SERS will be particularly important for near-field microscopy applications, where spatial contrast will be provided by enhanced light scattering in the vicinity of the metallized, scanning probe tip (coated with SERS active metals, e.g., Ag, Au) and the sample. Such apertureless NSOM (ANSOM) designs have recently appeared in the literature and have obvious advantage of eliminating the hollow fiber tip and its associated limitations.

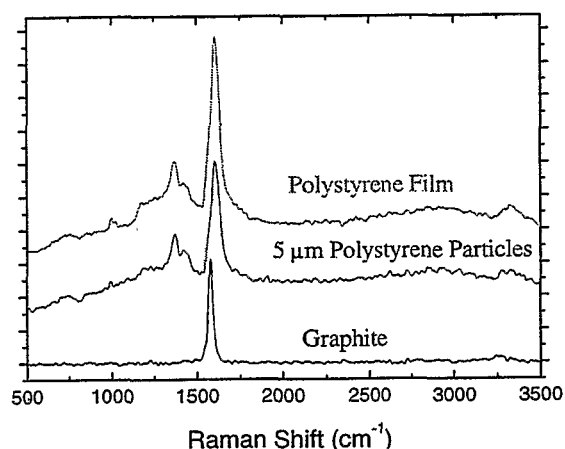
Initial studies focused on the sensitivity of UV Raman spectroscopy for detecting molecular adsorbates on metal and metal oxide surfaces at very low coverages. The second part of this project is to develop an ambient Raman microscope to engineer the basic optical configuration for spectroscopy

and assess the sensitivity for small, diffraction-limited spot sizes (~700 nm).

TECHNICAL PROGRESS AND RESULTS:

FY 2001: A UHV sample chamber was constructed for UV Raman sensitivity experiments on molecules adsorbed at low coverages on extended surfaces (metal foils, single crystals) and nanoparticle arrays. Studies of pyridine on Ag, benzenethiol on Cu and Au (see Figure), and sulfur dioxide on Ag and TiO₂ (100) surfaces indicate that for molecules with electronic states that can be accessed by the UV excitation (264.3 nm - 228.9 nm), UV Raman provides sufficient sensitivity to detect adsorbates at very low coverages.

FY 2002: A confocal UV Raman microscope was assembled and tested using a Leica optical microscope as the platform. The latter was modified to allow UV laser excitation and Raman scattered light collection through a custom supplied UV objective. Raman spectra were obtained by dispersing the scattered light by a 0.75 m monochromator onto a liquid nitrogen cooled CCD detector. Initial testing indicated that the spatial resolution was limited to ~1 μ m as result of the UV objective spot size (~700 μ m) and instabilities associated with the sample scanning stage. High quality Raman spectra could be obtained for small sample volumes as illustrated in the accompanying Figure for polystyrene particles used to calibrate sensitivity and spatial resolution. Data such as these indicate that UV Raman offers a promising approach to chemical imaging beyond the diffraction limit. Furthermore,



UV Raman (244 nm) spectra taken with the microscope focused a 5 μ m polystyrene particle supported on graphite. The Raman spectrum of bulk polystyrene is shown for comparison.

UV light collimation, collection, and transport were found to be relatively efficient and optically straightforward such that implementation in scanning probe instruments should present no major impediments.

Continued support for this project beyond FY2002 will be provided through a combination of NanoCenter Jump Start funds (pending) and limited support from the Chemistry NanoCatalysis NSET program (M. White, PI) and investigators from Rutgers University.

SPECIFIC ACCOMPLISHMENTS:

The UV Raman studies of adsorbates at low coverages will be submitted for publication as part of a larger study of vibrational spectroscopy of adsorbates on metal surfaces.

LDRD FUNDING:

FY 2001	\$ 96,203
FY 2002	\$ 99,850

Development of New Techniques for Improvements in PET Imaging of Small Animals and Other Applications

David Schlyer

01-28

C. Woody

PURPOSE:

The ultimate goal of this research is to design and build a detector that employs the latest technology in gamma ray detection to achieve the best possible energy and position resolution for PET imaging which can be used for a variety of applications such as freely moving small animal imaging and determination of blood radioactivity non-invasively. We will replace the photomultiplier tubes on standard PET tomographs with avalanche photodiodes, along with their individual readout electronics, on each crystal and compare the images and optimize the parameters of the system. We have broadened the scope of this LDRD slightly to include the use of this detector to measure blood flow in situ non-invasively. We feel this project should be focused on obtaining an arterial input function since this aspect has a more immediate impact on our program. This is a very innovative use of these detectors and could prove to be very valuable not only to Brookhaven but to the entire PET community. It would mean that the use of arterial lines (and the associated risks and pain) could be eliminated from kinetic PET studies. As a next step we will develop the microelectronics necessary for these arrays and use this assembly to image the levels of radioactivity in the blood as it passes through the wrist with high temporal resolution.

APPROACH:

The basic approach to the experiments is outlined below. We are currently in the midst of accomplishing goals one and two of this study.

1. Replace the phototube readout of the present module with avalanche photodiodes (APD) and compare the images. Optimize the image by tuning various parameters in the system, such as APD gain, electronic gain, noise, etc.
2. Achieve a two-dimensional image with the detector array and show that the sensitivity of the array is sufficient to obtain an arterial input function.
3. Replace the traditional electronics with integrated circuits that are compatible with the use as a blood monitoring system. If necessary the crystal arrays can be made larger to increase the sensitivity.

The risk associated with this approach is that the electronics do not exist in the form required to make this type of small ring detector. The development of these electronics would be a great leap forward in PET imaging technology. Other centers are working on such approaches, but no one to date has produced a final product. We feel we have the unique blend of resources to make this happen at Brookhaven.

TECHNICAL PROGRESS AND RESULTS:

The Lutetium oxyorthosilicate (LSO) blocks have been assembled with the APD arrays attached. All the associated electronics associated with reading out the signals from these detector blocks have been assembled and tested. The preliminary results from these tests looked very promising. Work continues to define the parameters that will be required in the final application specific integrated circuit that will be attached to the detector block in order to read out the

signals and convert them into an image. The first stage of the integrated electronic circuits has been sent out for fabrication. A dynamic phantom has been designed and tested to show that the wrist detector portion of this project is feasible in a clinical setting.

The software for the reconstruction of the images is complete and we are able to acquire two-dimensional images of the phantom. All our tests demonstrate that this project is feasible and will end in a useful device for clinical use.

The test set-up has been completed and data is being taken. The acquisition of all the electronics for this project was very time-consuming since we need 64 separate

channels for the data acquisition. We now have this data acquisition system in full operation and have obtained preliminary data.

SPECIFIC ACCOMPLISHMENTS:

We have filed a record of invention on the wrist detector device. The other section of this research dealing with the small tomograph to be attached to the rat head has recently been funded by a DOE Biomedical Engineering grant.

LDRD FUNDING:

FY 2001	\$86,322
FY 2002	\$89,885

Development of CZT Array Detector Technology for Synchrotron Radiation Applications.

D. Peter Siddons

01-30

PURPOSE:

Establishment of the technology to enhance the capabilities of NSLS beamlines by providing advanced detector capabilities. In particular, pixellated array detectors made from a high-Z material are not currently available, and such devices are essential for designing efficient experiments at x-ray energies greater than 10keV.

APPROACH:

As part of a CRADA project, scientists in the Instrumentation Division (ID) Large Scale Integration (LSI) group have recently developed a Complementary Metal Oxide Semiconductor (CMOS) charge-sensitive preamplifier which is optimized for use with solid-state detectors based on $Cd_xZn_{1-x}Te$. There are many instances for which silicon is ineffective as a detector material for x-rays. In particular, the absorption (and hence detection) efficiency falls very rapidly for photon energies greater than 10 keV. Many non-spectroscopic applications of synchrotron radiation are moving towards higher photon energies as a way to reduce sample absorption artifacts and to provide better bulk probes. Such applications would greatly benefit from the availability of a high-Z detector material and the technology for forming special-purpose arrays from this material. The main problems involved in applying Cadmium Zinc Telluride (CZT) to detectors are the crystal perfection required and the difficulty in making reliable surface electrical contacts to the material. Access to

the surface analytical tools available at NSLS should provide valuable scientific input to the contact problem, and diffraction imaging should at least allow us to select high quality areas of a wafer in a non-destructive way, and may provide valuable input to the crystal grower in steering growth technique developments.

We have succeeded in attracting a student, Edson Kakuno, and a young scientist, Giuseppe Camarda, to work on the project. The bulk of Kakuno's support will be provided by his country of origin, and that of Camarda by this LDRD. Kakuno arrived in March, and Camarda in August.

Our immediate goal was to arrive at a reproducible method which would allow us to fabricate array detectors with individual elements having a performance at least as good as commercially available single detectors.

In the previous year, we established the infrastructure necessary for semiconductor device fabrication. This included refurbishment of a disused clean room facility and obtaining raw materials and test and measurement instrumentation. All of this infrastructure has been put to good use in the past few months.

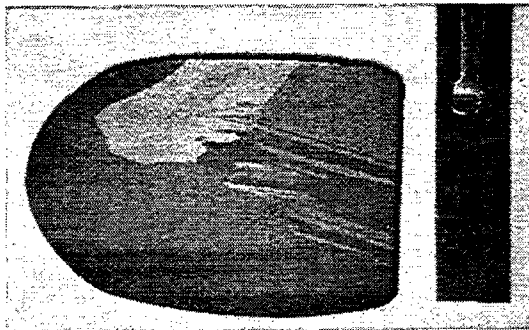
CZT (Cadmium Zinc Telluride) is a pseudo-binary alloy which is a semi-insulator. It has a band-gap of 1.56eV. This is significantly larger than that of silicon or germanium, the two most common semiconductors used for x-ray detectors. Two things follow. First, CZT detectors may be operated at room temperature and maintain low noise. This can be important in circumstances where space is at a premium and the device must work in varying orientations and positions. Second, the bulk resistivity of the material is very high, and devices are operated as

intrinsic photoconductors, not as reverse-biased diodes. This means that there is no need for forming doped layers on the material as is typical for silicon detectors. Thus, the fabrication of a device is in principle quite simple. Ohmic contacts are formed on either face of a slab of material and a large bias voltage applied across them. Electron-hole pairs produced by photoeffect in the material are swept toward opposite faces by this bias voltage. Currents are induced in the external circuit by these charge motions, and these constitute the detected signal.

TECHNICAL PROGRESS AND RESULTS:

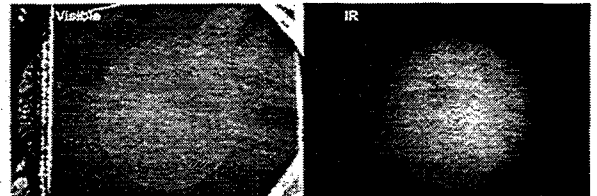
Herein we give a description of each process step required to take an ingot of CZT and transform it into a working x-ray detector.

Figure 1 shows a CZT slice as received from the crystal grower (in this case Yinnel Corp.)

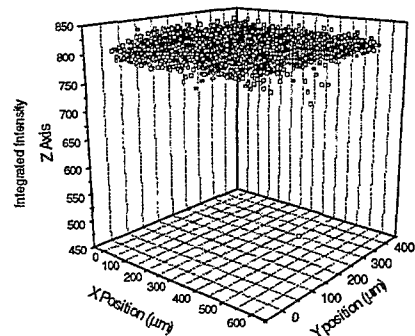


The varied texture on the slice is indicative of the fact that it is not a single crystal but contains large subgrains. This is far from ideal. Although each subgrain may be high-quality material, the grain boundaries are frequently decorated on the microscopic scale with impurities, precipitates, and other defects which lead, in general, to inferior electrical properties. In fabricating monolithic detector arrays, it is desirable to use a single grain for the entire array. The

arrays we have made so far have been small (~5mm x 5mm), and so this has not been a serious problem. We check for large buried defects (metallic precipitates, for example) using the infra-red imaging capabilities at NSLS. Such an image of the heavily-twinned area is shown below.



The left-hand image is a visible light image, where the light-colored circle delineates the area imaged in the infrared in the right hand image. This instrument can be configured to provide quantitative information about the material absorbance using a point-focussed beam in a raster scan. The figure below shows such a transmission map for a region 0.6mm x 0.4mm. The material appears to be locally quite homogeneous.



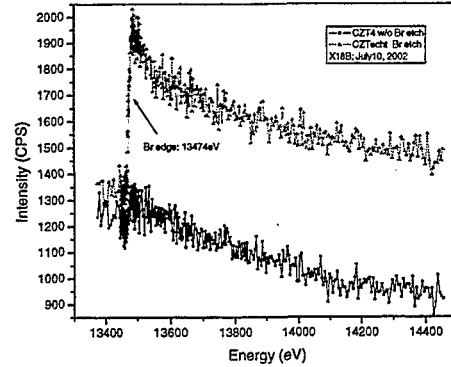
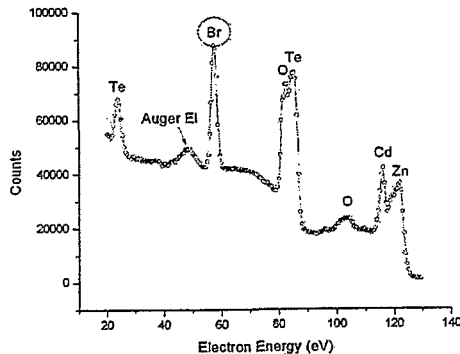
This slice is then diced into pieces suitable for array fabrication using a diamond-coated wire saw using water as a lubricant. Mechanical damage is known to result in problems. This machine allows a minimum of further mechanical surface treatment following cutting. Our samples are typically 5mm x 5mm x 2mm.

The next process is mechanical polishing to produce a mirror finish, free of visible

scratches. This is done by hand using a range of abrasive materials and a commercial sample manipulator.

The final step of surface preparation prior to forming electrical contacts is a chemical etching process which should remove any residual damage from the polishing step and leave a smooth surface for the subsequent lithography and metallization. Our best result comes from an etchant containing bromine, methanol and lactic acid.

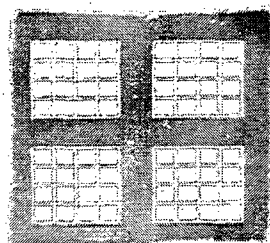
We have examined the etched surface using photoemission, and were surprised to see a large peak which we identified as a bromine level. We tried to remove the bromine by argon-ion sputtering, but were only partially successful. We checked this result using x-ray fluorescence analysis, and bromine is clearly visible. We would be surprised if the bromine did not play some role in the formation of electrical contacts, but are not aware of anyone considering this possibility. The photoemission and x-ray fluorescence data are shown below.



Following surface preparation, the next step is to form metallic contacts on opposite faces of the material. These contacts should be ohmic, that is, the bias voltage / current curve should be linear through the origin at least in the operating bias direction. Any departure from this indicates a surface preparation problem. Our best results so far have been from the chemical deposition method.

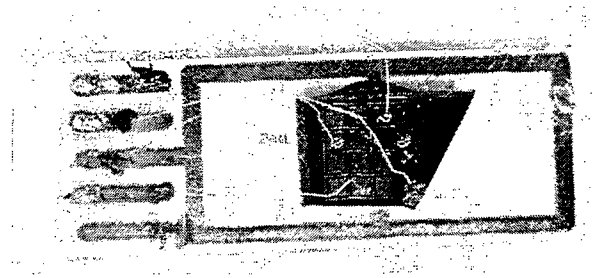
Since our primary goal is to make devices with custom geometries to suit particular synchrotron experiments, we felt that a lithographic method was essential. The metal of choice for ohmic contacts is gold, which is difficult to etch, and any etchant which removes gold will certainly destroy the underlying semiconductor. An alternative method is the so-called lift-off method. In this method, the lithographic step is made before the conductor is deposited. The lithography process is adjusted to form a slight undercut of the resist layer. Subsequent evaporation of the conductor forms a weakened layer at the resist edges, and the resist can be removed by a solvent carrying the unwanted metal with it. This method works well with CZT/gold, and we have fabricated devices using it. Unfortunately, we find that simple evaporation does not produce good ohmic contacts. We have developed an excellent technique which uses the chemical deposition method in conjunction with

lithography to make good ohmic contacts with well-defined geometry. As with the lift-off technique, the lithographic step is performed before the metallization step. The chemical metallization process involves simply immersing the material in a 5% solution of AuCl₃ in HCl. The gold is deposited on the exposed CZT. That which is protected by the photoresist receives no metal deposition. Subsequently, the resist can be removed by a solvent, leaving the metal pattern as required. Unless future work invalidates the chemical metallization process, we will continue to use this technique. The figure below shows our test lithography pattern. It consists of 4 groups of 16 detectors, each 1mm x 1mm, arranged in a square. We typically use one of these groups for our test detectors.



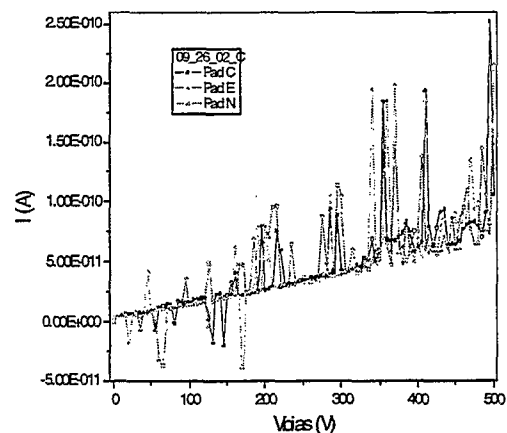
Each detector is surrounded by a guard electrode which serves to collect surface currents which would otherwise degrade the detector performance. With this pattern we can determine the level of these surface currents and separately measure the true bulk leakage current. The lithography process itself is quite standard, using a spin-coater to apply the photoresist and a UV lamp and contact mask-aligner to make the exposures. The reverse face of the detector is uniformly coated with gold, i.e. The lithography step is not applied.

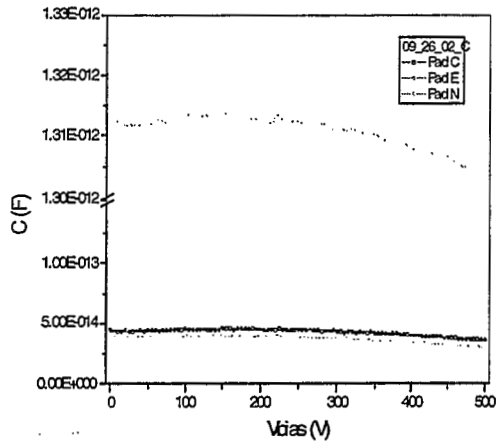
Next, we mount the detector onto a patterned ceramic substrate to facilitate electrical testing. A mounted detector is shown below. This image points out one aspect of our process which needs further work; application of wires to external circuits.



Currently, we apply connections to the detector elements using a tedious manual procedure using 1 mil gold wire and colloidal graphite suspension, manually under a microscope.

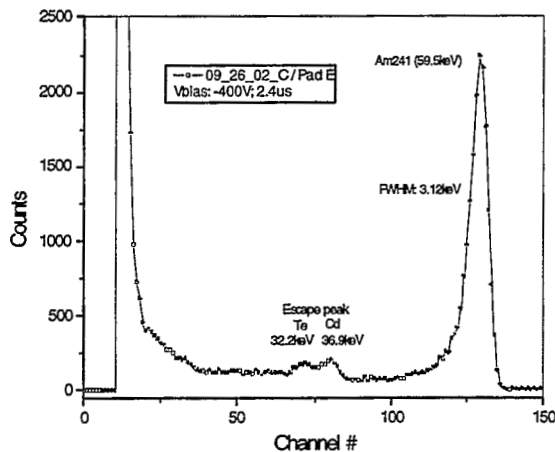
Electrical tests must be performed in darkness since the device is photosensitive. We have assembled a dark box and a set of measuring instruments and software to allow us to make automated C/V and I/V (C=capacitance, V=voltage, I=current) measurements. The figures show I/V and C/V results from 3 pixels of one of the test samples. They are typical of the test devices.



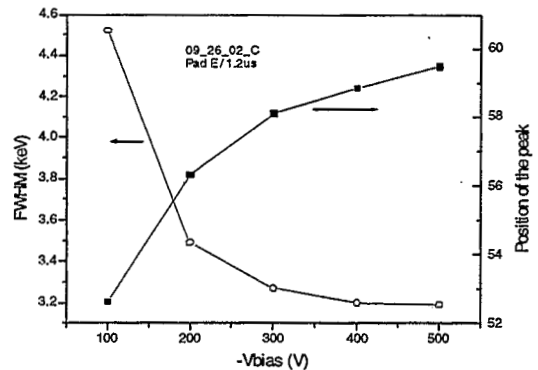
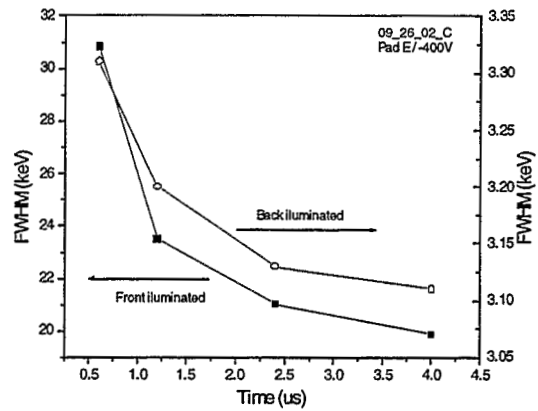


The tests indicate that the material is high quality, with leakage currents at the 100 pA level or less. The fact that the device capacitance is almost bias-independent shows that there are few free carriers in the material and no depletion layer forms.

We tested these devices as x-ray detectors by connecting the pixels to a readout integrated circuit developed by Paul O'Connor and Gianluigi De Geronimo specifically for CZT devices. The figure shows our best result to date. The radiation source was a heavily filtered ²⁴¹Am source such that only the 59.5keV line is observable. The observed resolution is around 5%, slightly better than individual commercial detectors we have measured.



Measurements of energy resolution as a function of bias voltage and pulse shaping time are shown below.



These curves indicate that the dominant contribution to detector noise is not leakage current. Leakage-induced noise in general increases with shaping time and with detector bias voltage. The observation that the resolution improves and the peak position moves towards higher charge values as the bias voltage is increased implies that charge trapping is the culprit. Increased bias increases the charge drift velocity, which reduces the time for charge collection. This reduces the probability for charge trapping and improves performance. It is clear from the curves that a bias of 400V is optimal. The large difference between front and rear illumination is a consequence of the fact that the electron and hole mobilities in CZT are quite different. Thus, electrons can travel further before being trapped. For 60keV

radiation, the photoabsorption occurs within 0.5mm of the entrance surface. If the entrance face is negatively biased, hole collection is optimal. If it is positively biased, then the holes must travel through the entire detector thickness before collection, giving a higher probability of being trapped. Thus, the performance of these devices for x-rays of 60keV or less is strongly dependent on the bias polarity and illumination geometry.

In summary, we have developed techniques which allow us to produce detector arrays of arbitrary planar geometry, with performance at least as good as that obtainable commercially for individual detectors. We

have observed, using photoemission and x-ray absorption spectroscopy, that bromine is present on the surface after etching. It is not clear what role this plays in the device operation, but we were surprised how persistent it was. Even heavy sputtering with high-energy argon ions did not remove it.

SPECIFIC ACCOMPLISHMENTS:

None

LDRD FUNDING:

FY 2001	\$106,592
FY 2002	\$ 68,399
FY 2003 (budgeted)	\$ 50,000

New Applications of Circular Polarized VUV-Light (NANO IV)

Elio Vescovo

01-31

H. Lee

S. Hulbert

PURPOSE:

Our goal is to provide the capability to conduct spin- and angular-resolved photoemission experiments with circular polarized light at U5UA beamline. This beamline is dedicated to the investigation of the magnetic properties of ultrathin films. The use of circularly polarized light will greatly benefit these studies. Particularly, electronic states which cannot be selected with linear light will be available for investigation with circular light; additionally, circular polarized light allows to directly resolve spin-orbit split electronic pairs; these electronic states are at the origin of magnetic anisotropy and their study is highly important both for basic understanding of magnetic materials as well as for device applications of the magnetic properties of thin films.

APPROACH:

In recent years, the availability of circularly polarized light (CPL) at synchrotron radiation sources has steadily increased. With the advent of third generation light sources, new insertion devices (e.g. elliptical undulators and wigglers) have provided more intense and brighter CPL than that from out-of-plane bending magnets. Consequently, more demanding experiments, e.g. photoemission and microscopy, have become practically feasible using CPL. However, the energy range usually covered by these new sources is in the soft x-ray region. These high photon energies are not

suitable for angle-resolved photoemission (ARPES), an experiment typically performed in the photon energy range 10-100 eV. Recently, it has been suggested that an efficient way to produce CPL at these low energies is to convert linearly polarized light into circularly polarized light using a quadruple-reflection (QR) circular polarizer.

The U5UA undulator beamline - an intense and highly linearly polarized VUV light source in the photon energy range 10-200 eV - is an ideal candidate for a QR polarizer. The addition of a QR circular polarizer is extremely convenient because it tailors the output polarization without any other change to the optical design of the beamline.

TECHNICAL PROGRESS AND RESULTS:

In FY 2001, a QR circular polarizer had been successfully installed and tested at U5UA.

In FY 2002, Dr. Hangil Lee has been hired to work on this project. To complete the project successfully it is mandatory to improve the electron collection efficiency in order to compensate for the decreased photon flux (in going from linear to circular light). This is obtained by substituting the current electron spectrometer with a more efficient one. A new end-station based on an Omicron 125 mm spherical analyzer (the old analyzer was 50 mm) has been designed, built, and assembled at the U5UA beamline. The new system is currently under commissioning and preliminary results do indeed indicate the expected increase in intensity.

Besides the increased collection efficiency, the new system constitutes an important improvement of the experimental apparatus in several respects. The energy resolution is considerably improved (about a factor 2).

Furthermore, the new vacuum system has been equipped with a sample fast-transfer load-lock which considerably reduces the downtime between experiments.

The new system is expected to become fully operational in about six months.

SPECIFIC ACCOMPLISHMENTS:

Hangil Lee, In-Gyu Baek, H.-J. Kim, and E. Vescovo, "Manipulating the surface anisotropy in Fe(110) Ultra-thin Films," NSLS user meeting (2202)

Hangil Lee, In-Gyu Baek, and E. Vescovo, "Spin-Reorientation Transition in Fe(110): the role of magnetoelastic anisotropy," MMM2002, Tampa, Florida (Nov. 11, 15).

LDRD FUNDING:

FY 2001	\$23,860
FY 2002	\$52,904
FY 2003 (budgeted)	\$50,000

Soft X-Ray Magnetic Speckle

Cecilia Sánchez-Hanke

01-32

C.-C. Kao

PURPOSE:

The main purpose of this proposal is to develop the necessary experimental technique and computational algorithm for measuring and reconstructing magnetic speckle patterns. The principal application of this work will be imaging magnetic domain structures with sub-micron spatial resolution and the study of magnetic domain dynamics. Both are important in the understanding of magnetism and the control of magnetic properties on the nanometer scale, a scientific thrust area in the Center for Functional Nanomaterials.

APPROACH:

To observe speckle patterns, spatially coherent light is necessary. With increasing brightness from undulators in synchrotron light sources, x-ray speckle patterns have been observed in hard as well as in the soft x-rays energy range. In the soft x-ray case there are two major advantages: (1) coherent x-ray flux is proportional to the square of wavelength, (2) large charge and magnetic resonant scattering amplitudes for 3d and 4f elements. Both factors together will make the technique sensitive to very small amounts of magnetic materials, such as self-assembled nano-magnetic particles and nano-patterned magnetic arrays. In addition, the wavelength of interest is on the order of a few nanometers, which means the spatial resolution of this technique will be on the order of tens of nanometers ideally suited for the study of nanometer sized magnetic systems.

Experimentally, a 10-micron pinhole will be used at the end of beamline X1B at NSLS to take out coherent soft x-rays. The scattered x-ray, i.e. the speckle pattern, will be recorded using a two-dimensional CCD detector. The speckle pattern will be recorded at selected wavelengths around an absorption edge of the element of interest to provide the phase information necessary for the reconstruction procedure. This is analogous to the multi-wavelength anomalous diffraction (MAD) method routinely used in solving the phase problem in protein crystallography.

T. O. Menteş, a graduate student in the Physics Department at the University of Stony Brook, has been recruited to assist in this project.

TECHNICAL PROGRESS AND RESULTS:

In FY 2001, a theoretical reconstruction algorithm was developed to recover a 2-D magnetic domain pattern from the magnetic speckle patterns. On the experimental side, magnetic speckle patterns were collected from a Pt/Co multilayer at the X-1B beamline at NSLS. The design of a new experimental chamber was started.

In FY 2002, the reconstruction algorithm was published. We also completed the assembling and testing of the new experimental chamber, in collaboration with the groups of J. Kirz and C. Jacobsen in the Physics Department at Stony Brook. On the experimental side, new measurements were carried out at the X1B NSLS beamline on the Pt/Co multiplayer and on arrays of magnetic nanodots using the new chamber. Experiments were also performed at the sector 4 beamline at APS where coherent circularly polarized soft x-rays can be used to enhance the magnetic contrast. These new results are currently being analyzed to

prove the consistency of the theoretical algorithm.

In FY 2003, we plan to perform further experiments under the support of DOE funding on arrays of nanomagnets and self-assembled magnetic particles. We also plan to further develop the technique by extending the transmission algorithm to reflectivity geometry. Finally, a new experimental diffraction chamber, operating in the reflection geometry, will be designed and constructed to increase the flexibility of this technique.

SPECIFIC ACCOMPLISHMENTS:

Publications:

“Reconstruction of Magnetization Density in Two-Dimensional Samples from Soft X-Ray Speckle Patterns Using the Multiple-Wavelength Anomalous Diffraction Method,” T. O. Mentes, C. Sánchez-Hanke and C. C. Kao, *Journal of Synchrotron Radiation*, Vol. 9, **90** (2002).

Presentations:

“Imaging Magnetic Domains with Soft X-Rays Speckles,” oral presentation at APS March meeting 2002.

“Imaging Magnetic Domains With Soft X-Rays Magnetic Speckles,” poster presentation at BNL Nanocenter (Center for Functional Nanomaterials) workshop in March 2002.

“Development of a Novel Apparatus for Experiments in Soft X-Ray Diffraction Imaging and Diffraction Tomography,” poster presentation at VII International Conference on X-ray Microscopy, August 2002.

LDRD FUNDING:

FY 2001	\$41,173
FY 2002	\$40,942

Prototype Approaches Toward Infrared Nanospectroscopy

G. L. Carr
L. M. Miller

01-35

PURPOSE:

Infrared microspectroscopy with synchrotron radiation is a probe of the local chemical and electronic properties of materials, achieving a spatial resolution of about 10 μm . But higher spatial resolution (1 μm or better) is needed for studying biological processes within single cells and the physical properties of heterogeneous materials found in environmental, geological, and even space sciences. This project intends to identify and test various methods for increasing the spatial resolution.

APPROACH:

The spatial resolution for conventional (far-field) infrared microspectroscopy is controlled by diffraction. One approach for improving spatial resolution parallels various techniques already in use for visible light microscopy, e.g., optical systems with increased numerical aperture, confocal optical systems, and image deconvolution. The practical limit on spatial resolution using these techniques is not known for infrared microspectroscopy. Though the resolution may never be significantly better than 1 μm , the data from far-field measurements can be readily interpreted according to standard spectroscopic analysis methods.

The alternative approach is based on near-field techniques where one uses an infrared source or probe having dimensions smaller than a wavelength (and the diffraction limit), and places the sample in close proximity to

this source/probe. The technique is very inefficient, and requires a very high brightness source to achieve an acceptable signal-to-noise. The resulting spectra can be difficult to interpret.

The approach offering the best performance and potential for use with synchrotron radiation is not known. We are actively studying far-field methods to determine the true limits and establish benchmarks for comparison to future near-field methods. We are monitoring near-field techniques to gain understanding in this area.

Milestones for FY 2002 were 1) testing of diamond-faced ZnSe hemispheres on realistic specimens to achieve a spatial resolution of $\lambda/3$ or better, 2) testing a type of near-field technique based on scanning thermal microscopy (from Columbia Univ.), and 3) writing software for performing point spread function (PSF) deconvolution for image enhancement.

TECHNICAL PROGRESS AND RESULTS:

In the first year of this project (FY 2001), an infrared microspectrometer was interfaced to the U4IR beamline, and the scanning stage was replaced with a higher precision unit. We completed the microscope upgrade this year by installing a custom silicon beamsplitter, extending the spectral range into the far-infrared. Surprisingly good performance was achieved down to a frequency of 20 cm^{-1} ($\lambda = 500 \mu\text{m}$), and is now being used by several research groups (NASA, Centre National de la Recherche Scientifique [CNRS], MIT).

Additional ZnSe hemispheres were obtained to test the solid-immersion lens method, but we encountered technical difficulties when optically contacting and cementing small diamond disks to the flat ZnSe faces (to

overcome the material's softness). We will continue this effort in FY 2003.

Based on the initial work with D. Adams and O. Cherniavsky (Columbia), scanning thermal probes (atomic force microscopy [AFM]-type cantilevers) were acquired and mounted for testing as direct detectors of infrared absorption in a specimen. One type of thermal sensor employs a thin Pt/Rh wire having a contact area of less than 5 μm . An electronics/pre-amp read-out scheme for the sensor was developed, and first spectra were acquired from materials attached to the tip.

Detailed calculations of the microscope's PSF were compared against experimental measurements and found to agree well. Additional calculations predicted some unusual artifacts for specimens with circularly shaped features, and these artifacts were later observed in actual measurements. Scans across the sharply defined edge of a photoresist film were subsequently deconvolved to improve the spatial resolution by a factor of about 3 beyond the traditional diffraction-limit.

SPECIFIC ACCOMPLISHMENTS:

- ◆ Far-infrared microspectroscopy was achieved and demonstrated on semiconductor and biological materials (DNA). The spectral range was extended a factor of 20 from 400 cm^{-1} (25 μm wavelength) to 20 cm^{-1} (500 micron).
- ◆ Our diffraction-based PSF calculation was confirmed in 2-D measurements of thin photoresist patterns, and a 1-D deconvolution of a line scan gave a 3-fold resolution improvement.
- ◆ Both mid (3 to 20 μm) and far (20 to 200 μm) infrared spectra have been acquired using a 5 μm (sub-wavelength) thermal probe.

LDRD FUNDING:

FY 2001	\$33,689
FY 2002	\$64,030
FY 2003 (budgeted)	\$65,000

Pressure-Induced Protein Folding Monitored by Small-Angle X-Ray Scattering and Fourier Transform Infrared Microspectroscopy

Lisa M. Miller

01-36

C.-C. Kao

PURPOSE:

The objective of this work is to develop novel time-resolved methods for studying the structure and dynamics of folding proteins monitored by synchrotron-based, small angle x-ray scattering (SAXS) and Fourier transform infrared microspectroscopy (FTIRMS). This project takes advantage of the high brightness of synchrotron radiation, where x-ray and infrared beams can be focused through the small aperture of a flowcell or diamond anvil pressure cell. The NSLS has several beamlines that are well suited for performing SAXS and FTIR microspectroscopy, and also has an accomplished user base in designing high-pressure diamond anvil cell devices. These new techniques will become key elements in the ongoing development of the Macromolecular Structure and Dynamics program at the NSLS.

APPROACH:

With over 3 gigabases of DNA in the human genome sequenced, more than 30,000 genes that code for individual proteins have been identified. The Human Proteome Project is the next step in deciphering the human genome and involves identification of the structure and function of each of these proteins.

A BNL initiative, the Human Proteome Project, seeks to develop BNL as a center for producing proteins and determining structures. X-ray crystallography has become the most commonly used technique for determining protein structure and "the NSLS is one of the most efficient of the synchrotrons that is the workhorse of structure production." However, crystal structures provide a "snapshot" of a protein in a single (most often native) state. Thus, it is difficult to learn about protein dynamics (e.g. protein folding and enzymatic function) with an x-ray crystal structure. Also, this technique is difficult to perform on macromolecular complexes and membrane-bound proteins.

This project involves the development of new methods for determining protein structure in solution (instead of the crystallized state) that takes advantage of the unique capabilities of the NSLS.

TECHNICAL PROGRESS AND RESULTS:

A rapid-mix flowcell was designed for determining time-resolved protein structures using Fourier transform infrared microspectroscopy. This work was done in collaboration with Dr. Mark Chance (Albert Einstein College of Medicine). Jaclyn Tetenbaum, an Energy Research Undergraduate Laboratory Fellowship Program (ERULF) student, determined the steady-state protein structure of soybean trypsin inhibitor in its native and disulfide-reduced, denatured state using a combination of circular dichroism (CD), x-ray absorption spectroscopy (XAS), and Fourier transform infrared microspectroscopy. Software for infrared data analysis was designed and written in Matlab by Dr. Haluk Utku (visiting scientist).

Dr. Lin Yang (postdoctoral fellow) designed and built an SAXS setup on the NSLS insertion device beamline, X21. Drs. Jim Ablett (postdoctoral fellow) and Lin Yang determined the structure of native and disulfide-reduced soybean trypsin inhibitor using SAXS. In addition, the structure of phosvitin, a model bone mineralization protein, was also determined using SAXS, CD, and FTIR. Finally, Dr. Jim Ablett began the design and construction of a diamond anvil cell for pressure-induced protein folding studies.

SPECIFIC ACCOMPLISHMENTS:

Publications:

N.S. Marinkovic, A.R. Adzic, M. Sullivan, K. Kovac, L.M. Miller, D.L. Rousseau, S.R. Yeh, M.R. Chance (2000). Design and implementation of a rapid-mixer flow cell for time-resolved infrared micro-spectroscopy. *Rev. Sci. Instr.*, **71**: 4057-60.

J. Tetenbaum, L.M. Miller (2001). A new spectroscopic approach to examining the role of disulfide bonds in the structure and unfolding of soybean trypsin inhibitor. *Biochemistry*, **40**: 12215-9.

N.S. Marinkovic, R. Huang, P. Bromberg, M. Sullivan, L.M. Miller, E. Sperber, S. Moshe, K.W. Jones, E. Chouparova, S. Franzen, S. Lappi, and M.R. Chance (2002). Center for synchrotron biosciences' U2B

beamline: An international resource for biological infrared spectroscopy. *J. Synchr. Rad.*, **9**: 189-97.

Abstracts:

L.M. Miller, D. Vairavamurthy, A. Vairavamurthy (2000). Disulfide bond formation in the folding of Ribonuclease A monitored by sulfur x-ray absorption spectroscopy. *Biophys. J.*, **78**: 44A.

J. Tetenbaum, L.M. Miller (2001). When bridges collapse: The role of disulfide bonds in the structure and folding of soybean trypsin inhibitor. *Biophys. J.*, **80**: 563A.

J. Tetenbaum, L.M. Miller, L. Yang, J. Ablett (2002). Using Synchrotron Light to Study Solution-State Protein Structure, Folding, and Dynamics. Soft Matter and Biophysics Workshop, Tarrytown, NY, Apr 25-27.

Grant Proposal Pending:

NIH-R01, "Metal ions and protein structure in protein folding diseases" 01/01/03 – 12/31/07, \$600,000.

LDRD FUNDING:

FY 2001	\$43,499
FY 2002	\$43,511
FY 2003 (budgeted)	\$50,000

Soft Condensed Matter Probed by Low-Energy Resonant Scattering

Wolfgang A. Caliebe

01-38

L. Yang

PURPOSE:

The purpose of this LDRD is to apply resonant scattering to the study of soft condensed matter. The resonantly scattering atom is a low Z atom, so that low-energy x-rays between 2 and 3keV have to be used. In resonant scattering, the scattering factor is a tensor, and the intensity of the scattered radiation depends on the dipole moment of the molecule. This allows the measurement of superstructure reflections that are not observable with conventional x-ray scattering techniques. The intensity and position of these superstructure reflections gives important information about the structure of the sample. The successful implementation of this technique will add another important tool for the investigation and study of soft condensed matter.

APPROACH:

Resonant scattering at conventional x-ray energies of 8keV has been proven to be an important tool in the research of magnetic materials, where the orientation of the magnetic moment results in a superstructure of the lattice. An analog in soft condensed matter is for example a thin free-standing liquid crystal film, in which the dipole moment of the molecule points into different directions in different layers. This superstructure has significant influence on the properties of the liquid crystal film and therefore on its technical application. Conventional methods like x-ray diffraction or laser scattering might just indicate the presence of the superstructure, but the actual

periodicity is not accessible. Measuring the superstructure reflections and determining their polarization dependence can solve this problem.

The research on liquid crystal films and similar systems is done in collaboration with Ron Pindak, NSLS, C.C. Huang and Andrew Cady from the University of Minnesota, where the laser scattering experiments are performed, and Philippe Barois from the University of Bordeaux, France.

The focus of the research at the NSLS is resonant scattering with polarization analysis. The main problem is to overcome the problem of absorption of low-energy x-rays by air, but to keep the sample still in a non-vacuum atmosphere. Most organic thin films are not stable in vacuum. Furthermore, the temperature of the films has to be controllable, and the film itself has to be observed with a normal microscope with polarization filters to determine its integrity and phase transitions.

Another important aspect is the development of a polarization analyzer. Most existing polarization analyzers are difficult to align or very heavy. This part is done in collaboration with Peter Siddons, NSLS.

TECHNICAL PROGRESS AND RESULTS:

In several experimental runs at beamline X19a studying liquid crystal films, new materials were investigated, and new methods and experimental configurations were tested.

The major achievements in FY 2001 was the determination of the orientational order in the chiral smectic-C*_{F12} liquid crystal phase. First experiments studying the order of banana-shaped compounds started in the end

of FY 2001. It was possible to make thin films of these compounds and measure superstructure reflections. These samples were studied in more detail in FY 2002 in one experimental run at X19a. The experiment clearly showed that only one of different competing models is possible. However, a polarization analysis of the superstructure reflection is still required to determine some finer details of the structure. These experiments were the first ones performed at the Cl K-edge, opening up a new class of compounds for resonant x-ray scattering.

Significant progress was also made in the investigation of lipid bilayers. The experiments were performed at X21, and a special set-up had to be designed and built. The idea was to first perform experiments off resonance at energies more favorable for diffraction. These experiments require area-detectors, and fast read-out time, so that a CCD-camera had to be used. This type of detector is not practical at low energies since the Be-window absorbs too many x-rays. However, these experiments are a big step forward resonant diffraction of biological materials. The research of lipid bilayers concentrated on an intermediate structure known as a stalk. It is speculated that a stalk is a key step in lipid bilayer fusion. Stable stalk structures were found to exist in a newly discovered lipid phase, where many stalks form a rhombohedral supramolecular crystal. Diffraction patterns from this crystal were measured, and the swelling method helped to determine the phases of the diffraction amplitudes and subsequently to calculate the structure of the stalk. Because of the limitations of the swelling method, additional evidence is necessary to ensure the correct choice of the phases. One possibility is to perform resonant diffraction at phosphor edge so that electron density contrast of the phosphor-containing head-groups of the lipids will be enhanced.

Diffraction amplitudes calculated from the structure obtained under non-resonant condition can now be compared with experiment to check the validity of the chosen phases.

Some progress was also made for the dedicated soft x-ray diffraction set-up. The design of the vacuum-compatible chamber was finished and the chamber and parts for the table ordered. The table and chamber will arrive in spring 2003. A design for a new oven for the diffractometer was also initiated during the summer. First ideas and sketches were compiled by Xifeng Han (Univ. Minnesota) and Lin Yang. This part of the research is financially supported by the NSLS.

The research on lipid bilayers also continues and focuses on the structure of these layers as a function of humidity, temperature. Different proteins and peptides are also added to the bilayers to investigate their influence on the structure.

SPECIFIC ACCOMPLISHMENTS:

Invited Talks:

P. Barois, "Resonant X-Ray Scattering from Smectic C phases with Antiferroelectric Order and Related Subphases in Bulk Geometry," 6th European Conference on Liquid Crystals.

R. Pindak, "Resonant X-Ray Scattering from Antiferroelectric and Ferrielectric Liquid Crystal Films," 6th European Conference on Liquid Crystals.

P. Barois, "Structural Studies of Soft Matter Systems by Resonant Scattering of X-rays – Application to Chiral and Non-chiral Liquid Crystals," *Frontiers for Synchrotron*

Research on Soft Matter and Biomaterials Workshop, Apr. 2002.

Publications:

Orientational ordering in the chiral smectic- C_{F12}^* liquid crystal phase determined by resonant polarized x-ray diffraction, A. Cady, J. A. Pitney, R. Pindak, L. S. Matkin, S. J. Watson, H. F. Gleeson, P. Cluzeau, P. Barois, A.-M. Levelut, W. Caliebe, J. W. Goodby, M. Hird, and C. C. Huang, Phys. Rev. E 64, 050702(R) (2001).

Interlayer structures of the chiral smectic liquid crystal phases revealed by resonant x-ray scattering, L.S. Hirst, S.J. Watson, H.F. Gleeson, P. Cluzeau, P. Barois, R. Pindak, J. Pitney, A. Cady, P.M. Johnson, C.C. Huang, A.-M. Levelut, G. Srajer, J. Pollmann, W.

Caliebe, A. Seed, M.R. Herbert, J.W. Goodby, M. Hird, Phys. Rev. E 65, 041705-1-041705-9 (2002).

Resonant X-ray scattering studies of the B2 phase formed by bent-core molecules, A. Cady, R. Pindak, W. Caliebe, P. Barois, W. Weissflog, H.T. Nguyen, and C.C. Huang, Liquid Crystals, 29, 1101-1104, (2002).

Observation of a Membrane Fusion Intermediate Structure, L. Yang and H.W. Huang, Science, 297, 1877-1879 (2002).

LDRD FUNDING:

FY 2001	\$32,873
FY 2002	\$50,401
FY 2003 (budgeted)	\$50,000

Femto-Seconds Electron Microscope Based on the Photocathode RF Gun

Xijie Wang
M. Babzien
Z. L. Wu

01-39

PURPOSE:

The objective of this work is to explore the photocathode RF gun technology for femto-second time-resolved electron microscope applications, especially the time-resolved electron diffraction. By taking advantage of higher energy and electron beam energy correlations from the photocathode RF gun, our approach would allow us to break the pico-second time barrier for the first time with an electron diffraction.

An electron microscope based photocathode RF gun can produce a high electron beam energy and a shorter electron pulse. Higher energy would make it possible to image bulk material, which is critical for biological applications. A shorter electron pulse will make it possible to study dynamics processes. Furthermore, an electron beam with a bunch length on the order of 100 fs is needed to investigate the deterministic process for chemical reactions (compared to slower, diffuse process). A femto-second electron microscope based on the photocathode RF gun could be used to study atomic rearrangements during the phase transition in condensed matter physics, ultra-fast structure transition in biology, and molecular movements during the chemical reactions.

APPROACH:

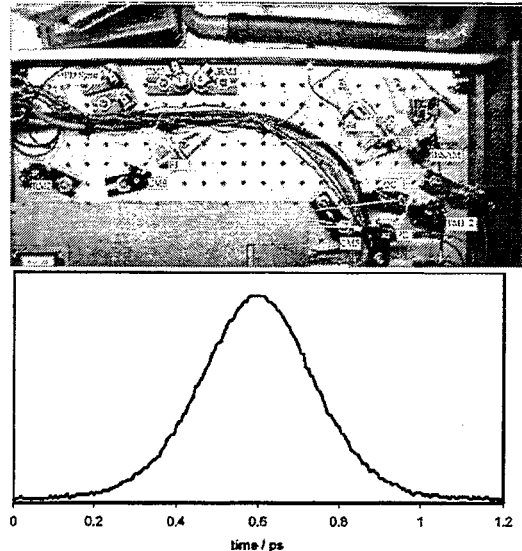
We focused our R&D this year on two fronts. The first is to continue studying the

high-brightness beam physics and technologies, such as photocathode RF gun laser system and ultra-short electron beam generation. The second front is to connect with possible future users to start to make scientific cases for femto-second electron diffraction based on the photocathode RF gun.

TECHNICAL PROGRESS AND RESULTS:

During FY 2002, we carried out R&D on all major components of the proposal:

1. Femto-seconds Yb:glass laser oscillator : We have commissioned a 200 fs (FWHM) (see figure below) Yb:glass oscillator in collaboration with H-Q Laser. Preliminary measurements show sub-picosecond timing jitter and less than 1% energy fluctuation.



2. High-duty factor photoinjector: For future pump-probe type electron diffraction experiment, kilo-Hz operation is preferable. We have carried out high-duty photoinjector R&D for the X-ray free electron laser (FEL) and electron micro-scope. For the X-ray FEL project (such as Linac Coherent Light Source [LCLS] in Stanford Linear Accelerator Facility [SLAC]), 120 Hz at

about 100 MV/m is required. For the electron micro-scope, kilo-Hz at 20 -50 MV/m is the operating condition. The heat load for these two cases is comparable. Our studies show it is possible to operate a photoinjector at kilo-Hz for the electron microscope.

3. Femto-second Kilo-Ampere High-brightness electron Beam: For the first time, we have shown that it is possible to produce an electron beam with 10 femto-second bunch length and peak current of about kilo-Ampere. This could lead to many applications.
4. L-band photoinjector: Our analysis for CW and high-duty factor photoinjector leads to 2.5 cell gun design. This idea now is widely adopted for BNL electron cooling and other projects.
5. Thermal emittance studies: our analysis and experiment show thermal emittance will not be the limiting factor for the performance of the photoinjector.

SPECIFIC ACCOMPLISHMENTS:

X. J. Wang, M. Babzien, X. Y. Chang, D. Lynch, S. Pjerov, M. Woodle, and Z. Wu, S-band High Duty Photo-injection System Proceeding of 2002 European Particle Accelerator Conference, Paris, France. June, 2002.

X. Y. Chang and X. J. Wang, Beam Dynamics Studies for a L-band Photoinjector, Proceeding of 2002 European Particle Accelerator Conference, Paris, France. June, 2002.

F. Zhou, J. H. Wu, X. J. Wang, M. Babzien, I. Ben-Zvi, J. Murphy, M. Woodle, R. Malone, V. Yakimenko, Surface Roughness Wakefield Measurement at Brookhaven Accelerator Test Facility, Proceeding of 2002 European Particle Accelerator Conference, Paris, France. June, 2002.

X. J. Wang, M. Babzien, R. Malone, and Z. Wu, Mg Cathode and its thermal emittance, Proceeding of Linac 2002 conference, Korea, August, 2002.

X. J. Wang and X. Y. Chang, Femto-seconds Kilo-Ampere High-brightness Electron Beam Generation, Proceeding of 2002 Free Electron Laser Conference, Chicago. September, 2002.

P. R. Bolton, J. E. Clendenin, D. H. Dowell, M. Ferrario, A. S. Fisher, S. M. Gierman, R. E. Kirby, P. Krejcik, C. G. Limborg, G. A. Mulhollan, D. Nguyen, D. T. Palmer, J. B. Rosenzweig, J. F. Schmerge, L. Serafini, X. J. Wang, Nuclear Instruments and Methods in Physics Research A 483 (2002) 296-300.

F. Zhou, I. Ben-Zvi, M. Babzien, X. Y. Chang, A. Doyuran, R. Malone, X. J. Wang, and V. Yakimenko, PHYSICAL REVIEW SPECIAL TOPICS - ACCELERATORS AND BEAMS 5, 094203 (2002).

LDRD FUNDING:

FY 2001	\$145,593
FY 2002	\$ 62,119
FY 2003 (budgeted)	\$ 65,000

First Principles Theory of the Magnetic and Electronic Properties of Nanostructures

Michael Weinert

01-45

PURPOSE:

To use first principles Density Functional Theory (DFT) to calculate electronic and magnetic structures of novel materials and nanoscale devices. Then to describe realistically metallo oxide compounds one has to treat electron-electron correlations of the open d shells in transition metals beyond the Local Density Approximation (LDA). Will use a LDA+U functional to model the correlation effects on the mean field level. To keep the *ab initio* status of the theory, it is necessary to provide a unique recipe to calculate input Hubbard parameters for LDA+U functional. For nanoscale devices it is planned to use DFT codes with open boundary conditions to calculate electronic structure of large molecules, which can be used as quantum dots, for example, metallo-porphyrins. Will apply bulk codes to calculate contact properties of the thiolate self-assembled monolayers on noble metal substrates such as Cu, Au, Ag. For instance, the lateral dispersion of the thiolate electronic states can dramatically change conduction properties of the designed devices.

APPROACH:

The electronic and magnetic properties of novel materials depend strongly on the strength of electron correlations. We designed a new scheme to calculate Hubbard parameters to be used in LDA+U mean field like approach or beyond the mean field treatments.

To make a predictive theory of nanoscale devices one has to model a system of few hundreds atoms in size, which is currently well beyond the reach of the first principles methods. To handle the situation, it is necessary to use DFT methods to extract parameters for model Hamiltonian to include kinetic energy, electron correlation effects and electron-phonon interactions. Once the model Hamiltonian is derived the transport properties of molecular wires, quantum dots, and surface properties of the contacts could be modeled using the Green's functions techniques.

TECHNICAL PROGRESS AND RESULTS:

In FY 2001, we used molecular code to calculate Jahn-Teller unstable benzene ions and to formulate the model Hamiltonian on Huckel level including the electron-phonon effects. The model Hamiltonian has been solved nonadiabatically for the vibrational spectrum to agree with the experiment.

In FY 2002, a new method to determine Hubbard parameters was developed. The Hubbard parameters has been extracted for a d shell of Ti atom in fluoride environment using the TiF_6^{2-} ion calculations. The LDA+U solution for electronic and magnetic properties of TiF_3 was found for these parameters.

The important accomplishments can be listed as following: (1) the benzene cation and anion have been solved for the vibrational spectra beyond the adiabatic approximation; (2) the method to calculate the input parameters for the LDA+U functional has been designed and applied to TiF_3 compound; (3) the electronic and magnetic structure of TiF_3 has been predicted and the nature of the observed structural phase transition has been understood.

SPECIFIC ACCOMPLISHMENTS:

None

LDRD FUNDING:

FY 2001	\$88,387
FY 2002	\$89,928

Cryo-EM for Solving Membrane Proteins

James F. Hainfeld

01-50

PURPOSE:

Membrane proteins play a vital role in cell function and are of central importance in many diseases and medical conditions. Such proteins serve as receptors that modulate cell responses, as determinants of immunological character, and as transport channels. Membrane proteins are the targets for 95% of drugs, and they compose about 30% of all proteins.

The structure of membrane proteins has been typically difficult to solve by standard crystal growing and x-ray crystallography techniques such as being used at synchrotrons (e.g., NSLS). This effort has been most successful with non-membrane, water-soluble proteins. This unfortunately leaves the structure of many important proteins and many uncovered by the proteome project inaccessible by standard techniques.

Cryo-electron microscopy (EM) has emerged as a useful tool to solve membrane proteins. Instead of growing relatively large 3-D crystals for x-ray studies, small 2-dimensional arrays or helices of proteins may be analyzed by electron microscopy. Rapid freezing and observation at near low temperatures has been shown to produce the best results, even to atomic resolution.

APPROACH:

This project seeks to establish the Cryo-EM Facility at BNL (which was previously non-existent) to examine frozen-hydrated membrane proteins by electron microscopy,

and to use these methods to solve unknown structures of important membrane proteins.

The scope of this work involved a) instrumentation, b) biochemistry, c) crystal growing, d) data collection, and e) data reduction. For instrumentation, existing EMs on-site were utilized and adapted for cryo work; additionally, cryo-EM facilities at another institution were used. Certain other specialized equipment was also necessary, such as a plunge freezer for preparing samples, a cryo transfer system, and a cold stage with regulated temperature and tilting capability. With respect to the biochemistry, membrane protein samples needed to be isolated and purified in their active state. This is more difficult with membrane proteins, since they require detergent or lipids, making it a two or more component system to handle and more difficult to produce units with atomic regularity for crystallization. Growing suitable crystals was implemented by using dialysis or vapor diffusion and changing a number of variables, such as concentration, salt, detergents, and temperature. Two-dimensional sheets of protein crystals were most desirable for EM work, but proteins can also form regular helical structures on lipid tubes or carbon nanotubes. Therefore, we also investigated the use of carbon nanotubes for growing protein crystals. Data collection consisted of examining the samples by electron microscopy first with negative staining to assess at medium resolution potential crystals. Prospective crystals were then quickly frozen in thin vitreous ice, and examined cold at very low electron dose (to preserve high resolution) along with collection of electron diffraction patterns. Data was transferred for analysis by high resolution scanning of the film plates. Three-dimensional reconstruction algorithms were installed on a multi-processor Silicon Graphics, Inc. (SGI)

workstation for computing and visualizing the protein structure.

TECHNICAL PROGRESS AND RESULTS:

In Year 1 of this project, a number of milestones were achieved: Two existing transmission electron microscopes at BNL were resuscitated, a Philips 300 in the Biology Department, and a JEOL 100CX that had been part of the Reactor Program. A cryo-transfer cold stage, capable of keeping frozen samples at -150°C was obtained and installed on the JEOL 100CX. A number of collaborations were established with other institutions to provide membrane protein samples or assist with this project. This included, Dr. Da-Nang Wang (New York University Medical School) who provided the GABA-receptor membrane protein, and important nerve receptor; Dr. Berhane Gehbrehiwet (Department of Immunology, SUNY-SB) who provided samples of the immune response receptor gC1q; Dr. Rod MacKinnon (Rockefeller University), who provided samples of the K^+ ion pump protein, important in nerve conduction and cell ion control; Dr. Neal Woodbury (Arizona State University), who provided samples of the photosynthetic reaction center protein; Dr. Robert Glaeser (Lawrence Berkeley National Laboratory), who provided samples of the membrane proton pump bacteriorhodopsin; Drs. John Sachs and Dwight Martin (Department of Medicine, SUNY-SB), who provided samples of the ion channel and pump, Na^+ , K^+ , ATPase; Dr. Michael Lewis (Skirball Institute, New York University), who assisted in using their Cryo-EM Facility; and Dr. Stan Wong (BNL and SUNY-SB), who assisted with carbon nanotubes.

Crystallization of the following proteins was attempted using membrane mediated

osmotic diffusion of detergents: 1) GABA-transporter, 2) gC1q-receptor, 3) K^+ pump, 4) photosynthetic reaction center, 5) bacteriorhodopsin, and 6) Na^+ , K^+ , ATPase isolated from the nasal gland of salt water adapted ducklings. Proteins solubilized with various detergent or lipids were placed in a glass tube with a dialysis membrane at one end. This was then placed in a solution containing various buffers (Fig. 1). As the detergent is dialyzed out, protein aggregation/crystallization occurs.

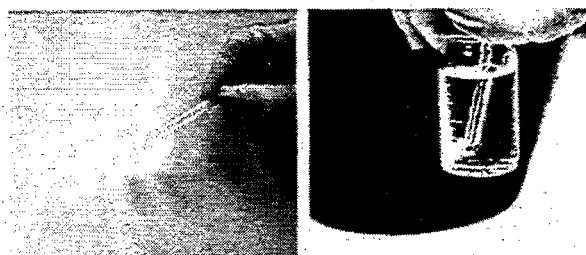


Fig. 1. Crystallization dialysis apparatus

Samples were taken at various time points and examined by electron microscopy (EM). Opalescence and optical rotation under a polarization microscope was observed and in a number of the samples indicated possible crystallization. No suitable high-resolution crystals were found. Crystallization efforts were continued in Year 2.

Carbon nanotubes were produced and purified. These were tested as templates to pattern protein adsorption into regular helical arrays. Although some proteins were adsorbed, the occupancy and ordering were not high enough to perform high-resolution structural determination.

Year 1 also included the starting of construction in BNL Shops of a plunge freezer for rapidly freezing samples that would then be kept cold and inserted into the microscope. This is an important step, since the freezing rate must be high enough to avoid ice crystals that would distort the

sample. The sample is placed on an EM grid, wicked down to a thin layer of water, then rapidly plunged with a pneumatic drive into liquid ethane. The cooling rate obtained produces vitreous ice.

Also, in year 2 the plunge freezer was completed. In year 2 crystallization of membrane proteins was continued, and two additional methods were implemented: a) Samples were suspended as hanging drops on coverslips mounted over wells in multiwell plates. This is a convenient format used by many crystallographers. b) crystals were grown directly on EM grids by floating them on the protein solution and allowing evaporation or diffusion to force insolubility. Both methods produced some crystals (Figs 2-3).

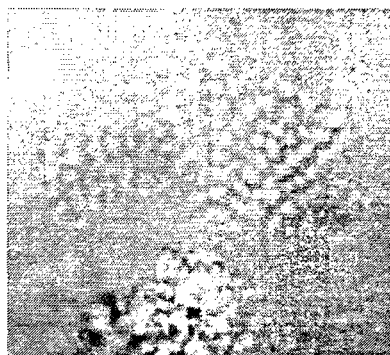


Fig. 2. Birefringent crystals of K⁺ channel. Light micrograph 1250x original magnification.



Fig. 3. Crystals of Na⁺K⁺-ATPase in EM.

However, those suitable for EM must be very thin, typically 1 to 3 unit cells thick, yet several microns in the other dimensions. This restriction eliminated a number of needle-like or thick crystals. Two crystals showing promise were those of bacteriorhodopsin (Fig. 4) and patches of Na⁺K⁺-ATPase (Fig.5).



Fig. 4. Low dose electron micrograph of crystal of the membrane protein bacteriorhodopsin. Note hexagonal edges and crystallinity. (512 nm full width).

The Na⁺K⁺-ATPase structure would be of great interest to solve in various metabolic states. Currently, the crystal patches are too small, and future work is needed to grow larger crystalline sheets so that the number of unit cells is sufficient for high-resolution analysis.

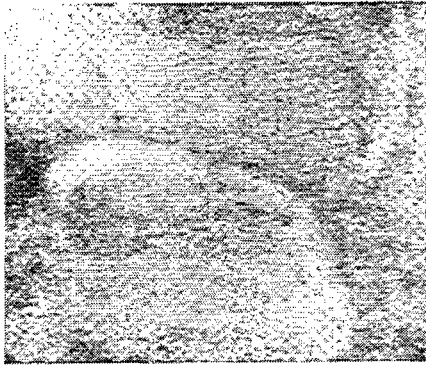


Fig. 5. EM at 100,000X of Na⁺K⁺-ATPase, negatively stained with uranyl acetate; Note crystal planes, but crystals need to be larger for high-resolution data. Full width 200nm.

The cryotransfer stage was modified with a copper specimen capsule to improve the cooling rate compared to original beryllium capsule.

The method for growing crystals directly on grids is now described: Gold EM grids were cleaned, covered with an 8nm holey film and coated with 4-8nm of carbon. The grids were baked for 1-12 hrs at 160°C. Some grids were treated to remove the formvar membrane following the carbon coating. Twenty µL of buffer was placed on a siliconized cover slip and two formvar carbon coated grids were placed on each droplet. Individual wells were sealed with plastic and the trays were incubated undisturbed at 4°C and 21-23°C. Samples were harvested at 19 and 24 hr incubations, and stained with 2% aqueous uranyl acetate (filtered, Millipore 0.22µm filter). An additional method utilized the same hanging drop technique at 20-21°C and 4°C, with the addition of an evaporation step before harvesting the last grid that allowed the droplet with grids to remain in air for 10 min before harvesting the grids. Grids were wicked after 23.5 hrs and 41 hrs incubation, stained with filtered uranyl acetate, and imaged by TEM.

Two computer analysis packages designed for analysis of CryoEM data have been obtained and installed on a SGI workstation in the Biology Dept. One is from the MRC lab in Cambridge, England (IMAGE 2000), and the other is from Wadsworth Center, Albany (SPIDER).

SPECIFIC ACCOMPLISHMENTS:

- Two NIH proposals including aspects of this work were submitted; the first one, P41 Facility Grant Renewal entitled, "STEM Mass Mapping & Heavy Atom Labeling of Biomolecules," J. Wall, Principal Investigator and J. Hainfeld, Co-Investigator, project period: September 30, 2002 – June 30, 2007 was funded. This proposal resulted in two project reviews: NIH STEM Site Visit, Biology Department, BNL, August 27, 2001, Presenters: J. Wall and J. Hainfeld; and NIH STEM Reverse Site Visit, Washington, DC, June 20-21, 2002, Presenters: J. Wall and J. Hainfeld.

LDRD FUNDING:

FY 2001	\$115,949
FY 2002	\$119,346

Human DNA Damage

Responses: DNA-PK and p53

Carl W. Anderson

01-51

PURPOSE:

In all cells, DNA double-strand breaks (DSBs) occur spontaneously and are caused by internal stresses as well as exposures to a variety of environmental insults including ionizing radiation, oxidative stress, metals, and natural and man-made genotoxic substances. In vertebrates, DSBs are repaired by two major pathways, homologous recombination (HR) and the non-homologous end-joining (NHEJ) pathway. The mis-repair of DSBs create mutations and genome rearrangements that may lead to cancer. The objective of this project is to develop and validate methods that will permit a determination of whether mutations and polymorphisms in the NHEJ DNA DSB repair genes result in increased susceptibility to cancer in humans. This objective will be attained through three specific aims. First, we will analyze sequences from several human cell lines surrounding the 86 exons of one of the NHEJ DNA repair genes, *PRKDC*, which encodes the catalytic subunit of the DNA-activated protein kinase, for mutations and polymorphisms. Second, we will develop a method to inactivate one allele of the *PRKDC* gene in human cell lines. This methodology would allow one to determine if a mutant or polymorphic allele in cells of a heterozygote containing one normal allele is defective. Third, in collaboration with others, we will create and analyze endogenous "knock-in" mutations that alter sites of posttranslational modifications in the murine p53 tumor gene. As described below, these studies are expected to lead to follow-on funding that enables a full

characterization of the consequences of both genetic variation in the NHEJ DNA repair system and its interaction with mechanisms that activate the p53 tumor suppressor system in response to DNA strand breaks.

APPROACH:

To test the hypothesis that polymorphisms in human NHEJ genes may be a risk factor for human cancer, DNA sequences from both normal and cancer populations can be analyzed. The sequence of the human *PRKDC* gene and other NHEJ genes, as appropriate, will be validated by analyzing a small number of cell lines that exhibit normal NHEJ function and one cell line that does not. These results are expected to provide necessary preliminary results to support proposals to the NIH or DOE for NHEJ gene polymorphism discovery.

To show that a specific polymorphism affects NHEJ function, it will be necessary to examine human cell lines or mice that are homologous for the sequence variation. To accomplish this task, a method to inactivate one or both alleles of the human *PRKDC* gene in established human cell lines will be developed. Deriving such mutant cells currently is technically challenging; for some genes, inactivating mutations may be lethal.

To examine the interaction of NHEJ and p53 as risk factors for cancer, and to develop methods for testing the role of specific polymorphisms in animals, methods will be developed for creating homozygous mutations in specific amino acids of the p53 gene of mice. These studies will be conducted in collaboration with E. Appella, NCI, NIH, and Y. Xu, University of California, San Diego. It is anticipated that the methods developed for p53 will translate to the murine *PRKDC* gene.

TECHNICAL PROGRESS AND RESULTS:

During FY 2002, efforts concentrated on analyzing the role of posttranslational modifications in regulating p53 activity. The p53 tumor suppressor protein preserves genome integrity by regulating growth arrest and apoptosis in response to DNA damage. In response to ionizing radiation (IR), ataxia telangiectasia mutated (kinase) (ATM), the gene product mutated in ataxia telangiectasia, stabilizes and activates p53 through phosphorylation of Ser15 and (indirectly) Ser20. Phosphorylation of p53 on Ser46, a residue important for p53 apoptotic activity, as well as on Ser9, in response to IR was shown to be dependent on the ATM protein kinase. IR-induced phosphorylation at Ser46 was inhibited by wortmannin, a phosphatidylinositol 3-kinase inhibitor, but not PD169316, a p38 MAPK inhibitor. p53 C-terminal acetylation at Lys320 and Lys382, which may stabilize p53 and activate sequence-specific DNA binding, required Ser15 phosphorylation by ATM and was enhanced by phosphorylation at nearby residues including Ser6, Ser9, and Thr18. These observations, together with the proposed role of Ser46 phosphorylation in mediating apoptosis, suggest that ATM is involved in the initiation of p53-dependent apoptosis after IR in human lymphoblastoid cells.

The mammalian Chk2 kinase is thought to mediate ATM-dependent signaling in response to DNA damage. In collaboration with the laboratory of N. Motoyama, National Institute for Longevity Sciences, Obu, Japan, the physiological role of mammalian Chk2 was investigated by generating Chk2-deficient mice. Although *Chk2*^{-/-} mice appeared normal, they were resistant to ionizing radiation (IR) as a result of the preservation of splenic lymphocytes.

Thymocytes and neurons of the developing brain also were resistant to IR-induced apoptosis. The IR-induced G₁/S cell cycle checkpoint, but not the G₂/M or S phase checkpoints, was impaired in embryonic fibroblasts derived from *Chk2*^{-/-} mice. IR-induced stabilization of p53 in *Chk2*^{-/-} cells was 50 to 70% of that in wild-type cells. Caffeine further reduced p53 accumulation, suggesting the existence of an ATM/Ataxia telangiectasia (mutated)-related (kinase) (ATR)-dependent but Chk2-independent pathway for p53 stabilization. In spite of p53 protein stabilization and phosphorylation of Ser23, the murine equivalent of Ser20 in human p53, p53-dependent transcriptional induction of target genes, such as p21 and Noxa, was not observed in *Chk2*^{-/-} cells. These results show that Chk2 plays a critical role in p53 function in response to IR by regulating its transcriptional activity as well as its stability. The work has potential implications for the development of countermeasures for long-duration space flight.

In collaboration with S. Kenney, Lineberger Cancer Center, University of North Carolina, the effect of the Epstein-Barr virus (EBV) immediate-early protein BZLF1 on p53 activation was examined to further characterize the role of p53 posttranslational modifications in cancer. BZLF1 is a transcriptional activator that mediates the switch between the latent and lytic forms of EBV infection, and BZLF1 inhibits p53 transcriptional function in reporter gene assays. We examined the effects of BZLF1 on p53 function using a BZLF1-expressing adenovirus vector, AdBZLF1. Infection of cells with AdBZLF1 increased the level of cellular p53 but prevented induction of p53-dependent cellular target genes such as p21 and MDM2. BZLF1 expressing cells had increased p53 DNA binding activity in

electrophoretic mobility shift assays (EMSA), increased p53 phosphorylation at multiple residues (including serines 6, 9, 15, 33, 46, 315, and 392), and increased acetylation on lysines 320 and 382. The inhibitory effect of BZLF1 on p53 transcriptional function cannot be explained by its effects on p53 phosphorylation, acetylation, or DNA binding activity. Instead, BZLF1 substantially reduced the level of cellular TBP in both normal human fibroblasts and A549 cells, and the inhibitory effect of BZLF1 on p53 transcriptional function could be partially rescued by over-expression of TATA-binding protein (TBP). Thus, BZLF1 has numerous effects on p53 post-translational modifications but likely inhibits p53 transcriptional function in part through an indirect mechanism involving suppression of TBP expression.

Analysis of the human *PRKDC* and *KU80* genes for polymorphisms is continuing. Primers for amplification of the 20 exons of *KU80* were prepared and validated using DNA from four cell lines. No coding polymorphisms were found; however, the first nucleotide of the first exon is heterozygous for C and T in all four-cell lines.

During FY 2003 primers to amplify segments containing the unique exons of *KARP1*, a radiation inducible product related to *KU80*, and additional *PRKDC* exons will be designed and validated. Polymorphism analysis of the *KU80* and *PRKDC* genes from 12 human breast cancer patients will be completed, six of which exhibit a phenotype of chromosomal breakage in response to ionizing radiation. Efforts will begin to develop knockout human cell lines lacking functional *PRKDC* genes. The use of RNAi techniques to phenotypically block Ku or DNA-PK_{cs}

expression will be explored. The analysis of p53 phosphorylation in response to genotoxic and non-genotoxic stress agents will continue to evaluate apparent differences in response between mice and men.

SPECIFIC ACCOMPLISHMENTS:

Publications:

Anderson, C.W.; Dunn, J.J.; Freimuth, P.; Galloway, A.M.; and Allalunis-Turner, M.J. Frameshift mutation in *PRKDC*, the gene for DNA-PK_{cs}, in the human, DNA repair-defective, glioma-derived cell line M059. *J. Radiat. Res.* 156, 2-9 (2001).

Saito, S.; Goodarzi, A.A.; Higashimoto, Y.; Noda, Y.; Lees-Miller, S.P.; Appella, E.; and Anderson, C.W. ATM mediates phosphorylation at multiple p53 sites, including Ser46, in response to ionizing radiation. *J. Biol. Chem.* 277, 12491-12494 (2002).

Takai, H.; Naka, K.; Okada, Y.; Watanabe, M.; Harada, N.; Saito, S.; Anderson, C.W.; Appella, E.; Nakanishi, M.; Suzuki, H.; Nagashima, K.; Sawa, H.; Ikeda, K.; and Motoyama, N. Chk2-deficient mice exhibit radioresistance and defective p53-mediated transcription. *EMBO J.* 21, 5195-5205 (2002).

Mausser, A.; Saito, S.; Appella, E.; Anderson, C.W.; Seaman, W.T.; and Kenney, S. The Epstein-Barr virus immediate-early protein, BZLF1, regulates p53 function through multiple mechanisms. *J. Virol.* (2002, in press).

LDRD FUNDING:

FY 2001	\$167,158
FY 2002	\$124,613
FY 2003 (budgeted)	\$105,000

Molecular Mechanisms Underlying Structural Changes in the Adult Brain: A Genetic Analyses

John J. Dunn

01-52A

PURPOSE:

One goal of this project is to develop methods for Serial Analysis of Gene Expression (SAGE) which use only small quantities of starting material, such as those obtained from brain punch biopsies. Another goal is increasing the length of the sequence tags to provide absolute identification of transcripts. During FY 2001-2002, a modified version of SAGE, called Long SAGE, was developed which generates 21-base long tags rather than the 14-bp long tags that are obtained following the published protocol. This advancement in SAGE technology greatly reduces the ambiguities associated with linking tags to expressed sequences since the probability of encountering a tag sequence at random decreases from once every 4^{14} or 2.68×10^8 bases for 14 base long tags to 4^{21} or 4.39×10^{12} bases when the tags are generated using the Long SAGE protocol. The uniqueness of these 21 bp tags allows them to be directly aligned to the draft human sequence with a high level of specificity. The correspondence of tag position relative to known and *ab initio*-predicted genes in draft sequences allows for direct validation of gene predictions, as well as identification of expressed regions that might have been overlooked without experimental data. This dramatic increase in tag length suggested to us that a Long SAGE DNA-based approach should allow for simultaneous detection, as well as quantification, of all the genomes present in a microbial assemblage.

Furthermore, this direct profiling of DNA in microbial communities would sample both cultivatable and currently uncultivable organisms and at the same time provide the sequence for probes that could be used to identify cloned segments of novel genomes in appropriate libraries. We have termed the method GST for Genomic Signature Tags.

APPROACH:

For many years our group has been involved in developing technologies based on the genetic elements of bacteriophage T7 in general and T7 RNA polymerase in particular. T7 RNA polymerase provides a means for unbiased amplification of low-abundance RNA samples, such as those obtained from brain punch biopsies. In collaboration with Dr. Wadi Bahou at SUNY-SB, we are studying the ability of T7 RNA polymerase to linearly amplify small amounts of RNA. Our preliminary results indicate that one round of amplification yields a 10^3 -fold high-fidelity increase in that amount of starting mRNA and two rounds yields about a 10^5 -fold increase. While this work was in progress, we also developed our Long SAGE protocol and verified the methodology by producing and sample sequencing a Long SAGE test library derived from a human erythroid leukemia cell line.

TECHNICAL PROGRESS AND RESULTS:

Two basic principles underlie the SAGE methodology: (i) a short sequence tag from a defined position contains sufficient information to uniquely identify an mRNA and (ii) the linking together of tags in a serial fashion allows for an increased efficiency in sequence-based analysis.

As mentioned above, a major breakthrough

in SAGE technology was achieved which generates 21-base long tags. This increase in tag length necessitated rewriting our SAGE analysis computer algorithms. We then expanded our analysis to include in silico Signature Analysis of Signature Tags (SAST) analysis of 21-base long tags derived from completely sequenced bacterial genomes listed in The Institute of Genetic Research's (TIGR) database. These computer simulations revealed that 21 base long SAST tags can distinguish closely related bacterial species from one another. This ability to interrogate the DNA of related strains and obtain a direct read out of the sequence tags has potential utility in our efforts to detect and respond to biological terrorism.

Summary: Long SAGE and SAST tags are important new methods to profile gene expression and genomic diversity. We are collaborating with several laboratories to verify the SAST technology and are attempting to obtain DOE support for using SAST for surveillance and identification of potential biological warfare agents.

SPECIFIC ACCOMPLISHMENTS:

A patent disclosure covering the emerging GST technology has been filed with BNL's Office of Economic Development and Technology Transfer ("Genome Sequence Tags," filed U.S. Patent Office, April 1, 2002, Serial Number 10/113,916, Inventors: J. Dunn, D. van der Lelie, and M. Krause). Both Long SAGE and GST were presented as enabling technologies at a meeting with funding managers at DOE Headquarters on November 6, 2001. This was followed by a presentation on November 9, 2001, to the BSA Science and Technology Steering Committee as part of a new initiative to develop a Center for the Molecular Analysis of Microbial Communities (CMAMC)

within the Biology Department. This work also formed the core for a large, multi-institution project to dramatically extend scientific and technical understanding of the genetic and metabolic diversity of the rhizosphere communities associated with maize and poplar that was submitted on April 2, 2002, in response to the DOE Program Announcement LAB 02-13 "Genomes to Life." This proposal entitled, "Diversity, Structure and Functional Interdependence of Microbial Communities in the Plant Rhizosphere," was not funded but did result in a DOE Reverse Site Visit in Washington, D.C. on May 30, 2002.

Publications:

- Dunn, J.J.; McCorkle, S.R.; Praissman, L.A.; Hind, G.; van der Lelie, D.; Gnatenko, D.V.; and Krause, M.K. Genomic signature tags (GSTs): A system for profiling genomic DNA. *Genome Res.* 12,1756-1765 (2002).
- Dunn, J. and van der Lelie, D. Diversity, Structure and Functional Interdependence of Microbial Communities in the Plant Rhizosphere. Informal Report BNL-52655 (2002).
- Gnatenko, D.V.; Dunn, J.J.; McCorkle, S.R.; Weissmann, D.; Perotta, P.; and Bahou, W.F. Transcript profiling of human platelets using microarray and serial analysis of gene expression. *Blood* (2002, in press).

LDRD FUNDING:

FY 2001	\$117,218
FY 2002	\$117,111

Catalytic Microcombustion Systems

C.R. Krishna

01-58A

PURPOSE:

Portable power generation systems of much higher energy densities than batteries are being sought to power computers, communication equipment, etc. by the military and also by commercial manufacturers for obvious reasons. This effectively requires, at least at the present juncture, using a petroleum liquid fuel and a miniature fuel cell or heat engine to convert the chemical energy to electric power. The goal of the project is to lead towards the development of a liquid fueled microcombustion system, which is at the heart of a miniature heat engine, more specifically a heat engine that uses a thermoconversion module, such as thermophotovoltaics (TPV), operating at ambient pressures. The objective is to provide a solution to the problems inherent in all components of such a combustion system, including fuel and air metering, injection and mixing; ignition; stable combustion in small combustion volumes; and from potentially excessive heat losses. The nature of the problems are both fundamental in scope in some of the processes and systemic to the whole. A successful completion could result in the development of new programs, for example with Defense Advanced Research Project Administration (DARPA), and complement the thermophotovoltaic initiative in the BNL institutional plan.

APPROACH:

We have previously investigated different types of fuel injection systems for different

fuels. Also, atomization techniques for small fuel flow rates have been pursued culminating in an air atomizer being adapted for the TPV system by Dr. Thomas A. Butcher who is a collaborator on the project. The current project requires the development of an injection system, which will operate at an even lower flow rate and which also has a lower parasitic loss. A variety of injection schemes were considered for the microcombustor before a capillary pump injection system was decided upon.

Based on the requirements defined by DARPA, and on the possible efficiencies of thermoelectric conversion achievable, it was calculated that a combustor fuel input of about 800 watts would be a reasonable design goal for the first attempt.

TECHNICAL PROGRESS AND RESULTS:

A capillary injection system was chosen from the samples available from a vendor to provide a fuel input of 1.27 ml per minute of diesel fuel corresponding to the design input of 800 watts. A cylindrical combustion chamber configuration was chosen and designed to give combustion intensity typical of small combustion systems. The small combustion system necessarily means a large surface to volume ratio and hence larger than normal heat losses potentially. Hence, it was decided to design the combustor with an annular outer wall and the air required for combustion was brought in through this annulus. This provides for regenerative heating of the air under steady operation and this preheat contributes to stable combustion. Such air preheating is also expected to increase system efficiency. For the laboratory tests, the air was supplied from a compressed gas cylinder. The combustor was instrumented with a number

of thermocouples on the walls. Two series of tests were run with the combustor axis horizontal and with the axis vertical to see whether the DARPA requirement of insensitivity to orientation was realized.

Figure 1 below shows the temperatures at various locations as the combustor is operating with the axis vertical. Similar results were obtained with the axis horizontal.

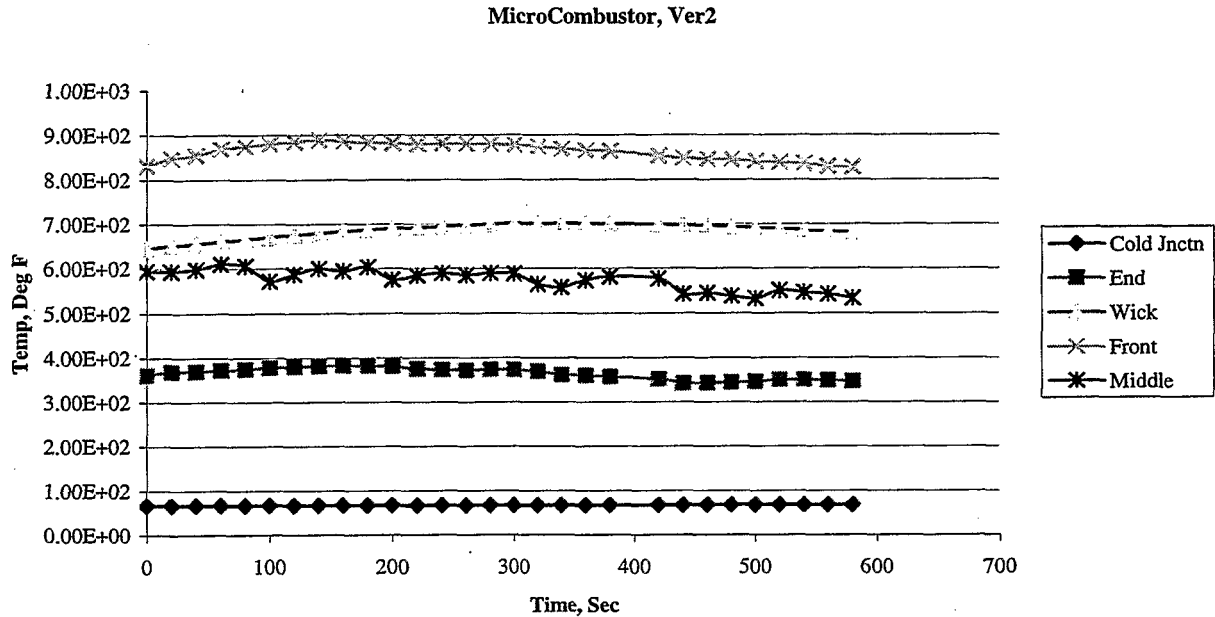
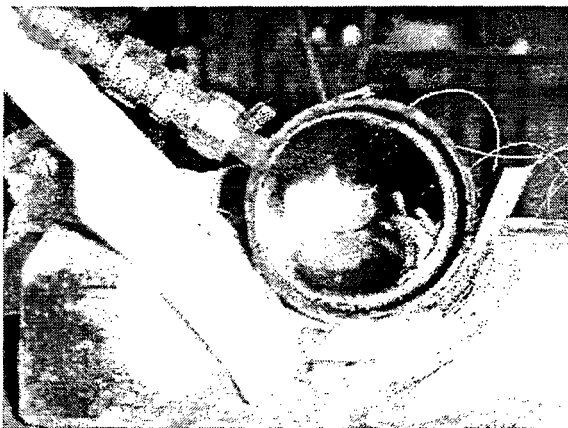


Figure 1.

Below is a photograph of the flame in the combustor with the axis horizontal. The non-uniformity of the flame volume is probably the result of non-uniform air injection and is indicative of one of the areas for improvement in the design. There are other areas needing improvement as well, as suggested by the testing.



SPECIFIC ACCOMPLISHMENTS:

None

LDRD Funding:

FY 2001	\$ 93,108
FY 2002	\$ 95,677

Mapping Electron Densities in Porphyrin Radical Crystals Using the NSLS

Kathleen M. Barkigia

01-62

PURPOSE:

Porphyrins are tetrapyrrole derivatives that mediate a spectrum of bioenergetic reactions ranging from solar photosynthetic energy transduction to conversion of carbon dioxide into fuel. Porphyrin cation radicals, i.e. oxidized porphyrins in which an electron is removed from the macrocycle rather than the metal, are important intermediates in the catalytic cycles of heme proteins and in photosynthetic processes. The objective of this work is twofold, namely to assess the stereochemical consequences of oxidation in porphyrin radicals at high resolution and high precision and to determine actual orbital occupancies of the metals and electron populations of the atoms that comprise the porphyrin skeleton. There are no electron density studies on radicals of any type in the literature and only a few such studies on porphyrins themselves.

APPROACH:

As part of the Porphyrin Chemistry Program (headed by Jack Fajer), we have designed a variety of biomimetic porphyrin radicals to address the consequences of oxidation in vivo. Building on methods for determining crystal structures at the NSLS that we have already implemented, we have broadened our scope to include extremely high-resolution data collection at beamline X3A1 at 20K. Our approach is systematic and entails comparison of the overall structures and derived electron populations from porphyrin radicals and their neutral precursors.

The research was conducted in collaboration with Mark Renner (Materials Science Dept., BNL) who prepared the crystals, Philip Coppens, an expert in charge density analysis (SUNY Buffalo) and Guang Wu, the beamline scientist at beamline X3A1. We thank Jean Logan (Chemistry Dept., BNL) for assistance with calculating d-orbital populations.

These experiments are performed entirely at the NSLS making innovative use of BNL facilities. They offer several fundamental advantages over conventional X-ray techniques. Among them are: 1) a highly intense X-ray beam eliminating the need for big crystals, 2) fast data collection on area detectors at 20K retarding crystal decomposition and enabling high data redundancy, and 3) short wavelength (0.394Å and 0.643Å) for maximizing resolution.

TECHNICAL PROGRESS AND RESULTS:

In FY2001, we collected and analyzed data on several porphyrin radicals and neutral precursors. These^a included the ZnOEP⁺ClO₄⁻ radical dimer, neutral Co-OETPP, two CoOETPP π -cation radicals, radical (dmf)(H₂O)Fe(III)-OETPP²⁺(ClO₄⁻)₂ and neutral (i-PrOH)₂Fe(II)(NO₂)₈TDCPP with an unusual high spin state. For the radicals, they represent the highest resolution X-ray data ever measured. Typical resolution for porphyrin radical datasets previously reported is ~0.75Å; the resolution on some of these data extends as far as 0.45Å.

Results from FY2002 are:

1. NiOEP (ruffled tetragonal form)

The results of two multipole refinements from data measured at 0.394Å and 0.643Å

are summarized in Table 1, along with the resolution of the data sets (0.32Å and 0.50Å) and the final agreement indices (0.027 and 0.021). The populations of the d-orbitals are in excellent agreement with each other, but differ slightly from the values predicted by ligand field theory for low spin Ni(II). Most notably, there is some electron density in the dx^2-y^2 orbital, where ligand field theory predicts none and depletion in the dxz, dyz orbitals; this can be explained by covalency effects.

	NiOEP ($\lambda=0.394\text{\AA}$)	NiOEP ($\lambda=0.643\text{\AA}$)
data/parameters	32/1	22/1
R-factor	0.027	0.021
resolution	0.32Å	0.50Å
dx^2-y^2 %	14 [0]*	9
dz^2	21 [25]*	24
Dxy	24 [25]*	28
Dxz,dyz	41 [50]*	40

*expected for Ni(II) with low spin d^8 configuration

2. ZnOEP(py) and ZnOEP⁺ClO₄⁻

The ZnOEP⁺ClO₄⁻ radical exhibits an unusual pattern of short and long bond alternation in the inner 16-member ring; this effect has been attributed to mixing of the two highest occupied orbitals and a pseudo Jahn-Teller distortion. In contrast, the bond distances in ZnOEP(py) for each bond type are remarkably equivalent and do not vary. Bond distances for both are compared in Table 2. In order to better understand the bonding in the radical and the electron populations at each of the atoms of the porphyrin, we have initiated electron density calculations. A model electron density map calculated after a multipole refinement is presented in Figure 1.

Table 2. Comparison of Bond Distances in ZnOEP⁺radical and neutral ZnOEP(py) at 20K

	ZnOEP ⁺	ZnOEP(py)
Zn-N	2.066(1)	2.070(2)
C α -N	1.353(2)	1.371(2)
C α -N	1.390(2)	-
C α -C m	1.382(2)	1.395(3)
C α -C m	1.427(2)	-
C α -C β	1.471(2)	1.453(2)
C β -C β	1.369(2)	1.365(3)

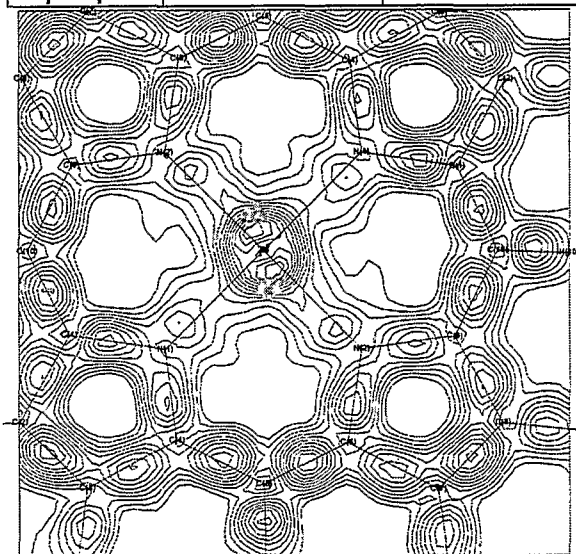


Figure 1. Electron density in the plane of the nitrogens for ZnOEP⁺ClO₄⁻

3. Co(III)OETPP(im)₂(PF₆)

As part our efforts to assess the consequences of oxidation in Co(II) porphyrin radicals, we studied the related Co(III) cation, where the electron is abstracted from the metal, rather than from the porphyrin π -system. The results in the form of linear displays (Figure 2) contrast the dramatic changes in conformation upon oxidation of the neutral porphyrin to the radical vs. oxidation of the metal to Co(III).

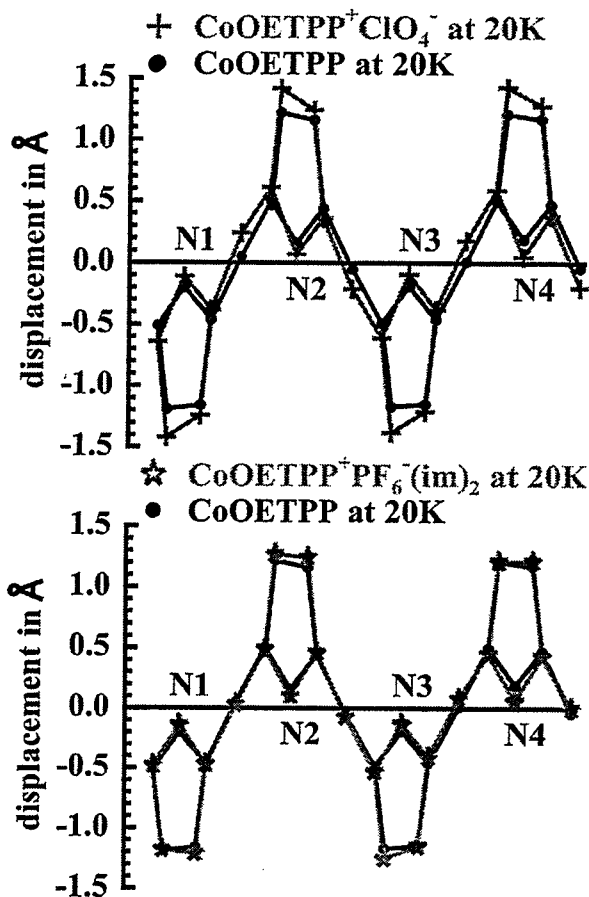


Figure 2. Linear displays of the displacements of the atoms of the porphyrin from the 24-atom plane of the macrocycle. The horizontal axis is not-to-scale.

4. NiOEP⁺ClO₄⁻

Preliminary analysis of this radical clearly indicates that the unusual bonding pattern in ZnOEP⁺ is not observed.

5. Other compounds studied

In addition, we have collected high resolution data at 20K for (n-PrOH)₂Fe(II)-(NO₂)₈TDCPP, another Fe(II) species in the rare high spin state and planar triclinic NiOEP. At lower resolution, we have characterized two chlorin (hydroporphyrin) radicals and their neutral precursor.

^aAbbreviations: OEP (octaethylporphyrin); OETPP (octaethyltetraphenylporphyrin);

TDCPP (tetra-2,6-dichlorophenylporphyrin); DMF (dimethylformamide); i-PrOH (isopropanol); py (pyridine); im (imidazole), n-PrOH (n-propanol).

SPECIFIC ACCOMPLISHMENTS:

Results were presented at the 25th DOE Solar Photochemistry Research Conference, sponsored by the Office of Basic Energy Sciences, June 9-12, 2002.

K.M. Barkigia, M.W. Renner, and G. Wu, "Mapping electron densities in porphyrins from high resolution x-ray data," poster #2.

M.W. Renner, K.M. Barkigia, K.M. Smith, and J. Fajer, "Structural consequences of oxidation in nonplanar chromophores. Molecular structures of a Co(II)porphyrin, its Co(II) π -cation radical and Co(III)cation at 20K," poster #35.

LDRD FUNDING:

FY 2001	\$29,102
FY 2002	\$69,694

High Sensitivity Mass Spectrometer

Peter E. Vanier

01-67

J. Warren

L. Forman, SUNY Stony Brook

PURPOSE:

The aim of the project is to demonstrate a significant improvement in signal strength from a 90-degree sector magnetic mass spectrometer by extracting more ions from the ionization volume using multiple slits and combining the resulting signals in the detection plane by means of a coded aperture approach. The advantage of multiple ion beams within a single analyzing permanent magnet should lead to more compact designs of fieldable mass spectrometers for detection of explosives and illegal drugs.

APPROACH:

The concept grew out of previous work on thermal neutron imaging with coded apertures, in which non-focusable radiation passing through multiple openings casts a shadow that can be mathematically processed to reconstruct the image of the original source. Although the ions created at one end of a magnetic sector mass spectrometer can be focussed on a detector at the other end, there is an inherent limitation in performance due to the width of the source slit and the analyzing slit. These slits simultaneously control the mass resolution and the detected beam current. Using an extended source and multiple slits, spaced according to an algorithm that generates a Uniformly Redundant Array, the total beam current can be increased significantly without loss of mass resolution. The advantage obtained is roughly equivalent to operating several identical mass spectrometers simultaneously and

combining their individual signals. The multiplexing of these signals does not add to the weight of the single-beam instrument. The use of high-performance permanent ceramic magnets allows the necessary field strengths to be achieved without excessive weight or power consumption.

TECHNICAL PROGRESS AND RESULTS:

In FY 2001, a commercial ion source was tested with one wide slit to verify that it produced a beam wide enough to be divided into multiple high-resolution beamlets with reasonable uniformity. Computer simulations were performed to model the source focussing. A new set of coded source slits and a set of analyzer slits were fabricated out of silicon using anisotropic wet etching. A vacuum pumping station was purchased, and a prototype spectrometer was designed. Permanent magnets for the analyzer were designed and purchased.

In FY 2002, the magnets were tested for field strength and uniformity, and deemed to be adequate for the prototype design. The main spectrometer components, including a 90-degree sector and a multiple-port ion-detection chamber were fabricated. A programmable pico-ammeter was purchased from Keithley Instruments to measure the ion currents and transfer digital outputs to the controlling computer. A compact, integrated power supply to provide accelerating and focussing voltages under computer control was constructed for the source. Software to adjust all the voltages, scan the mass, and acquire the current readings was developed using National Instruments' "LabView" graphical programming application. Initial testing of the system with a single slit showed successful creation, focussing and transport of an ion beam through the 90-degree sector and separation of residual gas ions into a

mass spectrum. The hardware and software were shown to be very flexible for carrying out a variety of experiments such as detecting the ion beam with a suspended wire collector. Achieving this capability was a major step towards testing the basic principle of the proposal. Full-blown proposals for a new project can now be submitted to interested agencies in order to exploit this equipment.



Figure 1. Peter Vanier and Leon Forman with Coded Slit Mass Spectrometer (CoSMaS) experimental equipment. Micrograph shows pattern of coded aperture fabricated from silicon (in round boxes) by John Warren. Black box under laptop computer contains custom-built power supplies for spectrometer, at lower right.

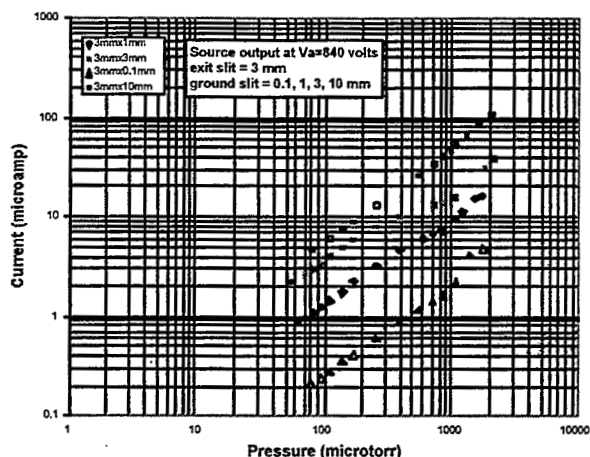


Figure 2. Dependence of signal intensity on residual gas pressure at different slit widths. The coded aperture makes use of the ions available to a wide slit, but maintains the mass resolution of a narrow slit. This data shows a factor of 6 increase in current is feasible.

SPECIFIC ACCOMPLISHMENTS:

White paper entitled "Compact Coded Slit Mass Spectrometer (CoSMaS)" submitted to DOE/NA-22, March 2002.

LDRD FUNDING:

FY 2001	\$117,574
FY 2002	\$120,988

Development and Application of Cavity Ringdown Spectroscopy to the Detection and Monitoring of Trace Chemical Species in the Atmosphere

Arthur J. Sedlacek

01-78

PURPOSE:

The objective of this LDRD project was to develop and evaluate a fieldable instrument based on the Cavity Ringdown technique for the ultra-high sensitivity detection of trace atmospheric species. The proposed work focused on the detection of ambient mercury vapor (parts-per-trillion levels) and the examination of the efficacy of cavity ringdown (CRD) towards the real-time detection and monitoring of ambient ammonia.

APPROACH:

Over the past decade a new technique known as CRD spectroscopy has provided practitioners of absorption spectroscopy a tool to realize parts-per-billion (ppb) to parts-per-trillion (ppt) detection sensitivities without complex modulation techniques. CRD spectroscopy has been able to achieve this level of sensitivity because this approach measures the *rate of absorption* rather than directly monitoring the change in the probe light intensity. By measuring the rate of absorption, the CRD measurement process becomes independent of light source intensity fluctuations thereby increasing attainable detection sensitivities.

In CRD, a monochromatic light pulse is injected into a high Q-value optical cavity.

A detector is positioned at the exit end of the cavity to monitor the light leakage of the injected light pulse per round trip. Using very highly reflective mirrors, the injected laser pulse will make several thousand round trips between the two cavity mirrors. Each round trip will result in a slight loss of intensity due to transmission losses at each mirror and other finite losses in the system. This loss will follow a simple exponential decay. When an absorbing sample is then placed in the cavity, the loss per round trip will exceed that of the empty cavity thereby resulting in a different decay. When this measurement is conducted as a function of wavelength, a high-sensitivity absorption spectra can be reconstructed for a given chemical species. The time necessary for the intensity (amplitude) of the injected light pulse to decay to $1/e$ of its initial value is referred to as the "ringdown" time, and from which this spectroscopy derives its name. Typically, the decay time to the $1/e$ value is on the order of tens of microseconds, but is very dependent upon the reflectivity of the mirrors. Consequently, a CRD signal is collected for each laser pulse and subsequently averaged until the desired signal-to-noise ratio (SNR) is achieved.

TECHNICAL PROGRESS AND RESULTS:

During FY 2001, efforts focused on the construction of a deep-ultraviolet cavity ringdown system and examining the efficacy of this technique towards the *open-path*, real-time detection of ambient ammonia. As ammonia's basic nature and high water solubility make it a significant player in atmospheric chemistry, the ability to monitor this chemical species is of great interest in the atmospheric community. This examination revealed that an open-path CRD system should be able to realize the detection of ammonia at the 10^5 of part-per-trillion loading levels in the atmosphere.

This ultra-high sensitivity can be achieved, in part, because of the large absorption cross-section of ammonia in the mid-IR, and the availability of very highly reflective mirrors that can approach 0.99995.

Activities during this second and final year of support focused on the detection of ambient levels of elemental mercury in air. Since levels of elemental mercury are typically on the order to 10s of parts per trillion, it's detection is ideally suited for the CRD technique.

Shown in figure 1 is a plot of two representative CRD signals collected "on" and "off" the Hg atomic absorption line centered at 253.65 nm. As can be seen in the plot, the rate of decay ("ringdown") is slightly faster for the "on" resonance measurement. Shown in the inset is a plot of the measured ringdown time as a function of excitation wavelength. It should be noted that because of the many different Hg isotopes and pressure broadening, the nominal linewidth of the Hg transition is ~ 0.9 cm⁻¹ full width at half maximum (FWHM).

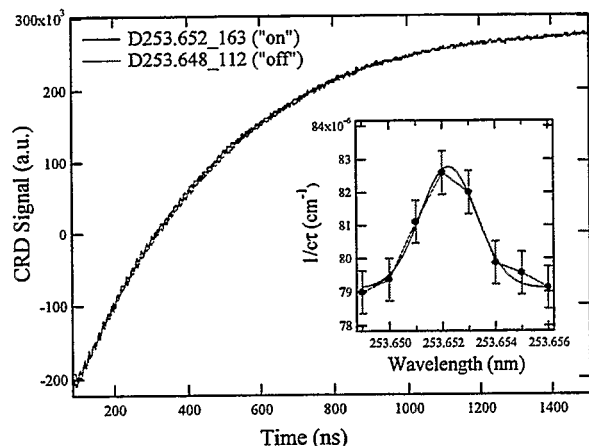


Figure 1: CRD signal for ambient levels of Hg. Inset: 1/ringdown time vs. laser wavelength.

Based on this data and the present state-of-the-art for mirror coatings (which directly impact the sensitivity of the CRD technique)

the following sensitivity curve for elemental Hg detection was developed.

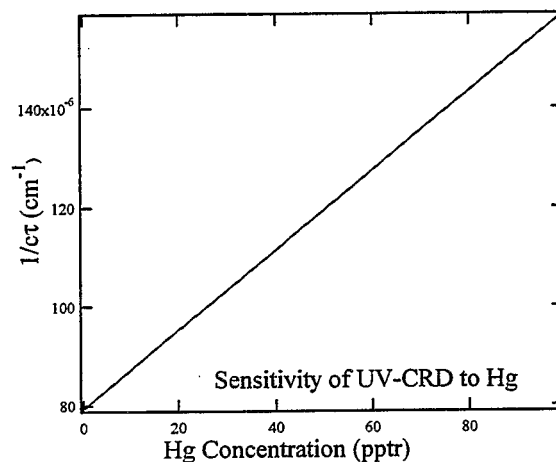


Figure 2: CRD sensitivity towards elemental Hg

These experiments revealed that the CRD technique is mature enough for deployment as an ambient ammonia chemical sensor. This conclusion is based on the coupling the very large IR absorption cross-section with the very high reflectivity mirrors available in the mid-IR (>99.999%). Furthermore, the availability of high-efficiency, small footprint, tunable, quantum cascade diode lasers make an ambient ammonia sensor based on the CRD technique a low-risk development effort. While the latter point represents an engineering issue, for field deployment, such issues must be considered. This is perhaps best illustrated when considering the detection of ambient elemental Hg. Work performed under this LDRD has confirmed that UV-CRD is a viable technique for the detection of low parts-per-trillion loading of Hg. This detection sensitivity was achieved primarily because of the exceedingly large atomic absorption cross-section at 253.65 nm; nominally 3.3×10^{-14} cm²/atom. However, in poignant contrast to the ammonia case, the state-of-the-art cavity mirrors available for the deep UV are only 99.8% reflective, which translates to limited dynamic range and lower limit sensitivity. Specifically, 99.8% mirrors give an empty ringdown time

(1/e) of ~800 ns. Thus, measurement of the decrease in the ringdown becomes limited by the speed of the detector/electronics subsystem and the bit resolution of the Analog to Digital (AD) converter (i.e., trade off between speed and signal resolution). Another issue with respect to a fieldable Hg detector is the laser source. Experiments conducted under this LDRD utilized Optical Parametric Oscillator/Optical Parametric Amplifier (OPO/OPA) technology to reach the desired atomic transition of Hg. However, the very large size and hypersensitivity of this type of laser system to vibrations and alignment effectively limit its use as a laser source to the laboratory. A far better choice is a tripled Alexandrite laser as this source has many favorable attributes such as being all solid-state and of straightforward, robust design.

Of the issues often brought up with respect to field deployment of CRD-based detectors is the sensitivity of the system to alignment. While this is still very much a concern for the “traditional” approach of injecting the laser pulse through the center of the CRD cell, work recently published by other researchers in CRD have demonstrated that an off axis injection of the laser pulse into the cell can eliminate this technique’s hypersensitivity to alignment. The other issue raised regarding field deployment is cleanliness of the cavity mirrors. While this will always remain a valid concern, schemes involving filtering and nitrogen flow across the mirror surface are easy to envision lengthening the time between cleanings.

Using the data collected under this LDRD, the PI will pursue solicitations in the areas of environmental monitoring and clean-up and other related research areas. In addition, the PI will be analyzing samples collected at a NJ/EPA harbor drudge site for trace Hg.

ACCOMPLISHMENTS:

- Presentation of UV-CRD technique for Hg detection at an EPA-sponsored Optical and Remote Sensing Workshop, July 29-31, 2002
- White paper submitted to EPA office in NJ on UV-CRD for Hg monitoring of waste incineration.
- UV-CRD system successfully built and tested for the detection of parts-per-trillion levels of Hg.

LDRD FUNDING:

FY 2001	\$ 86,743
FY 2002	\$ 89,625

Development of a High Field Magnet for Neutrino Factory Storage Rings

Ramesh Gupta
B. Parker

01-79

PURPOSE:

The purpose of this LDRD was to develop a dipole magnet design that allows a compact Neutrino Factory Storage Ring. The magnet design minimizes the energy deposition on the superconducting coils due to showers initiated by muon decay products. A compact storage ring minimizes the environmental impact by keeping the entire machine above the ground water table at BNL. The applications of such magnet designs go well beyond that of a Neutrino Factory. In particular, they are applicable in the interaction region magnets of next generation hadron colliders.

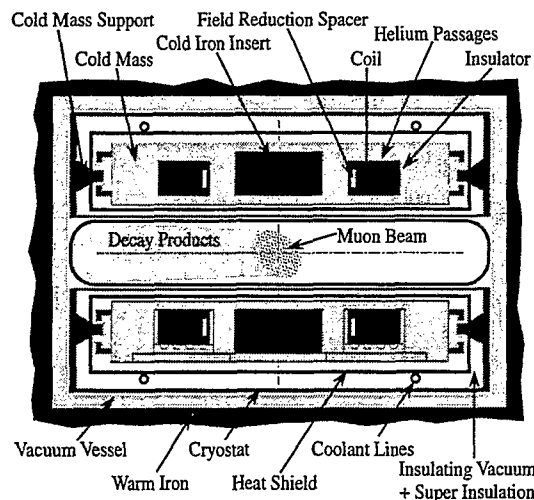


Figure 1: Cross section, with main features labeled, of neutrino factory muon storage ring magnet that avoids decay particles directly hitting superconducting coils.

APPROACH:

A racetrack coil magnet design with open midplane gap keeps decay particles away from directly hitting superconducting coils. This

eliminates the need for a "tungsten liner" which is expensive and occupies a critical real estate in high field magnets. The flat racetrack coils have a large bend radius in the ends. A large bend radius allows the use of "react and wind" magnet technology that is suitable for Nb_3Sn and High Temperature Superconductors.

TECHNICAL PROGRESS AND RESULTS:

A dipole magnet design for the proposed Neutrino Factory Storage Ring has been developed. The dipole operating field is 6.93 T and the design quench field is over 8 T for an operating field margin of over 15%. The cross-section of this design is shown in Figure 1.

The maximum field on the conductor at quench is significantly higher than the central field and excludes using NbTi at 4.2 K. The coils therefore are made from brittle Nb_3Sn superconductor. A large bend radius in the ends and a simple pancake coil (racetrack) geometry allows the use of "react and wind" magnet technology.

The superconducting collared coils inside a cryostat clear the magnet midplane region where most of the decay energy goes. A warm iron yoke structure around the coils then allows heat generated by decay particles to be removed efficiently at a higher temperature.

The superconducting coils are contained in cold masses surrounded by a heat shield and cryostat. Large vertical forces, that could be either attractive or repulsive, depending on the configuration, are contained with the help of support keys mounted to the yoke. The overall magnet structure is designed to minimize the heat leak through the support keys while containing the large Lorentz forces.

Finite element analysis codes were used to minimize the deflections and stresses on

superconducting coils and on the support structure. The analysis shows that the deflections are less than 10 mil and stresses are less than 50 kpsi.

The design of support keys provided another challenge. It must balance between the conflicting requirements of low heat leak and low deflections. The material of the support keys and cryogenic structure was chosen carefully. An optimum support key design was developed where the deflections were less than 5 mil (0.125 mm) and stresses were less than 80 kpsi. The estimated heat load is about 7 Watts.

To maintain field strength, we minimize the vertical distance between the coils and the beam cavity. The cryostat wall thickness is minimized on the side near the beam tube. The beam tube is warm and its thickness is as small as possible. Surrounding both cold masses and the beam cavity is an outer vacuum vessel that eliminates differential pressure on the cryostats and beam tubes and prevents them from collapsing under vacuum.

SPECIFIC ACCOMPLISHMENTS:

We have developed a new magnet design that allows compact Neutrino Factory Storage Rings to be constructed at the BNL site. It was observed, during the course of this LDRD, that a skew quadrupole lattice avoids the direct hit of a large number of decay particles on quadrupole magnets as well. A lattice with skew quadrupole has been developed and presented in the following paper:

B. Parker, Skew-Quadrupole Focusing Lattices and Their Applications, 2001 Particle Accelerator Conference, Chicago, 18-22 June, 2001.

In addition, a novel magnet system design has been developed where all focusing is provided in the ends. This concept has been presented in the following paper:

B. Parker, M. Anerella, A. Ghosh, R. Gupta, M. Harrison, J. Schmalzle, J. Sondericker, and E. Willen, Magnets for a Muon Storage Ring, 2001 Particle Accelerator Conference, Chicago, 18-22 June, 2001.

The following are other significant publications related on Neutrino Factory and Muon Collider that are based on the work performed under this LDRD:

S. Ozaki, R. Palmer, M. Zisman, and J. Gallardo ed., Feasibility Study-II of a Muon-Based Neutrino Source, BNL-52623 (2001).

N. Mokhov, C. J. Johnstone, B. Parker, Beam-Induced Energy Deposition in Muon Storage Rings, 2001 Particle Accelerator Conference, Chicago, 18-22 June, 2001.

In addition, several talks were given by principal investigators at various meetings. These include Muon Collider Collaboration Meetings, Editorial Meetings on Neutrino Factory Feasibility Study, Symposium on Neutrino Factory Study II and presentations at Snowmass 2001.

LDRD FUNDING:

FY 2000	\$ 98,066
FY 2001	\$100,659

DNA-Nano Wires that AutoConnect in 3 Dimensions (NANO III)

James F. Hainfeld

01-82

PURPOSE:

Current computer chip technology is based on lithographic methods that limit components to ~0.3 microns in size, due to the wavelength of light, and the coating/etching processes. The size directly determines computer speed, complexity and cost, and advances in computers over the years have mostly been due to reduction in component size. It is here proposed to construct nanowires that are approximately 2 nm in diameter, or 150 times smaller than currently available. For 2-dimensions, this translates into a $150^2 = 22,500$ -fold computational advantage. Additionally, 3-dimensional construction may be possible using self-assembly, bringing the potential improvement factor to 3,375,000. While it is probably unrealistic that this factor of packing density can be fully achieved, even several orders of magnitude improvement over current technology would be significant.

The purpose of this project is to investigate the use of DNA strands coated with small gold clusters which can be further metalized as novel and extremely small nanowires that may be connected at their ends to target junctions by base-pairing hybridization. This could produce wires 150 times smaller than those currently used to make computer chips, permit 3-dimensional wiring, and potentially increase the power of computers by 3,000,000 times.

APPROACH:

We have previously coupled nanometer-sized gold clusters to antibodies and other proteins to visualize molecular sites using the Brookhaven Scanning Transmission Electron Microscope (STEM). The approach was to extend this technology to attach 1.4 nm gold clusters in high density to strands of DNA to make a nanowire. Although the 1.4 nm gold clusters used have a 0.6 nm organic shell, their high density might permit tunneling conduction. Additionally, we may make conduction more certain by coalescing adjacent gold clusters that are first deposited in high density by using the particles' catalytic properties to deposit additional metal. This could be used to form continuous metal nanowires. E-beam lithographic grids were constructed as test jigs to determine conduction of bridging DNA. An additional aspect of the approach was to study the hybridization of DNA-gold cluster constructs to demonstrate their usefulness in making specific connections. This would be assayed by mixing complementary strands and observing hybridization both by increase in hydrodynamic size in solution and direct visualization by electron microscopy. For ultimate circuit wiring, DNA may be self-organized to form ordered circuit patterns. To investigate this, DNA oligonucleotides that form Holliday junctions were designed that were capable of self-assembly into ordered patterned arrays. Modified DNA bases were used to provide chemical links to gold clusters to form a nanowire array. These were then assayed by electron microscopy in order to study the programmed assembly of electronic nanostructures by DNA scaffolding. Methods to carry out this work included: a) chemical synthesis of appropriate functionalized gold clusters, b) synthesis of DNA strands capable of forming self-

assembled nanostructures, c) biochemical techniques to handle and purify DNA constructs, d) use of STEM to visualize products, e) e-beam lithography to produce small electrodes for measuring conductivity, f) optimization of catalytic metal deposition to produce continuous metal nanowires.

TECHNICAL PROGRESS AND RESULTS:

In the first year of support of this two-year project, double stranded DNA was labeled to high density using 1.4 nm gold nanoparticles. This is shown in Fig. 1.



Fig. 1. Double stranded DNA labeled with 1.4 nm gold nanoclusters. Full width 128 nm.

This result verified an important proof-of-principle, that individual DNA strands, which are only 2 nm in diameter, could be targeted and loaded with small nanometer-sized gold particles. The method employed was to make use of the polyphosphate backbone of DNA which is negative and therefore will bind positively charged gold particles. Electrical conduction could be achieved by either: a) tunneling between nanoparticles, if they are close enough, or b) depositing additional metal around each

nanoparticle “seed” thus growing it until it coalesced with adjacent ones, thus forming a continuous metal nanowire.

The principle of coalescing nanoparticles into continuous metal structures was also proven on the nanoscale. Small metal particles can act as “seeds” for further specific metal deposition because they have a different redox potential than free metal ions. Under the right chemical conditions, additional metal ions, e.g., gold or silver, can be catalytically deposited specifically on the nanoparticle surface. Controlling the growth permits termination when coalescence is achieved, as shown in Fig. 2.

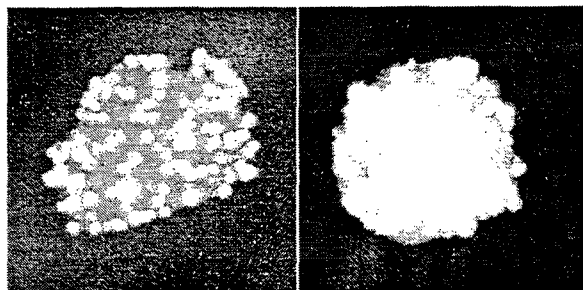


Fig. 2. Nano-sized gold clusters nucleating further gold deposition so that they become contiguous. Here, 1.4 nm gold clusters were integrated onto a liposome, and metal deposition stopped at coalescence. Note that no development occurs randomly or without a “seed.” Left image after 5 min, right after 10 min. BNL STEM micrograph; full width of each image 230 nm.

The work in year 1 was also expanded to labeling single-stranded nucleic acids (Fig. 3), which are of even smaller diameter, and may be used to hybridize to other “targeted” DNA or RNA sites.

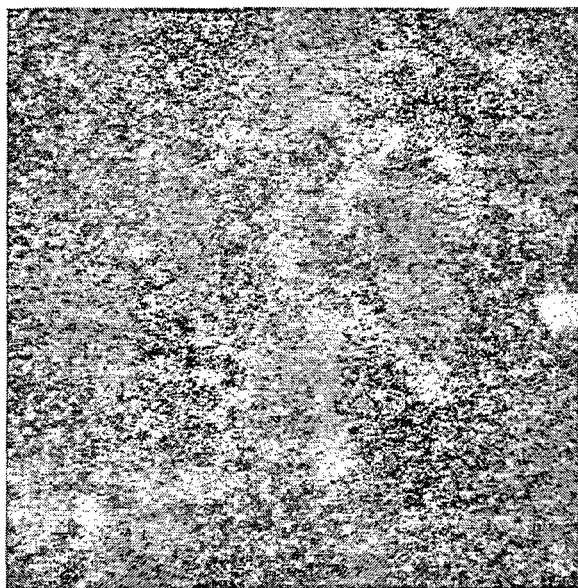


Fig. 3. M13 Phage single-stranded DNA after gold cluster binding and separation on A0.5M column from unbound gold. STEM micrograph, 128-nm full width.

In order to test the hybridization properties of gold-labeled DNA, short 26-mer oligonucleotides were made that were complementary to one another. Gold was bound again by the charge mechanism. Stable gold-DNA complexes could be purified.

Year 2 continued this work and perfected hybridization conditions such that two separately gold labeled complementary strands could be hybridized and isolated. These were shown to have an increased hydrodynamic radius and were directly visualized by STEM microscopy (Fig. 4).

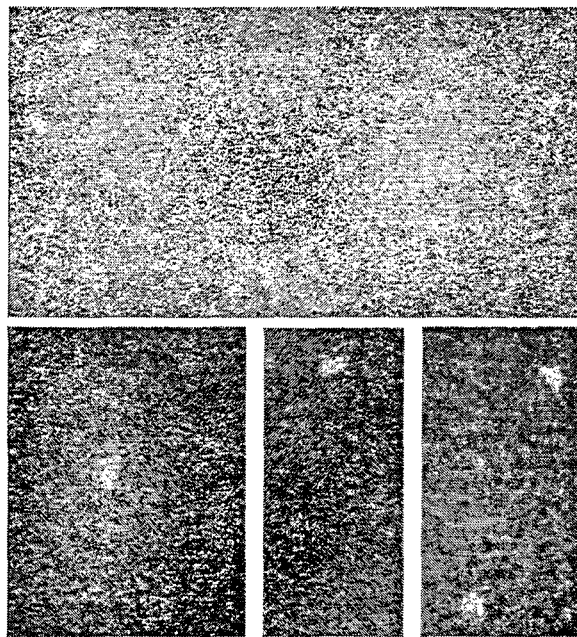


Fig. 4. Top image shows single 26-mer oligonucleotides with gold labels. Two or three gold particles will fit on an oligo this size. The lower images are taken after two complementary strands were separately gold labeled, then hybridized. Note the double row of labeling. STEM micrograph; full width 180 nm.

This is the first time small single oligonucleotides have been visualized, and the sensitivity far exceeds any other DNA detection method devised.

Gold nanoparticle-DNA intercalators were constructed by chemically reacting gold clusters with known intercalators. Labeling of DNA thus far has not been as extensive as with charge labeling.

Long pieces of DNA may be required for longer wires. pBR322 dsDNA was labeled with gold, and strands as long as 2 microns were achieved (Fig. 5).

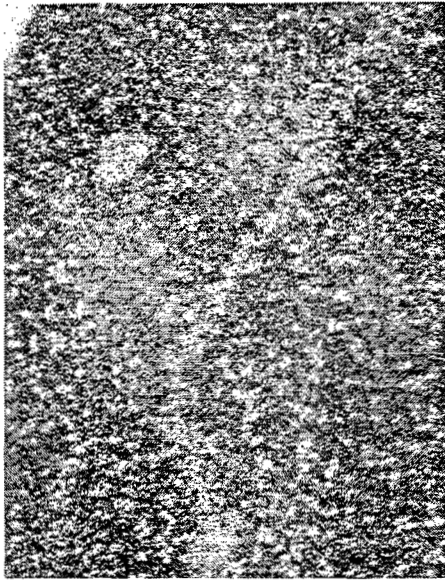


Fig. 5. Section of a 2-micron piece of DNA that was gold labeled (arrow).

Several electron beam lithographically produced micro-electrode arrays were constructed so that conductivity of the DNA wires could be studied (Fig. 6).

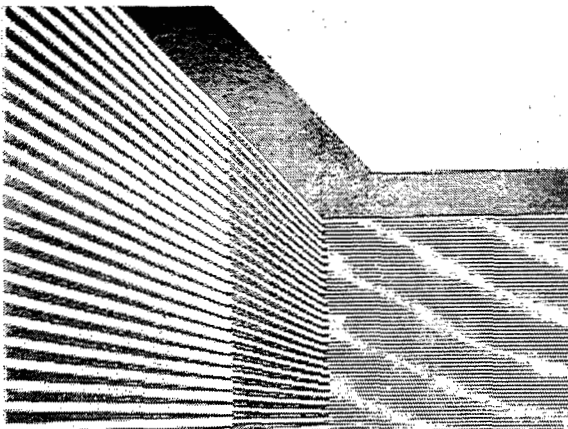


Fig. 6. E-beam metal electrode array for measuring DNA wire conductivity. Grid spacing is 1 micron. Scanning electron micrograph.

DNA nanowires made from T7 DNA and 1.4 nm gold clusters were applied to the array. Upon catalytic silver deposition, conductivity was established between the array electrodes. Measurement of the conduction properties of single DNA strands was beyond the scope of this project.

Finally, connection of nanowires into useful circuits requires designed self-assembly. In order to explore this, DNA Holliday junction technology was utilized to design self-assembled arrays of various dimensions. Chemical hooks were incorporated into certain bases so that gold clusters could be attached after assembly of the array. Fig. 7 shows a Holliday junction and method of self-assembly. Completed structure with gold nanospheres is shown in Fig. 8.

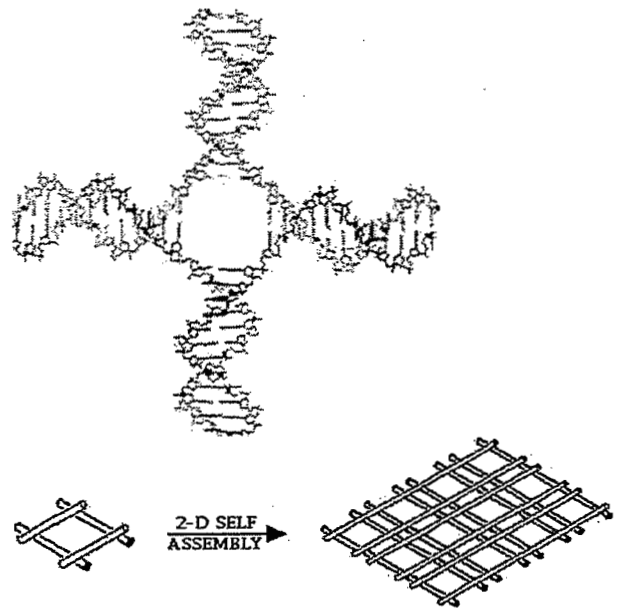


Fig. 7. Holliday junction (top), and self assembly using complimentary oligo hybridization (bottom)



Fig. 8. DNA 2-D array with gold labeling. Note gold only on alternate dense rows as expected (indicated by arrows). Full width 256 nm. In collaboration with Rick A. Kiehl (University of Minnesota) and Nadrian C. Seeman (New York University).

This was the first time that assembly of nanoparticle arrays on DNA scaffolding has been demonstrated.

SPECIFIC ACCOMPLISHMENTS:

- Hainfeld, J. F.; Furuya, F. R.; Powell, R. D.; and Liu, W. DNA Nanowires. Proc. 59th Ann. Mtg., Micros. Soc. Amer.; Bailey, G. W.; Price, R. L.; Voelkl, E.; and Musselman, I. H. (Eds.); Springer-Verlag, New York, NY, pp. 1034-1035 (2001).
- Xiao, S.; Liu, F.; Rosen, A. E.; Hainfeld, J. F.; Seeman, N. C.; Musier-Forsyth, K.; and Kiehl, R. A. Assembly of nanoparticle arrays by DNA scaffolding. *J. Nanoparticle Res.* **4**, 313-317 (2002).
- This work was submitted to the DOE Nanotechnology Initiative in the BNL proposal, "Charge Injection and Transport in Nanoscale Materials." Although funding was received from this multi-departmental effort, a decision was

made to drop Bio-Nanotechnology from the BNL Nanotechnology Program.

- Two NIH proposals including aspects of this work were submitted; the first one, P41 Facility Grant Renewal entitled, "STEM Mass Mapping & Heavy Atom Labeling of Biomolecules," J. Wall, Principal Investigator and J. Hainfeld, Co-Investigator, project period: September 30, 2002 – June 30, 2007, was funded. This proposal resulted in two project reviews: NIH STEM Site Visit, Biology Department, BNL, August 27, 2001, Presenters: J. Wall and J. Hainfeld; and NIH STEM Reverse Site Visit, Washington, DC, June 20-21, 2002, Presenters: J. Wall and J. Hainfeld.

LDRD FUNDING:

FY 2001	\$58,814
FY 2002	\$60,337

Carbon Nanotube Chemical Probes for Biological Membrane Attachment Quantification

Barbara Panessa-Warren
S. Wong

01-85

PURPOSE:

Explore altering single walled carbon nanotubes (SWNTs) and develop visually recognizable nanometer scale probes, compatible with living biological cell systems (human tissue culture and bacterial cells), that could be "functionalized" with membrane proteins, and monoclonal antibodies to the latter. Antibodies attached to the SWNT probes, allowed dynamic experiments with living tissue culture cells incubated with bacterial cells (and spores), which showed the distribution and localization of a specific membrane protein, gClq-R (associated with bacterial invasion). By combining the skills and resource personnel in nanofabrication and nanomaterials involved in the newly developing Center for Functional NanoMaterials at BNL, SWNTs were cleaned, cut and joined into individual nanoloops and functionalized with gClq-receptor protein, two different monoclonal antibodies to gClq-R and a third control non-specific antibody. These immuno-nanoprobes were visible by field emission scanning electron microscopy (FESEM), transmission electron microscopy (TEM), and by oil immersion light (LM) microscopy (following the use of a modified Gram stain). The newly engineered carbon "nanoloops" were stable during cell culture and *Listeria sp.* bacterial attack, as well as *Clostridial* and *Bacillus* spore attachment and invasion studies. This project utilized nanofabrication to create a new tool for visualizing specific membrane proteins on

living human cells, during bacterial attack and invasion.

APPROACH:

Carbon nanotubes have a carbon lattice with unique mechanical properties, even though the diameter of the nanotubes can be quite small (2-5nm). Investigators have found that SWNTs can be functionalized by attaching proteins to the carbon lattice in such a way that these proteins retain their biological activity. By combining this approach with the technology to cut and bend the SWNTs into loops, a 25-60nm diameter nanoloop was developed in our laboratory, which when functionalized with monoclonal antibodies to a specific human membrane protein, was used as an immuno-probe compatible with living cells that could be imaged by light and electron microscopy.

Collaborators:

Prof. George Tortora, Head of the Clinical Microbiology Laboratory, University Hospital, SUNY Stony Brook. Isolated, purified and maintained bacteriologic organisms. Provided microbiological expertise in developing experimental procedures, setting-up an anaerobic hood, and developing safety procedures for all cell culture and bacterial handling.

John Warren, Instrumentation Division, BNL. Cleaned, cut and made carbon nanotubes. Maintained and supervised FESEM analysis.

Prof. Berhane Ghebrehwet, Dept. of Med SUNY at Stony Brook. Isolated and provided the purified membrane associated gClq-Receptor protein, and monoclonal antibodies.

TECHNICAL PROGRESS AND RESULTS:

In FY 2001 SWNTs were cleaned using several methods, but all of the conventional cleaning techniques left metal ions, graphite debris or clumps/bundles of tubes. Modifying the known cleaning procedures produced a method for cleaning the nanotubes and forming them into 3 types of structures:

1. caterpillars, 3-5 um in length
2. "bucky balls", 1-3um in diameter
3. single carbon nanotube loops, 25-60nm diameter (Fig. 1).

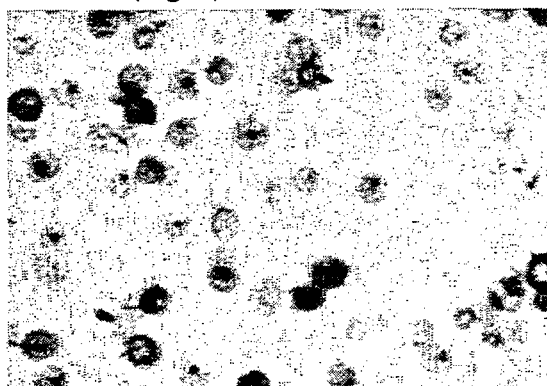


Fig.1. Antibody functionalized carbon nanoloops stained with uranyl acetate .TEM 53,750X

In December 2001, the carbon nanoloops were found to be the most compatible nanofabricated structures to be used with tissue culture cells. The other structures were too large for use as membrane probes. The original process for functionalizing the nanoloops was long and resulted in the loss of many samples, and was subsequently modified by using ultracentrifugation. TEM, atomic force microscopy (AFM) and FESEM monitoring of all functionalized nanoloop preparations showed that the protein was not only attached to the carbon lattice but also was held in the central hole of the loop (Fig.2).

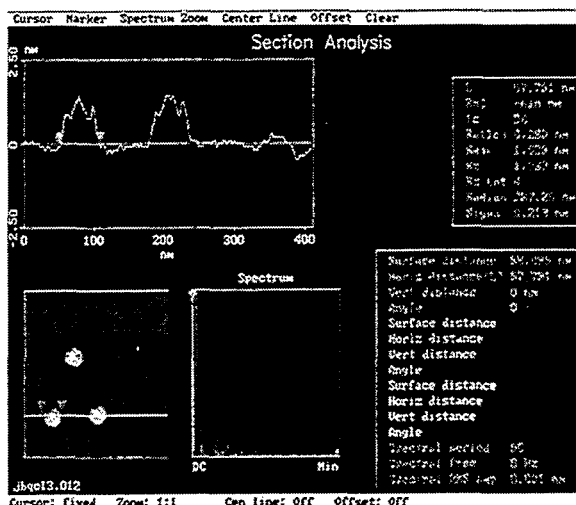


Fig. 2. AFM image of 3 nanoloops functionalized with gClq-R protein. An AFM tracing of 2 of the nanoloops (between arrows) shows that the loops contain hydrated material at their center.

Experiments performed with *Listeria monocytogenes*, *Clostridium difficile*, and *Bacillus cereus* organisms attacking tissue culture cells, showed that the antibody labeled nanoloops became bound to the apical host cell surface only when bacterial attack had begun. During bacterial attack of human tissue culture cells, the antibody functionalized carbon nanoloop probes attached primarily to microvilli in close proximity to attached bacteria or bacterial spores (Fig.3).

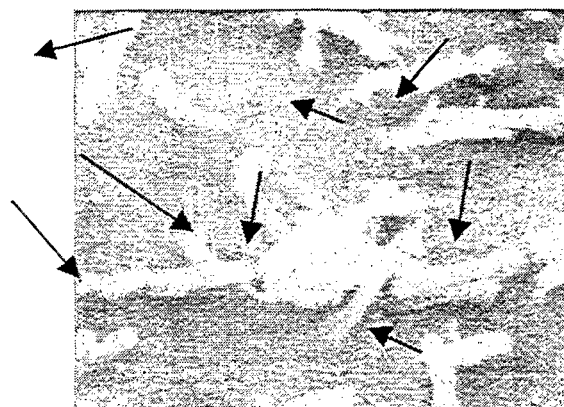


Fig. 3. Surface of human Caco-2 cell showing many antibody functionalized nanoloops (arrows), specifically attached to microvilli and a *B. cereus* endospore. FESEM. 30,660X.

These results suggested that in the first stages of bacterial attack, attachment and invasion was linked to gClq-R localization on host cell microvilli. Control tissue culture preparations incubated with bacteria alone, showed invasion of the host cell membrane in areas with large microvillous processes.

A staining technique was developed that allowed clusters of protein functionalized nanoloops to be seen as blue-purple dots by oil immersion LM (1000X mag). This enabled us to monitor cells that were not chemically fixed, using light microscopy, which enabled us to eliminate artifactual attachment of the nanoloops to cells due to glutaraldehyde crosslinking. By FESEM and LM, antibody functionalized nanoloops were found to attach to the outer membrane of *B.cereus* endospores, but not to attach to the mucoid layer covering the colon and lung tissue culture cells. Control nanoloops with non-specific mouse IgG, or with purified gClq-receptor protein, did not attach to the host cell membranes, nor to the bacterial spores. During the duration of this program it was not possible to do TEM serial thin sectioning of the plastic embedded nanoloop reacted tissue culture cells. Therefore, it is not known at this time if the antibody functionalized nanoloops actually blocked bacterial invasion by inactivating the host cell membrane bound gClq-R. FESEM images suggest that when anti-gClq-R nanoloops and tissue culture cells were subjected to bacterial attack, bacteria were inhibited from entering the host cells. Quantification of functionalized nanoloop probes and their fate (TEM analysis) during bacterial attack will depend on the sectioning of the plastic embedded tissue from this study. Hopefully this final work will be done in the future for publication. Statistical characterization of the nanoloops (functionalized with protein and non-functionalized) by AFM software

metrology revealed that the size, morphology and functionalization with biologically active proteins was reproducible from experiment to experiment with different batches of probes made in the laboratory.

In summary, we were able to nanofabricate 3 types of SWNT structures. The 25-60nm diameter nanoloop structure was chosen for functionalization with 3 different antibodies and a purified membrane protein. These nanofabricated membrane probes were used in living tissue culture preparations under control (non-bacterial attack) and experimental conditions (bacterial attack), and produced repeatable results. The data showed that gClq-receptor protein (involved in bacterial entry into specific types of human cells) is seen on the host cell membrane under attack; and specifically in Caco-2 cells, on the microvilli adjacent to attached bacteria, or bacterial spores*. Later during attack, the anti-gClq-R labeled nanoloops were found to cluster on the surface membrane of the cell, surrounding and attaching to intact and destroyed bacterial cells. By LM antibody functionalized nanoloops exhibited a specific type of clustering on the host cell membranes in the presence of bacteria called capping or patching, which is consistent with biochemical and immunological findings in the literature.

* The findings with the bacterial endospores is especially interesting in light of the recent anthrax spore attacks on the US Postal Service, and high profile political and news personnel. The *B.cereus* strain that was used in this study was reported to be genetically identical to anthrax (with the exception of toxin production), and therefore these data represent the first experiments on the possible role of gClq-R in anthrax-type, endospore attachment/ invasion of human cells.

The development of this SWNT nanofabricated membrane-protein probe has provided data on the appearance and movement of a specific membrane associated protein in living human cells undergoing bacterial attack. This type of functionalized SWNT nanostructure offers the possibility of using this type of nanotechnology for studying specific membrane proteins in living cells, blocking microbial invasion of host cells, and as an antibody delivery system for specific target cells, or receptor sites, within a living organism.

SPECIFIC ACCOMPLISHMENTS:

1. Goethermal and Pathogenic Clostridial and Bacillus Endospore Ultrastructural Attachment Mechanisms. Panessa-Warren, B.; Tortora, G.; and Warren, J. SCANNING 23 (2):122-123, May 2001.

2. Bacillus and Clostridial Endospore Attachment Begins Colonization/ Invasion Process. Panessa-Warren, B.; Tortora, G.; and Warren, J. 102nd Proceedings of the Amer. Soc. for Microbiology, Salt Lake City, Utah, (abstract J19) May 23, 2002.

3. Carbon Nanotube Membrane Probes, Panessa-Warren, B.; Wong, S.; Ghebrehiwet, B.; Tortora, G.; and Warren, J. Workshop for the BNL Center for Functional Nanomaterials, BNL March 2002.

4. Carbon Nanotube Membrane Probes: Immunolabelling by LM, TEM & FESEM. Panessa-Warren, B.; Wong, S.; Ghebrehiwet, B.; Tortora, G.; and Warren, J. Microscopy and Micro-analysis 2002 Proceedings, Springer Verlag (NY) August 2002.

5. (invited paper) Functionalized carbon nanotube loops for identifying gClq-receptor protein on human cells. Panessa-Warren, B.; Wong, S.; Warren, J.; Ghebrehiwet, B.; and Tortora, G. American Chemical Society, March 23-27, 2002

LDRD FUNDING:

FY 2001	\$48,378
FY 2002	\$50,113

Self-Organized Nanoparticles for Probing Charge Transfer at Metallic/Organic Interfaces

Myron Strongin
J.F. Tu

01-86

PURPOSE:

This proposal is concerned with using nanoparticle arrays to study the transfer of charge from metals to organic molecules.

APPROACH:

The approach is to form arrays of metal clusters by evaporation onto substrates held at 10K. Organic molecules are then condensed onto the surface and changes in the conductivity and optical properties are measured.

TECHNICAL PROGRESS AND RESULTS:

During the duration of this project several goals have been achieved. A new ultra high vacuum chamber for obtaining optical data on ultra thin films is well underway and is at the point where, with some adjustments to the mirror holders, the optics can be installed. The main part of the program involved making thin films of Au on glass and on Ge covered glass substrates (held at temperatures from 78K to room temperature), and measuring the transport properties. Some attention has been paid to the influence of the substrate on the properties and nucleation of the films and whether different grain sizes in the initial nucleation stages can be controlled. Work was done to see if decanethiol exposure changed the conductivity of the films. However, future work will be more concerned with characterizing the film

structure before interactions with molecules will be studied.

We have discovered an anomaly in the optical conductivity of both ultra thin Au and ultra thin Pb films. The size of the grains in these systems is of the order of one nm, and this is a regime that had not been studied optically. It is thought that this anomaly occurs when the dielectric constant of the film becomes large at the percolation transition from the insulating to metallic state. Another fascinating aspect of this result is that the transition indicates that in the case of Pb the transition from the insulating to metal state occurs at a different value (a lower resistance) than the transition to the superconducting state. This type of system with grains near 1 nm would also be of great interest in our studies of the effects of organics on charge transfer. Realizing that the nucleation properties and the actual physical properties of films deposited at cryogenic temperatures are not understood, most of the recent work on films has focused on transport properties of films made under different conditions. For example, during the period of this LDRD we have investigated the transport and annealing properties of films made by deposition of gold onto about 1nm of previously deposited Ge. We are investigating the possibilities that amorphous substrates, such as Ge and probably also Si, provide an almost universal substrate for growing ultra-thin films since the deposited metal lowers the surface energy of the system by combining with uncompensated bonds on the amorphous substrate surface.

PUBLICATIONS:

Optical properties of ultra thin films: evidence for a dielectric anomaly at the insulator to metal transition, J.J. Tu, C.C. Homes, and M. Strongin. Phys. Rev. Lett. (accepted).

PATENT SUBMITTED:

“A Universal Method for Making Ultra-Thin Films and Nanoscale Metallic Clusters that are Stable at Room Temperature,” Myron Strongin and Jiufeng Tu, submitted November 2002.

LDRD FUNDING:

FY 2001	\$46,504
FY 2002	\$49,321

Charge Transfer on the Nanoscale: Theory

Marshall D. Newton

01-87

PURPOSE:

The objective of this project is to model the energetic and electronic structural characteristics controlling charge transfer dynamics in extended (tens of angstroms) oligomeric systems comprised of organic or organometallic building blocks. The work is exploratory, in comparison with current techniques typically employed for chemical systems of modest size, in that it 1) includes a full account of many-electron and final- as well as initial-state effects, and 2) is tested by application to quite large-scale molecular assemblies (≥ 100 atoms and ≥ 300 electrons, including transition metal atoms), so as to assess limitations due to issues of convergence and numerical precision. The results will be of value in critically evaluating the merits of common mean-field approaches which generally suppress state-specific and multi-particle effects. Success in this venture will be valuable as an adjunct to evolving plans for the BNL Nanoscience Center.

APPROACH:

The massive current interest in designing and characterizing nanoscale conductive junctions constitutes a major opportunity for exploiting the power of contemporary techniques of computational quantum chemistry and electron transfer theory in modeling the requisite molecular properties governing the overall conductive behavior. This project specifically deals with evaluation of long-range electronic coupling of localized donor and acceptor sites, the modulation of such coupling by vibrational motions (electron-phonon coupling), and the

sensitivity of the coupling (and hence, the conduction mechanism) to tuning of relevant energy gaps (e.g., by chemical substitution).

The theoretical models are implemented computationally using a variety of many-electron quantum mechanical techniques, including configuration interaction and density functional (DF) methods. Models for charge transfer kinetics employ the Golden-rule dynamical model or suitable semiclassical extensions. In collaborative work with Dr. Vasili Perebeinos (BNL Physics), model Hamiltonians based on results from DF calculations are formulated for study of metal-mediated electronic and vibronic coupling in extended conducting junctions based on Green Function methods.

TECHNICAL PROGRESS AND RESULTS:

FY 2001

A systematic study was completed for long-range electronic coupling in a family of homologous systems of generic type DSA (donor, spacer [i.e., "wire"], acceptor), monitoring sensitivity of coupling with respect to chemical substitution (on both D, S, and A units), molecular conformation (oligomer torsion angles), electronic spacer type (saturated vs. unsaturated) and length (number of spacer units), donor electronic state type (in cases of quasi-degenerate transition metal complexes), and charge carrier type (electron vs. hole).

FY 2002

Building on the progress in FY 2001 (focused primarily on electronic structure), the FY 2002 work involved enhanced modeling of electronic structural effects on tunneling propensities in conductive junctions, but with new emphasis on the role of nuclear modes (both molecular modes of

the junction and low-frequency modes of background polar media) in modulating the coupling underlying electron tunneling. Fluctuations controlling thermal activation of charge transfer in polymeric systems with low charge-injection gaps (≤ 1 eV, as e.g., in the case of DNA duplexes) were shown to exert a strong modulating influence on tunneling, with detailed behavior depending on the precise charge transfer characteristics (charge separation vs. charge shift, electron vs. hole carriers). These conclusions emerged from a newly-developed linear response formalism, broadly applicable to charge transfer processes, and amenable to detailed computational implementation, using either continuum or molecular-level models for the medium. Crucial tests of basic models for charge transfer dynamics were carried out by quantitative comparisons of experimental conductance and electrochemical kinetics data for a common set of homologous molecular wires. The overall agreement obtained from these demanding comparisons (within one or two orders of magnitude) provided important support for the underlying theoretical framework. Encouraging preliminary results were obtained from implementations of a new hybrid model for medium dielectric response to charge transfer, combining a molecular-level treatment of inertial response and a continuum treatment of optical response.

SPECIFIC ACCOMPLISHMENTS:

Funding

DOE proposal: "Charge Injection and Transport in Nanoscale Materials," for the period FY 2001-2004.

PI in BNL Center for Functional Nanomaterials, funded Spring 2002.

Refereed Publications

Rapid Electron Tunnelling..., H.D. Sikes et al, *Science* **291**, 1519-1523 (2001)

Distance-Dependent Activation Energies for Hole Injection..., Davis, W.B. et al, *J.A.C.S* **124**, 2422-23 (2002)

Application of the Linearized MD Approach for Computing Equilibrium Solvation Free Energies..., M.V. Vener et al, *J. Phys. Chem. A* (in press)

Electronic Coupling of Donor/Acceptor Sites ..., M.D. Newton in *ACS Symposium Series* (in press)

Heterogeneous Electron Transfer Kinetics for Ruthenium and Ferrocene Redox Moieties..., J.F. Smalley et al, *J. Phys. Chem. B* (in press)

Charge Transfer on the Nanoscale. D. Adams et al, *J. Phys. Chem.* (submitted)

Estimate of Reorganization Energy for Charge Transfer in DNA – K. Siriwong et al, *J. Phys. Chem.* (submitted)

LDRD FUNDING:

FY 2001	\$43,063
FY 2002	\$54,429
FY 2003 (budgeted)	\$18,000

Charge Transport Through Dye-Sensitized Nanocrystalline Semiconductor Films

Bruce Brunschwig

01-88

PURPOSE:

The conversion of solar energy into electricity has been accomplished primarily by semiconductor photovoltaic devices. Over the past few years a new type of solar conversion device has been developed based on liquid junction photovoltaic cells. The cells make use of dye-sensitized charge injection into a nanocrystalline TiO₂ film. While the initial charge injection step is very fast, the subsequent conduction of the charge through the TiO₂ is much slower. The proposed research focuses on the nature of the charge injection into TiO₂ particles.

APPROACH:

First, we developed synthetic methods that allow the preparation of nanoscale TiO₂ particles of various sizes. These particles were characterized by various physical methods. A sensitizing dye was then added to the particle. Finally, Electroabsorption (Stark) spectroscopy was used to characterize the initially formed charge transfer state of the dye-adsorbed system. No previous work of this type has been reported.

The study of charge transfer phenomena on the nanoscale is part of the BNL initiative to develop new research programs in the size region between the molecular and the micro (or the region where bulk materials begin). The new programs are formalized in the Charge Transfer nano proposal *Charge Injection and Transport in Nanoscale Materials* that has been funded through DOE and the Nanocenter proposal

Brookhaven Center for Functional Nanomaterials that has been submitted to DOE. The work described here is an outgrowth of our DOE-funded charge transfer work on the molecular scale.

The research proposed will characterize the initially formed charge transfer state in dye-sensitized systems. Two types of dye sensitization have been reported. One involves direct injection of the charge from the dye to the nanoparticle. The second involves indirect injection in which an excited state of the dye molecule is initially formed that then injects charge into the particle. The direct injection mechanism results from excitation in a new absorption band that is formed when the dye is attached to the particle while no new absorption features are present in the indirect mechanism. Stark spectroscopy affords a means of characterizing the charge transfer state: determination of the distance of the initial charge transfer and the changes in the dipole moment and polarizability between the ground and initially formed Franck-Condon state. For the direct injection mechanism this should yield information about whether the Franck-Condon state is part of the conduction band of the particle or localized on an individual titanium center. For the indirect mechanism it will allow one to assess whether the excited state of the dye has different properties when it is free in solution or attached to the nanoparticle. The Stark spectra for a number of different donors (both direct and indirect) and for nanoparticles freely suspended in solution and attached in nanocrystalline films will be compared.

We have begun work with Drs. E. Galoppini (Rutgers), Dr. T. Rajh (ANL), and G. Meyer (Johns Hopkins University). Other collaborations with Dr. David Thompson (Memorial University, Newfoundland), Dr. Edward Castner (Rutgers-New Brunswick),

and Dr. Stanislaus Wong (SUNY Stony Brook) are being developed. Within BNL collaborations on nanoscale research are underway with Drs. C. Creutz, N. Sutin, E. Fujita, and J. Hanson.

TECHNICAL PROGRESS AND RESULTS:

FY 2001:

1. **Equipment:** A dynamic light scattering (DLS) instrument and a high-speed centrifuge have been purchased. The DLS instrument is used to screen the preparations while the centrifuge is used in the separation. Also an electron-microscope has been reconditioned (under Dr. C. Creutz) and was used in the characterization of the TiO₂ particles.
2. Synthesis of TiO₂ by literature methods was initiated.
3. Initial Stark spectra were taken.

FY 2002:

1. **Synthesis of TiO₂ nanoparticles:** A new synthetic method that produces TiO₂ particles in the size range of 6 to 20 nm has been developed. Titanium (IV) isopropoxide (2 mL) was dissolved in 50 mL of anhydrous ethylene glycol. The solution was heated to 140 (6 nm), 160 (10 nm), or 180 (21 nm) °C and equilibrated at this temperature (the mixture turns milky white). Water (2 mL) was injected under vigorous stirring (the solution becomes clear again). The mixture was removed from heat after 1 hour, allowed to cool to room temperature, and mixed with 50 mL of 0.5 M HCl. This method together with modification of published methods has allowed the synthesis of nanoparticles in the range of 2 to 25 nm (Figure 1). All

particles were characterized by dynamic light scattering with the crystalline one also characterized by X-ray powder diffraction and transmission electron microscopy (Figure 2).

2. **Stark Spectra of Fe(CN)₆-TiO₂:** The first Stark spectra of a dye attached to a nanoparticle that exhibits a new charge transfer band have been collected and interpreted (Figure 3). The charge transfer distance determined from the spectra is $\approx 5\text{\AA}$ (Table 1) and closely matches the distance between the Fe center and the Ti^{IV} that is coordinated to the nitrogen end of one of the CN ligands of the ferrocyanide complex. This result is the first to show conclusively that the direct charge injection is to an individual titanium site and not into the conduction band of the particle.
3. **Postdoctoral Associate:** Dr. Mikhail Khoudiakov departed on October 11, 2002, for a position at Old Dominion University to work on carbon nanotubes.

SPECIFIC ACCOMPLISHMENTS:

1. **Electroabsorption Spectroscopy of (NC)₅Fe^{II}(CN)Ti^{IV} Systems.** A. R. Parise, B. S. Brunschwig, and N. Sutin. Poster given at the Twenty-Fourth DOE Solar Photochemistry Research Conference, Tahoe City, CA, June 3-7, 2001
2. **Charge Injection and Transport through Colloidal Nanoparticles and Nanocrystalline Semiconductor Films** Section in Charge Injection and Transport in Nanoscale Materials. A proposal for DOE Laboratory Activities in Nanoscale Science, Engineering and Technology, C. Creutz 2001.

Figures:

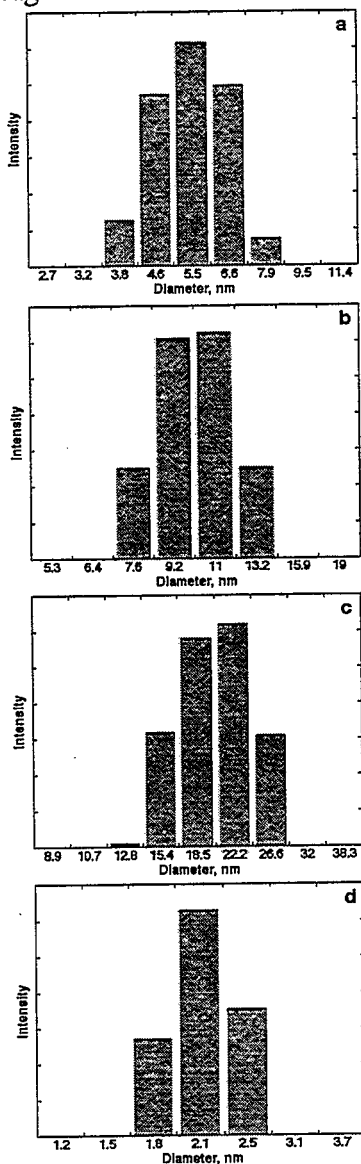


Figure 1. Size distribution of TiO₂ nanoparticles obtained by the hydrothermal procedure at 140 °C ($D_h = 5.6$ nm, panel a), 160 °C ($D_h = 10.2$ nm, panel b), 180 °C ($D_h = 20.5$ nm, panel c), and by hydrolysis in strongly acidic water/ethylene glycol mixture ($D_h = 2.2$ nm, panel d).

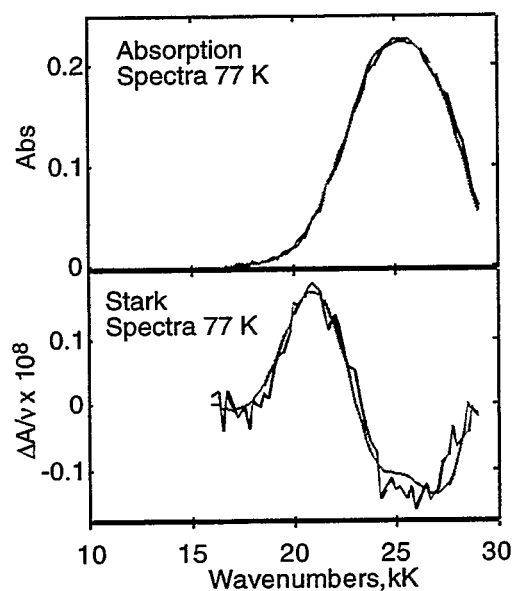


Figure 2. Electroabsorption spectra of Fe(CN)₆⁻ TiO₂(nanoparticle): Experimental data in blue and fit in green.

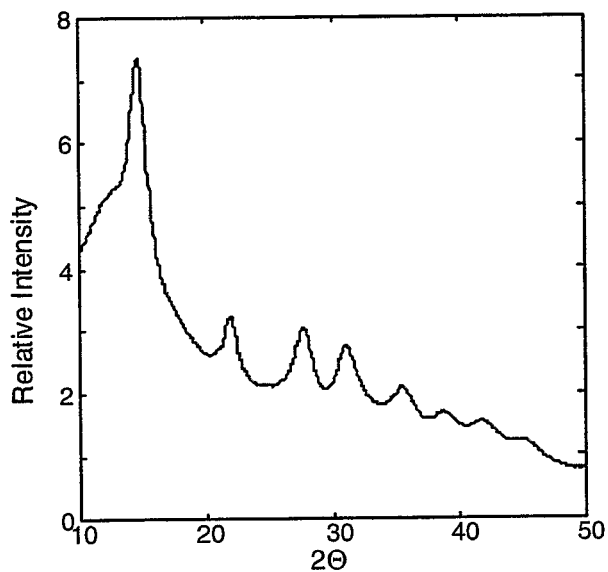


Figure 3. X-ray powder diffraction pattern of ~3 nm diameter TiO₂ nanoparticles.

Magnetic Nanodispersions

Laura H. Lewis
C.-C. Kao

01-91

PURPOSE:

This work is a study of the magnetic properties of well-characterized thin-film systems of two magnetic phases, "magnetic nanodispersions." The objective of the work is to obtain an understanding of the nature and extent of interparticulate magnetic interactions and how these interactions are mediated by the intervening matrix. This work supports the BNL institutional strategy because it constitutes a significant portion of the proposed DOE/Basic Energy Sciences Nanoscience Center "Magnetic Nano-assemblies" Thrust Area. Furthermore, the research represents a unique effort to increase both the degree of research collaboration between BNL and SUNY SB as well as augment the BNL materials synthesis capabilities and experience. The research is both innovative and high risk because neither the materials synthesis route, the nanoarchitecture, nor the combination of phases has been employed before in the scientific literature.

APPROACH:

Multi-phase nanostructured thin-film samples were successfully deposited using the novel technique of reactive ion beam assisted deposition (RIBAD) in the laboratory of Prof. R. J. Gambino at SUNY Stony Brook. RIBAD uses a focused Ar ion beam from a deposition source to sputter metal atoms from a target onto a substrate surface. Concurrent with the primary beam deposition a secondary ion beam from an assist source produces a controlled Ne/O₂ mix beam. The mix beam combines with the flux of metal atoms to oxidize the most

thermodynamically-susceptible metal ion and thereby synthesize nanocomposite metal and metal-oxide film dispersions. Thin films of MnO + Co and MnO + Pd of 50 nm thickness were deposited and investigated with standard materials characterization techniques as follows. Table I summarizes the film's compositions and preliminary results of characterization. 4-point probe conductivity measurements were carried out as a rough check of the oxide content of the films, and a Tencor AlphaStep Profiler was used to measure the thickness of the deposited films. Scanning electron microscopy/energy-dispersive x-ray spectroscopy (SEM/EDX) was utilized to check the films' compositions, laboratory x-ray diffraction (XRD) was carried out to identify phase and microstructure, and Auger electron spectroscopy (AES) provided information on the thickness of the oxide layer on top of the films. Preliminary transmission electron microscopy (TEM) and electron energy-loss spectroscopy (EELS) was performed to further examine the films' nanostructure and phase content. Detailed *ac* (dynamic) and *dc* (static) SQUID magnetometry was performed as functions of both temperature and field to examine the films' magnetic response. Properties that were clarified with magnetic measurement include uniformity of particle size, interparticulate interactions, and the properties of the blocking temperature, which marks the energy balance of the nanoparticles' magnetic response and temperature.

TECHNICAL PROGRESS AND RESULTS:

CoMn-O samples of average thickness of 50 nm have been deposited with nominal oxygen contents ranging from 0% to 29% and have been characterized by various techniques as described earlier. While the amount and scope of characterization per-

formed on the extremely large sample set is impressive, by its very size it precludes understanding of magnetic phenomena in the films. This is because of the appearance of non-systematic magnetic behavior and phase constitution with increased O₂ content in the films. Efforts are ongoing at BNL to understand the magnetic behavior exhibited by the samples. In particular, novel magnetic behavior as a function of applied field was discovered in films with low oxygen content. This behavior hints at a very unusual magnetic coupling between the antiferromagnetic particles and the matrix in the films. It appears that the antiferromagnetic particles induce a magnetic polarization of the matrix surrounding the particles that is opposite to that of the majority of the matrix. Thus a "compensating"-type magnetic behavior is found much like that found in the temperature dependence of ferrimagnets.

The presence of the antiferromagnetic oxide was signaled by a significant increase in the coercivity and onset of an exchange bias shift at $T \sim 150$ K in the major hysteresis loops. Temperature-dependent magnetization measurements made between 10 K and 330 K under different field-cooling conditions reveal a maximum 80% decrease in the saturation magnetization of Co at 10 K, as shown in Fig. 1. This magnetization compensation decreases with increased cooling field, indicating the exchange field between the ferromagnetic cobalt matrix and the antiferromagnetic MnO particles is the same order of magnitude as the applied field. Quantitative determination of the moment compensation reveal that a significant portion of the cobalt matrix surrounding the

MnO nanoparticles must couple in an antiferromagnetic manner to uncompensated spins on the oxides' surface.

SPECIFIC ACCOMPLISHMENTS:

Refereed Journal Article:

J. van Lierop, L. H. Lewis, K. E. Williams, and R. J. Gambino, "Magnetic exchange effects in a nanocomposite Ni/NiO film," *J. Appl. Phys.*, **91** 7233 (2002).

Poster presentation, "Magnetic exchange effects in a nanocomposite Ni/NiO film" 46th Annual Conference on Magnetism and Magnetic Materials, Seattle, WA, Nov. 12 – 16, 2001.

J. van Lierop, L.H. Lewis, and Qiang Li, "A Magneto-Optical Study of Exchange Bias in a Thin Film Dispersion of MnO Nanocrystalite in Co," submitted (but not accepted) for presentation at the 2002 MRS Fall Meeting, December 2-6, 2002, Boston, Massachusetts

J. van Lierop, M. A. Schofield, L. H. Lewis, and R. J. Gambino, "Strong exchange bias in a thin film dispersion of MnO nanocrystalites in Co," manuscript in preparation.

L. H. Lewis, J. van Lierop, and Richard J. Gambino, "Magnetic Compensating Behavior in Nanocomposite Metal-Oxide Films" manuscript in preparation.

LDRD FUNDING:

FY 2001	\$71,175
FY 2002	\$72,892

Table I: summary of film composition and physical characteristics.

Sample + % O ₂ /Ar mix	Thickness (Å)	$\rho_S(\mu\Omega/m)$	at% (Mn/Co)
Co ₉₆ Mn ₄ +0%	538 ± 23	16.9 ± 3.4	3.75 ± 0.04
Co ₉₆ Mn ₄ +2%	403 ± 20	35.8 ± 7.2	3.75 ± 0.04
Co ₉₆ Mn ₄ +6%	490 ± 25	159 ± 32	4.10 ± 0.04
Co ₉₆ Mn ₄ +8%	475 ± 25	140 ± 28	
Co ₉₆ Mn ₄ +10%	495 ± 26	109 ± 22	3.90 ± 0.04
Co ₉₆ Mn ₄ +14%	560 ± 27	152 ± 30	3.70 ± 0.04
Co ₉₆ Mn ₄ +29%	463 ± 23	124 ± 25	3.75 ± 0.04

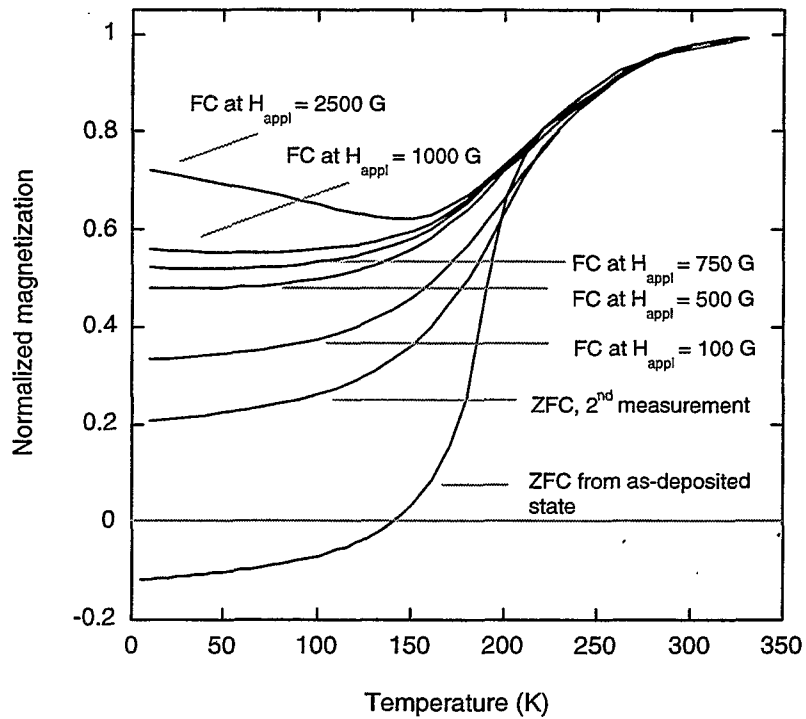


Figure 1. Magnetization curves of Co₉₆Mn₄+29% O₂ nanocomposite film that shows normalized magnetization data taken in the temperature range 10 K ≤ T ≤ 330 K at an applied field of 500 G upon warming from different field-cooling conditions. The results are normalized to the magnetic moment value of cobalt at T = 0 K.

High Resolution Magneto-optical Study of Magnetic Nanostructures, Nanocomposite Functional and Superconducting Materials

Qiang Li

01-93

PURPOSE:

A high-resolution magneto-optical technique has been developed to provide a novel and versatile characterization tool for investigating properties of magnetic nanostructures, nanocomposite functional, and superconducting materials. The success of this technique will greatly broaden BNL's capability of both conducting fundamental scientific studies and pursuing practical application of various functional materials. It is an important element of BNL's strategic effort on building a state-of-the-art functional-material and nano-science center.

APPROACH:

One of the greatest challenges in the studies of magnetic properties in various materials is to develop a versatile technique which can "visualize" the static and dynamic interaction of magnetic structures at a wide range of length scales. The magneto-optical effect is one of a very few techniques that provides a direct interaction between the magnetic domain and photons.

Based on the magneto-optical Faraday effect, the proposed technique allows for a nondestructive and direct observation of change in local magnetic structures at the scale of micrometers to millimeters. Using the magneto-optical effect, we are able to image, as well as study the phenomena associated with, the nucleation of various magnetic domains (like spin-flop and antiferromagnetic domains), domain wall motion, magnetic interface, and

antiferromagnetic coupling, as well as magnetic flux motion in superconductors. Another unique strength of this technique is being able to study the dynamic behavior of magnetic properties and its interaction with the structural defects simultaneously and nondestructively. The information obtained from the high resolution magneto-optical technique is extremely valuable and is unattainable with other existing methods, like transmission emission microscopy (TEM), magnetic force microscopy, X-ray scattering and diffraction method.

TECHNICAL PROGRESS AND RESULTS:

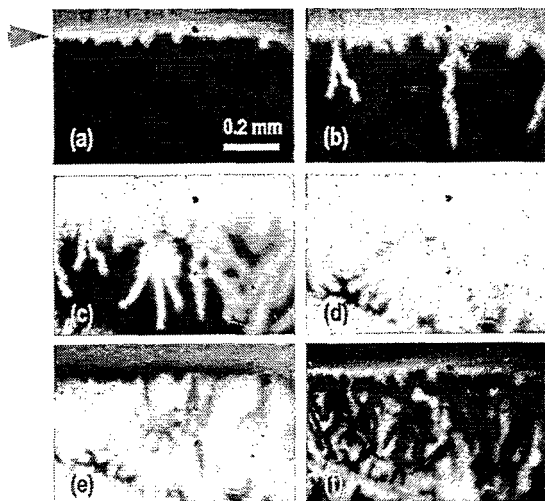
It is emphasized that the entire project started from ground zero in October 2000 when it received LDRD funding. In the first part of FY 2001, we purchased and installed an optical microscope with polarizer/analyzer and digital camera with software for image capture. A new Ph. D. graduate student from SUNY at Stony Brook was hired in February 2001 to participate in this project. We custom-designed (and subsequently purchased) a low vibration, liquid helium continuing flow cryostat with Janis Corp. used for temperature control under microscope. Image capturing and analysis software was tested. In the second half of FY 2001, we installed a turbo-pump based vacuum system and successfully tested the temperature control system. We custom designed, winded and tested a copper coil magnet for the cryostat capable of producing up to 1000 Oe magnetic field.

In August-October 2001, we put the system in a milestone test by imaging the magnetic field distribution profile in a newly discovered MgB₂ superconducting film. It was a remarkable success where the stability and reproducibility of this homemade magneto-optical system surpassed all the

performance parameters we had expected from an optical microscope. We found that our homemade instrument can be operated continuously from 350 K down to 2 K and under magnetic field up to 1000 Oe with excellent stability.

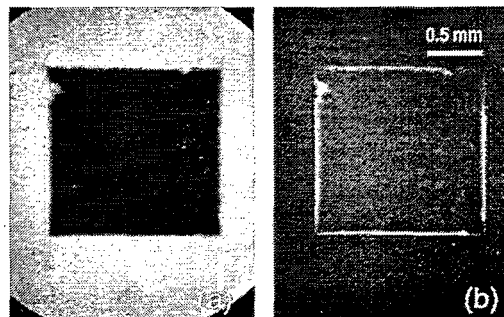
Since October 2001, we have used this system extensively for studies of magnetic properties of nano-dispersed CoMnO system and flux penetration and trapping in various superconductors. The following examples highlight some of the results we obtained with this system.

The following figures show complex dendritic flux penetration and trapping sequence (image brightness represents flux density) into the zero-field-cooled superconducting state of a *c*-axis oriented MgB₂ thin film (arrow indicating the film edge) at 4.2 K. The respective images were taken at *H* (perpendicular to the film) ~ 30 (a), 200 (b), 300 (c), 1000 (d), 500 (e), and 0 Oe (f).

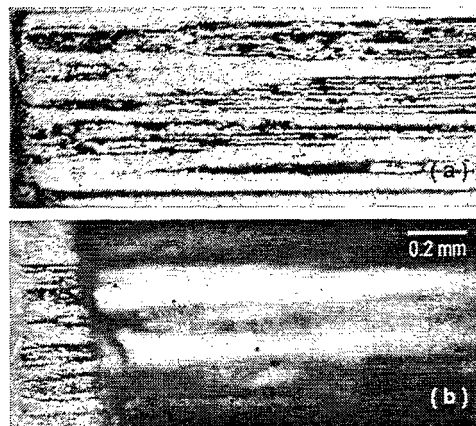


The following figures show the magneto-optical images of the same area of a square-disk-shaped bulk MgB₂/Mg nano-composite taken at 4.2 K. At the maximum external field of 1100 Oe applied to the zero-field-cooled sample (a). We found that the magnetic field was completely screened outside the samples demonstrating strong coupling of MgB₂ nano-

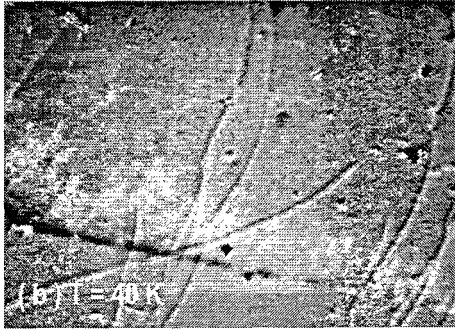
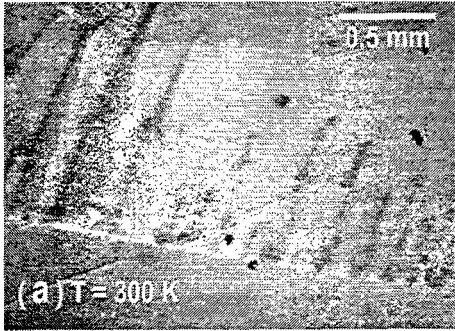
grains. Surface pinning was observed in the remnant state (b) after the external field was decreased from 1100 Oe to zero.



The following figures show corresponding conventional light optical (a) and magneto-optical (b) of the same cross section of a Bi2212 multifilament wire. The magneto-optical image shows the remnant state after *H*_m = 1000 Oe at 4.2 K. The supercurrent flow across the filaments demonstrates that the filaments in the sub-bundles are coupled.



The following figures show our studies of exchange bias in a thin film dispersion of MnO nanocrystallites in Co. At room temperature, regular domain wall motion was observed at *H*_c = 200 Oe after *H*_m = -1000 Oe, while a band of reverse domain was found pinned near the edge in a 200 nm thin film Co₉₀Mn₁₀ - 5%O₂/Ar at 40 K.



SPECIFIC ACCOMPLISHMENTS:

Publications:

“Magneto-Optical Studies of Critical States in c-axis Oriented MgB₂ Thin Film and Bulk MgB₂/Mg Nano-composites,” Zuxin Ye, Qiang Li, G. D. Gu, J. J. Tu, W. N. Kang, Eun-Mi Choi, Hyeong-Jin Kim, and Sung-Ik Lee (IEEE trans on Appl. Supercon. in press)

“Comparative Studies of MgB₂/Mg Nano-Composites and Press-Sintered MgB Pellets,” Qiang Li, L. Wu, Y. Zhu, A. R. Moodenbaugh, G. D. Gu, M. Suenaga, Z. X. Ye, and D. A. Fischer G. D. Gu, and Y. Zhu (IEEE trans on Appl. Supercon. in press.)

“High critical current density in robust MgB₂/Mg nano-composites,” Qiang Li, G. D. Gu, and Y. Zhu (submitted to Appl. Phys. Lett.)

Presentations:

“Critical Current, Flux Pinning and Microstructure of Superconducting MgB₂/Mg Nano-composites and MgB₂ Films,” Qiang Li,

APS March Meeting, Indianapolis, In, March 18-22, 2002.

“Superconducting and Microstructural Properties of MgB₂/Mg Nano-Composites,” Qiang Li, MRS Fall meeting, Boston, Nov. 26-30, 2002.

“Magneto-Optical Studies of Critical States in c-axis Oriented MgB₂ Thin Film and Bulk MgB₂/Mg Nano-composites,” Z. Y, Qiang Li, et.al. Applied Superconductivity Conference, Houston USA, Aug. 4-9 2002.

“Superconducting and Microstructural Properties of MgB₂/Mg Nano-Composites,” Applied Super-conductivity Conference, Houston USA, Aug. 4-9 2002.

“Studies of High Angle Off-basal-plane Tilt Grain Boundaries in BI2212 Superconductors,” Qiang Li, Z. X. Ye, M. Suenaga, and A. Ghosh, MRS Fall meeting, Boston, Nov. 26-30, 2002.

“Magneto-optical Studies of AC Loss in YBCO Thin Film and the Effect of Non-uniform Flux Pinning on the Critical Current in HTS,” Qiang Li, Zuxing Ye and M. Suenaga, APS March Meeting 3-7, 2003; Austin, TX.

“Magneto-optical Studies of the Critical State in Superconducting Thin Films” Z. X. Ye and Qiang Li," APS March Meeting 3-7, 2003; Austin, TX.

LDRD FUNDING:

FY 2001	\$32,748
FY 2002	\$45,797
FY 2003 (budgeted)	\$26,000

Size Selected Quantum Dots Under Environmentally Controlled Conditions

Dan Imre

01-97

PURPOSE:

This program aims to explore nanoparticles along two parallel lines: 1. Use ultrafast spectroscopy to study the electronic dynamics and optical properties of semiconductor nanoparticles, and 2. develop a method for generating size selected nanoparticles and investigate their thermodynamic behavior.

APPROACH:

The electronic dynamics are studied using a femtosecond laser system in a pump-probe mode, in which the first frequency doubled laser pulse populates the excited state. A second time-delayed pulse at the fundamental frequency is used to measure the transient absorption.

In most studies size selected nanoparticles are produced by using an atomizer and a Differential Mobility Analyzer (DMA) to select a narrow size distribution for study. To investigate the thermodynamics of solvation and crystallization on the nanoscale arrested electrospray of electrolyte solution, a method of single size nanoparticle generation is used. The thermodynamics of these particles is investigated using a second DMA and a controlled humidity region in-between.

TECHNICAL PROGRESS AND RESULTS:

1. Ultrafast Power Dependent Dynamics of CdS(Se) Quantum Dots in Glass

Semiconductor quantum dots (QDs) are nanoparticles that exhibit novel optical and electrical properties due to confinement of their charge carrier wave functions in three dimensions. Confinement phenomena become important when the radius of the semiconductor nanoparticle becomes equal to or smaller than its Bohr exciton radius. The most characterized and well-understood confinement phenomenon is the blue shift of the ground state absorption, due to exciton confinement, analogous to the quantum-mechanical particle-in-a-box. Although the effect of confinement on the absorption spectrum is well understood, its effect on the relaxation dynamics such as exciton-exciton recombination is poorly understood. This is despite the fact that the dynamics of these systems have important implications for the integration of QDs into electro-optical devices.

Studies of the electronic dynamics in QDs have thus far produced many contradictory and irreproducible results. The observations show two relaxation pathways with lifetimes and probabilities that tend to be laser power and preparation dependent. CdS QDs of vastly differing surfaces, sizes, electronic structures, and in various solvents all show a fast (1.5-4ps) decay component whose amplitude increased with laser power and a longer decay on the order of 50ps. The rapid decay was assigned to exciton-exciton annihilation, which under high intensity and where multiple photoexcited charge carriers are created in each quantum dot is dominant, leading to trap state saturation and an accumulation of band edge excitons. It was also shown that the power dependent decay is only weakly dependent on surface, size, and electronic structure.

The studies described here aim to unravel the electronic relaxation pathways and to develop an understanding of their mechanisms. The present work uses two

different commercial samples of CdS and CdSe nanoparticles embedded in glass, each with different sulfur-to-selenium ratios, to study the nature of the species responsible for the short decay times. The new laser system made it possible to achieve higher excitation powers than in previous studies.

The static absorption and fluorescence spectra of the two samples (GG495 and OG515) are shown in Figure 1. The absorption spectra, Figure 1a, shows absorption onsets of 495 nm for GG495 and 515 nm for OG515. The fluorescence spectrum, Figure 1b, of sample GG495 shows some band edge emission around 480-505 nm as well as an emission peak at 528 nm. The overall quantum emission yield is less than 1%, indicating that the majority of charge carriers relax non-radiatively.

The dependence of the 790 nm transient absorption of sample GG495 on the 390 nm pump power is shown in Figure 2. Note that three different time scales are shown. The fitting (not shown) consisted of a pulse width limited rise (~ 250 fs) and a double exponential decay, with time constants of 1.5 ps and 50 ps, plus an offset. The offset and the 50 ps decay time constants, which were determined from 0-600 ps scans, were held constant for all fits.

The slower (tens of picosecond decay) was shown to be power independent and can be assigned to the trapping of charge carriers which is consistent with the time-resolved fluorescence studies reported by others.

In a previous experiment, nanosecond fluorescence experiments showed that there was an accumulation of band edge excitons as the photoexcitation power increases. Thus, at high power, a new decay mechanism may arise due to exciton-exciton interactions. This decay mechanism is

known as exciton-exciton annihilation, which is most likely responsible for the power-dependent, 1.5 ps transient absorption decay we have observed. A power-dependent excitonic bleach has also been observed in $Zn_xCd_{1-x}S$ QDs, where the fast, power-dependent decay time constant of the bleach decreased from 1.3 to 0.8 ps as the power was increased.

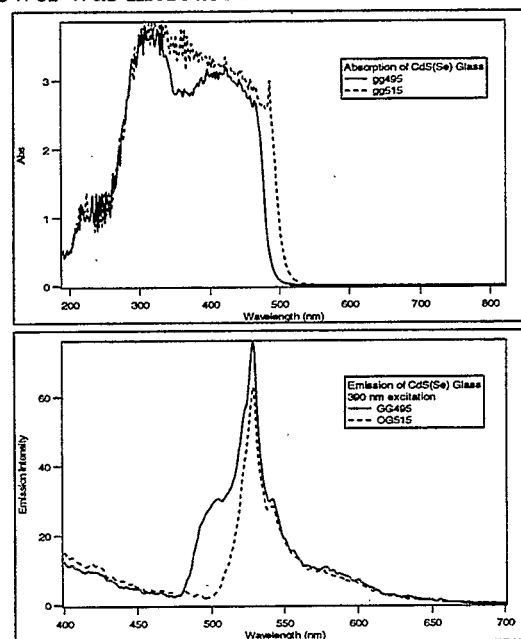


Figure 1: Absorption (top) and fluorescence spectra (bottom)

2. Thermodynamics on the Nanoscale

A significant fraction of atmospheric particles are hygroscopic by nature and exhibit the properties of deliquescence and efflorescence. Recent field studies have observed large nucleation events of hygroscopic particles, and there are noted discrepancies between predicted and observed particle growth rates after nucleation. These growth rates are governed, in part, by the thermodynamic properties of particles only a few nanometers in diameter. However, little thermodynamic information is currently available for nanometer-sized particles. The Kelvin relation indicates that the surface tension of a particle less than 100nm in diameter can dramatically affect the thermodynamics, and

surface states may begin to influence the bulk physical properties in these small particles with high surface to volume ratios.

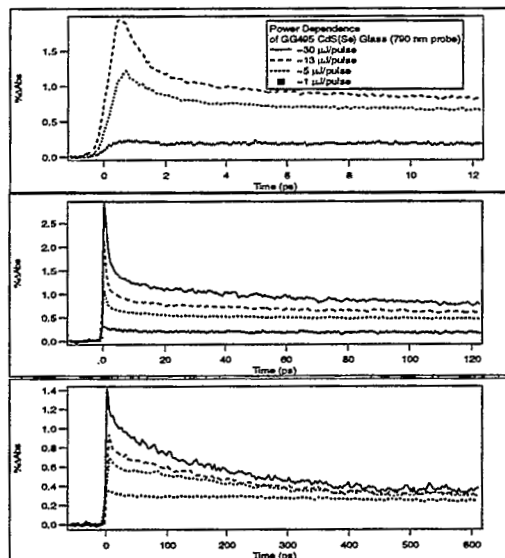


Figure 2: Power dependent transient absorption signals at 790 nm.

In this context, we are investigating the thermodynamic properties, including pre-deliquescence water adsorption, deliquescence, efflorescence, and supersaturated particle compositions of nanoparticles with mobility diameters in the range of 5 to 50 nm. We have developed a temperature and humidity-controlled laboratory-based Nano Differential Mobility Analyzer (NDMA) system to characterize the hygroscopic properties of the common atmospheric salt particles as a function of size. Two different aerosol generation systems have been used to cover the full-size range. The first system (>20nm diameter) relies on an Atomizer (TSI 3076) to produce particles which are size-selected using an initial DMA. For particle sizes smaller than 20 nm, the Electro spray Aerosol Generator (EAG, TSI 3480) has been employed as a particle source. The EAG characteristically provides narrow size distributions, comparable to the monodisperse size distribution from a DMA, but with higher number concentrations. Once generated, the monodisperse aerosol flow is then

conditioned with respect to humidity at a constant temperature and subsequently analyzed using a TSI Ultrafine Condensation Particle Counter (CPC Model 3010) modified for Pulse-Height Analysis. The dry particle sizes are also continually monitored by an external Switch Mode Power Supply (SMPS) system (TSI 3936) to rectify errors in the calculated growth factor resulting from any drift in the dry particle size. The size changes of the humidified particles are directly correlated with the relative humidity and temperature. Our results of ammonium sulfate particles from 5 - 50 nm in diameter are consistent with those predicted from the Kelvin relation (Figure 3). The particle size affects both deliquescence and efflorescence of the homogeneous salt particles: the deliquescence relative humidity increases and the efflorescence decreases as particles become smaller. In addition, we observed a sharp deliquescence transition for all of the particles from 5 to 50 nm.

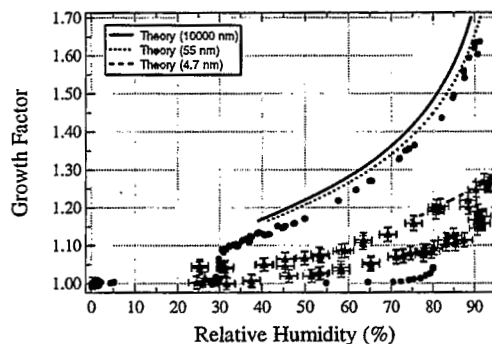


Figure 3: Hygroscopic properties of ammonium sulfate particles 4.7 nm (Δ) and 55 nm (\bullet) in diameter.

SPECIFIC ACCOMPLISHMENTS:

The work has been presented in two professional meetings and 2 publications are in preparation.

LDRD FUNDING:

FY 2001	\$87,349
FY 2002	\$89,705

Crystallization and X-ray Analysis of Membrane Proteins

DaXiong Fu

02-02

PURPOSE:

The purpose of this project is to develop a general approach for crystallization and structure analysis of integral membrane proteins, and to elucidate the structural basis for transmembrane active processes mediated by membrane channels and transporters. Toward these ends, we will proceed from gene cloning through protein expression, purification, and crystallization toward x-ray analysis and structural determination in a three-year timeline. This proposed research meets the general characteristics of the LDRD program in the following three ways: (1) Transmembrane active processes are fundamental and ubiquitous biological phenomena that have not yet been studied at a chemical level due to a lack of a general methodology for crystallization of membrane proteins. This project will enhance the ability of the Laboratory to be in this forefront area of Life Sciences. (2) Insights gained during our recent crystallization and structural determination of an integral membrane channel resulted in new hypotheses and new concepts that are needed to be further tested and generalized. (3) One major focus of this project is to crystallize and solve the structures of membrane transporters involved in the process of detoxification of heavy metals. Bioremediation is one of DOE's focuses.

APPROACH:

The central idea revolves around the considerations for dual physicochemical properties of membrane proteins that are

destined to be in the polar, non-polar environments of the lipid bilayer. This biphasic feature of membrane proteins makes structural analysis almost entirely inaccessible to current biochemical and biophysical approaches that have been developed for studying polar globular proteins. In this proposed research, we will explore new approaches to convert membrane proteins to the equivalents of globular proteins using detergents and other amphipathic reagents. We will also tailor the methodology of general protein crystallization to parameters of integral membrane proteins. The convergence of these two efforts should allow crystallization of membrane proteins using similar principles as for globular proteins.

TECHNICAL PROGRESS AND RESULTS:

This project supports the efforts of setting up a new biochemistry and crystallization laboratory in the Biology Department. The laboratory was re-designed with added multi-disciplinary capacity of molecular biology, protein chemistry, and protein crystallization. With the exception of a crystallization facility, lab renovation is nearly complete.

All milestones in FY 2002 were met as planned, including cloning eight representative membrane channels and transporters from *Escherichia coli.*, conducting mini-scale protein expression and purification, defining solubilization conditions to extract each of the eight proteins from membranes and optimizing protein expression. Among these selected membrane proteins, four of them could be over-expressed and purified at a high level suitable for structural, functional, and crystallographic studies.

Starting in FY 2002, our experiments were focused upon YiiP, a heavy metal transporter that showed excellent solution stability in certain detergent conditions. The function of YiiP was characterized by liposome reconstitution and transmembrane flux/uptake measurements. Using metal sensitive fluorescent indicators, we showed that YiiP catalyzes translocation of Zn (II) and Cd (II) across the lipid bilayer. Detailed kinetic characterization of the YiiP-mediated transmembrane processes is planned for the coming months. The binding of YiiP to heavy metal ions was examined by titration calorimetric analysis. The binding affinities to Zn(II) and Cd(II) were determined in the micromolar range with a 1:1 stoichiometry. The secondary structure of YiiP was determined in detergent micelles by circular dichroism spectroscopy and in lipid bilayer by FTIR spectroscopy. These experiments indicated that YiiP is an alpha-helical protein in which about 60% of the residues are folded in alpha helical conformation. To further examine the membrane topology of YiiP, we mapped solvent accessibility of all charged residues in YiiP by protease digestion and mass spectrometric analysis. The pattern of residue accessibility showed an excellent agreement with the profile of hydrophobicity distribution in the primary structure, leading to the identification of possible transmembrane spanning segments. Further topological studies using a combination of site-directed chemical labeling, protease digestion, mass spectrometry and western-blotting analyses concluded that YiiP is a five-span membrane protein with c-and n-termini facing outside and inside of the cell respectively. The purification of YiiP was streamlined and scaled up to the 100-mg range. The purified YiiP showed marked stability in certain detergent conditions. Crystallization screening was initiated and several possible leads began to emerge.

Milestones planned for FY 2003 include: defining initial crystallization conditions, setting up fine grid screening to plow through several "initial hits," optimizing crystallization conditions, developing cryo methods to flash-freeze crystals, initiating X-ray analysis, determining space group and cell dimension. In addition, we plan to carry out a series of structural-functional studies to examine: the mechanism of metal binding by Cd¹¹³ NMR analysis, the location of metal sites by site directed mutagenesis and chemical labeling, and the oligomeric state of YiiP by a combination of dynamic light scattering, cross-linking and HPLC analysis.

SPECIFIC ACCOMPLISHMENTS:

Our studies on YiiP revised two fundamental misunderstandings in the metal transporter field about structure and function of YiiP and its representative protein family. Two papers are in preparation for refereed journals.

Heavy metal transporters are of critical importance both in human health and in bioremediation. Preliminary studies funded by LDRD laid the groundwork for future NIH and DOE funding.

LDRD FUNDING:

FY 2002	\$380,454
FY 2003 (budgeted)	\$396,000
FY 2004 (requested)	\$414,400

***In Vitro* Investigation of the DNA Double Strand Break Repair Mechanism by Non-Homologous End-Joining in the Context of Chromatin**

Elena S. Lymar

02-03

PURPOSE:

The DNA double-strand breaks (DSBs) cause chromosomal fragmentation and, if not repaired, may result either in cell death or cancer. The DSBs occur under cell exposure to genotoxic stress (e.g., oxidative stress, chemotherapy, ionizing radiation) as well as under normal physiological conditions. The predominant mechanism of DSB repair in humans is non-homologous end-joining (NHEJ). The defects in NHEJ have been implicated in a number of pathological conditions including severe immunodeficiency, tumorigenesis, radiosensitivity, accelerated morbidity, mental and growth retardation. Despite the progress in NHEJ research, there is still no precise mechanistic understanding of DSB repair *in vivo*, which to a great extent, is due to the lack of appropriate *in vitro* model.

This project is aimed at the development of a novel, advanced and physiologically relevant model for studying molecular mechanisms of DSB repair. The model will be based on chromatin templates, providing the closest possible approximation of the *in vivo* conditions. This model will allow the investigation of the most fundamental aspects of DNA damage and repair, which are not amenable to all presently available *in vitro* models based on the usage of free DNA. Specifically, we will address the following questions: (1) how DNA repair complex assembles on the site of damage in the context

of chromatin; (2) what type of chromatin remodeling complex assists this process; (3) which proteins mediate communication between these two complexes. We anticipate that the development of the unique and advanced experimental system for studying DSB repair *in vitro* as well as demonstration of its potency will help to secure the follow-on funding for further, in depth investigations of the mechanisms of DSB repair in human cells.

APPROACH:

To reconstitute the NHEJ protein complex *in vitro*, we will clone and express all of its components as recombinant proteins: DNA-PK_{cs}, Ku70, Ku80, Rad50, Mre11, Nbs1, Ligase4, and XRCC4. We will also express the proteins that have been shown to interact with the NHEJ complex and to regulate its function: C1D, HMG1, and HMG1. The proteins will be purified using conventional and affinity chromatography. As an additional benefit, having these proteins purified will enable structural characterization of the NHEJ repair complex.

To reconstitute human physiological chromatin *in vitro*, we will develop a novel and unique assembly system based on human recombinant chromatin remodeling complex. The only presently available recombinant chromatin assembly system is based on *Drosophila* proteins. They may not cooperate with human NHEJ proteins, since the NHEJ mechanisms in *Drosophila* and human differ. Thus, a chromatin assembly system based on human proteins will be more appropriate for studies of NHEJ in human. Our system will be composed of cloned human components: ACF1, ISWI (2H or 2L), TopoI, Chrac15, Chrac17, DNA and histones purified from human cells. It will be useful for studying any process on DNA when approximation to the natural conditions is desired. Moreover, it

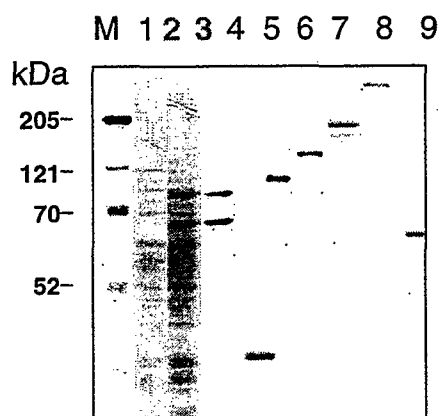
will be necessary for the other ongoing project in our laboratory on tumor suppressor p53, and will help to provide preliminary data to support a DOE or NIH proposal for the investigation of the role of p53 covalent modifications in gene regulation.

To study the mechanisms of NHEJ repair in the context of chromatin, we will have to design and establish a novel experimental system. All presently available *in vitro* models are based on free DNA. However, *in vivo*, DNA does not exist as a free species. In a cell, DNA is wrapped around histone octamers and forms a structure called chromatin, an actual substrate for both damage and repair. Chromatin is compact and largely inaccessible for protein binding. It can be unraveled and become accessible only by the action of specific chromatin remodeling complexes. How NHEJ repair proteins gain access to the site of damage in chromatin and which remodeling complexes are involved is not known and cannot be investigated without having a chromatin-based DNA repair model. Establishing this model is the most challenging part of this project. When this task is accomplished, we will have a unique tool for investigating DSB repair at the most advanced level, which will provide a strong basis for NIH grant applications.

TECHNICAL PROGRESS AND RESULTS:

The proposed technical goals for FY 2002 were largely accomplished. We cloned, sequenced, expressed, and purified the proteins necessary for the reconstitution of the NHEJ DNA repair complex. Since it was not possible to express these proteins in bacteria (the proteins are either insoluble or easily degradable), we established a more sophisticated protein expression system based on the usage of the insect embryonic cell line and

baculovirus infection. The system was successfully set up and proved suitable for the expression of functional proteins within a wide range of molecular weights (from 10 to 300 kDa). The figure below demonstrates the achieved purity of the recombinant proteins.



- 1 and 2: crude cellular lysate
- 3: 70 and 86kDa (Ku70/Ku80)
- 4: 40 kDa (XRCC4)
- 5: 100 kDa (Topo I)
- 6: 130 kDa (ISWI-2H)
- 7: 180 kDa (ACF1)
- 8: 300 kDa (P300)
- 9: 200 ng protein standard

To ensure efficient purification, we equipped the recombinant proteins with specific tags, which can be cleaved later, if necessary. To attach the tags, we used either commercially available vectors or vectors that we constructed ourselves. The latter allowed addition of Flag- or myc-tag for the easy one-step protein purification, GST-tag for protein interaction studies, and His-tag for a large-scale purification of two associated proteins simultaneously expressed from the same baculovirus.

We developed the human chromatin assembly system. For this system, the human proteins ACF1, ISWI-2H, ISWI-2L, Chrac15, Chrac17, TopoI were cloned, sequenced, expressed in the insect cells, and purified

using affinity chromatography. Histone proteins H2A, H2B, H3 and H4 were purified from the human cell line by conventional chromatography. DNA was purified by CsCl equilibrium centrifugation. The designed system was capable of deposition of H3/H4 tetramers onto DNA but required one more factor, histone chaperone Nap1, for the efficient deposition of H2A/H2B dimers. So far, Nap1 protein is the only protein of non-human origin in our system and will be substituted for its human homolog as soon as cloning of the latter is completed.

To summarize, during FY 2002 we finished the major preparative work, which is the most labor-intensive and time-consuming part of the project. We (1) constructed specific expression vectors; (2) established baculoviral protein expression system; (3) cloned, sequenced, expressed, and purified the proteins needed to reconstitute the NHEJ complex and the chromatin assembly system; and (4) developed the human recombinant chromatin assembly system. During FY 2003 our major efforts will be directed toward the establishment and characterization of the chromatin-based NHEJ DNA repair system.

SPECIFIC ACCOMPLISHMENTS:

“Characterization of Human Recombinant Chromatin Assembly Systems.” Symposium on the Eukaryotic Nucleus, March 8-11, 2003.

LDRD FUNDING:

FY 2002	\$63,659
FY 2003 (budgeted)	\$62,600
FY 2004 (requested)	\$65,400

Creating a MicroMRI Facility for Research and Development

Helene Benveniste

02-08

PURPOSE:

The goal of this project is to analyze the utility of a joint high field, high-resolution magnetic resonance imaging (microMRI) laboratory at Brookhaven National Laboratory (BNL) and at the University of Stony Brook (USB). The microMRI laboratory will serve as a research facility for several federally funded BNL and USB investigators whose research requires functional and high-resolution anatomical imaging of small animals and/or plants. A small-bore (20-cm) high field MRI instrument dedicated to imaging will become available at BNL and USB. The microMRI instrument will add great value to the current imaging infrastructure at BNL.

APPROACH:

The scientific interest in microMRI technology has escalated over the last few years as a consequence of the increase in genetically engineered mouse models of human disease. The need to visualize structural and functional anatomy in transgenic mice, targeted mutations or chemically induced mutations in mice during progression of disease and during therapeutic interventions has driven the MRI field into refining hardware and software for this purpose. Clinical MRI instruments are not suitable for small animal (rodent) imaging and special hardware such as actively shielded strong gradient systems (400mT/m-950mT/m) and high magnetic field are needed to facilitate the generation of MR images on 30-gm mice at the necessary microscopic spatial resolution of <100 microns. The Laboratory has

purchased a state-of-the-art 9.4T MR instrument, which will allow BNL and USB investigators to take advantage among others of the vast knowledge on the mouse genome. This LDRD is providing the dedicated technical expertise necessary to run the 9.4T MR instrument. This technical expertise will facilitate the use of the 9.4T instrument by the primary PI and the following other investigators: Nora Volkow (BNL), Peter Thanos (BNL), John S. Gately (BNL), Joanna Fowler (BNL), W. Rooney (BNL), Charles Springer Jr. (BNL), Stella Tsirka (USB), Brenda Andersen (USB), Ira Rampil (USB), Louis Pena (BNL/USB), and Marcello Vazques (BNL/NASA).

TECHNICAL PROGRESS AND RESULTS:

As described in the first report the initial LDRD Milestone Schedule was planned to incorporate installation of the microMRI instrument and on-site training during the first six months followed by actual initiation of research projects (cf. Table 1).

Table 1. LDRD Milestone schedule.

0-6 months	1. Install microMRI instrument 2. On-site Training 3. Animal protocols & compliance
6-12 months	1. Anatomical imaging 2. Physiological equipment 3. Initiate fMRI experiments

Refurbishing of space for 9.4T MR instrument.

The PI has worked closely with the BNL and Bruker Engineering teams to finalize the 9.4T MRI laboratory design. Progress meetings with the teams have lead to the establishment of starting and completion dates for the refurbishing project. A contractor has been chosen and started renovation November 6, 2002, and is

expected to complete the project by middle of March 2003.

Hiring of technical expertise

The current LDRD funding has enabled us to recruit a highly suitable competent biomedical engineer, Dr. Congwu Du, PhD, who will be dedicating research time to manage the microMRI 9.4T instrument. Dr. Du has worked in the field of biomedical engineering since 1993 and has also trained with Dr. Alan Koretsky at the NIH microMRI facility. We are very fortunate to have recruited Dr. Du to our microMRI program.

Small animal physiological equipment for MR imaging.

We have started to prepare for the arrival of the 9.4T MR instrument and other infrastructure for the subsequent many projects that will require monitoring of multiple physiological parameters. Through funding from the NYSTAR award we have purchased MR compatible small animal (rodent) physiological monitoring systems, which we have set up and tested on the 4T human MR scanner at BNL. All systems are in place and ready to be implemented in the small animal MR imaging laboratory.

SPECIFIC ACCOMPLISHMENTS:

None

LDRD FUNDING:

FY 2002	\$ 94,494
FY 2003 (budgeted)	\$196,000
FY 2004 (requested)	\$180,000

Targeting Tin-117m to Estrogen Receptors for Breast Cancer Therapy

Kathryn Kolsky

02-09

PURPOSE:

Most malignant tumors express one or more receptor proteins that are absent or subdued in normal cells. Targeting such exclusive proteins with radionuclides to image or treat tumors is a very attractive approach. The targeting moiety most often is an analog of the natural ligand for the receptors. In this project, we propose to synthesize Sn-117m labeled precursors that will selectively bind to the estrogen receptor on malignant breast carcinoma, while sparing the surrounding normal tissue. A majority of breast cancer cells express high levels of estrogen receptors that could be targeted for radiotherapy using short-range β^- or other electron emitters. Sn-117m emits abundant low-energy, high linear energy transfer (LET), monoenergetic conversion electrons that are lethal within a range of 200-300 nm from the site of localization. No significant efforts to label estrogen receptor ligands with radiometals have been made, despite some success that has been demonstrated using In-111-labeled octreotide that targets somatostatin receptors on neuroendocrine and a few other tumors. Radiohalogens, such as Br-80m or I-125 have been used for targeting estrogen receptors in very limited studies, but the results were only mildly encouraging. Radiometals promise prolonged residence time in the tumor by virtue of their slow metabolic efflux, and thus estrogens labeled with Sn-117m are expected to have better therapeutic efficacy than I-125 or Br-80m in terms of tumoricidal index.

APPROACH:

We propose to synthesize (17 α , 20E/Z) tributyltin estradiol and other similar derivatives, and through a structure-activity relationship study on these molecules, select 2-3 successful analogs. We will label them with Sn-117m and test their efficacy for estrogen receptor targeted therapy of breast cancer in SKBR-5 xenografted nude tumor mice. Based on these results, we will extend the study to synthesize more hydrophilic, long-circulating estrogens by attaching hydrophilic polymers to the steroid molecules. If successful, these investigations are expected to extend the application and use of Sn-117m and other high LET radiometals for therapy using, in addition to the steroids which will be the focus of this project, to other bio-engineered molecules including peptides, and antibodies.

TECHNICAL PROGRESS AND RESULTS:

A research associate, Dmitry Kosynkin, was hired to synthesize the required ligand molecules and started to work on the project in July 2002. Rooms 32 and 33 in Building 801 were equipped with Schlenk line, solvent distillers, a low-pressure hydrogenator and glassware. The inventory of chemicals was brought in full Chemical Management System (CMS) compliance and extended to accommodate the requirements of the project. State of the art was analyzed for steroidal and nonsteroidal estrogens with respect to their structure – receptor binding affinity relationships. A set of synthetic models was designed based on known synthetic methodologies and crystal structures of complexes of several unrelated estrogens with estrogen receptor ligand binding domain. High yielding, large-scale preparations for the synthetic precursors of the benzothiophene

moiety of the target molecules were developed as a result of optimization of published procedures.

In 2003 we anticipate to complete the synthesis of the first generation of the benzothiophene series of target molecules and conduct studies of the binding affinity with the ligand binding domain of the estrogen receptor for both native molecules and their complexes with non-radioactive tin isotopes. Contingent on the results of the binding studies, the investigation of biodistribution of complexes of the target molecules labeled with tracer levels of radioactive tin in animal models (rats) will commence.

In addition, a source for Sn-113, a long-lived stand-in for Sn-117m was developed with Los Alamos National Laboratory. Sn-113 will be used in place of Sn-117m until its production method has been developed.

SPECIFIC ACCOMPLISHMENTS:

An initiative for proliferation prevention (IPP) Thrust 2 project, entitled "Production of High Specific Activity SN-117m," was written and funded to develop a source of no-carrier-added Sn-117m radionuclide.

LDRD FUNDING:

FY 2002	\$ 56,000
FY 2003 (budgeted)	\$100,000
FY 2004 (requested)	\$ 50,000

Biomining of Actinides: A Mechanistic Study of the Genesis of Novel and Stable Compounds

A. J. Francis

02-16

C. J. Dodge

J. B. Gillow

G. Vazquez

PURPOSE:

Elucidate the fundamental mechanisms of stabilization of soluble actinides (organic- and inorganic-complexes and colloidal forms) by naturally occurring phosphate and polyphosphate-producing microorganisms. Specifically, we are investigating (i) the nature of association of U with phosphate minerals formed as a result of microbial action, and (ii) the stability of U-phosphate minerals by elucidating the mechanisms of dissolution of U and phosphate.

Results of this basic research should lead to (i) a better understanding of the environmental conditions likely to foster retardation of actinide mobility and transport, and (ii) strategies for engineered long-term immobilization of actinides in waste repositories and in contaminated soils, sediments, and wastes.

APPROACH:

In this study we are (i) elucidating the fundamental mechanisms of stabilization of soluble actinides (organic- and inorganic-complexes and colloidal forms) by naturally occurring phosphate and polyphosphate-producing microorganisms; (ii) determining the factors that favor the formation of stable actinide mineral phases by the addition of Ca and other elements; (iii) characterizing the nature of the association of actinides with the phosphate mineral; (iv) evaluating

the stability of actinides with newly formed phosphate mineral phases; and (v) establishing a structure-function relationship with broad application to immobilization of other actinides and toxic metals of interest.

Uranium was used as a model compound in the initial studies. We selected (poly)phosphate-producing organisms for detailed study and determined the speciation and molecular association of uranium in various U-phosphate minerals and selected bacteria.

TECHNICAL PROGRESS AND RESULTS:

Selection of microorganisms. Several aerobic and anaerobic bacteria (halophilic and non-halophilic, and archaea) were tested for their ability to bioaccumulate uranium. These include *Pseudomonas fluorescens*, *Bacillus subtilis*, *Clostridium sp.*, *Halobacterium halobium*, *Haloanaerobium praevalens*, and *Halomonas sp.* When exposed to uranyl nitrate these bacteria accumulated uranium both extracellularly and intracellularly to varying degrees. Uranium distribution and its association in



Figure 1A. TEM of thin section of *Halomonas sp.* shows intracellular accumulation of uranium as granules.

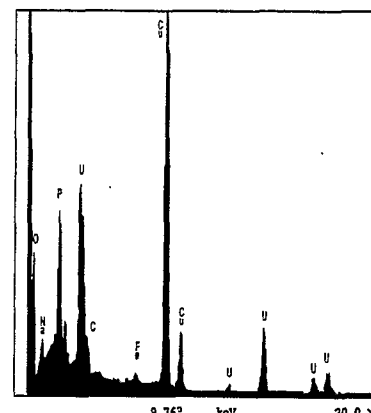


Figure 1B. EDS spectra shows U and P are the major constituents of the intracellular granules.

the cells was determined by Transmission Electron Microscopy (TEM), Energy Dispersive X-ray Spectroscopy (EDS), and Extended X-ray Absorption Fine Structure (EXAFS). In *Bacillus subtilis* uranium accumulated at the cell surface as irregularly shaped mineral grains and in *Pseudomonas fluorescens* it was found at the cell surface. In *Halomonas* sp. uranium accumulated both intracellularly and extracellularly and uranium was localized as electron dense granules inside the cell (Figure 1A and B). TEM and EDS spectra were obtained through collaboration with T.J. Beveridge, University of Guelph, Ontario, Canada. We selected *Halomonas* sp. for further study.

Speciation of uranium and its molecular association with various synthetic phosphate minerals and bacteria. The oxidation state and the association of U with various phosphate minerals, and with bacterial cells were determined by X-ray Absorption Near-edge Spectroscopy (XANES) and EXAFS at the National Synchrotron Light Source (NSLS).

Uranium standards consisting of uranyl hydrogen phosphate $\text{UO}_2\text{HPO}_4 \cdot 2\text{H}_2\text{O}$, Chernikovite $(\text{H}_3\text{O})[\text{UO}_2\text{PO}_4]_2(\text{H}_2\text{O})_8$, and meta-autunite $(\text{Ca}[(\text{UO}_2)\text{PO}_4]_2(\text{H}_2\text{O})_6)$ were synthesized using standard methods. Short and long chain U-polyphosphate species were obtained commercially. The samples were analyzed in the fluorescence mode using a Passivated Implanted Planar Silicon detector (PIPS) detector on beamline X23A2 at the NSLS. Preliminary analysis of the raw EXAFS data shows the polyphosphate to be most similar to Chernikovite (Figure 2). Fitting of the Fourier-transform data is in progress. Chernikovite is an important, though potentially short-lived, mineral in the paragenesis of uranyl phosphates. The mineral may also replace uranyl oxyhydroxides in low phosphate bearing regions.

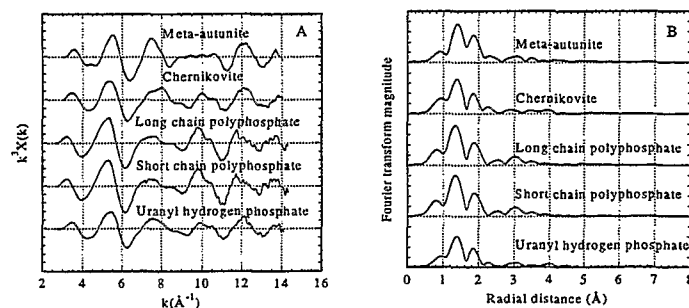


Figure 2 A and B. EXAFS spectra at the U L_3 edge showing (A) raw k^3 -weighted EXAFS spectra (2.9 to 14.1 \AA^{-1}) and (B) Fourier transformed spectra showing U association with phosphate minerals and with a short- and a long-chain polyphosphate.

Bioaccumulation of Uranium in *Halomonas* sp. Uranium was associated with *Halomonas* sp. predominantly as uranyl hydrogen phosphate ($\text{UO}_2\text{HPO}_4 \cdot 2\text{H}_2\text{O}$). Cell fragments of lysed *Halomonas* sp. cells also showed complexation with phosphate, as well as with carboxylate groups as a bidentate complex. Addition of U to the cell lysate of *Halomonas* sp., which contained cellular phosphate and other cellular components, resulted in the precipitation of U. These results show that the bacterial cells are rich in cellular inorganic phosphate, which have a strong affinity for U, and bind a significant amount of U despite the presence of other functional groups in bacteria.

These initial results indicate stable U-phosphate mineral species may be obtained from bacterially generated phosphate following an equilibration period.

The stability of U-phosphate minerals will be determined by elucidating the mechanisms of microbial dissolution of U bound to various phosphates by (i) direct enzymatic action involving reductases for U transformation and polyphosphate kinase

(PPK) for polyphosphate transformation, and (ii) indirect action due to production of extracellular metabolites. Fundamental understanding of the nature of association of uranium with phosphate minerals and their interactions with microorganisms at the molecular and biochemical level will be useful in the selection of appropriate microorganisms for the biogenesis of phosphate containing mineral phases and the long-term immobilization of actinides and toxic metals. Future work will involve extension of these studies to other actinides and toxic metals.

Milestones Planned for FY 2003.

- Identify the U-P minerals formed as a result of bacterial action.
- Elucidate the mechanisms (enzymatic and non-enzymatic) of U dissolution from microbially formed phosphate minerals under aerobic and anaerobic conditions.
- Determine the factors which favor formation of stable U-P mineral phases.
- Determine the structure function relationship (degree of crystallinity, nature of bonding, nearest neighbor, etc).

SPECIFIC ACCOMPLISHMENTS:

Francis, A.J.; Gillow, J.B.; Dodge, C.J.; Harris, R.; Beveridge, T.J.; and Papenguth, H.W. Association of Uranium with Halophilic and Non-halophilic Bacteria and Archaea. [manuscript to be submitted to *Radiochimica Acta*].

LDRD FUNDING:

FY 2002	\$88,871
FY 2003 (budgeted)	\$93,000

Using Mini-LIDAR for Verification and Long-Term Monitoring of Cover Systems

John Heiser

02-17

PURPOSE:

The Environmental Research and Technology Division (ERTD) at BNL developed a novel methodology for verifying and monitoring caps and cover systems (covers) used to remediate hazardous and/or radioactive waste sites. The technology uses gaseous perfluorocarbon tracers (PFTs) to determine the flaws (e.g., holes or cracks) and high permeability areas in covers. This project will develop an optical (laser-based) technique for the detection of PFTs for use in environmental monitoring. A Mini-LIDAR system and above-grade air monitoring will replace the traditional soil-gas sampling and gas-chromatographic analysis of the PFT(s).

Long-term monitoring and verification of covers is of great interest to DOE-EM. With the increased focus on accelerated clean up at the various DOE sites, there is considerable concern about long-term stewardship issues in general, and verification and long-term monitoring (LTM) of caps and covers, in particular. DOE-EM set up a national committee of experts to develop a long-term capping guidance document. The PI for this project was on the committee and served as the verification/LTM expert.

In the recent past, the ERTD received funding through the Office of Science and Technology (OST) Subsurface Contaminants Focus Area (SCFA) to develop PFT verification and monitoring for caps and cover systems. This LDRD

focuses on developing a new and novel detection technology. Once developed, the technology would also be useful for monitoring and surveying for contaminants such as volatile organic compounds (VOCs). We will leverage the LDRD in an attempt to secure new funding in the area of LTM and will also pursue funding for *in-situ* real-time monitoring of VOCs in such areas as dynamic underground stripping of VOCs from groundwater.

APPROACH:

The BNL cover verification/monitoring technology uses gaseous tracers, which are injected below a cover and searched for on the top-side of the barrier. The sampling grid, concentration and time of arrival of the tracer(s) are used to determine the size and location of flaws and to determine relative permeability of the barrier.

Traditionally, detection of the PFTs has been done using gas chromatography techniques developed at BNL. While this analytical method is very sensitive and allows detection of part per quadrillion levels, it also requires gas sampling ports placed on 5 to 10 foot spacing throughout the barrier and air sampling equipment to draw the samples either into storage bags or directly into a field gas chromatograph (GC). Installation of the ports is time consuming and requires penetrations into the ground. Any penetrations into the ground, even if they do not penetrate the cover itself, introduce additional potential failure points. It may be as simple as causing water or wind erosion points (due to turbulent flow around the stand pipe) or water ingress pathways. Sampling a typical one-acre site with 5 foot spacing would also require 800 sampling ports. GC analysis of this many ports is time consuming and can be very expensive (currently ~\$75 per sample). The GCs used for PFTs are also prone to failure if used in a

typical long-term monitoring application. The GC would be expected to operate one to four times each year and remain “dormant” the rest of the time. Experience shows that GCs are not best utilized in such a manner and heavy-duty cycle GCs typically require full-time operation.

BNL collaborator, Art Sedlacek, has considerable experience with laser systems and in particular LIDAR. Mini-LIDAR systems appear to be ideally suited to the detection/monitoring needs of PFTs in the application of cover system verification and monitoring. Differential Absorption Lidar (DIAL) has routinely achieved detection sensitivities on the order of low parts-per-million (ppm) to high parts-per-billion (ppb) levels. Literature suggests that for PFTs, detection limits as low as 0.1 ppb may be achievable. We plan on using Mini-LIDAR over a far more restricted distance (10 to 100 feet) than typical LIDAR systems are used (kilometers). This will help in our efforts to increase the sensitivity of the Mini-LIDAR to the ppb range. A Mini-LIDAR system would be set up at a cover system and the laser then scans the entire field. The system would simultaneously measure concentrations and locations of PFTs above the cover system. This information would be translated to assess the performance of covers in a manner similar to using conventional GC analysis.

TECHNICAL PROGRESS AND RESULTS:

During FY 2002, a project review and safety analysis was performed and required documentation was completed and approved prior to the beginning of laboratory work. A tunable, CO₂ laser was refurbished and brought into operating condition. The laser emits in the infrared region required for absorption studies of the PFTs. A detector was found that operated in the region of

interest and was wired to an amplifier and mounted onto a laser table with the CO₂ laser. Optics and a one-meter gas cell were positioned on the laser table such that a simple two-pass (out and back) LIDAR configuration was obtained. The system schematic is depicted in Fig. 1, and the actual laboratory set-up is pictured in Fig. 2.

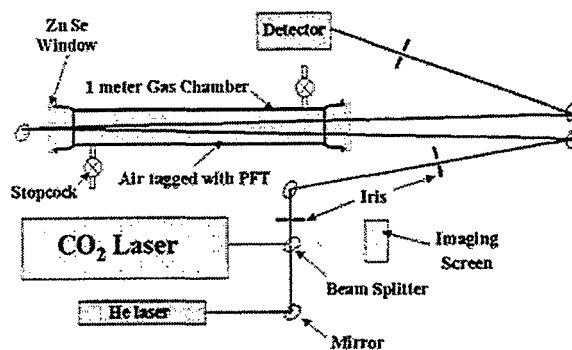


Figure 1. Schematic of laboratory test set-up for PFTs

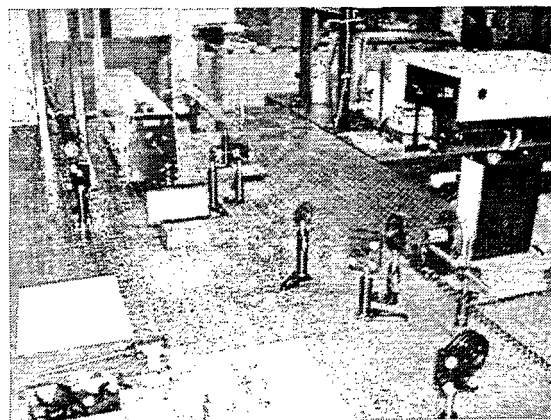


Figure 2. Photograph of laboratory set-up (with laser path appended)

After aligning the optics and detector, a series of experiments were completed to determine the maximum absorbing line for the laser using the PFT pmch. The gas cell was filled with air containing nominally 350 ppm of tracer. The laser was directed through the cell and the absorption measured. After each measurement the output wavelength of the laser was changed. This was done until the peak absorption was

found. All later experiments were completed using the peak wavelength.

With the laser system optimized, absorption versus concentration curves were generated. The beam was chopped as it entered the detector to provide a differential output curve. The gas cell was filled with tracer-spiked air and the peak height was measured (average of 250 samples). After each measurement the cell contents were sampled into gas-sample bags and sent to an on-site laboratory for analysis of the chosen PFT, perfluoromethylcyclohexane (PMCH) concentration. The tracer concentration in the cell was then changed and the procedure repeated.

Figure 3 gives a series of absorption curves for the PMCH. The peak height was plotted versus concentration to obtain the absorption cross-section for PMCH (see Figure 4). The value obtained was the same order of magnitude compared to literature values for other perfluorocarbon compounds.

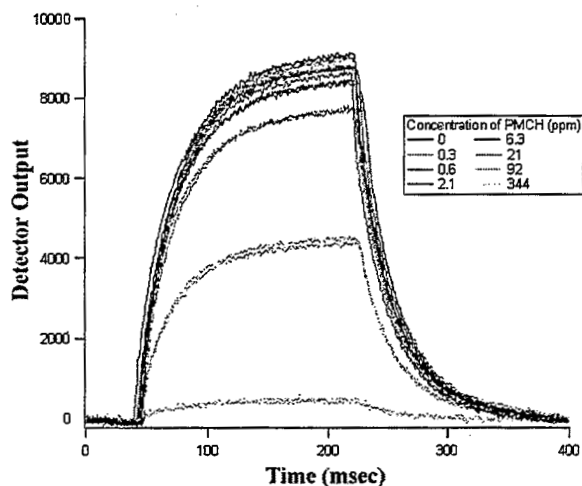


Figure 3. Absorption curves for PMCH in air (August 2002).

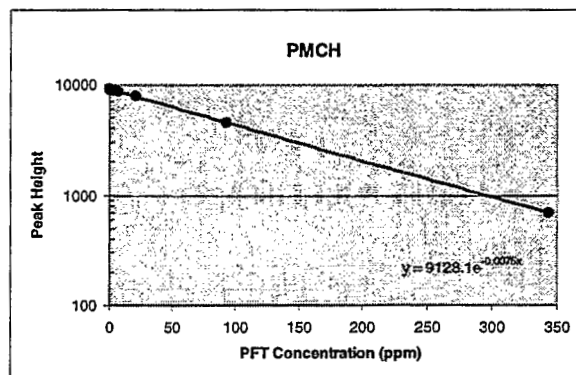


Figure 4. Peak height versus tracer (PMCH) concentration (August 2002)

The first round of experiments achieved a resolution of approximately 30 ppb. The laser output was then more carefully stabilized using a feedback loop to the high voltage. This resulted in a resolution increase and detection down to 10 ppb was accomplished.

We have not yet reached the desired resolution of 1.0 to 0.1 ppb. To accomplish this we plan to perform FTIR on the tracer PMCH to make certain that we are not missing a more desirable absorption line. In addition, a better detector may also increase sensitivity.

For FY 2003, we expect to move from the laboratory to hallway and/or field experiments. A field deployable LIDAR will be used to measure PFTs that will be released in a small “puff.”

SPECIFIC ACCOMPLISHMENTS:

None

LDRD FUNDING:

FY 2002	\$125,000
FY 2003 (budgeted)	\$125,080

Electrical Systems Reliability

Robert A. Bari

02-22

PURPOSE:

The purpose of this research is to develop a methodology for a probabilistic assessment of the security of electrical energy distribution networks including the future grid system, which relies heavily on the communication industry for monitoring and protection. The identification of potential failure modes and their likelihood will permit informed decisions on potential modifications to the network including hardware, monitoring instrumentation, and protection systems. We will extend the technology developed and apply the techniques to address the electrical configuration of the Consolidated Edison (Con Ed) system. We are currently working collaboratively with Con Ed. The management in KeySpan and the Long Island Power Authority (LIPA) also have expressed their interest in collaborative projects with BNL in this area. Successful achievement of this research by developing and demonstrating the methods could establish BNL as a frontier laboratory in the areas of reliability assessment of electrical power grids.

APPROACH:

The traditional approach to electrical grid reliability is based on deterministic analyses for congestion and transient response under normal conditions or a condition that satisfies "a single failure criterion." Such methods have shown to be effective and have resulted in sound designs which are robust to major single failures. However, past events have shown that multiple cascading failures under unfavorable conditions have been the major contributor

to losses of electrical distribution systems. Another factor in the evolution of the electrical grid systems is their ever-increasing reliance on communication infrastructures for protection and monitoring, which are not easily amenable to traditional deterministic analysis.

Powerful reliability methods have been developed in the past three decades in the nuclear industry, which could be tailored for use in evaluating the reliability of the existing and the future electrical grid system. These methods have the capability of, systematically and in an efficient manner, incorporating the deterministic models for congestion and transient response analyses.

Others have developed methods for identification of the potential vulnerability of a large grid system using the grid topology (e.g. application of "small world" techniques), and use of empirical fault propagation using epidemiological models. These methods are macroscopic in nature and do not address the detailed design issues of a grid system. At best they can identify portions of the grid that are suspected of potential vulnerabilities.

In contrast to these models, our model is microscopic in nature and relies heavily on the specific design of the portion of the grid being analyzed. It extensively models the types of faults the grid could potentially experience, the response of the grid, and the specific design of the protection schemes. The importance of fault detection and protection schemes is heavily emphasized, and the role of future reliance on the communication infrastructure is addressed. Finally, the methods proposed are quantitative in nature, thereby allowing prioritization, reliability allocation to different modules, and the verification of the

design that meets the allocated reliability goal.

TECHNICAL PROGRESS AND RESULTS:

This research began with a review of the existing literature pertinent to the problem. In order to focus on a particular system, cooperation with Con Ed was sought and assured. This led to familiarization and understanding of Con Ed's electrical distribution system and their reliance on communication technology for control and protection of their network. A site visit to a Con Ed substation was arranged and occurred. A meeting was also held with Verizon because they provide one of the redundant communication paths in the Con Ed system. A Confidentiality Agreement was established between Con Ed and BNL to allow us to obtain access to their system configurations and operational and failure data.

A preliminary evaluation of an electrical energy distribution system coupled to a control/protection system has been done. In concert with this activity, a computer model of the network system, intended to simulate an actual system, was initiated.

Important progress was realized in the development of a reliability database for the electrical system and the development of a reliability database for the communication system pertinent to electrical grid application. This was followed by the development and tailoring of the reliability methods for application to an electrical grid system.

The pilot application to the Con Ed grid subsystem has been partially completed: events trees for the key failure event have

been developed and preliminary quantification of fault trees has occurred.

During FY 2003, we will continue to apply our expertise in reliability and risk to develop a methodology for a vulnerability assessment for electrical distribution networks operated by Con Ed. The identification of these configurations will be able to provide informed decisions on potential modifications to the network including hardware, monitoring instrumentation, and system control aspects. Upgrades to a network and improvements in emergency procedures would demonstrate their effectiveness in providing an enhanced distribution network segmentation capability and greater flexibility in responding to multiple contingency situations.

SPECIFIC ACCOMPLISHMENTS:

A paper entitled "Electrical Systems Reliability and Related Communications Infrastructure" will be submitted to an appropriate refereed journal in the second quarter of FY 2003.

LDRD FUNDING:

FY 2002	\$ 85,000
FY 2003 (budgeted)	\$100,000
FY 2004 (requested)	\$157,000

Liquid Fuel Gasifier for Combustion and Fuel Cells

Thomas Butcher

02-24

PURPOSE:

Liquid fuels provide high energy densities and this provides a great advantage particularly for remote or mobile applications. In many applications however, a gaseous fuel offers critical advantages in emissions, heat transfer, and flame control. Conversion of oil to gaseous fuels in practical systems can be complicated by coke and deposit fouling. The purpose of this project is to develop oil-to-gas conversion methods via vaporization and partial oxidation which can lead to ultra-low NO_x oil combustors and oil reformers for fuel cells.

APPROACH:

A major problem which has been encountered in prior related work is successful vaporization and partial oxidation of oil without the formation of soot, deposits, and coke. This depends on the chemical structure of the fuel and on the process in the vaporizer/partial oxidizer. Conventional vaporizers have a separate feed of air and atomized fuel to the processing zone. Our group has developed a low- pressure air atomization concept in burner applications, where the fuel spray and air are nearly premixed in the nozzle and a flame with a high internal recirculation rate. This patented concept is now being used in several other burner development projects. In this project we are exploring the deployment of this concept for a liquid fuel, partial oxidation gas generator.

Following vaporization, oxidation of the fuel under "cool flame" conditions is being

studied as a method of generating a fuel gas which will not recondense on downstream surfaces. These cool flame reactions occur between 320 and 400 C and have been studied in some detail with model compounds (n-heptane). Some results in the literature have shown that these reactions can be used with practical fuels, such as diesel oil, followed by porous surface burners. There is, however, no available data on the products of the low temperature oxidation step with practical fuels. This is needed to allow system design optimization, extension to other conditions, and comparison with other technical options which do not include this step.

Planned work in this area includes a detailed review of prior work in this area, design of a facility at BNL which will enable study of these reactions with a practical fuel, using the BNL air atomization concept, and experimental studies.

Project collaborators at BNL include Dr. C.R. Krishna, Dr. Abdallah Naidja (FY 02), and Dr. Devinder Mahajan.

TECHNICAL PROGRESS AND RESULTS:

A detailed review of the prior literature in this area has been completed. From this the key issues to be evaluated have been identified as well as a preliminary reaction model. Following from the review a test reactor, air heater, and atomizer concept have been designed and construction of this facility has been started. A computational fluid dynamics (CFD) simulation of the atomizer flow and droplet vaporization in this reactor has been completed. Also completed is an analytical plan for characterization of the hydrocarbons produced in the low temperature oxidation step.

Much of the prior work in this area has been done by a research group in Aachen, Germany. Contact has been made with this group and a visit paid to their laboratory. They have also visited BNL, and we have had detailed discussions of our research plans in this area. Future collaboration is under active discussion.

During Fiscal Year '03 the test reactor system will be completed and operated. Work will then focus on characterization of the products and analysis of applications to ultralow NOx oil burners and fuel cell reformers.

SPECIFIC ACCOMPLISHMENTS:

Major review paper submitted to a peer review journal:

Oxidation of Fuels in the Cool Flame Regime for Combustion and Reforming for Fuel Cells, Naidja, A.; Krishna, C. R.; Butcher, T.; and Mahajan, D. Submitted to Progress in Energy and Combustion Science, August 2002 BNL 69349

LDRD FUNDING:

FY 2002	\$ 73,000
FY 2003 (budgeted)	\$109,000

Study of a Power Source for Nano-Devices

Mow S. Lin

02-31

PURPOSE:

It is possible to build nano-devices out of nano-wire, tube or other blocks, however, to power such devices on a nano-scale is challenging.

A naturally occurring powerhouse will be used to prove the concept. This natural powerhouse built as part of the nano-device will be driven by solar energy, converting photo-energy into electric potential, thus avoiding transmission of power via direct wiring. The molecular power supply to be tested is bacteriorhodopsin (BR), a purple-colored membrane protein isolated from *H. halobium*, which displays outstanding stability and non-linear optical properties.

The object of the proposed research is to integrate the photo-driven proton pump (BR) with functional groups in nano-devices in order to overcome power transmission problems inherent to such devices (especially free moving ones).

This feasibility study may lead to the development of a process for fabricating nano-electronics, ultra fast photoactive on-off switch and random access memory, biosensor and solar energy converter.

The project fits well into the BNL strategy planning of the newly funded nano-technology center.

APPROACH:

As originally proposed studies of self-assembly on silicon surface will be systematically tested on a variety of pure and

doped silicon crystals. The first step is to arrange the BR molecule at specific positions on silicon surfaces. Other molecules for example, fullerenes, porphyrins, conjugated polyenes and thiophenes may be tested as back up using different self-assembly techniques.

- The assembly of molecules will be accomplished by using Langmuir-Blodgett (LB) techniques, either by evaporating a thin monolayer film of the molecule or by dip-and-pull from a monolayer film formed in a trough. This step will allow for spontaneous assembly on silicon, Si (100), surface templates. Then molecules with specific properties (e.g. conduction, charge transfer or fluorescence quenching moiety) will be attached in conjugation with specific properties of BR. The synthesized molecules of nanometer size can be recovered from the template and characterized. Molecules with special properties will be used as building blocks or subject to further reactions for building complex materials.
- Different templates: Si (100) surface template will be tested for their sensitivity to pH and surface modification agents in an attempt to alter the template for different syntheses. Other surfaces e.g. Si (111), semiconductor, GaAs, tin oxide (ITO) and other metal oxides will be tested for use as different templates.
- Field and medium effects: The synthesis will be carried out under the magnetic or electric field in an attempt to change the orientation of the absorbed molecule on the template.
- Critical-state control: Setting up two systems adjacent to phase transition or

defects such that the synthesis can be conducted along the interfaces in controlled orientation.

- Atom manipulation method using scanning probe microscopy (SPM) will be tested on BR or atoms on silicon surfaces.

TECHNICAL PROGRESS AND RESULTS:

Materials for the first phase of the experiments have been purchased. A Langmuir-Blodgett trough (LB trough) obtained through the DOE excess property program has been repaired and restored, it is currently operational. The bacterium *H. halobium* has been cultured and its membrane protein bacteriorhodopsin has been isolated and purified to the highest quality. The monomeric protein unit has been extracted from the membrane with a Triton X-100 detergent and purified by dialysis out of the detergent. It has been compressed into a monolayer film in the restored LB trough. The self-assembly experiment has been performed to spread a monolayer of bacteriorhodopsin units on a (100) silicone wafer. Structure determination by using Atomic Force Microscopy (AFM) in J. Wall's Scanning Transmission Electron Microscope (STEM) group in the Biology Department has shown good progress. Further structure study by using X-25 beam line in NSLS has been arranged for beam time in late January 2003 in collaboration with M. Becker of the Biology Department.

The project has progressed on the funded scale and schedule.

In the continuation of this work, the structure of self-assembled BR monolayer will be determined. A second monolayer of the functional group will be assembled on top of the first layer of bacteriorhodopsin. Chemical reactions will be conducted to connect the two assembled layers. The structure of the resulting unit will be determined and its electronic function will be studied using Scanning Probe Microscopy (SPM), which will be studied in collaboration with S. Wong in the Material Science Department in FY 2003.

SPECIFIC ACCOMPLISHMENTS:

A spin-off project titled "Molecular Engineering: The Next Generation in Gas Purification Technology" is recently funded by DOE Natural Gas and Oil Technology Partnership Program (NGOTP) at \$250K/yr for 3 years. The project is aimed to develop molecular imprint technique for separating methane from other gases ie. carbon dioxide, nitrogen and higher hydrocarbons in natural gas and thus purify the low-grade natural gases.

LDRD FUNDING:

FY 2002	\$ 99,920
FY 2003 (budgeted)	\$100,000
FY 2004 (requested)	\$165,000

Ultrafast Nonlinear Spectroscopic Studies of Model Catalytic Surfaces

Nicholas Camillone III

02-42

PURPOSE:

The goal of this project is to develop ultrafast nonlinear optical methods directed at the molecular-level study of the kinetics, dynamics and structure of organic molecules interacting on model catalytic surfaces in gaseous environments, spanning pressures ranging from 10^{-10} to 10^3 Torr, and in liquid environments. The application of such capabilities in the context of nanostructured surfaces will provide unique kinetic and dynamic insights into structure-reactivity relationships, and as such are relevant to furthering the development of chemical nanosciences at Brookhaven.

APPROACH:

Over the last decade, sum frequency generation (SFG) and second harmonic generation (SHG) have been demonstrated to be valuable probes of interface structure, reaction kinetics and adsorbate dynamics.¹ Paralleling these developments, recent advances have been made in the control of interface structure at the nanoscale by physical, chemical and electrochemical methods. Work in other laboratories is demonstrating the value of combining nonlinear optical techniques with nanoscale preparation methods, for example, in determining differences in adsorbate structure on supported nanoparticles as compared to single crystal surfaces.² This convergence of technologies opens new opportunities for molecular-level probing of the chemistry of catalysis by innovative application of the nonlinear optical techniques to the kinetics

and dynamics of molecule-nanoparticle interactions.

Thus, the approach to be taken in this LDRD project is the design, acquisition, construction and development of the instrumentation for nonlinear optical probing of chemical reactions in real time with optical SHG in ultrahigh vacuum, atmospheric pressure and liquid ambients. Once developed, this infrastructure will be positioned to make significant contributions to the BNL Nanocenter by fostering collaborative user-based efforts.

The risk in these experiments is low signal levels expected as a consequence of the low concentrations characteristic of nanoparticle assemblies. Strategies to be explored in overcoming this difficulty include the use of high peak power femtosecond lasers and exploitation of signal enhancements due to surface plasmon resonances.^{3, 4, 5}

TECHNICAL PROGRESS AND RESULTS:

The initial stage of construction involved acquisition of a solid-state-pumped, mode-locked Ti:Sapphire femtosecond laser system and preparation of the laboratory for Class IV laser operation including design and installation of an interlock system. A homebuilt autocorrelator was built to characterize the pulsewidth of the laser light. Figure 1(a) illustrates some early results.

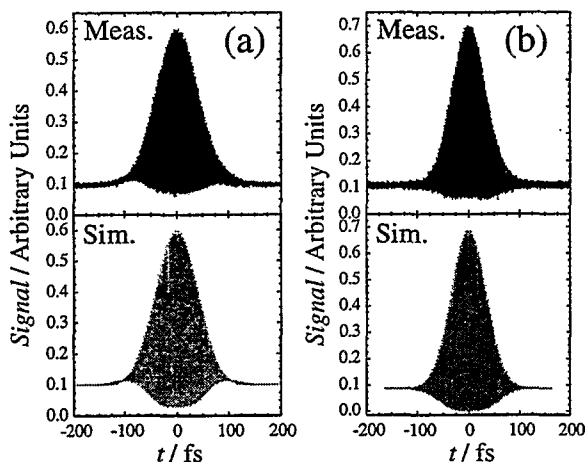


Figure 1. (a) Measured and simulated interferometric autocorrelation patterns. Simulation indicated an 80 fs pulsewidth and a linear frequency “chirp” of $3 \times 10^4 \text{ fs}^{-2}$. (b) Measured and simulated post GVDC compensation interferometric autocorrelation patterns indicated a 52 fs pulsewidth with no indications of a frequency “chirp.”

Optical components for controlling and directing the laser and detecting the second harmonic (SH) signal were designed, acquired, and installed. A schematic of the experimental optical setup is shown in Figure 2. A zero order $\frac{1}{2}\lambda$ waveplate (HWP) is used in tandem with a polarizer (P1) to control the incident laser intensity and polarization orientation. A red filter (F1) is positioned just prior to the experimental surface to block any spurious SH light generated in the optics. The large majority of the reflected light at the fundamental wavelength is blocked by a blue/green filter (F2). The SH light is directed into an enclosure containing a monochromator to attenuate ambient and residual fundamental light. The SH signal is detected by a photomultiplier tube and processed by a photon counter.

To maximize the field at the experimental surface, a group velocity dispersion compensator (GVDC) was constructed. Figure 1b illustrates a measurement and simulation of pulses compressed by the GVDC. Post-GVDC pulsewidths were confirmed to be Fourier Transform limited.

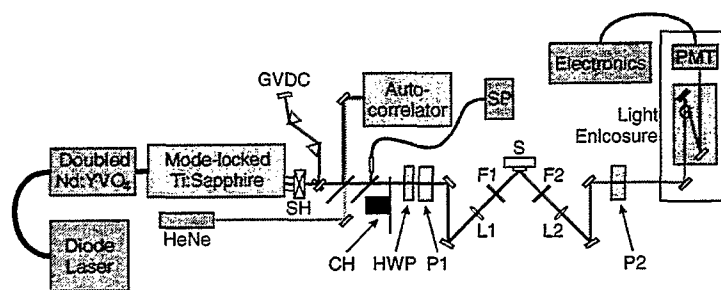


Figure 2. Optical scheme for SHG experiments.

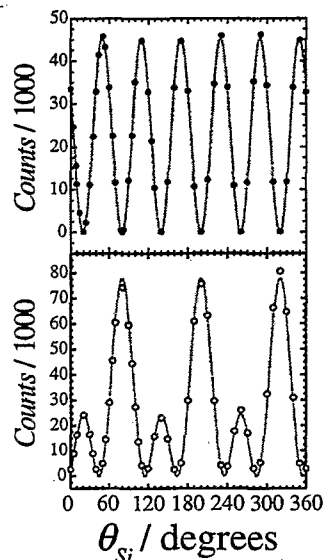


Figure 3. Measured SH rotational anisotropy of the $\text{SiO}_2/\text{Si}(111)$ interface in air for *s*-polarized incident radiation and *s*- (top) and *p*-polarized (bottom) SH radiation.

The surface SHG system was validated by comparison of measurements of the rotational anisotropy of SH from the $\text{SiO}_2/\text{Si}(111)$ interface in air, as illustrated in Figure 3, with those found in the literature.⁶

Apparatus for measuring surface reaction kinetics in a liquid environment was designed, constructed, and tested. The apparatus consisted of a sample mounting assembly, a spectrochemical cell, a solution reservoir bottle and two peristaltic liquid pumps. The sample holder and cell, illustrated in Figure 4, were constructed from chemically inert materials. Solvent is

circulated through the system by the peristaltic pumps and a reservoir bottle allows for nitrogen bubbling, mixing, filtering and the abrupt introduction of solutions into the system, while maintaining a low level of turbulence in the cell. The sample is mounted on a tilt stage which is suspended from a computer controlled rotation platform, allowing *in situ* measurements of the SH rotational anisotropy.

Experiments using SHG to measure the flow rate dependence of the self-assembly of decanethiol on Au(111) surfaces were performed. The results are shown in Figure 5. To the best of our knowledge, these measurements are the first demonstrating a systematic dependence of adsorption rate on flow rate for self-assembling amphiphiles from solution. Analysis of these data is currently in progress, and their implications regarding the self-assembly mechanism are the subject of a paper currently in preparation.

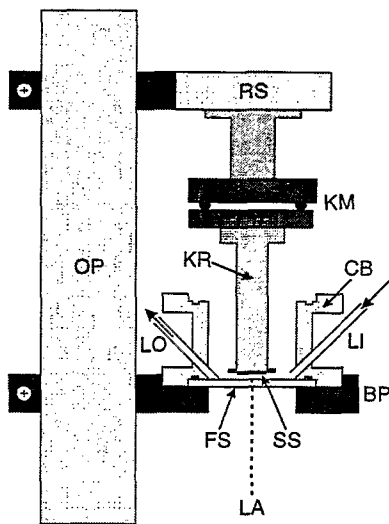


Figure 4. Schematic of the spectrochemical cell. Key: OP-optical post, RS-rotational stage, KM-kinematic mount, KR-Kel-F rod, CB-Teflon cell body, LI-liquid input, LO-liquid output, FS-fused silica window, LA-laser access plane, SS-sample surface, BP-base plate.

In addition, an ultra high vacuum (UHV) surface analysis system with attached atmospheric-pressure reaction chamber was

designed and all major chamber and analytical components have been acquired. Assembly of the system, as well as design and construction of peripheral components is currently underway.

Software written included two data collection programs — (1) for SHG kinetics data acquisition and (2) for SHG rotational anisotropy data acquisition — and one data simulation program for interferometric autocorrelation pattern simulation.

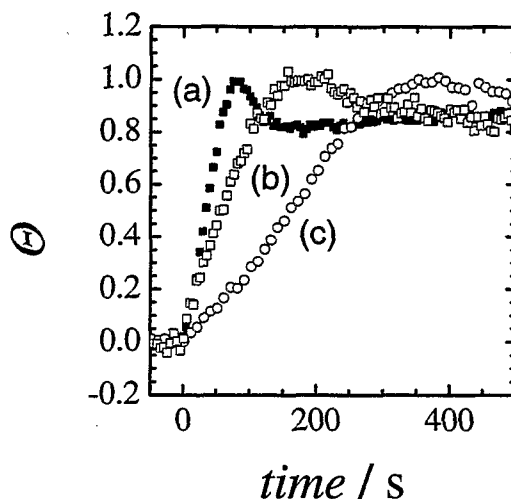


Figure 5. Surface coverage as a function of time as measured *in situ* during self-assembly of decanethiol on Au(111) in 2 μM solution showing an increasing rate of adsorption with an increasing solution flow rate ($a > b > c$).

Continuation of this work over the next fiscal year is anticipated. Plans include completion of the UHV surface preparation and analysis facility and atmospheric-pressure reaction chamber. Addition of electrochemical capabilities to the spectrochemical cell, in collaboration with R. Adžić (Materials Science), is also planned. Specific experiments planned involve SHG measurements of molecular adsorption on nanoparticles in solution (collaboration with C. Creutz, Chemistry), specific adsorption of nanoparticles on solid surfaces, and probing the kinetics of nanoparticle growth in UHV and in solution.

Finally, during the coming fiscal year a focused effort directed towards securing longer term DOE office of BES support for this effort is planned. Collaborations with J. Hrbek, M. White, and J. Rodriguez (Chemistry) and funding for extension of the system's capabilities to include pump-probe SFG for dynamics as part of the catalysis effort will be pursued.

SPECIFIC ACCOMPLISHMENTS:

N. Camillone participated as Co-Principal Investigator in a proposal submitted Jan. 2002 in response to the DOE office of BES *Nanoscale Science, Engineering and Technology* solicitation for DOE laboratory activities. The proposal was entitled: "*Preparation and Characterization of Metal and Alloy Nanoparticle Electrocatalysts*" Co-Principal Investigators: J. McBreen, R. Adžić, and S.S. Wong.

Manuscript in preparation for submission to *Surface Science*:

N. Camillone III, "*An optical second-harmonic generation measurement of the kinetics of self-assembly of decanethiol monolayers on Au(111).*"

REFERENCES:

1. J.I. Dadap, T.F. Heinz, "Nonlinear Optical Spectroscopy of Surfaces and Interfaces," Ch. B1.5 in *Encyclopedia of Chemical Physics and Physical Chemistry*, J.H. Moore, and N.D. Spencer, Eds. (Institute of Physics, London, 2001).
2. G. Rupprechter, *Phys. Chem. Chem. Phys.*, **3**, 4621 (2001).
3. T. Götz, M. Buck, C. Dressler, F. Eisert, F. Träger, *Appl. Phys. A*, **60**, 607 (1995).
4. R. Antoine, P.F. Brevet, H.H. Girault, D. Bethell, D.J. Schiffrin, *Chem. Commun.*, **1997**, 1901 (1997).
5. C.L. Haynes, R.P. Van Duyne, *J. Phys. Chem. B.*, **105**, 5599 (2001).
6. C.W. van Hasselt, M.A. Verheijen, Th. Rasing, *Phys. Rev. B*, **42**, 9263 (1990); J.E. Sipe, D.J. Moss, H.M. Driel, *Phys. Rev. B*, **35**, 1129 (1987)

LDRD FUNDING:

FY 2002	\$ 184,847
FY 2003 (budgeted)	\$ 185,000

Combined Use of Radiotracers and Positron Emission Imaging in Understanding the Integrated Response of Plants to Environmental Stress

Richard Ferrieri

02-45

D. J. Schlyer

M. Schueller

M. Lerdau (SBU)

M. Holbrook (Harvard U.)

PURPOSE:

Unlike many questions of plant response that can be studied using cell culture and/or destructive techniques, the integration of plant stress responses requires a *non-invasive* approach that allows repeated measurements from the same plant. Standard methods of functional plant biology such as discrete measurements of water transport capacity and gas exchange do not provide a complete picture of the interrelationship between different transport processes. A complementary approach is needed that addresses this integration by allowing visualization and quantification of molecular movement and disposition across the scale of the entire plant.

Visualizing and quantifying whole plant responses using short-lived positron emitting radioisotopes in combination with positron imaging and positron annihilation detection provides a unique opportunity to unravel the many complex biochemical pathways involved in plant nutrient assimilation and transport during stages of development and/or during periods of environmental stress.

APPROACH:

These radioisotopes, including carbon-11 ($t_{1/2}$ 20.4 m) as $^{11}\text{CO}_2$, nitrogen-13 ($t_{1/2}$ 9.97 m) as $^{13}\text{NH}_4^+$ and $^{13}\text{NO}_3^-$, and oxygen-15 ($t_{1/2}$ 2.0 m) as H_2^{15}O , decay by emitting energetic positrons or positively charged electrons ranging in energy from 0.99 MeV to 2.65 MeV. The high energy of these particles enables a significant portion of them to exit the plant tissue before they have a chance to annihilate with an electron yielding a pair of coincident photons in return. Because of this, it is possible to image with extremely high resolution (50 μm), the spatial distribution of radioactivity using a phosphor-plate that is sensitive only to the particle energy and not the photon. The rapid decay rate also enables imaging to be performed with brief exposures of the plate to provide real-time feedback of transport. Additionally, strategically placed photon counters provide real-time feedback and quantification of nutrient transport dynamics. More importantly, the same plant serves as its own control in a plant challenge study design as well as be used in retests for longitudinal response changes. These aspects are unique in plant physiology and can have major implications for investigating impacts of environmental stressors on plants. Other areas of potential application include plant soil chemistry, more specifically phytoremediation, as well as screening of transgenic plant responses relative to nutrition allocation under stress.

We are currently in the midst of validating system performance with regard to carbon-11 and nitrogen-13 assimilation and transport using photon counting techniques and positron imaging, and are establishing experimental protocols for inducing plant water stress as our first planned environmental manipulation. We also

anticipate having the first $H_2^{15}O$ tracer results by 2003 with the commissioning of the new Ebc Cyclotron in December of this year.

The risk associated with this technological approach is that radiation induced cell damage could impact on plant performance thus confounding interpretations. We established in one of our first experiments that a single bamboo plant subjected to a series of repeat doses of $^{13}NO_3^-$ tracer over two weeks time, responded in the same way.

TECHNICAL PROGRESS AND RESULTS:

We have designed and constructed an integrated plant metabolism chamber (Figure 1) that is fully integrated with a photosynthesis cell (Figure 2), infrared gas exchange instrumentation and electronic gas flow controllers. We have recently demonstrated the feasibility of non-destructively visualizing and quantifying the assimilation, transport and disposition of carbon (using $^{11}CO_2$) in plants.

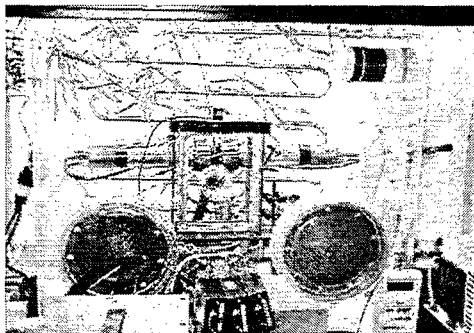


Figure 1. This is a photograph of the main environmental control chamber used during tracer studies which provides lighting to $450 \mu mol m^{-2} s^{-1}$, humidity control, and temperature control between 20-30°C. This chamber also houses the leaf photosynthesis cell and coincidence detectors.

A significant technological breakthrough this year involved manipulating radioactive $^{11}CO_2$ gas in rapid impulse feeding to the

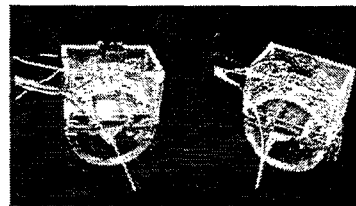


Figure 2. Leaf photosynthesis cell with light control to $800 \mu mol m^{-2} s^{-1}$, humidity control, CO_2 control from 0-834 ppm in air and temperature control to $\pm 0.1^\circ C$. The cell interfaces with an infrared gas exchange instrument.

plant. This feature allowed direct measurement of carbon-11 fixation, as well as plant photorespiration during times of photosynthetic activity. The underlying feature behind this technology involved selective adsorption of $^{11}CO_2$ onto Ni(0) catalyst, and later flash desorption into a stream of air as a discrete pulse that is feed to the plant leaf. Figure 3 shows the module we constructed from this technology.

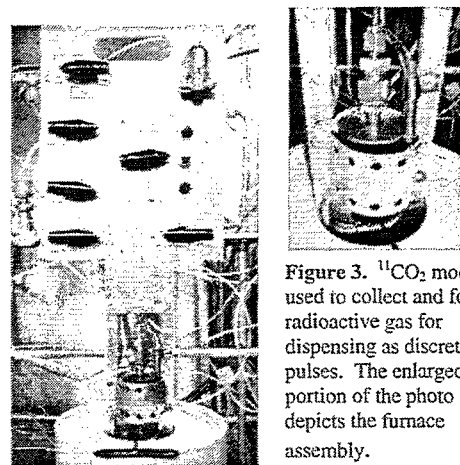


Figure 3. $^{11}CO_2$ module used to collect and focus radioactive gas for dispensing as discrete pulses. The enlarged portion of the photo depicts the furnace assembly.

Our first pulsed $^{11}CO_2$ experiments were performed this past July on cut paper birch (*Betula*) leaves. The series of images seen in Figure 4 were acquired at 5, 30 and 120 minutes post pulse feeding while maintaining full environmental control.

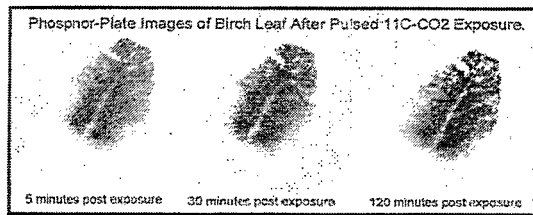


Figure 4. Phosphor plate images of the same cut paper birch leaf exposed to a 30 second, 9 mCi pulse of ^{11}C of which 25% remained fixed.

Considerable surface heterogeneity was noted with regard to carbon fixation, as well as a lack active assimilate transport.

Pulsed ^{11}C studies were also performed on hydroponically grown wheat and corn plants this past September. Transport dynamics for ^{11}C -sucrose were monitored in both species at similar transport distances. Figure 5 represents time-activity curves for both species. Corn transports more rapidly than wheat, but doesn't achieve saturation within the time monitored.

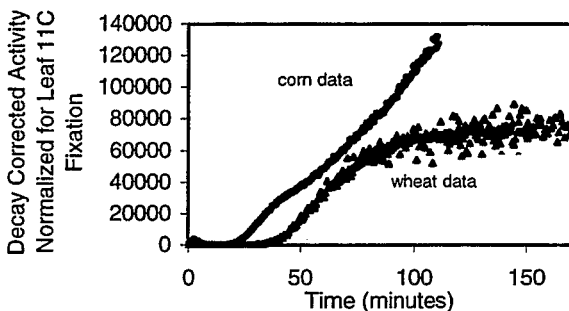
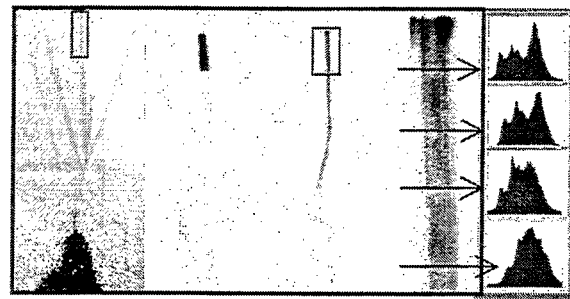


Figure 5. Time-activity curves from ^{11}C pulse-feedings to intact healthy wheat and corn plants. Data is decay corrected and normalized for fixed-carbon-11 activity on the exposed leaflet.

Imaging whole plant radioactivity distribution after feeding an intact wheat plant ^{11}C (Figure 6) reveals strong ^{11}C fixation within the exposed leaf area, but also clearly shows strong phloem loading within the individual vascular bundles, as well as export to other shoots and leaves.



Figures 6A-E. Figure 6A depicts a photograph of the wheat plant indicating the leaflet portion that was pulse-fed ^{11}C . Figure 6B depicts a 10 second acquired image of the entire plant taken 90 minutes after tracer administration. Figure 6C depicts a 12 minute acquired image with that portion of the exposed tissue shielded. More export features are seen in the adjacent shoots and leaves. Figure 6D depicts an enlarged view of the highlighted portion indicating transport vascular. Figure 6E depicts lateral radioactivity distribution across $5\mu\text{m}$ wide cuts of the leaf indicating phloem leakage on transport.

As seen in Figure 7, 4% of the fixed activity was repartitioned throughout the plant within 60 minutes.

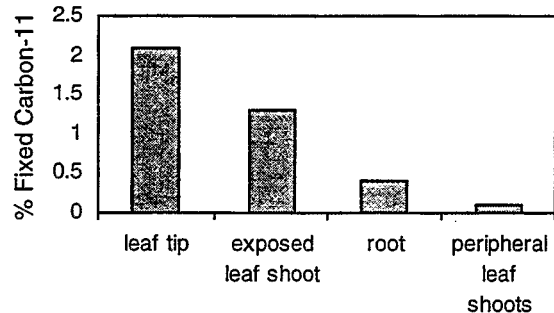


Figure 7. ^{11}C -sucrose partitioning within the wheat plant at 90 minutes post pulse.

Additionally, we have established experimental protocols allowing root administration of nitrogen-13 as $^{13}\text{NH}_4^+$ and $^{13}\text{NO}_3^-$ and have successfully carried out longitudinal studies within a single plant to assess nitrogen pool capacity. Results in Figure 8 show the response over time of a nitrogen deprived bamboo plant that is challenged with nitrate.

The plant's capacity to deplete the newly established nitrogen pool was monitored using sequential administrations of $^{13}\text{NO}_3^-$.

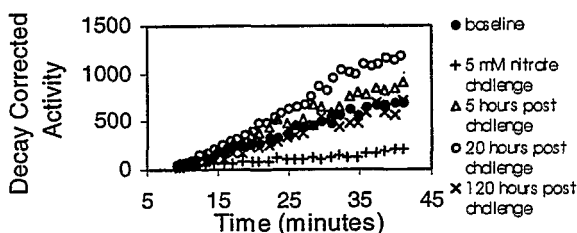


Figure 8. Time activity curves representing ^{13}N transport from baseline through a nitrogen challenge.

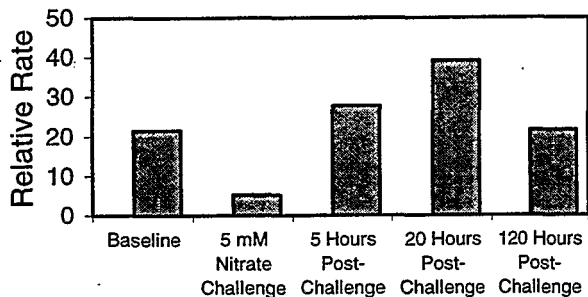


Figure 9. Relative rates for ^{13}N transport subsequent to a nitrate challenge on a nitrogen deprived bamboo plant.

Results in Figure 9 indicate that the plant returned to baseline response from its original nutrient deprived state within five days time demonstrating the power of this tracer technique for continued monitoring.

SPECIFIC ACCOMPLISHMENTS:

An invited talk entitled, "Imaging Long-Range Transport in Plants using short-Lived Radioisotopes" was presented at the Harvard Forest International Workshop on Long-Range Transport (Oct 18-21, 2002).

A record of invention was filed with the BNL Office of Intellectual Property and Industrial Partnerships on rapid impulse feeding of $^{11}\text{CO}_2$ to plants with real-time positron imaging.

Grant application entitled, "Imaging and Quantifying Effects of Elevated Ozone and Carbon Dioxide on Soybean Plant Capacity to Fix and Transport Carbon and Nitrogen"

has been submitted with the USDA, Plant Response to the Environment Program.

A second FWP proposal entitled, "Using PET and Positron Imaging in *Thlaspi caerulescens* Ecotypes to Investigate the Relationship Between Carbon Allocation and Plant Capacity to Hyperaccumulate Zn and Cd" was submitted to DOE/BER as part of the Joint Interagency Program on Phytoremediation Research.

Submitted manuscript to Science (*Brevia*) entitled, "Sink-Source Signaling in Maize."

LDRD FUNDING:

FY2002	\$ 99,200
FY2003(budgeted)	\$100,000

Arranging Nanoparticles Into Arbitrary Patterns With Optical Trapping

Christopher Fockenberg

02-46

J. P. Kirby

T. J. Sears

PURPOSE:

Propose to combine optical trapping (laser tweezers) and self-assembly to form two-dimensional structures of metallic (*e.g.*: gold) nanoparticles. Optical trapping is used to hold nanoparticles at key positions in the desired structure followed by “filling in” of the gaps exploiting attractive and/or repulsive interaction among the nanoparticles established by suitable molecules adsorbed on their surfaces. The objective of this work is to determine the feasibility of our idea. In this respect, synthesizing capping molecules for, and trapping of, gold nanoparticles as well as creating multiple optical traps are the technical challenges of this experiment.

If the molecular links between the metal particles could be made to function as molecular wires, these structures could be operated as practical electronic circuits. Therefore, this work could potentially be incorporated into the Nanoscience Application program of the BNL Nanocenter. Optical traps can also be used for spectroscopic studies of single particles or their surface coverage, which could be exploited as a new tool to investigate the surface chemistry in the liquid phase, with implications for research on nanocatalysts.

APPROACH:

In contrast to the “top-down” methods used in traditional microfabrication, today’s nanoscience favors self-assembly as the tool

in an indirect construction technique for nanoscale objects. Currently there is quite poor controllability. However, optical trapping (known as “optical tweezers”) has been widely used to manipulate micrometer-sized particles, and its extension to the nanoscale is possible. Although optical trapping in the focus of a laser beam applies mainly to dielectric particles, small metallic spheres (particle diameter $\ll \lambda_{\text{laser}}$) can be trapped in a similar manner. In addition, multiple traps have been generated by using spatial light modulators creating the desired pattern by way of diffraction.

Thiols can form highly ordered, self-assembled monolayers at the gold surface by hydrogen bonding (amidinium-carboxylate salt bridge) among the molecules. Di-, tri-, and tetrathiol compounds were also used to link two or more gold nanoparticles together forming stable dimers, trimers, or tetrahedra. Moreover, gold nanocrystals covered with simple alkanethiols have been shown to arrange in crystal structures (molecular nanocrystals). Instead of using gold-thiol bonds to link two particles, we envision to utilize amidinium-carboxylate salt bridges.

The long-term goal of this project is to combine all of the aspects mentioned above and to create a simple two-dimensional network of metallic nanoparticles. Immediate questions that this investigation tries to answer are: Can a simple dynamic, trapping structure be generated using a digital micromirror device as a diffractive optical element, and do gold-nanoparticles form stable molecular nanocrystals on their own by establishing salt-bridges?

TECHNICAL PROGRESS AND RESULTS:

The basic setup for the laser tweezers has been built including general and microscope optics and image acquisition. Trapping of

single dielectric particles (0.5 μm and 30 nm) and multiple dielectric particles (0.5 μm) using an off-the-shelf, static diffractive optical element could be demonstrated (see Figure 1). Trapping times range from a few to 100 seconds depending on laser intensity and particle size. The particles were observed by imaging the light reflected by the particle onto a digital (CCD) camera. Two computer programs in LabVIEWTM were written to calculate Fresnel diffraction patterns (image) from given hole masks (aperture pattern), and vice versa. The reverse calculation is based on an iterative genetic algorithm to find the best solution for the aperture pattern. Based on the results from the diffraction calculations, we will decide which type of diffractive optical element (digital mirror device or spatial light modulator) is best suited for this experiment to generate dynamic optical traps. Also, using the blue light from the Ar ion laser, separate illumination of the nanoparticles will be attempted for darkfield microscopy.

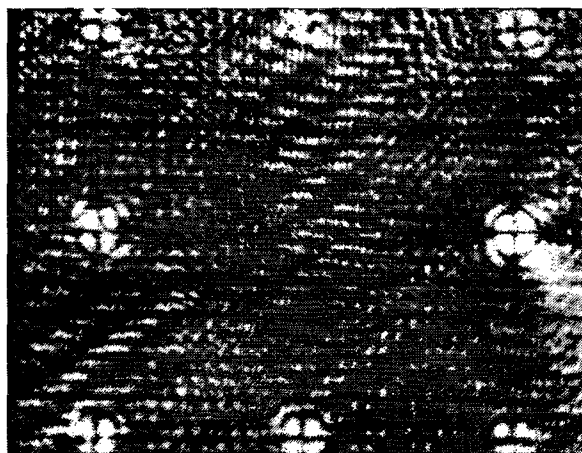


Fig. 1: Box of trapped polystyrene particles (diameter = 0.5 μm) in water. The distance between the particles is approximately 5 μm .

Gold nanoparticles have been prepared from gold salts using the citrate reduction technique. This method yields citrate-coated nanoparticles, where the size of the gold nanoparticles has been determined by either visible absorption spectroscopy or scanning electron microscopy (SEM). In the visible absorption experiment, solution samples are assessed for the peak wavelength of the surface plasmon band, which is dependent on the gold nanoparticle diameter. To confirm the size of the gold nanoparticle, SEM images were obtained to assess the size directly. Using these techniques, we have prepared samples of citrate coated gold nanoparticles ranging in sizes from 5 nm to 50 nm diameters. Currently we are attempting to synthesize thiol-amide and thiol-carboxyl ligands as capping material for the gold particles.

In addition to the extension of the imaging system, we plan to investigate the trapping efficiency of gold nanoparticles with our setup and attempt to grow molecular crystals from these particles capped with the thiol ligands mentioned above.

SPECIFIC ACCOMPLISHMENTS:

None

LDRD FUNDING:

FY 2002	\$119,860
FY 2003 (budgeted)	\$120,000

Advanced Multidimensional Techniques to Explore the Biochemical and Behavioral Consequences of VOC Exposure

M.R. Gerasimov

02-48

PURPOSE:

The technical objective of this work is two-fold: 1) to develop a viable methodology for exposing laboratory animals to precisely measured and controlled levels of volatile organic compounds (VOCs) under environmentally safe conditions; and 2) to develop a fully automated computer-assisted algorithm for monitoring animal behavior under several experimental protocols. To our knowledge this is the first demonstration of a successful animal model for the inhalants abuse potential. This methodology set a stage for further exploring the factors contributing to the predisposition, development, and potential treatment of inhalant abuse. Additionally, the use of this new technique will allow for the exploration of the neurotransmitter systems implicated in the co morbidity between inhalants abuse and addiction to other drugs, which are the focus of BNL research such as cocaine, nicotine, heroin, and alcohol.

APPROACH:

Work-related as well as voluntary inhalation of solvents such as toluene, is wide spread with the incidence increasing over the past decade, especially among adolescents. Notwithstanding the high rate of exposure, the current research has not adequately addressed the need for establishing a reliable animal model to assess the abuse liability of the inhalants.

Since the main route of exposure to the VOCs is inhalation (the other ones being skin penetration and ingestion), we pursued the goal of creating reproducible levels of solvents within dynamic exposure animal chambers. Our second objective was to monitor on-line and to change the concentrations of vapors according to the indices of the animal's behavior.

We utilized the approach of mixing different proportions of pure compressed air and the stream of air saturated with solvents vapors produced by a simple liquid bubbler. Flame ionization detection (SRI Instruments) in conjunction with gas chromatography (for calibration purposes) was selected for monitoring the vapors concentrations within the animal's behavioral chambers. These chambers were custom designed and built upon our request by MedAssociates Inc.

We chose the technique of conditioned place preference (CPP) as a measurement of drug-seeking behavior and the technique of nose-poke as an assessment of self-administration potential.

Co-investigators are W. Schiffer and S. Dewey. The expertise of Mr. David Alexoff (bioengineer) and Dr. R. Ferrieri (physical chemist) proved to be invaluable for this project. ERULF student, J. Taibali (Fall Semester 2002), and CSI student, Abbi Ferrieri (summer semester 2002), also contributed to this effort.

TECHNICAL PROGRESS AND RESULTS:

Over the period of October 2001-2002:

- We have purchased and installed all the proposed equipment, developed specific procedures, prepared and got the

approval of the appropriate Environmental Safety Review.

- We performed independent calibration of the FID and correlated this response with the levels of solvent vapors achieved in the CPP and nose-poke apparatus (see Fig. 1).
- We created a fully integrated computerized interface for the solvent delivery and behavioral measurements (time spent in a particular chamber, number and duration of nose-poking).
- We performed two groups of the experiments: validation of the nose-poking procedure to assess self-administration potential of the inhalants (Fig 2) and the demonstration of the feasibility of CPP using solvents vapors as a conditioning factor (Fig 3).

Our results confirm the notion that inhalants possess rewarding/reinforcing properties in animals. This is in agreement with extensive clinical evidence accumulated over the past four decades. Under specific conditions, these effects can be quantified, and subsequently, distinct neurotransmitter systems involved in mediating the response to the inhalants can be identified and further explored by using various pharmacological perturbations.

The unique, completely automated design of data acquisition system removes any potential bias and sets the stage for the further development of the program aimed at addressing the following questions:

- What are the underlying mechanisms of the addictive liability of inhalants;
- Are the inhalants really the “gateway” drugs and if there is a distinct

neurobiological mechanism responsible for this predisposing effect;

- What are the potential neurotransmitter systems that can be targeted for the treatment and/or prevention of inhalant abuse and neurotoxicity associated with environmental and voluntary VOCs exposure.

This project involves vertebrate animals (Sprague-Dawley rats) that are used under the approved IACUC protocol #240 “Investigation into Abuse Potential of Inhalants” 07/24 02-07/09-03.

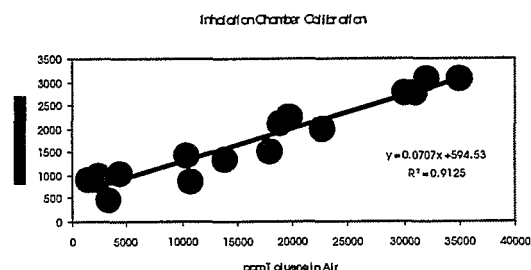


Figure 1.

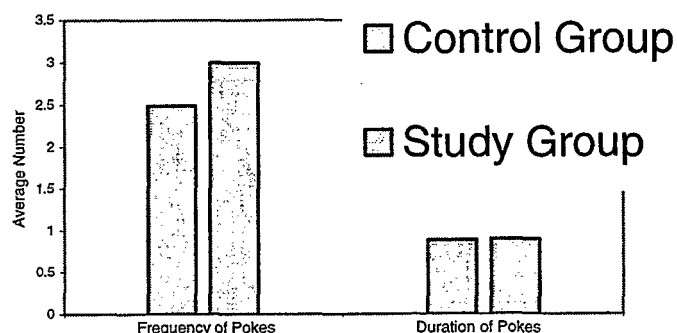


Figure 2.

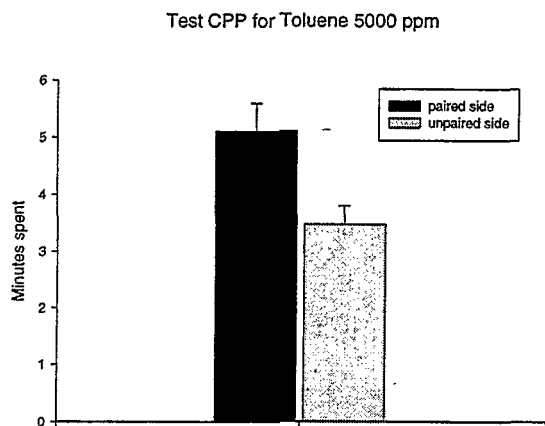
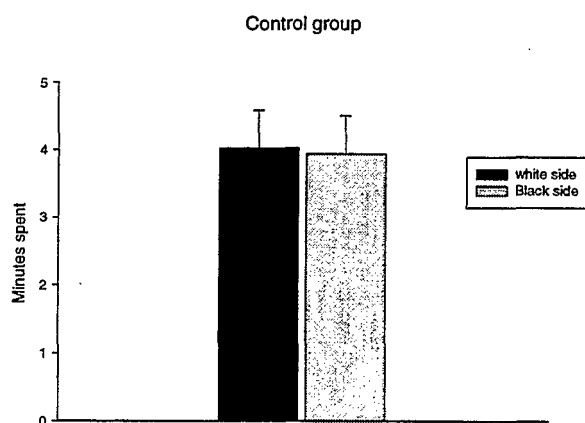


Figure 3.



SPECIFIC ACCOMPLISHMENTS:

Toluene vapors produce conditioned place preference in Sprague-Dawley rats. Gerasimov, M.R.; Taibali, J.; Ferrieri, R.; Dewey, S.; Alexoff, D. *Drug and Alcohol Dependence* (Submitted) 2002.

Abuse liability of toluene: behavioral study. Gerasimov, M.R.; Taibali, J.; Ferrieri, R.; Alexoff, D. Abstract submitted to the Annual Meeting of College on Problems of Drug Dependence (CPDD), June 2003.

LDRD FUNDING:

FY 2002	\$119,827
FY 2003	\$ 95,000

Project to Detect pp and ^7Be Solar Neutrinos in Real Time: LENS, the Low Energy Neutrino Spectrometer

Richard L. Hahn

02-49

PURPOSE:

The goal of the low energy neutrino spectrometer (LENS) is to develop a neutrino detector that can measure in real time the fluxes and energy spectra of the most prevalent (>99.9%) neutrinos that are emitted from the Sun, those from the low-energy pp and ^7Be solar branches (at energies 0.1 - 1 MeV).

To date, these low-energy neutrinos have only been detected in the (^{37}Cl and ^{71}Ga) radiochemical neutrino detectors. During the past few years, the phenomenon of neutrino flavor oscillations has been convincingly demonstrated in two real-time detectors, but only for neutrinos from 5 MeV up to ~ 1 GeV. There is great interest in confirming that the proposed mechanisms of neutrino oscillations also apply at low energies.

The International LENS Collaboration was formed by scientists from the U.S. (including BNL), France, Italy, Germany, Japan, and Russia. If LENS R&D and prototype testing prove successful, the plan is to build a ~ 100 -ton neutrino detector and to share the costs among the participating countries.

APPROACH:

A major obstacle to the successful operation of any low-energy neutrino spectrometer is the natural large background that exists below ~ 5 MeV, even in deep underground

physics laboratories. To suppress these backgrounds significantly, LENS is currently focusing on using indium as the target for neutrino interactions. Neutrino capture in ^{115}In has a threshold of only 118 keV, which makes it ideal for detecting the pp neutrinos. This capture process produces a distinctive signal that is composed of three successive events over a time interval $< 5 \mu\text{s}$: a positron followed by a ~ 100 -keV electron or gamma ray followed by a ~ 500 -keV gamma ray. This triple coincidence in time and space cleanly distinguishes neutrino events from the backgrounds.

The approach being followed in LENS is to dissolve the indium target in sufficient concentration in a liquid-scintillating (LS) medium so as to maximize the amount of light that is produced by the neutrino capture reaction. The chemical requirements to do so are formidable.

The LS is an organic liquid, and the concentration of dissolved indium must be relatively high, $\sim 10\%$ by weight. The indium must thus form an organic chemical complex that is soluble in the LS ("In-LS"). The mixture must be chemically stable over periods of years, with no hydrolysis, gel formation, or precipitation occurring. Also, the In-LS must have a light yield of several thousand photons per MeV of deposited energy, and the liquid must have an attenuation length of > 2 m, to provide an intense signal to the photomultiplier tubes (PMTs) that will view the detector.

The BNL Group has taken on the task, in collaboration with the LENS Spokesman, R. S. Raghavan, who is at Bell Labs, to develop the In-LS. In addition to the P.I., Research Associate Dr. Zheng Chang, Assistant Chemist Dr. Minfang Yeh, and Research Subcontractor Dr. Claude Musikas are all working on this LENS R&D project. Only Chang is funded by this LDRD account.

TECHNICAL PROGRESS AND RESULTS:

In FY 2002, we found that complexes of indium with carboxylic acids and/or organophosphorus compounds satisfied many of the requirements for the In-LS. Various chemical synthesis methods were tested. Scores of samples were prepared.

Several analytical chemistry methods were developed and/or applied to these samples: (1) A spectrophotometric (UV-visible) method was used to measure the indium concentration. (2) Apparatus for the Karl Fisher method was purchased and used to measure the amount of water that is entrained in the organic In-LS, since H₂O can lead to the formation of hydrolysis products. (3) X-ray fluorescence was used to determine Cl and In concentrations in the organic liquid. Cl is a quencher that can reduce the LS light output. (4) Potentiometric acid-base titrations were done, to determine the effects of pH. Besides hydrolysis, dimers and trimers of the In-carboxylates can possibly form as the pH is raised. (5) Infrared spectroscopy, FTIR and Raman, was used to study speciation of the indium and of the organic constituents in the In-LS.

Besides using UV-visible spectrophotometry to measure the light absorption in In-LS samples over pathlengths ≤ 10 cm, we built a system to measure light loss over pathlengths ≥ 1 m, comparable to those in the LENS detector design. The system employs a 450-nm laser as the light source. Testing of the system will begin soon.

We also built a system to measure the light yield of the In-LS solution, for comparison with the yield of the neat LS, whose light output characteristics are well known. The system employs a radioactive gamma-ray

source to excite the LS, and a PMT plus associated electronics to measure the resulting energy spectrum.

We made excellent progress in the past year in identifying and solving problems in the preparation and chemical analysis of the In-LS, and in characterizing the In-LS samples that we prepared. We learned a lot about what works, and what does not.

During the next several months, we will perfect our synthesis and analysis methods. The BNL group will then go into a production mode, to prepare multi-liter samples of In-LS that will be used by us and others in LENS, to test detector-module designs, both in the U.S. and at the underground Gran Sasso Laboratory (GSL) in Italy. These prototype detectors will teach us about the detector's response to gamma radiation (as stand-ins for neutrinos), energy thresholds, energy resolution, electronic timing, background suppression, etc.

If we conclude from these tests that a LENS-type detector is feasible, the collaboration will then develop a proposal to build a full-scale detector. The current idea is that LENS will be a modular array containing at least 10 tons of indium in an In-LS solution of at least 100 tons, interspersed with modules that contain pure LS (to help us suppress certain types of background events).

The anticipated cost of the LENS detector will most likely be \geq \$50 M. One possible site for the detector is the Gran Sasso Laboratory in Italy. Another is the new, dedicated laboratory for underground physics that is being contemplated for the U.S., possibly at the Homestake Mine in South Dakota.

In the event that LENS construction does win approval, the BNL Group will have to

grow, to be able to participate effectively in the Sudbury Neutrino Observatory (SNO) project and in LENS. DOE's Office of Nuclear Physics will be asked to increase funding of the BNL Group's R&D program. Substantial additional funds will be requested by BNL and LANL, another major U.S. player in LENS, for construction.

SPECIFIC ACCOMPLISHMENTS:

Presentations:

"Recent Work at BNL on Preparing M-LS," Zheng Chang and Richard L. Hahn, LENS Collaboration Meeting, December 14, 2001.

"Recent BNL Chemical Studies of In-LS Preparations," Zheng Chang, Richard L. Hahn, Minfang Yeh, Claude Musikas, LENS Collaboration Meeting, June 21-22, 2002.

"The Current Status of Solar Neutrino Research," Richard L. Hahn, at Physics

Departments at: (a) Purdue University, December 6, 2001; (b) Australian National University, January 29, 2002; (c) University of Sydney, February 4, 2002; (d) BNL, April 25, 2002.

"LENS, the Low-Energy Neutrino Spectrometer," Richard L. Hahn, American Chemical Society National Meeting, Boston, August 17, 2002.

"LENS, the Low-Energy Neutrino Spectrometer," Richard L. Hahn, NESS02 Conference on the Future of Underground Science, Washington, D.C., September 18, 2002.

LDRD FUNDING:

FY 2002	\$70,248
FY 2003 (budgeted)	\$70,000

Combined Theoretical and Experimental Study of Crystal Lattice Defects in Complex Transition Metal Oxides

James Davenport

02-53

Y. Zhu

D. O. Welch

PURPOSE:

The purpose of this project is to provide first principles calculations of complex transition metal surfaces and compounds for comparison with experiments using the transmission electron microscope at BNL as well as x-ray studies from the National Synchrotron Light Source.

APPROACH:

First principles density functional calculations are being performed to obtain the energy, charge density, and electron energy loss spectra for the relevant materials. These are obtained with the full potential linear augmented plane wave method and are run in parallel on the Linux cluster in the Center for Data Intensive Computing. Calculations of this type have not been compared previously in detail with experiments, and there is a risk that the comparison will reveal that further advances in theory will be needed.

TECHNICAL PROGRESS AND RESULTS:

There was important progress in two systems which are examples of the joint theoretical and experimental program that is envisaged. First, because of the high spatial resolution of the transmission electron microscope it has been possible to study the angular dependence (relative to the

crystalline axes) of the electron energy loss spectra (EELS) in the newly discovered superconductor magnesium diboride. MgB_2 has not been available in large single crystals, so the TEM has been the only way to study angular effects since individual crystallites could be resolved. EELS spectra parallel and perpendicular to the crystalline c axis have been recorded and analyzed. First principles calculations have shown that the spectra can be understood in terms of the wave functions and matrix elements for the transitions from the core state to the unoccupied valence states. However, further work is needed to precisely define the angular behavior of the detectors and their energy resolution.

The second project is an outgrowth of the current interest in nanoscience. It has recently become possible to prepare linear chains of cobalt one atom wide and with lengths of approximately 80 atoms when adsorbed onto a stepped platinum surface. These chains have been investigated by magnetic circular dichroism and display the largest orbital magnetic moment (as opposed to spin moment) of any 3d transition element. Our first principles calculations model the system as a supercell with both cobalt and platinum. They show strong moments on the Co and essentially no moment on the Pt consistent with experiments. However, the magnitude of the orbital moment is lower by a factor of roughly 2 than the experimental one. This can be corrected with an empirical on-site Coulomb interaction, but further work will be needed to fully understand the experimental results.

Future work will involve similar first principles calculations on the magnetic properties of cobalt and other 3d transition element oxides and sulfides. In particular, the results of more extensive surface, grain boundary and other imperfections will be

explored along with a more detailed analysis of the angular detection efficiencies of the TEM.

SPECIFIC ACCOMPLISHMENTS:

Unraveling the Symmetry of Hole States near the Fermi Level in the MgB₂ Superconductor, Y. Zhu, A. R. Moodenbaugh, G. Schneider, J. W. Davenport, T. Vogt, Q. Li, G. Gu, D. A. Fischer, and J. Tafto. *Phys. Rev. Lett.* **88**, 247002 (2002).

Valence electron distribution in MgB₂ studied by accurate diffraction measurements and first principle calculations, L. Wu, Y. Zhu, T. Vogt, H. Su, J. W. Davenport, and J. Tafto, Submitted.

X-ray absorption study of the boron K near edge in MgB₂, R. Moodenbaugh, D. A. Fischer, Q. Li, G. Gu, Y. Zhu., H. Su, D. O. Welch, and J. W. Davenport, Submitted.

From the bulk to monatomic wires: An ab-initio study of magnetism in Co systems with various dimensionality, M. Komelj, C. Ederer, J. W. Davenport, and M. Fahnle, *Phys. Rev. B*, in press.

Comment on the analysis of angular-dependent x-ray magnetic circular dichroism in systems with reduced dimensionality, C. Ederer, M. Komelj, J. W. Davenport, and M. Fahnle, Submitted.

LDRD FUNDING:

FY 2002	\$39,678
FY 2003 (budgeted)	\$66,825

Chemical Sensors: Immobilization of Organometallic Complexes into Sol-gel Matrices

Mark W. Renner

02-55

PURPOSE:

Characterization of organometallic compounds (porphyrins) immobilized in sol-gel matrices as chemical sensors for the detection of toxic chemicals or heavy metals. In order to develop porphyrin/sol-gel sensors, it is necessary to understand how the sol-gel matrix influences the chemical and physical properties of the sensor. This research will aid in the rational design of sensors with enhanced chemical selectivity and sensitivity.

APPROACH:

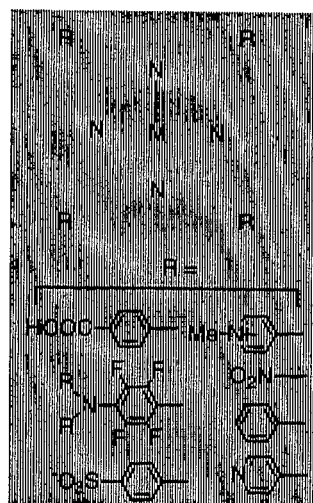
Previously, researchers have investigated the encapsulation of porphyrins into sol-gels or other polymers as sensors, magnetic materials, non-linear optic materials and catalysis. Sol-gel matrices are attractive polymer supports due to their optical transparency and porous nature, as well as their chemical, thermal, and structural stability.

We will investigate the immobilization of porphyrin-based sensors into sol-gel matrices. Using a variety of spectroscopic techniques, the stability of the porphyrin-matrices and their reactivity will be monitored. The methods used to characterize these materials will consist of magnetic resonance techniques, optical and FT-IR spectroscopy. X-ray absorption techniques may be used to follow changes in the metals oxidation, ligation and geometry upon sol-gel formation. Some of the porphyrins were provided through collaborations with K.

Smith (Louisiana State University), M. Senge (Freie Universität Berlin), and D. Mansuy and P. Battioni (Université Paris V).

TECHNICAL PROGRESS AND RESULTS:

A mild method for preparing optically transparent and crack-free, porphyrin-doped sol-gels monoliths was devised. Sol-gel/porphyrin complexes with a variety of peripheral functional groups were prepared, see below.



Water-soluble porphyrins with cationic functional groups interact with the siloxide (SiO⁻) groups on sol-gel walls to form stable complexes. The stability varies as follows: cationic > anionic > nitro > organic.

The optical changes for a freebase porphyrin/sol-gel complex as a function of pH and metal ion are shown in Figure 1. These have potential applications for pH and/or metal ion detection. Zinc porphyrins are often difficult to prepare using conventional sol-gel synthetic methods and pH variations. We have shown that zinc and other metals can be added to the freebase porphyrin sol-gel in order to prepare the Zn(II)porphyrin sol-gel, see below. This may be a convenient method to prepare lanthanide porphyrins, in which the metal is

lost during normal sol-gel synthesis. These are of interest due to their non-linear optical properties.

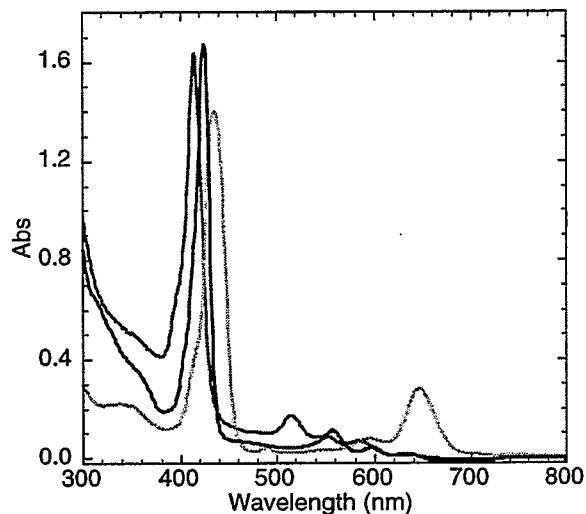


Figure 1. The optical spectra of freebase porphyrin (red), Zinc(II)porphyrin (blue) and freebase diacid porphyrin (green).

One unexpected result is that the sol-gel SiO⁻ groups can also interact with the central metal of the porphyrin. These findings explain why some researchers have observed decreased or no metal reactivity in metalloporphyrin/sol-gels. We have shown that the metal can be protected using axial ligands (pyridine, imidazole, or carbon monoxide) or by using cationic surfactants. Surfactants are often used during sol-gel synthesis as drying agents to prevent cracking, but also protect the metal from SiO⁻ binding.

We have recently prepared a ruthenium(II)-CO porphyrin sol-gel in which the metal's sixth coordination site is open for ligand binding and which exhibits optical changes upon substrate binding. The axial carbon monoxide, which protects the metal from ligation by the sol-gel SiO⁻ groups, can be removed by photolysis using a xenon lamp, see Figure 2.

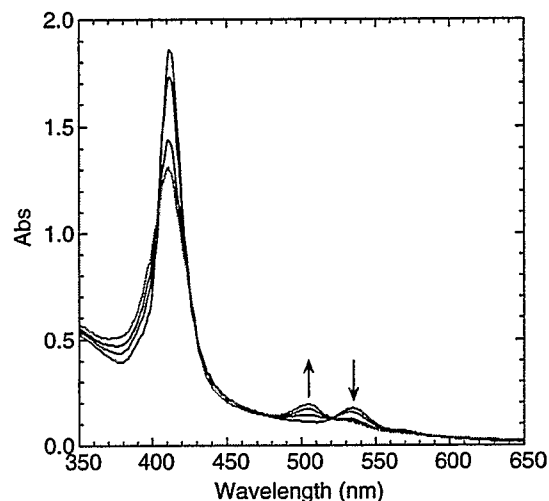


Figure 2. Optical changes upon photolysis of Ru(II)TPP-CO(pyr) sol-gel in EtOH.

During FY 2003: In the upcoming year, we will continue characterizing the chemical and physical properties of new sensors in sol-gels. We have prepared a series of brominated water-soluble porphyrins in order to alter the reactivity of the sensors and their sol-gel chemistry will be studied. An alternative route to preparing porphyrin-doped sol-gels is the ion-exchange of porphyrins containing cationic functional groups with surfactant bound sol-gels. Preliminary results indicate that this may be a convenient method of preparing porphyrin/sol-gels. We also propose to study the role of surfactants during sol-gel synthesis. Surfactants have been used as structural modifiers in the synthesis of zeolites and this may be extended to sol-gels synthesis.

SPECIFIC ACCOMPLISHMENTS:

None

LDRD FUNDING:

FY 2002	\$81,940
FY 2003 (budgeted)	\$86,000

Size Dependence of Catalytic Reactivity of Iron Oxide Nanocrystals

Stanislaus S. Wong

02-56

PURPOSE:

The goal of the project is to synthesize iron oxide nanocrystals of a variety of different morphologies and sizes and to analyze the catalytic reactivity of these nanocrystals for the purpose of quinoline degradation. We have also further generalized our initial objectives to study the synthesis, characterization, and properties of nanocrystal-nanotube heterostructures, as well as more specifically, chemical derivatization strategies involving nanotubes.

Nanocrystals are unique in that the number of surface atoms is a large fraction of the total and that their intrinsic properties are transformed by quantum size effects. Hence, they exhibit strongly size-dependent optical and electrical properties. Research on nanoparticles and nanotubes with size-dependent optical, chemical, and electronic properties is motivated by potential applications, including those for novel optical components of catalytic convertors with enhanced performance.

APPROACH:

We have chosen to synthesize novel nanostructures by carefully studying growth conditions in solution as well as rational chemical derivatization strategies appropriate for predictable functionalization of nanotubes and nanocrystals. With these data, we are then exploring the physical dependence of the catalytic reactivity and optical properties of our nanomaterials.

TECHNICAL PROGRESS AND RESULTS:

I. Iron Oxide Nanoparticles.

We have employed a hydrolysis reaction to form uniform distributions of nanoparticles ranging in size from tens to hundreds of nm. We have attempted to form particles of varying aspect ratios (including spherical, peanut, ellipsoidal, spindle-type, and platelet), based on using a number of different precursors and additives (i.e. varying concentrations of acid and base) as well as different reaction/aging times (ranging from minutes to weeks).

II. Derivatization of Carbon Nanotubes with Metal-containing Complexes.

Raw and oxidized carbon nanotubes have been reacted with Vaska's complex. It has been found that Ir coordinates to these nanotubes by two distinctive pathways. With raw nanotubes, the metal attaches as if the tubes behaved as electron-deficient alkenes. With oxidized nanotubes, the reaction occurs by coordination through the increased number of oxygen atoms, forming a hexacoordinate structure around the Ir atom. The reaction process significantly increases oxidized nanotube solubility in dimethylformamide.

Another compound analyzed was Wilkinson's complex. It has been found that the Rh metal similarly coordinates to these nanotubes through the increased number of oxygenated species. The functionalization reaction, in general, appears to significantly increase oxidized nanotube solubility in dimethylsulfoxide (>150 mg/L) as well as to a certain extent in dimethylformamide and tetrahydrofuran. The derivatization process results in exfoliation of larger bundles of carbon nanotubes and may select for the presence of distributions of smaller diameter tubes. Optical data on the derivatized adducts suggest the possibility of interesting charge transfer behavior across the metal-nanotube

interface. An application has been made of this system as support for homogeneous catalysis, specifically in the hydrogenation of cyclohexene to cyclohexane at room temperature.

III. Rational Synthesis and Characterization of Nanotube-Nanocrystal Heterostructures.

In another set of experiments, oxidized carbon nanotubes have been reacted with cadmium selenide nanocrystals (quantum dots) as well as with titanium dioxide nanocrystals to form nanoscale heterostructures, characterized by transmission electron microscopy and infrared spectroscopy. Based on the types of intermediary linking agents used, we have demonstrated a level of control over the spatial distribution of nanocrystals on these tubes. Optical data on the derivatized adducts suggest the possibility of interesting charge transfer behavior from the nanocrystal to the nanotube in the CdSe-nanotube system, whereas in the TiO₂-nanotube system, charge transfer is expected to occur from nanotube to nanocrystal.

IV. Goals for FY 2003.

In terms of the iron oxide work, we intend to characterize the hematite nanocrystals by atomic force microscopy (AFM), UV-visible spectroscopy, electron microscopy, and similar analytical techniques. Regarding the derivatization project, we intend to analyze other metal-containing complexes to demonstrate catalytic activity. Moreover, we will continue with nanotube-nanocrystal derivatization with the intent of tuning the size, shape, and chemistry of these component nanostructures to create a sharp junction interface, whose properties are manipulable and hence, predictable. In all instances, we are interested in developing adequate structure-property correlations with a predictive potential.

SPECIFIC ACCOMPLISHMENTS:

- Sarbajit Banerjee and Stanislaus S. Wong, "Structural Characterization, Optical Properties, and Improved Solubility of Carbon Nanotubes Functionalized with Wilkinson's Catalyst," *J. Am. Chem. Soc.*, **124**, 8940-8948 (2002)
- Sarbajit Banerjee and Stanislaus S. Wong, "Synthesis and Characterization of Carbon Nanotube-Nanocrystal Heterostructures," *Nano Letters*, **2(3)**, 195-200 (2002).
- Sarbajit Banerjee and Stanislaus S. Wong, "Functionalization of Carbon Nanotubes with a Metal-Containing Molecular Complex," *Nano Letters*, **2(1)**, 49-53 (2002).

Presentations:

- "Nanotube Functionalization Strategies," *American Chemical Society National Meeting*, Boston, MA, August 18-22, 2002.
- "Strategies for Carbon Nanotube Functionalization," *Scanning Probe Microscopy, Sensors, and Nanostructures*, (sponsored by *Ultramicroscopy*) Las Vegas, NV, May 26-29, 2002. Nanostructures Session Chair – May 27.
- "Charge Transfer in Functionalized Nanomaterials" (Breakout Session entitled 'Charge Transfer on the Nanoscale')
- Invited Presentation given at the *Discussion of Emerging Science and Instrumentation Opportunities*, Planning Workshop for the BNL Center for Functional Nanomaterials, Brookhaven National Laboratory, Upton, NY, March 7-9, 2002.

Data from these studies were used as material in BNL nanoscience proposals, including that for the *BNL NanoCenter*, submitted to DOE in FY 2002.

LDRD FUNDING:

FY 2002	\$ 84,575
FY 2003 (budgeted)	\$104,000

Femtosecond Synchronization for Ultra-Short Pulse DUV- FEL Radiation

William Graves

02-58

J. B. Murphy

J. Rose

B. Sheehy

T. Shaftan

X. J. Wang

L. H. Yu

PURPOSE:

The objective of this work is to develop technologies to support Deep Ultra Violet Free-Electron Laser (DUV-FEL) R&D and future NSLS upgrade. Synchronization between laser and electron beam plays an important role in both schemes for the possible future X-ray FEL, such as self-amplified spontaneous emission (SASE) and the high-gain harmonic generation (HG HG). BNL is actively pursuing HG HG because of its many advantages over SASE, such as better radiation stability and longitudinal coherence. For HG HG to reach shorter wavelength, cascading of several stages of HG HG is necessary. Timing jitter control and electron beam qualities are two critical areas for the success of the cascaded HG HG. Timing control is critical for cascaded HG HG in three aspects. First, electron beam generation in a photoinjector, where timing jitter between the photocathode RF gun drive laser and RF system needed is less than 500 fs. A factor of two improvement is required for the first stage laser seed in electron beam modulation. The fresh bunch technique in cascading multi-stage HG HG imposes even more stringent timing control, better than 100 fs.

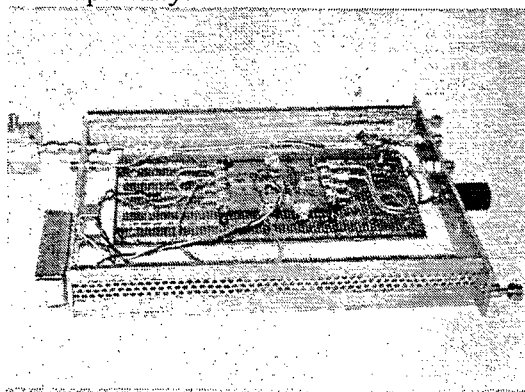
APPROACH:

Develop technologies capable of delivering the performance required, we have a plan to attack these challenges on several fronts. First, we have identified that a laser and a low-level RF system are critical for timing control. Improvement of their environments, such as better temperature and vibration control, is the key. Second, we will develop femtosecond timing jitter diagnostics tools. Laser and RF pickup will be non-interceptive techniques, which we are now investigating. Third, is feedback control of the timing jitter. Solid state S-band (2856 MHz) I-Q modulator will be developed for a low-level RF system.

TECHNICAL PROGRESS AND RESULTS:

During FY 2002, we have accomplished:

1. Solid State S-band I-Q modulator: Three sets of I-Q modulators (see picture below) were designed, constructed, and installed during FY 2002. We have demonstrated 0.1 degree (100 fs) RF control capability.



2. Electron beam and laser seed synchronization: We have demonstrated sub pico-second synchronization between the electron beam and seed laser for HG HG and laser seeded FEL.

3. Success of HGHG and laser seeded FEL: The best illustration of the success of the timing control system is the saturation of laser seeded FEL and HGHG at 266 nm.

3. A. Doyuran, W. Graves, R. Heese, E. D. Johnson, S. Krinsky, H. Loos, J. Murphy, G. Rakowsky, J. Rose, T. Shaftan, B. Sheehy, J. Skaritka, X.J. Wang, L.H. Yu, "Observation of Sase and Amplified Seed of the DUV-FEL at BNL," FEL 2002, Chicago.

SPECIFIC ACCOMPLISHMENTS:

1. W. Graves, "Microbunching and CSR experiments at BNL's Source Development Lab," presented at the Workshop on Coherent Synchrotron Radiation and Its Impact on the Beam Dynamics of High-brightness Electron Beams, DESY-Zeuthen, Berlin, Germany, January 14-18, 2002.

4. A. Doyuran, W. Graves, R. Heese, E. D. Johnson, S. Krinsky, H. Loos, J.B. Murphy, G. Rakowsky, J. Rose, T. Shaftan, B. Sheehy, J. Skaritka, X.J. Wang, L.H. Yu, "First SASE and Seeded FEL Lasing of the NSLS DUV-FEL at 266 & 400 nm," FEL 2002, Chicago.

2. H. Loos, A. Doyuran, W. Graves, J. Rose, T. Shaftan, B. Sheehy, L.H. Yu, "Electron Bunch Compression and Coherent Effects at the SDL," Advanced Accelerator Concepts Workshop, Mandalay Beach, CA, June 23-28, 2002.

LDRD FUNDING:

FY 2002	\$134,883
FY 2003 (budgeted)	\$135,000
FY 2004 (estimated)	\$135,000

Rapid Wavelength Tunability for the DUV-FEL

Brian Sheehy

02-62

PURPOSE:

The deep ultraviolet free electron laser (DUV-FEL), located in the NSLS at the Source Development Laboratory (SDL), is an important test bed of FEL physics and beam dynamics as well as a growing user facility. It has and will have important impacts on the design of next-generation sources, and its applied experimental program is opening new territory in chemical dynamics. A central part of this facility is an ultrafast laser system that generates the electron bunch in the RF gun, provides seed radiation to generate coherent FEL output, and produces reference beams for various diagnostics and experiments. Integrating these functions with control of the electron beam dynamics in a seamless way is necessary for smooth operation of the facility. It is important for the success of both the FEL and the user programs that the flexibility of the laser system and the beam machine (RF gun, accelerator, undulators, etc.) be developed to permit the rapid changes in configuration and wavelength required to meet all of the needs of the SDL program.

APPROACH:

Accomplishing this requires significant development on several fronts: seed light generation, transport and synchronization, output diagnostics, and beam machine controls.

Generation of a stable seed requires temporal shape control independent of the photocathode drive pulse that generates the electron bunch. This is done with a separate

compression stage for the amplified infrared pulse, with the proper seed wavelength synthesized using nonlinear optical methods. As pulse temporal profiles are critical in both seed and drive pulse, high-resolution diagnostics must be developed, and methods of pulse-shaping are highly desirable. Pulse shapes are measured by cross-correlation with the oscillator. Optimally, pulse shaping would be done coherently, modulating spectral amplitude and phase in the oscillator pulse. As this requires some investment, we have used simpler, cruder methods first to do some important proof-of-principle experiments.

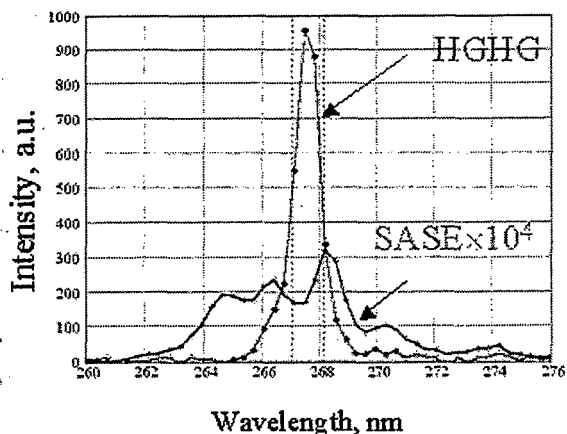
Transport and synchronization of the seed require an optical relay stable over the 35-meter transport distance, and diagnostics to control synchronization and spatial overlap with the electron beam. These are integrated into the control system for the beam machine as a whole, in order that both optical and electron beam parameters can be cooperatively controlled. Output diagnostics are required to analyze the spectral, temporal, and spatial characteristics of the output beam.

This work is carried out by the scientists and postdocs collaborating in the SDL: G. L. Carr, Louis DiMauro, Adnan Doyuran, William Graves, Richard Heese, Steve Hulbert, Erik Johnson, Henrik Loos, Jim Murphy, Jim Rose, Sam Krinsky, George Rakowsky, Timur Shaftan, John Skaritka, Xijie Wang, Zilu Wu, and Li Hua Yu.

TECHNICAL PROGRESS AND RESULTS:

We have successfully completed the design and construction of an independent pulse-compressor and frequency tripler for the direct seeding of the FEL. A stable transport line was designed and constructed, first for 266 nanometer light, intended to directly

seed the FEL, and subsequently for 800 nm light, which is used in High Gain Harmonic Generation (HG HG). HG HG is a technique in which the FEL is seeded by a subharmonic of the desired output radiation in a separate undulator. The resultant energy modulation induces microbunching in the electron bunch in a following dispersive section, and this yields coherent radiation at the shorter wavelength in the radiator. The direct seeding was demonstrated in August 2002, yielding 40 uJ pulses at 266 nm. HG HG with an 800 nm seed was first demonstrated in October-November 2002 with pulse energies above 100 uJ attained at 266 nm. Spectral profiles are shown below, showing the dramatic line-narrowing indicative of HG HG relative to the much weaker ($\sim 10^{-4}$) self-amplified spontaneous emission (SASE) that is emitted in the absence of the seed.



Extensive diagnostic development has also been accomplished this year. An output diagnostic end station has been implemented for spectral, temporal, and spatial analysis of the FEL output. An extensive electron-beam monitoring system comprising Ce:YAG pop-in monitors was integrated with an optical alignment system and computer control to permit rapid beam alignment and electron bunch measurements including emittance, slice emittance, and high-resolution (50 fsec) temporal profiles. Pop-

ins also permit step-wise measurement of the output build-up in the radiator. Scanning and single-shot cross-correlators have been designed and constructed. These give temporal profiles of optical pulses with a resolution of 250 femtoseconds. Using the above diagnostics, we have refined new techniques of time-resolved measurement of beam parameters and conducted extensive studies on beam dynamics during compression, an issue critical to FEL development. We have also shaped the temporal profile of the photocathode drive pulse, using frequency masks in the optical compressor and phase mis-matching in the frequency tripler, and studied its effects on beam dynamics and radiation from the electron bunch. This has proven to be a very useful tool in studying electron bunch dynamics questions that are critical to future FEL development, and for pursuing the promising question using modulated electron bunches to generate intense Terahertz radiation.

Experimental work with HG HG has just begun. In the next year we will fully characterize it and extend our studies to include coherent measures of the FEL output. This will enable us to examine the possibility and limits of compressing that output, another critical FEL development issue. It is also necessary to refine our control system to better accommodate the user program and develop synchronization techniques.

SPECIFIC ACCOMPLISHMENTS:

A. Doyuran, W.S. Graves, E.D. Johnson, S. Krinsky, H. Loos, G. Rakowsky, J. Rose, T.V. Shaftan, B. Sheehy, J. Skaritka, J.H. Wu, L.H. Yu, Y. Zhao. *Diagnostics System for the NISUS Wiggler and FEL Observations at the BNL Source Development Lab*. European Particle Accelerator Conference Paris, France, June 3-7, 2002 (hereafter "EPAC'02")

H. Loos, A. Doyuran, W.S. Graves, E.D. Johnson, S. Krinsky, J. Rose, T.V. Shafan, B. Sheehy, J. Skaritka, J.H. Wu, L.H. Yu. *Experiments in Coherent Radiation at SDL*. EPAC'02

T.V. Shafan, A. Doyuran, W.S. Graves, E.D. Johnson, S. Krinsky, H. Loos, J. Rose, B. Sheehy, J.H. Wu, L.H. Yu, D.H. Dowell. *Electron Bunch Compression in the SDL Linac*. EPAC'02

T.V. Shafan, L.F. DiMauro, A. Doyuran, W.S. Graves, E.D. Johnson, S. Krinsky, H. Loos, J. Rakowsky, J. Rose, B. Sheehy, J. Skaritka, J.H. Wu, L.H. Yu, Y. Zhao. *Beam-based Trajectory Alignment in the NISUS Wiggler*. EPAC'02

C. Limborg, P. Bolton, J.E. Clendenin, D.H. Dowell, P. Emma, S. Gierman, B. Murphy, J. Schmerge, W.S. Graves, H. Loos, T.V. Shafan, B. Sheehy. *PARMELA vs Measurements for GTF and DUVFEL*. EPAC'02

B. Sheehy, G.L. Carr, L. F. DiMauro, A. Doyuran, W.S. Graves, R. Heese, E.D. Johnson, S. Krinsky, H. Loos, J.B. Murphy, G. Rakowsky, J. Rose, J. Rudati, T. Shafan, J. Skaritka, J.H. Wu, L.H. Yu, Y. Zhao, C.P. Neuman, L. Mihaly, D. Talbayev, D. H. Dowell, P. Emma, C. Limborg, P. Piot. *Deep Ultraviolet Free Electron Laser Source at BNL's Source Development Laboratory*. Gordon Research Conference on Multiphoton Processes, Tilton, NH, June 30 - July 5, 2002

T. Shafan, J. Wu, W. Graves, H. Loos, A. Doyuran, L.H. Yu, E.D. Johnson, S. Krinsky, J. Rose, B. Sheehy, D.H. Dowell. *Bunch Compression in SDL Linac*. 24th International Free Electron Conference and 9th FEL Users Workshop, Argonne, Ill, Sep. 9-13, 2002 (hereafter FEL'02)

T.V. Shafan, H. Loos, L.F. DiMauro, A. Doyuran, W.S. Graves, E.D. Johnson, S. Krinsky, J. Rakowsky, J. Rose, B. Sheehy, J. Skaritka, J. Wu, L.-H. Yu, Y. Zhao. *Beam-Based Trajectory Alignment in the NISUS Wiggler*. FEL'02

A. Doyuran, W.S. Graves, H. Loos, T. Shafan, B. Sheehy, L.-H. Yu, L.F. Dimauro, R. Heese, E.D. Johnson, S. Krinsky, G. Rakowsky, J. Rose, J. Skaritka, J. Wu, Y. Zhao. *Observation of SASE at the BNL Source Development Laboratory*. FEL'02

J.G. Neumann, P.G. O'Shea, W.S. Graves, B. Sheehy. *Coherent Radiative Phenomena Driven By a Pre-Modulated Electron Beam*. FEL'02

LDRD FUNDING:

FY 2002	\$135,269
FY 2003 (budgeted)	\$135,000
FY 2004 (estimated)	\$135,000

High-Gain Harmonic- Generation at the DUV-FEL

Li Hua Yu

02-66

PURPOSE:

We investigate the performance of a high-gain harmonic-generation (HG HG) free-electron laser at the Deep Ultra Violet – Free Electron Laser (DUV-FEL) facility. The HG HG approach utilizes a laser-seeded FEL to produce amplified, longitudinally coherent, Fourier-transform-limited output at a harmonic of the seed laser. In 1999-2000, we had successfully demonstrated the HG HG FEL in the infrared in an experiment performed at the BNL Accelerator Test Facility (ATF). Recently we have carried out the Self Amplified Spontaneous Emission (SASE) experiment at 400 nm using Near Infra-red Scalable Undulator System (NISUS). Here, we plan to extend this work into the visible and then down to 100 nm at the DUV-FEL. In the long-term development of the HG HG FEL, a key objective is to move the output radiation down to shorter wavelengths, with the ultimate goal of providing an intense, highly coherent source of hard x-rays. To accomplish this, it will be necessary to cascade several stages of high-gain harmonic-generation. Therefore, in addition to the experimental investigations at the DUV-FEL facility outlined above, we plan to carry out theoretical studies of the cascading process, investigating its potential and sensitivities.

APPROACH:

The conventional approach to X-ray FEL is to use the SASE method. The SASE output is not longitudinal coherent, its bandwidth is larger than spontaneous radiation, our theory showed that using HG HG approach, we can

achieve coherent output with stable, narrow bandwidth output. We use the photocathode RF electron gun and the NISUS undulator at the Source Development Laboratory (SDL) to demonstrate the HG HG operation and generate Deep UV output for application in chemistry. The collaborators include A. Doyuran, H. Loos, T. Shaftan, B. Sheehy, W. Graves, and J. Murphy.

TECHNICAL PROGRESS AND RESULTS:

During FY 2001, we accomplished SASE at 400 nm, at 266 nm and achieved near saturation of seeding at 266 nm. These showed that the trajectory in the NISUS undulator and the electron beam quality is appropriate for HG HG to generate 266 nm radiation from 800 nm with a micro joule output at 88 nm. Based on this result, we installed the modulator and dispersion magnet. Beginning from FY 2002, we installed seeding optics for 800 nm input, and commissioned the new electron beam line. In short, we have achieved three milestones: 400 nm SASE, 266 nm SASE and 266 nm seeding. The commissioning of the new electron beam line with the modulator, dispersion magnet and the seeding beam line installed means we are ready to commission the HG HG experiment now.

SPECIFIC ACCOMPLISHMENTS:

Acquired funding from Air Force Office of Scientific Research/Finance Department (AFOSR/PIF), Medical FEL Research Program, Agreement Number NMIPR015203751.

Publications:

- L.H. Yu, L.F. DiMauro, A. Doyuran, W. Graves, E. Johnson, S. Krinsky, S. Mikhailov, G. Rakowsky, J. Skaritka, T.

- Shaftan, B. Sheehy, J.H. Wu, "The DUV-FEL Development Program, p.2830, Proceedings of PAC 2001, Chicago (2001).
- Juhao Wu and Li Hua Yu, "High Gain Harmonic Generation UV to DUV-FEL at NSLS," 2719, Proceedings of PAC 2001, Chicago (2001).
 - A. Doyuran, W. Graves, E.D. Johnson, S. Krinsky, H. Loos, J. Rose, J. Skaritka, T.V. Shaftan, B. Sheehy, J. Wu, L.H. Yu, G. Rakowsky, "Diagnostic System of the NISUS Wiggler and FEL Measurements in SDL," EPAC 2002.
 - T.V. Shaftan, A. Doyuran, H. Loos, L.H. Yu, S. Mikhailov, J. Skaritka, S. Krinsky, W. Graves, B. Sheehy, E.D. Johnson, J. Wu, J. Rose, Z. Yu, J. Rakowsky, "Beam-based Trajectory Alignment in the NISUS Undulator," EPAC 2002.
 - T.V. Shaftan, A. Doyuran, W. Graves, E.D. Johnson, S. Krinsky, H. Loos, J. Rose, J. Skaritka, B. Sheehy, J. Wu, L.H. Yu, Z. Yu, "Electron Bunch Compression in SDL linac," EPAC 2002.
 - A. Doyuran, W. Graves, E.D. Johnson, S. Krinsky, H. Loos, G. Rakowsky, J. Rose, T.V. Shaftan, B. Sheehy, J. Skaritka, J. Wu, L.H. Yu, "Diagnostic System of the NISUS Wiggler and FEL Measurements in SDL," EPAC (2002).
 - Li Hua Yu, Juhao Wu, "Theory of High Gain Harmonic Generation - an Analytical Estimate," Proceedings of 23rd International Free Electron Laser Conference, Darmstadt, August 20-24, 2001.
 - A. Doyuran, W. Graves, R. Heese, E.D. Johnson, S. Krinsky, H. Loos, J. Murphy, G. Rakowsky, J. Rose, T. Shaftan, B. Sheehy, J. Skaritka, X.J. Wang, L.H. Yu, "Observation of SASE and Amplified Seed of the DUV-FEL at BNL," FEL 2002, Chicago.
 - A. Doyuran, W. Graves, R. Heese, E.D. Johnson, S. Krinsky, H. Loos, J.B. Murphy, G. Rakowsky, J. Rose, T. Shaftan, B. Sheehy, J. Skaritka, X.J. Wang, L.H. Yu, "First SASE and Seeded FEL Lasing of the NSLS DUV-FEL at 266 & 400 nm," FEL 2002, Chicago.

LDRD FUNDING:

FY 2002	\$134,947
FY 2003 (budgeted)	\$135,000

Biomaterialization: a Route to Advanced Materials

Elaine DiMasi

02-67

PURPOSE:

Biomaterialization is the process by which living organisms produce high-performance composite materials with exceptional physical strength, toughness, and flexibility. The structure, morphology, and hierarchical organization of the mineral crystals are controlled on nanometer to micron length scales; comparable design has not been achieved in synthetic materials so far. In pursuit of nanoscale functional materials, the biomaterialization process has been under intense study for the last several years. Most of the open questions involve the relationship between mineral growth and accompanying organic species, and the current lack of understanding can be attributed to the dearth of in-situ structural studies up to now. By using synchrotron X-ray scattering to study mineralization at organic templates, we clarify the competing mechanisms of biomaterialization. Our work motivates BNL programs in nanoscale templating and organic thin films (Physics Dept.), new micro-diffraction capabilities (NSLS), and studies of diatom genetics and silicification (Biology Dept.), with proposals funded or pending in each of these areas.

APPROACH:

Biogenic minerals are complicated: The cells supply proteins, ions, and insoluble organics that all act together to control crystallization. From the viewpoint of materials science, it is feasible to study mineralization in "biomimetic" systems with a few well-chosen ingredients to direct mineralization, not necessarily into a copy of a biomineral, but into a form that can be

designed by the scientist. This is an exciting approach, but the field was limited by the inability to monitor mineralization in-situ. Our innovation is to use surface-sensitive X-ray scattering to study mineralization from solution onto organic monolayers and films.

One important problem is to understand how monolayer films nucleate or "template" the growth of mineral films. In the literature, the necessity for a structural match between "template" and mineral polytype is often taken for granted, but without any structural evidence to support it. Our synchrotron measurements probe template and mineral structure directly. A second very important issue is the kinetics of mineralization. Previous optical and electron microscopy techniques could not access nm-scale structures at early growth stages, but the X-ray measurements can be done directly in the mineralizing solution. For example, we have made the first direct measurements of the time dependence of amorphous calcium carbonate film formation.

Collaborators include Laurie Gower (U. Florida, Gainesville), who studies polymer-induced amorphous mineral precursors; Christine Orme (LLNL), studying electrochemistry of coated titanium bone implant alloys; and Mehmet Sarikaya (U. Washington, Seattle), who provides marine biominerals for study. Laser light scattering experiments on polymer-induced mineral droplets were done in collaboration with Tianbo Liu (BNL Physics).

TECHNICAL PROGRESS AND RESULTS:

We first focused on calcium carbonates, scrutinizing the assumptions underlying previous studies of nucleation at monolayers. Fig. 1 shows the morphologies of CaCO_3 grown under different conditions.

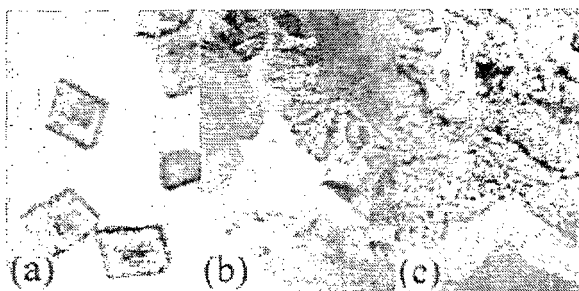


Figure 1. (a) Calcite rhombs favored during fast mineralization. (b) Vaterite florets favored during rate-inhibited mineralization. (c) Bi-refringent calcite thin film grown with polymer additives. Height of each optical micrograph panel is 200 μm .

Previous workers believed that vaterite crystals (Fig. 1b), unstable polymorphs compared to calcite (Fig. 1a), grow by structural matching of their (001) faces to the fatty acid monolayer. Our surface X-ray measurements showed conclusively that the crystals are not oriented beneath this layer, and that no clear relationship exists between the vaterite and monolayer structures. Cation binding measured by X-ray scattering is a factor of five less than the template model predicts, and it can vary with solution composition. Here, kinetics determines the mineral polytype, and we showed this by varying the supersaturation time dependence in template-independent ways.

Milestone (6 months): Verified experimental approach. Concluded structural assessments of template, and completed dilution study.

We next examined the effect of soluble acidic polymers. In solution, polyacrylic and polyaspartic acids mimic proteins that affect biomineralization. In our experiments, the polymers force mineralization to proceed via an amorphous precursor phase. Our ability to monitor the details of mineralization is exemplified in Figure 2, which shows how we can probe the density and growth rate under varying conditions. We identified the regime where this system is rate-limited by gas diffusion, and began to explore the

behavior where the kinetics depends upon polymer concentration. We also determined that the amorphous film does not crystallize through hydrous crystalline phases, but as a mixture of vaterite and calcite. No evidence for template matching was obtained.

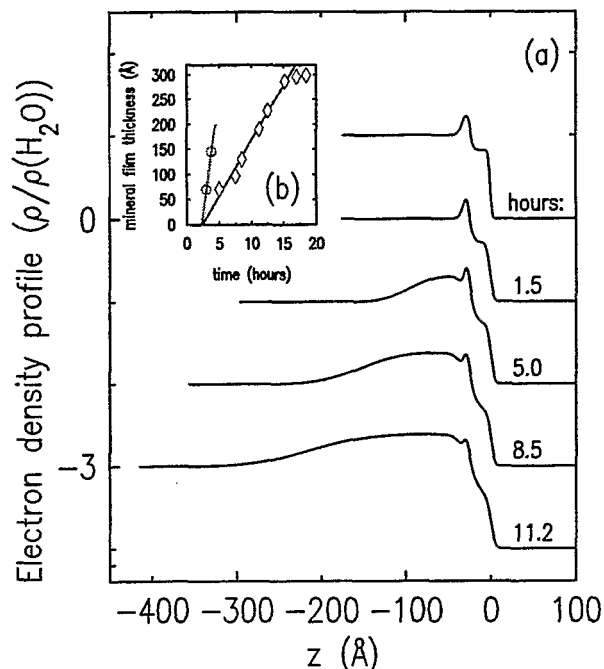


Figure 2. (a) Time series of film density profiles determined by X-ray reflectivity, showing the bound cations and the mineral region growing into the subphase. (b) Time-dependent mineral thickness under fast (circles) and slow (diamonds) diffusion conditions.

Milestone (1 year): Comparative time and density studies completed. Concluded that no template matching mechanism exists in CaCO_3 -fatty acid system.

Our results suggest that in calcium carbonates, nucleation proceeds from local charge redistributions, which are enhanced near the template. Work will therefore continue in the context of patterned templates, which closely mimic the mineralization matrices in avian eggshells and marine shells.

Sketch of new milestones: Year 2, homogeneous monolayer film studies completed. Identification of self-assembling domain-forming film for mineralization. Year 3, establish program on solid patterned substrates, to be studied by microdiffraction.

SPECIFIC ACCOMPLISHMENTS:

Programmatic Funding

Nanotemplate Directed Assembly of Soft and Nanomaterials, NSET, BNL Physics/NSLS, funded FY 2003. **NOTE:** Funds to be shared among 5 PI's cannot provide sole support to continue the biomineralization research.

Engineering Titanium for Improved Biological Response, LLNL, LDRD funded FY 2003. Supports bone implant coating work.

Refereed Publications, FY 2002

Synchrotron X-ray Observations of a Monolayer Template for Mineralization. E. DiMasi and L. B. Gower, MRS Symp. Proc. **711** (2002) 301.

Polymer-Controlled Growth Rate of an Amorphous Mineral Film Nucleated at a Fatty Acid Monolayer. E. DiMasi, L. B. Gower, et al., *Langmuir* **18** (2002) 8902.

Cation Binding, Polymer Inhibitors, and Amorphous CaCO₃ Film Formation at Fatty Acids. E. DiMasi, L. B. Gower, et al., in preparation (to submit to *Phys. Rev. E*).

Coalescence and Mineralization of Polymer-Induced Mineral Precursor Droplets Observed by Laser Light Scattering. T. Liu, L. B. Gower, and E. DiMasi, in preparation (to submit to *Nano Letters*).

When is Template Directed Mineralization Truly Template Directed? E. DiMasi et al., in preparation (submit as Letter to Science).

Internal Reports: NSLS Activity Abs. FY02

Effect of Hydrogen Peroxide on the Native Oxide of a Titanium Surface. E. DiMasi, C. Orme, J. Bearinger, J. Muryko.

Growth Rate of Polymer-induced Calcium Carbonate Films: Concentration and CO₂ Dependence. E. DiMasi, V. M. Patel, M. J. Olszta, M. Sivakumar, G. Sivakumar, Y. P. Yang, L. B. Gower.

Microdiffraction from Abalone Shell: Microstructure and Crystallite Orientation at the Nacre-prismatic Boundary. E. DiMasi and M. Sarikaya.

Presentations and Reviews in FY 2001/FY 2002

4 contributed conference presentations:

"Synchrotron X-ray Observations of a Polymer-induced Amorphous Calcium Carbonate Film," Materials Research Society, Boston MA, December 2000.

"Mineralization at a Monolayer Template: Direct Observations by Synchrotron X-ray Scattering," Materials Research Society, Boston MA, December 2001.

"Direct Observation of Biomimetic Mineral Nucleation by Surface X-ray Scattering," Symposium on Biological and Biomimetic Materials, Materials Research Society, San Francisco CA, April 2002.

"When is template directed mineralization really template directed?" Gordon Research Conference on Biomineralization, New London NH, August 2002.

3 invited conference presentations:

“Biomineralization: “Organic” Methods of Calcium Carbonate Growth.” Workshop on Synchrotron X-ray methods in Soft Matter and Biomaterials, sponsored by Brookhaven National Laboratory, Tarrytown NY, April 2002.

“Mineralization at a Monolayer Template: Direct Observations by Synchrotron X-ray Scattering.” United Engineering Foundation Conference on Biomimetic Engineering, Desin FL, March 2002.

“When is template directed mineralization truly template directed?” Materials Research Society Spring Meeting, San Francisco CA, April 2003.

Recognition by Materials Research Society, December 2001.

LDRD FUNDING:

FY 2002	\$ 99,935
FY 2003 (budgeted)	\$105,400
FY 2004 (estimated)	\$111,000

Theory of Electronic **Transport in Nanostructures and Low-Dimensional Systems**

Alexei Tsvelik

02-70

PURPOSE:

To study combined effects of strong correlations, low dimensionality and disorder on transport properties and correlation functions. All these three factors determine physics of nanoscale systems and hence their understanding is crucial to creation of nanoscale technology.

APPROACH:

This research employs well-developed non-perturbative techniques such as exact solutions and conformal field theory. The distinct feature of low-dimensional world is that its physics is dominated by collective excitations. Nanoscale devices may become systems where this physics strongly manifests itself and thus could provide realizations for scenarios of behavior which used to exist only in theorists dreams.

The investigation conducted so far in this project concerns two types of problems. The line of research pursued with M.J. Bhaseen (BNL) is related to study of correlation functions in the model where excitations carry fractional quantum numbers. This model describes a frustrated spin-1/2 Heisenberg magnet with short-range interactions in arbitrary number of dimensions. It was formulated by A. A. Nersesyan (ICTP) and A. M. Tsvelik (Phys. Rev. B67, 02422 (2003)) and still remains the only example of a model (beyond the Fractional Quantum Hall) where existence of fractional quantum number excitations was rigorously proven. To calculate

correlation functions we use the so-called formfactor approach method.

The research conducted by B. N. Narozhny concerns effects of interaction in experimentally available two-dimensional devices such as Si-MOSFET's. The methods employed are standard methods of mesoscopic theory (perturbative diagram expansion, Keldysh technique).

TECHNICAL PROGRESS AND RESULTS:

In FY 2002 the most important result is the demonstration of a possibility of independent extraction of Fermi liquid parameters from transport measurements in mesoscopic systems. It is now necessary to complete the work on dephasing time in the presence of magnetic impurities. Such impurities are ubiquitous and strongly affect transport properties being a strong source of inelastic scattering. The latter is quenched at low temperatures due to the Kondo effect. The temperature dependence of the corresponding dephasing time has never been calculated.

It is also necessary to continue the research in fractional spin magnets. Some early results indicate that this research may be relevant to the problem of quantum computing.

SPECIFIC ACCOMPLISHMENTS:

Narozhny, B.N., Zala, Gábor, and Aleiner, I.L. Interaction Corrections at Intermediate Temperatures: Dephasing Time. *Phys. Rev. B*65, 180202 (2002). BNL 69243

Publications in preparation:

B. L. Altshuler, B.N. Narozhny and A.M.Tsvelik, Electron Dephasing Time in the Presence of Magnetic Impurities.

M. J. Bhaseen, $SU(N)$ Generalization of
RVB: Exact Results.

LDRD FUNDING:

FY 2002	\$134,268
FY 2003 (budgeted)	\$139,900
FY 2004 (requested)	\$145,500

Pressure in Nanopores

Thomas Vogt

02-71

Y. Lee

PURPOSE:

The purpose of this project was to study the structural changes in nanoporous materials, which result from pressure-induced chemical reactions within nanopores. Various interactions between the species inherent or introduced under pressure inside a given nanopore leads to unusual property changes, such as pressure-induced swelling or trap-door exchange, which may open new types of applications of these materials.

APPROACH:

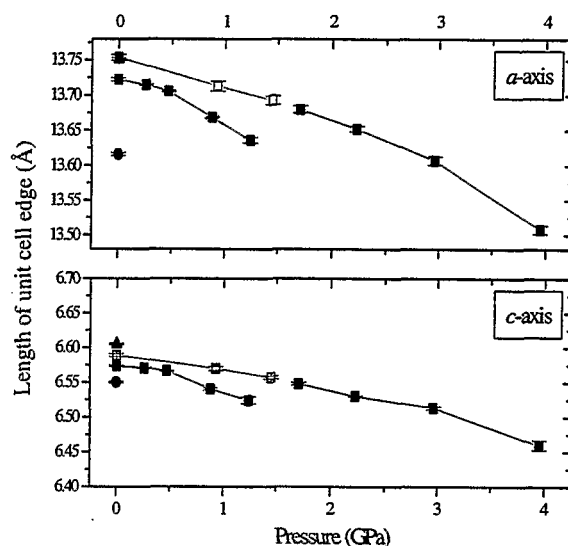
The project began with deciphering the mechanism of pressure-induced swelling in zeolite natrolite. We used micro-focused monochromatic synchrotron X-ray powder diffraction at beamline X7A and diamond-anvil high-pressure cells. Other related nanopore-guest species systems were subsequently investigated in an attempt to tune and exploit this phenomenon.

Collaborators include J.A. Hriljac (U Birmingham, UK), J.B. Parise (USB), G. Artioli (U Milano, Italy), S.J. Kim (KIST, Korea), J.E. Post (Smithsonian), P.M. Woodward (OSU), and J.C. Hanson (BNL).

TECHNICAL PROGRESS AND RESULTS:

In FY 2002, we have investigated more than 20 nanopore-guest species systems using the high-pressure experimental technique described above. Among those, successful modification of the pressure-induced swelling was achieved in a potassium gallosilicate zeolite, which retains the high

pressure expanded state upon pressure release, and significant increase in ion-exchange capacity was observed in a sodium aluminosilicate zeolite utilizing the pressure swelling effect. These results imply that using pressure some nanopores may be used to immobilize tritiated water or other chemical pollutants.



Furthermore, we successfully implemented high-pressure measurements using an imaging plate area detector at beamline X7B. This will serve us either as a screening tool for suitable systems for follow-up X7A runs or studying structurally simpler materials which do not require the higher resolution available with PSD at X7A. Future upgrades in our high-pressure capability will include increase in working pressure range and simultaneous cooling or heating under pressure.

SPECIFIC ACCOMPLISHMENTS:

Awards

1. **Sidhu Award** (2002), Pittsburgh Diffraction Conference, Pittsburgh, Pennsylvania, Oct. 3-5.
2. **Alvin Van Valkenburg Award** (2002), Gordon Conference on "Research at

High Pressure" Meriden, New Hampshire, June 23-28.

3. **Certificate of Excellence** from the Director of Brookhaven National Laboratory and **Poster Session Award** during 2002 NSLS Annual Users' Meeting.

Invited Talks:

1. Sidhu Award Lecture (2002), *Pressure in Nanopores*, 60th Pittsburgh Diffraction Conference, Pittsburgh Diffraction Society, University of Pittsburgh, Pittsburgh, Pennsylvania, Oct. 3-5.

Publications:

1. Lee, Y.; Vogt, T.; Hriljac, J.A.; Parise, J.B.; Hanson, J.C.; and Kim, S.J. (accepted) *Non-framework cation migration and irreversible pressure-induced hydration in a zeolite*. **Nature**

2. Barnes, P.W.; Woodward, P.M.; Lee, Y.; Vogt, T.; Hriljac, J.A. (submitted) *Pressure-induced cation migration and volume expansion in the defect pyrochlores ANbWO₆*. **J. Am. Chem. Soc.**

3. Lee, Y.; Vogt, T.; Hriljac, J.A.; Parise, J.B.; Artioli, G.; and Studer, A. (submitted) *Anisotropic compression of fibrous zeolites (natrolite, edingtonite, thomsonite) to 7 GPa at room temperature*. **Phys. Chem. Mineral.**

4. Lee, Y.; Vogt, T.; Hriljac, J.A.; and Parise, J.B. (2002) *Discovery of a Rhombohedral Form of the Li-Exchanged Aluminogermanate Zeolite RHO and Its Pressure-, Temperature-, and Composition-induced Phase Transitions*. **Chem. Mater.**, 14, 3501-3508.

5. Lee, Y.; Vogt, T.; Hriljac, J.A.; Parise, J.B.; and Artioli, G. (2002) *Pressure-Induced Volume Expansion of Zeolites in the Natrolite family*. **J. Am. Chem. Soc.**, 124, 5466-5475.

6. Lee, Y.; Hriljac, J.A.; Vogt, T.; Parise, J.B.; and Artioli, G. (2001) *First*

Structural Investigation of a Super-hydrated Zeolite. **J. Am. Chem. Soc.**, 123, 12732-12733.

7. Lee, Y.; Hriljac, J.A.; Vogt, T.; Parise, J.B.; Edmondson, M.J.; Anderson, P.A.; Corbin, D.R.; and Nagai, T. (2001) *Phase Transition of Zeolite Rho at High-Pressure*. **J. Am. Chem. Soc.**, 123, 8418-8419.

Poster Presentations:

1. Lee, Y.; Vogt, T.; Hriljac, J.A.; Parise, J.B.; Hanson, J.C.; Artioli, G.; Post, J.E.; Kim, S.-J. (2002) *Gordon Conference on "Solid State Chemistry I"*, New London, NH.

2. Hriljac, J.A.; Anderson, P.A.; Readman, J.E.; Lee, Y.; Vogt, T., (2002) *Gordon Conference on "Solid State Chemistry I"*, New London, NH.

3. Lee, Y.; Vogt, T.; Hriljac, J.A.; Parise, J.B.; Hanson, J.C.; Artioli, G.; Post, J.E.; Kim, S.-J. (2002) *Gordon Conference on "Research at High Pressure"*, Meriden, NH.

4. Lee, Y.; Vogt, T.; Hriljac, J.A.; Parise, J.B.; Post, J.; Artioli, G. (2002) *National Synchrotron Light Source (NSLS) Annual User Meeting*, Upton, NY.

5. Lee, Y.; Vogt, T.; Hriljac, J.A.; Parise, J.B.; Post, J.; Artioli, G. (2002) *BNL Nanocenter Workshop*, Upton, NY.

6. Lee, Y.; Hriljac, J.A.; Vogt, T.; Parise, J.B.; Corbin, D.R.; and Nagai, T. (2001) *American Crystallographic Association (ACA) Annual Meeting*, Los Angeles, CA.

LDRD FUNDING:

FY 2002	\$80,000
FY 2003 (budgeted)	\$82,600
FY 2004 (estimated)	\$86,700

Genomic SELEX to Study Protein DNA/RNA Interactions in *Ralstonia Metallidurans* CH34 Regulating Heavy Metal Homeostasis and Resistance

Daniel van der Lelie

02-84A

PURPOSE:

The aim of this proposal is to use SELEX (Systematic Evolution of Ligands by Exponential enrichment) approach to establish a protein-nucleic acid linkage map for heavy metal resistance and homeostasis in *Ralstonia metallidurans* CH34.

APPROACH:

The SELEX approach, which was carried out in collaboration with S. Taghavi and J. Flanagan, involves the following logical steps: Selection of key-regulator genes; cloning, over-expression and purification of proteins; strategy for the generation of random DNA/RNA fragments; and SELEX enrichment of nucleotide fragments interacting with regulatory protein.

TECHNICAL PROGRESS AND RESULTS:

Set-up of New Laboratory: Considerable time was spent with the set-up of a new laboratory, including the purchase of the necessary equipment.

Phylogenetic analysis of heavy metal resistance regulators: After a BLAST search of the nearly completed sequenced genome of *Ralstonia metallidurans* CH34, 10 PbrR/MerR like regulators were identified. These regulators could, based on sequence similarity and functional linkage to

structural resistance proteins, be divided in four major groups. Members of the different groups were chosen for cloning in protein over-expression vectors. At present the work concentrates on members of the MerR family (*merR* genes from the contigs 691, 663 and Tn4378), where identical regulators were found to be involved in the regulation of three mercury resistance genes, and on the PbrR-like regulator from contig 710. The *pbrR*-like gene on contig 710 was not physically linked to any structural heavy metal resistance gene. Therefore, SELEX is an ideal approach to identify the PbrR710 regulated functions that are located physically distant on the chromosome. The *merR*-like and *pbrR*-like regulators were cloned as His-tag fusions in pET28 and pET30 and checked for over-expression. The proteins are presently being purified.

In addition, several loci were identified in the *Ralstonia metallidurans* CH34 genome that, based on sequence homology, are expected to be involved in copper homeostasis and resistance. These include the *copH*, *copG* and *copR* genes, which were cloned as His-tag fusions in pET28 and pET30.

Random DNA fragments for SELEX enrichments: A library of random DNA fragments for SELEX enrichment was constructed based on the following principles (Fig. 1):

- random 40bp DNA fragment, flanked by well-defined ends:
 - One end allows conversion into RNA using the T7 promoter
 - RNA can be converted into ss-DNA
 - ds-DNA is obtained by simple PCR amplification

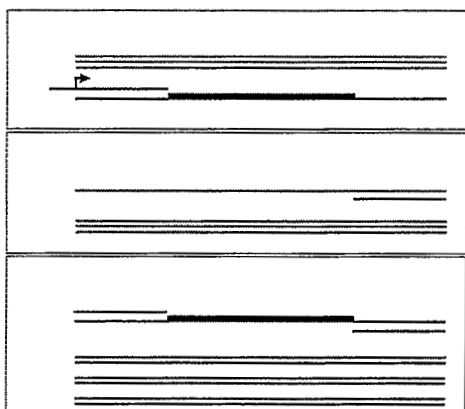


Figure 1: Strategies for generating Random DNA / RNA fragments for SELEX enrichment.

Reorientation of the Work: Although regulatory pathways are one of the goals of DOE's Genomes to Life (GTL) Program, our strategy is not suitable for high throughput identification of protein-nucleotide interactions as is solicited for by DOE. Therefore, part of the effort of this LDRD was reoriented towards the analysis of the composition and functioning of microbial communities, especially microbial communities associated with contaminated sites, which is also a goal of DOE's GTL Program.

SPECIFIC ACCOMPLISHMENTS:

A proposal is presently in preparation on rhizosphere bacteria and their role in phytoremediation of heavy metals and radionuclides, this in response to Office of Science Financial Assistance Program Notice 03-04: Joint Interagency Program on Phytoremediation Research.

As part of the reorientation of the work the following two reports and proposals were written:

- Diversity, Structure and Functional Interdependence of Microbial Communities in the Plant Rhizosphere.

J. Dunn and D. van der Lelie, Informal Report BNL-52655 (2002).

- An Integrated Functional Genomics Consortium to Increase Carbon Sequestration in Poplar: The Poplar-Mycorrhizal Symbiosis as a System to Improve Terrestrial Carbon Sequestration. D. van der Lelie and J. Dunn, Informal Report BNL-69188 (2002).

The work on the characterization of the PbrR/MerR regulators is part of a paper for FEMS Microbial Reviews that is presently in preparation.

In addition the following paper is presently in preparation:

Vallaey, T.; Benotmane, R.; Wattiez, R.; Noel-Georis, I.; Borremans, B.; Monchy, S.; Toussaint, A.; Mergeay, M.; Dunn, J.; Taghavi, S.; and van der Lelie, D. Analysis of the copper response in *Ralstonia metallidurans* CH34.

LDRD FUNDING:

FY 2002	\$163,972
FY 2003 (budgeted)	\$170,900
FY 2004 (requested)	\$ 49,900

Lead Resistance in *Ralstonia Metallidurans* CH34

Daniel van der Lelie

02-84B

PURPOSE:

The purpose of this project is to further elucidate the functioning of the *pbr*TRABCD lead resistance operon of *Ralstonia metallidurans* CH34, and to determine the role and interactions of the different lead resistance proteins.

APPROACH:

In order to study the role of the different components of the *pbr*TRABCD lead resistance operon of *Ralstonia metallidurans* CH34, the operon was cloned and subsequently a library of different knock-out mutants was constructed. Sequence analysis was used to identify different *pbr* mutants. This work was carried out in collaboration with S. Taghavi.

To study the functioning of the *pbr* proteins, we cloned them in a pET protein expression system. This work was carried out in collaboration with J. Flanagan.

As part of the effort to sequence and analyse the genome of *Ralstonia metallidurans* CH34 we identified and studied different PbrR and MerR like regulators. Work on the *Ralstonia metallidurans* CH34 genome is done in collaboration with Prof. Max Mergeay, Center for Studies of Nuclear Energy, Mol, Belgium.

LuxCDABE fusions were constructed in collaboration with S. Taghavi to study the role of PbrR-like regulators. Biosensor applications are part of a collaboration between BNL and Vito, the Flemish

Institute for Technological Research, Belgium.

TECHNICAL PROGRESS AND RESULTS:

Set-up of New Laboratory: Considerable time was spent with the set-up of a new laboratory, including the purchase of the necessary equipment.

Isolation of *pbr* Mutants: Using the EZ::Tn(Km2) *in vitro* transposition system we constructed a library of *pbr*::Tn(Km2) mutants (Fig. 1). A total of 89 mutants were obtained from which 7 were analyzed by sequencing. Among these we successfully obtained mutants in the *pbrT* and *pbrA* genes. Other mutants are presently being analyzed.

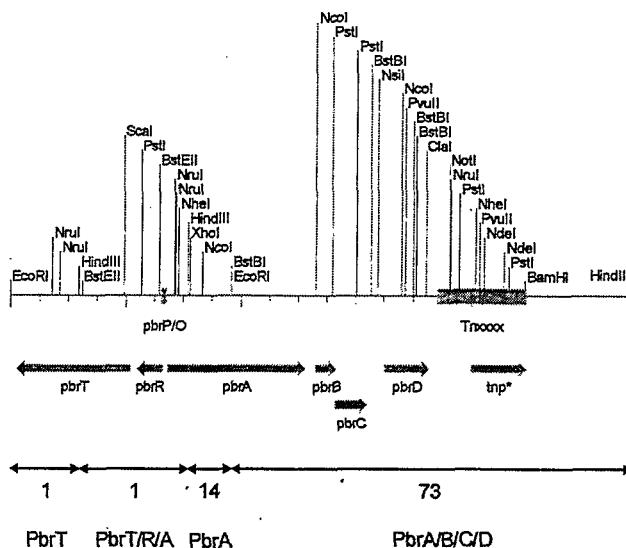


Figure 1. Map of the *pbr* operon of *Ralstonia metallidurans* CH34 and the position and numbers of the different EZ::Tn(Km2) insertion mutants.

Phylogenetic Analysis of PbrR-like Regulators: After a BLAST search of the nearly completed sequenced genome of *Ralstonia metallidurans* CH34, 10 PbrR/MerR like regulators were identified. These regulators could, based on sequence

similarity and functional linkage to structural resistance proteins, be divided in four major groups.

Construction of *luxCDABE* Fusions with Alternative *pbrR* Regulators: The second group of regulators consists of PbrR, the regulator of the CH34 lead resistance operon that is located on contig 692, and two regulators found on contigs 691 and 710, respectively. Like for the *pbrTRABCD* operon, the *pbrR*-like gene of contig 691 is linked to a heavy metal efflux ATPase, most similar to a Cd-efflux ATPase, and a *pbC* like gene. However, homologues of *pbrT*, *pbrB* and *pbrD* are lacking. In addition, a *luxCDABE* based gene fusion comprising the *pbrR*-like regulator and the 5'-end of the ATPase gene failed to show metal dependent induction of transcription (the metals tested were Zn, Cd, Cu and Pb), indicating that the operon is most likely silent.

Reorientation of Work: Based on our past experience (at Vito, Belgium) with the construction, testing and evaluation of bacterial biosensors and the interest for these sensors in the scientific community, we decided to reorient part of our efforts to the application of bacterial biosensors to evaluate the bioavailability of heavy metals in environmental samples. We successfully demonstrated the possibilities of these biosensors by evaluating heavy metal bioavailability in sludge from the NY/NJ harbor.

SPECIFIC ACCOMPLISHMENTS:

Based on the experience with the *lux*-based heavy metal biosensors we successfully applied for a project entitled "The Impact of Surface Precipitation on Sequestration and Bioavailability of Metals in Soils," as a subcontract with the Center for the Study of Metals in the Environment, University of Delaware.

The work on the characterization of the PbrR/MerR regulators is part of a paper for FEMS Microbial Reviews that is presently in preparation.

Publications:

van der Lelie, D.; Schwitzguebel, J.-P.; Glass, D. J.; Vangronsveld, J.; and Baker, A. Assessing phytoremediation's progress in the United States and Europe. *Environ. Sci. Technol.* 35, 446A-452A (2001).

Schwitzguebel, J.-P.; van der Lelie, D.; Glass, D. J.; Vangronsveld, J.; Baker, A. Phytoremediation: European and American trends, successes, obstacles and needs. *J. Soil Sediments* 2, 91-99 (2002).

LDRD FUNDING:

FY 2002	\$161,408
FY 2003 (budgeted)	\$170,100

Design of a *Ralstonia* *Metallidurans* Two-Hybrid Protein System for Studying Signaling Pathways Regulating Heavy Metal Homeostasis and Resistance

Safiyh Taghavi

02-85

PURPOSE:

This proposal aims at developing a two-hybrid protein system for elucidating at the protein level the signaling pathways that control heavy metal resistance and homeostasis in *Ralstonia metallidurans* CH34.

APPROACH:

Construct a suitable Two-Hybrid protein system for the construction and screening of libraries from *Ralstonia metallidurans* CH34.

TECHNICAL PROGRESS AND RESULTS:

Set-up of New Laboratory: Considerable time was spent with the set-up of a new laboratory, including the purchase of the necessary equipment.

Construction of a Modified Vector System for Two-Hybrid Studies: Three available Two-Hybrid vector systems were evaluated for their performances using the regulatory genes of the *cnr* cobalt-nickel resistance system of *Ralstonia metallidurans* CH34: (1) BacterioMatch Two-hybrid System (Stratagene): This is based on interaction between λ CI repressor protein and RNAP (RNA polymerase). This system was found suitable but the pBT (bait) vector would

need improvement to make it suitable for library construction. (2) T25-T18 fragments of the *Bordetella pertussis* adenylate cyclase; complementation restores cAMP synthesis in *cya*⁻ strain. This system looked promising, but was abandoned due to unacceptable conditions for technology transfer with the Pasteur Institute (Paris, France). (3) GFP complementation: The control constructs with antiparallel leucine zipper-protein reassembly did not work in our hands, and the system was abandoned.

The BacterioMatch system was improved by adding a linker to the 3' end of the λ CI repressor of the pBT (bait) vector. This allows making better fusion libraries with the λ CI repressor protein. In addition, a number of unique restriction sites were added to facilitate the cloning of blunt-end restricted fragments.

Evaluation and Proof of Principle: We used the regulatory system of the *cnr* cobalt-nickel resistance system of *Ralstonia metallidurans* CH34 to evaluate the pBT-linker vector. To do so we cloned *cnrY*, a predicted anti- σ factor regulating *cnr* expression, in the pBT-linker vector. In order to destroy the predicted transmembrane region of the CnrY protein we replaced two Phe by Glu. In addition, the *cnrH* gene encoding a predicted ECF70 σ factor that transcribes the *cnr* operon was cloned in pTRG. Introduction of both plasmids in the same cell resulted in expression of the Two-Hybrid reporter phenotype (ampicillin resistance and β -galactosidase activity), confirming that the vectors are working and that the CnrY and CnrH proteins are physically reacting with each other as part of the regulation of the *cnr* operon.

Construction of Two-Hybrid Protein Libraries from the Genome of *Ralstonia*

metallidurans CH34: The system is presently being used for a random screening of protein-protein interactions using genomic libraries of *R. metallidurans* CH34. To do so, randomly generated DNA fragments (obtained by sheering) were cloned in both vectors. Subsequently, the libraries are being introduced in the same *Escherichia coli* strain, where they will be screened for expression of the Two-Hybrid reporter phenotype (ampicillin resistance and β -galactosidase activity).

Reorientation of the Work: Although regulatory pathways are one of the goals of DOE's Genomes to Life (GTL) Program, our strategy is not suitable for high throughput identification of protein-protein interactions as is solicited by DOE. Therefore, part of the effort of this LDRD was reoriented towards the analysis of microbial communities, especially microbial communities associated with plants, which is also a goal of DOE's GTL Program.

SPECIFIC ACCOMPLISHMENTS:

A proposal is presently in preparation on endophytic bacteria and their role in phytoremediation, this in response to Office of Science Financial Assistance Program Notice 03-04: Joint Interagency Program on Phytoremediation Research.

Publication:

Lodewyckx, C.; Vangronsveld, J.; Porteous, F.; Moore, E. R. B.; Taghavi S.; and van der Lelie, D. Endophytic bacteria and their potential applications. *Critical Rev. Plant. Sci.* (2002, in press).

LDRD FUNDING:

FY 2002	\$168,188
FY 2003 (budgeted)	\$173,900
FY 2004 (requested)	\$ 51,200

Ultrafast X-Ray Science

Steve Dierker

02-86

B. Sheehy

C.-C. Kao

PURPOSE:

Developing new X-ray sources and techniques and making them available to the user community is an important part of the NSLS mission. In recent years, some of the most important developments in the field have concerned time-resolved studies using X-rays. These promise to open new frontiers in chemical dynamics, material science, and biology, as simultaneous resolution at both molecular time scales and atomic spatial scales becomes a reality. New sources are capable of producing subpicosecond bursts of X-rays, and new techniques are being used to obtain subpicosecond resolution using synchrotron sources. Existing resources at the NSLS can be adapted for these purposes, and the purpose of this project is to carry this development forward.

APPROACH:

The Source Development Laboratory (SDL) contains a Ti:Sapphire laser system capable of producing 0.5 Terawatt peak power pulses in the infrared (800 nm wavelength). Such a source is capable of producing intensities between 10^{17} and 10^{18} W/cm² and so is an ideal candidate for a laser-driven plasma X-ray source. In such a source, the laser is focused on a metal target, forming an ultradense plasma. Energetic electrons are produced and decelerated rapidly, producing continuous bremsstrahlung radiation to energies on the order of 10 keV. Electrons penetrating the surface also eject core electrons, producing prompt K_α and K_β lines as well. In order to achieve this, certain

improvements have to be made to the laser. The contrast – the ratio between the main laser pulse and a precursor pulse which is due to the amplification method – must be brought above 10^6 . Some of this will be done with improvements in the amplifier design, which will also correct a mode problem that would otherwise prevent diffraction-limited focusing. A pulse cleaner will also be implemented after the first amplifier. We will also experiment with using the laser's second harmonic for the X-ray generation since, in addition to improving the contrast, this may improve the efficiency of the device.

On the synchrotron rings, we will expand the program in time-resolved experiments by developing ultrafast detection methods. This will include optical pump – X-ray probe experiments and the development of an X-ray streak camera.

TECHNICAL PROGRESS AND RESULTS:

One of the two postdoctoral researchers approved for this project has been hired. Yuzhen Shen joined the staff in October 2002.

In the ultrafast X-ray source project, design work on the laser modifications has been done, necessary parts have been specified, and ~80% have been delivered. A collaboration has been formed with Professor Christoph Rose-Petruck of Brown University, who will assist us in the target fabrication and other source development issues. A number of logistics issues are being resolved: the source will be located in the laser room in the SDL, and this requires considerable modification of that enclosure. These modifications will take place during a scheduled SDL shutdown December 2002 – January 2003.

A laser has been purchased (from NSLS capital funds) to support the optical pump – X-ray probe program on the synchrotron rings. A design was developed with the vendor that will permit the laser to operate initially in the ultraviolet, for a currently-planned program of nanosecond experiments. The laser can subsequently be converted to a pump laser for an ultrafast system for future experiments. The X6B beamline is currently being refitted to accommodate the nanosecond experiments.

A collaboration with Professor Jean-Claude Kieffer of the University of Quebec has been formed for the X-ray streak camera project.

Professor Kieffer is a leader in this field and will assist us in developing the instrument at BNL. A second postdoc will be hired for this project.

SPECIFIC ACCOMPLISHMENTS:

As this project is currently still in the construction phase, there are no publications or reports to date.

LDRD FUNDING:

FY 2002	\$100,018
FY 2003 (budgeted)	\$105,000

X-Ray Photon Correlation Spectroscopy Studies of Nanostructured Block Copolymers

Steve Dierker

02-88

PURPOSE:

The objective of the proposed research is to use the technique of X-ray Photon Correlation Spectroscopy (XPCS) to study the short length scale dynamics of both binary homopolymer blends and also nanostructured block copolymers. The goal of the study is to provide an experimental base from which a theoretical understanding of the short wavelength dynamics might be constructed. As a prelude to the block copolymer studies, the previously unexplored dynamics of both the highly entangled regime as well as dynamics on length scales comparable to and smaller than the polymer radius of gyration will be investigated in homopolymer blends. In the block copolymers, the previously unexplored dynamics in the unentangled regime, as well as the little explored behavior near the critical wave vector for microphase separation will be studied.

APPROACH:

On a macroscopic level, the miscibility, phase behavior, and rheology of polymers have been extensively studied. The static properties of both binary polymer blends and block copolymers have been investigated by a variety of different scattering techniques, including light scattering, small angle x-ray scattering, and mainly small angle neutron scattering. The dynamic properties, on the other hand, are relatively less well explored, especially in nanostructured block copolymers, despite their obvious

importance in understanding the microscopic origins of their tremendously variable macroscopic rheology. Essentially all previous experiments have been limited to studying the long wavelength dynamics of polymers, which provide little if any information as to how the dynamics evolve as one probes to shorter length scales comparable to the nanostructure of the polymer. The objective of this research is to use XPCS to make experimental results on the short length scale dynamics of polymers available for the first time. Since it utilizes a coherent x-ray beam, the XPCS technique necessitates a high brilliance x-ray source. Coherence and high brilliance are distinguishing characteristics of the planned NSLS Upgrade, and this project contributes expertise and scientific justification for the NSLS Upgrade.

TECHNICAL PROGRESS AND RESULTS:

A graduate student and two research associates were supported during the first year of this project. One of the research associates, TaeJoo Shin, joined the staff in September 2002 and will be continuing for a full two years.

Sample cells for the polymer XPCS experiments were fabricated. A series of Small Angle X-ray Scattering (SAXS) and XPCS measurements on homopolymer mixtures of polystyrene and polybutadiene were performed in several synchrotron runs at the NSLS and at the APS. Data were collected on the static and dynamic critical behavior at the order-disorder transition from a homogeneous mixture to a macroscopically separated phase. These data are currently being analyzed and the results prepared for publication. These experiments will continue in the coming year and will be followed by a series of experiments in a block copolymer blend.

In another aspect of the project, a prototype gas detector which shows promise for greatly improving the time resolution of XPCS measurements is being tested. This work is being carried out in collaboration with the Instrumentation Division. Initial tests of the detector are underway, and we plan to demonstrate its use in an actual XPCS experiment in the coming year. A second postdoc will be hired for this project.

SPECIFIC ACCOMPLISHMENTS:

None

LDRD FUNDING:

FY 2002	\$ 90,212
FY 2003 (budgeted)	\$105,000

Fine Grain Gas and Silicon Detectors for Future Experiments in Nuclear Physics at High Energies

Timothy Hallman
C. Woody

02-91

PURPOSE:

The purpose of this work is to investigate several new technologies which could be of great importance in the future of nuclear physics experiments at high energies. These are high-resolution gas tracking devices based on so-called micropattern detectors, and high granularity silicon pixel detectors. The objective is to determine whether any of these new technologies could be used for the next generation of detectors at RHIC that would enhance their physics capabilities or improve their performance in future years. If these technologies prove to be useful at RHIC, there would be significant scientific benefit to the RHIC program, and additional funding to continue this project could be expected from DOE Nuclear Physics.

APPROACH:

The physics program at RHIC is presently in a new discovery phase in studying high-energy heavy ion and polarized proton collisions. The current suite of RHIC detectors have proven to work extremely effectively in investigating these new phenomena, but there are potentially new discoveries which require further enhanced capabilities for these detectors. These include the measurement of low mass dilepton pairs and vector mesons, and a detailed systematic study of heavy quark production in heavy ion collisions. To study these phenomena, new detector technologies are required. Two such technologies are high precision tracking detectors capable of identifying and rejecting Dalitz pairs and photon conversions in high multiplicity heavy

ion collisions, and very high-resolution vertex detectors capable of resolving secondary vertices at the level of a few tens of microns. This project investigates the use of micropattern detectors for high-resolution particle tracking and silicon pixel detector for vertex finding. Specifically, we have studied the properties of Gas Electron Multipliers (GEM) and MicroMega detectors for use in a fast, compact Time Projection Chamber (TPC), and Hadron Blind Detector (HBD) which would be used as a device to reject Dalitz pairs and conversions, and both hybrid and active silicon pixel detectors as possible high-resolution vertex detectors. This work is being carried out in collaboration with members from both the PHENIX and STAR collaborations.

TECHNICAL PROGRESS AND RESULTS:

During FY 2002, a number of small micropattern detectors were obtained for testing and evaluation, including several multistage GEM detectors and a MicroMega detector. An example of one of the GEM detectors is shown in Figure 1.

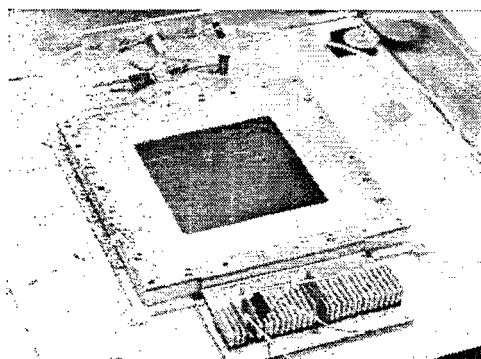


Fig. 1. Multistage GEM detector tested in FY 2002

These devices were tested in BNL's Instrumentation Division in order to study the properties of these detectors that would be important for their performance in our application. This included studies of gas gain, uniformity of response, rate dependent effects, the rate of ion feedback, and energy and position resolution.

Two of the most critical parameters for use in a fast, compact TPC detector are spatial resolution and the rate of ion feedback. Tests were carried out which showed that the size of the charge cloud at the last stage of a GEM was on the order of 500 microns, as shown in Figure 2. Further tests showed that a spatial resolution of less than 100 microns can be achieved with various types of interpolative readout. This quantity is very important in terms of designing a readout plane for a TPC, as well as the required readout electronics.

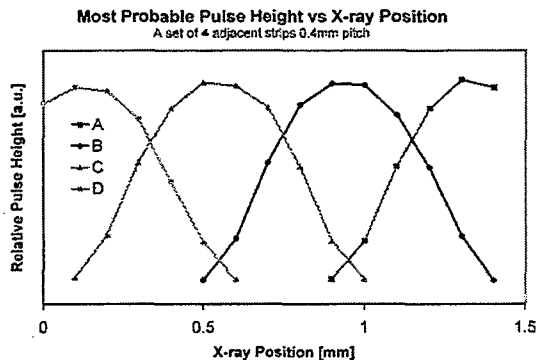


Fig. 2. Measurement of the size of the charge cloud at the last stage of a multistage GEM detector

Tests also showed that the positive ion feedback in these detectors is important and must be reduced for use at very high rates, such as would be required for the highest luminosities foreseen at RHIC.

An apparatus was also built that will allow the study of these detectors as a readout device for a TPC using a full-length drift cell.

In FY 2002, an investigation was also made of several types of silicon pixel detectors. This included a study of the ALICE/NA60 hybrid pixel detectors and their associated readout electronics, and new active pixel detectors that are being developed in collaboration with LBL. The test of the hybrid pixels involved a beam test of the first set of detectors at CERN, and the study of the active pixel detectors included a beam test at LBL. The results of both of these tests were very encouraging in

terms of achieving the spatial resolution required for an application at RHIC.

SPECIFIC ACCOMPLISHMENTS:

Presentations:

- A Study of GEM Characteristics for Application in a MicroTPC, B.Yu et al., paper to be presented at the 2002 IEEE Nuclear Science Symposium, Norfolk, VA, November 10-16, 2002, and to be submitted for publication in the IEEE Transactions on Nuclear Science.
- A Fast, Compact Time Projection Chamber for Tracking and Electron Identification in Heavy Ion Collisions, N.Smirnov et al., paper to be presented at the 2002 IEEE Nuclear Science Symposium, Norfolk, VA, November 10-16, 2002 and to be submitted for publication in the IEEE Transactions on Nuclear Science
- Upgrade Plans for PHENIX, C.L. Woody, 18th Winter Workshop on Nuclear Dynamics, Nassau, Bahamas, January 28, 2002.
- R&D Plans for PHENIX Upgrades, C.L.Woody, STAR Workshop on Future Physics and Detectors, Bar Harbor, Maine, June 18, 2002.
- Quarkonium Measurements with MiniTPC + Pad Chambers, N. Smirnov, STAR Workshop on Future Physics and Detectors, Bar Harbor, Maine, June 18, 2002.
- PHENIX AA Related Upgrades, C.L.Woody, RIKEN Workshop on Current and Future Directions at RHIC, BNL, August 9, 2002.

LDRD FUNDING:

FY 2002	\$100,000
FY 2003 (budgeted)	\$100,000

Appendix A

2003 Project Summaries

Appendix A BNL FY 2003 Projects

- (03-099) The microPET Study of Gene Expression in Rodents
P. Thanos (FY 2003 Funding \$100,000)

Examine the capability of micro Positron Emission Tomography (PET) in studying non-invasively, in vivo, genes and their function in rodents that are critical to future studies in various areas of gene research.

- (03-100) Investigation of the "Early Response" in Functional MRI
T. Ernst (FY 2003 Funding \$240,000)

Propose to utilize and study the small signal that can be detected with functional magnetic resonance imaging (MRI) with 500 milliseconds after a stimulus (e.g. a flash of light). Develop techniques and scan 60 normal subjects in order to answer these three questions: 1) whether we can see the "early response" more clearly before the regular BOLD response starts; 2) whether signal changes in the large blood vessels will affect the early response; 3) whether a contrast agent (gadolinium) that stays within the blood vessels will affect the early response.

- (03-101) PET Imaging of Violent Behavior
G.-J. Wang (FY 2003 Funding \$100,000)

Propose to assess the value of Positron Emission Tomography (PET) imaging to investigate differences in the brain of individuals that may make them vulnerable to engage in violent and/or terrorist acts based on the hypothesis that metabolism in frontal cortex and limbic regions of the brain will be increased in subjects who enjoy the viewing of video depicting violent scenes when compared with those who find this aversive since the frontal cortex is involved in controlling and inhibiting impulsive actions and the limbic system is involved with aggressive behavior.

- (03-103) PET Study of Acetaldehyde Distribution and Metabolism to Better Understand Alcohol Related Diseases
Zizhong Li (FY 2003 Funding \$100,000)

Prepare carbon-11 labeled acetaldehyde for evaluating acetaldehyde disposition in living system with positron emission tomography (PET) in order to conduct studies of acetaldehyde metabolism in tomographically isolated organs in living human subjects.

- (03-104) Hydrogen Atom Transfer from Carbon to Metal – Relevance of a Novel Reaction to Catalyzed Hydrocarbon Conversions
M. Bullock (FY 2003 Funding \$80,000)

Carry out fundamental studies to investigate a novel type of chemical reaction that could have significant practical utility in homogeneously catalyzed hydrocarbon conversions. Investigate the feasibility of achieving a new method of activation of carbon-hydrogen (C-H) bonds, through hydrogen (H) atom transfer reactions from a carbon to a metal.

Exhibit A

Director's Office
Laboratory Directed Research and Development Program



Building 815E
P.O. Box 5000
Upton, NY 11973-5000
Phone 631 344-4467
Fax 631 344-2887
newman@bnl.gov

managed by Brookhaven Science Associates
for the U.S. Department of Energy

Memo

date: February 7, 2003
to: Distribution
from: L. Newman L.N.
subject: Laboratory Directed Research & Development Program (LDRD) Proposals

This is to solicit proposals for the annual LDRD competition. Proposals must be submitted by April 2, 2003, through the respective Chairperson and the Associate Laboratory Director to the Administrator for LDRD (Kevin Fox in Bldg. 460). Electronic versions of the Proposal Information Questionnaire submission form can be obtained by going to <https://sbms.bnl.gov/ld/ld03/ld03d011.htm> or from greco@bnl.gov. The BNL LDRD Policy, which defines the LDRD Program, can be reviewed at this web site. In my capacity as Scientific Director for LDRD, I am available to counsel individuals to aid them in their preparation of a successful proposal.

Please note that we require an abstract to fit on the first page of the form and a proposal which is not more than three pages in length. Also, note that LDRD projects are restricted to a maximum of three years. However, projects should be tailored to a two-year schedule. Along with your proposal you are requested to include a milestone schedule of activities to be completed with planned accomplishments and dates of completion of for example: lab setups, test runs or trials, compiled data sets, reports to be issued on results, etc. In addition, this year we are requesting a one-page vita. In each year there is a mid-year review of all programs to assess the extent of progress.

Research conducted under LDRD should be highly innovative, and an element of high risk as to success is acceptable. This year we will be especially pleased to receive proposals in the areas of advances in computational sciences, materials sciences, and biotechnology. Over the years the budget allocation has been increased to \$8.5 million, and as a consequence we should have approximately two to three million dollars for new starts.

The Selection Committee will be chaired by the Scientific Director for LDRD and includes the Director for Science and Technology along with the Associate Laboratory Directors and is augmented by selected distinguished scientists. The committee starts meeting in April to evaluate proposals for selection for funding in FY 2004.

Exhibit A

For your convenience and planning purposes, note the following calendar for LDRD activities and the attached copy of the new Proposal Information Questionnaire.

February 7, 2003	Call for FY 2004 Proposals
April 2, 2003	FY 2004 Proposals Due
April 1-3, 2003	FY 2003 Mid-Year review
April 28 –May 31, 2003	Selection of FY 2004 LDRDs
August 15, 2003	FY 2004 Plan Due to DOE
October 1, 2003	Funding of FY 2004 Projects
October 10, 2003	Call for FY 2003 Annual Reports
November 13, 2003	Annual Reports Due on FY 2003 Projects

LN:kjf
Attachments

Distribution:

Associate Laboratory Directors
Department Chairpersons

cc: G. Fess
K. Fox
W. Hempfling
D. Johnson
N. Narain
P. Paul
Assistant Laboratory Directors
Division Managers

Exhibit B

BROOKHAVEN NATIONAL LABORATORY PROPOSAL INFORMATION QUESTIONNAIRE LABORATORY DIRECTED RESEARCH AND DEVELOPMENT PROGRAM

PRINCIPAL INVESTIGATOR	PHONE
DEPARTMENT/DIVISION	DATE
OTHER INVESTIGATORS	
TITLE OF PROPOSAL	
PROPOSAL TERM (month/year)	From _____ Through _____

SUMMARY OF PROPOSAL

Description of Project:

Expected Results:

INSTRUCTIONS

Under **Description of Project**, provide a summary of the scientific concept of the proposed project including the motivation for the undertaking and the approach that will be used to conduct the investigation. Also indicate how the project meets the general characteristics of the LDRD Program and how it is tied to the DOE Mission. Under **Expected Results**, clearly enunciate what are the expected results and how they will impact the science. These items should not exceed the space remaining on this page, using the given font and size. Follow this page with an extended Proposal of no more than three (3) pages in length plus a Milestone Schedule. In addition, include a one-page Vita of the Principal Investigator; fill out the page with citations to recent pertinent publications. Do not include any additional attachments, as these will be discarded. Complete the Questionnaire, obtain the required approvals, and provide a Budget in the format on the form supplied. Break down the funding by fiscal year and by the broad categories of labor, materials and supplies, travel (foreign & domestic), services and subcontracts. LDRD funds cannot be used to purchase capital equipment. Indicate the intent to use collaborators, postdoctoral research associates, and/or students. Identify the various burdens applied, i.e., organizational, materials, and contracts. Include any other charges but the Laboratory G&A should not be applied. Go to the LDRD web site (www.bnl.gov/lldr/) for further information. **(This paragraph should be deleted before you input the requested information.)**

PROPOSAL

VITA (Principal Investigator)

LDRD MILESTONE SCHEDULE

Date	Planned Accomplishments
6 months	
1 year	
18 months	
2 years	
30 months	
3 years	

1. HUMAN SUBJECTS (Reference: DOE Order 1300.3)

Are human subjects involved from BNL or a collaborating institution?

If **yes**, attach copy of the current Institutional Review Board Approval and Informed Consent Form from BNL and/or collaborating institution.

Y/N _____

2. VERTEBRATE ANIMALS

Are vertebrate animals involved?

If **yes**, has approval from BNL's Animal Care and Use Committee been obtained?

Y/N _____

Y/N _____

3. NEPA REVIEW

Are the activities proposed similar to those now carried out in the Department/Division which have been previously reviewed for potential environmental impacts and compliance with federal, state, local rules and regulations, and BNL's Environment, Safety, and Health Standards? (Therefore, if funded, proposed activities would require no additional environmental evaluation.)

Y/N _____

If **no**, has a NEPA review been completed in accordance with the Subject Area National Environmental Policy Act (NEPA) and Cultural Resources Evaluation and the results documented?

Y/N _____

(Note: If a NEPA review has not been completed, submit a copy of the work proposal to the BNL NEPA Coordinator for review. No work may commence until the review is completed and documented.)

4. ES&H CONSIDERATIONS

Does the proposal provide sufficient funding for appropriate decommissioning of the research space when the experiment is complete?

Y/N _____

Is there an available waste disposal path for project wastes throughout the course of the experiment?

Y/N _____

Is funding available to properly dispose of project wastes throughout the course of the experiment?

Y/N _____

Are biohazards involved in the proposed work? If yes, attach a current copy of approval from the Institutional Biosafety Committee.

Y/N _____

Can the proposed work be carried out within the existing safety envelope of the facility (Facility Use Agreement, Nuclear Facility Authorization Agreement, Accelerator Safety Envelope, etc.) in which it will be performed?

Y/N _____

If **no**, attach a statement indicating what has to be done and how modifications will be funded to prepare the facility to accept the work.

5. TYPE OF WORK

Basic/Applied _____

6. CATEGORY OF WORK (select one by placing an X)

Advanced Sensors & Instrumentation	_____	Engineering & Manufacturing Processes	_____
Biological Sciences (including medical)	_____	Materials Science and Technology	_____
Chemistry	_____	Mathematics and Computing Sciences	_____
Earth and Space Sciences (including environmental)	_____	Nuclear Science and Engineering	_____
Energy Supply and Use	_____	Physics	_____

7. POTENTIAL FUTURE FUNDING

Identify below the Agencies and the specific program/office, which may be interested in supplying future funding. Give some indication of time frame.

APPROVALS

Department /Division Administrator	_____	
	Print Name	Signature
Department Chair/Division Manager	_____	
	Print Name	Signature
Cognizant Associate Director	_____	
	Print Name	Signature

BUDGET REQUEST BY FISCAL YEAR

(Note: Funding for more than 2 years is unlikely and cannot exceed 3 years)

COST ELEMENT	FISCAL YEAR _____	FISCAL YEAR _____	FISCAL YEAR _____
Labor * Fringe Total Labor Organizational Burden @ ____ %			
Materials Supplies Travel Services Total MST Materials Burden @ ____ %			
Sub-contracts Contracts Burden @ ____ %			
Electric Power ITD Charge Other (specify)			
TOTAL PROJECT COST			
* Labor (indicate names, type of staff and level of effort, and where names are not known indicate TBD)			
List all materials costing over \$5000			

Exhibit C

LDRD DATA COLLECTION FORM

Read and then remove the instructions before attempting to complete this form and return it electronically by November 13 to D. J. Greco (greco@bnl.gov)

LDRD PROJECT NUMBER:

PROJECT TITLE:

PRINCIPAL INVESTIGATOR(S):

PUBLICATIONS

TOTAL _____

List all refereed publications originating in whole or in part from this LDRD including those that have been submitted but do not include any that are in preparation. Provide the total number above.

Example of style

Ozone production in the New York City Urban Plume. Kleinman, L. I., Daum, P. H., Imre, D. G., Lee, J. H., Lee, Y.-N., Nunnermacker, L. J., Springston, S. R., Weinstein-Lloyd, J., and Newman, L. J. *Geophys. Res.*, 105, 14,495-14,511 (2000).

MEETINGS, PROCEEDINGS AND ABSTRACTS

TOTAL _____

List all formal presentations originating in whole or in part from this LDRD including those that have been accepted for presentation but not yet presented. Provide the total number above.

Example of style

Ozone production in the New York City urban plume. Kleinman, L., Daum, P. H., Imre, D., Klotz, P., Lee, J. H., Lee, Y.-N., Nunnermacker, L. J., Springston, S., Weinstein-Lloyd, J., and Newman, L. American Geophysical Union Fall Meeting, San Francisco, CA, Dec. 8-12, 1997.

REPORTS

TOTAL _____

List all formal reports originating in whole or in part from this LDRD including those that have been accepted for publication but do not include any that are in preparation. Provide the total number above.

PATENTS, LICENSES AND COPYRIGHTS

TOTAL _____

List all patents licenses and copyrights originating in whole or in part from this LDRD including those that are pending but not any that are in preparation. Provide the total number above.

Exhibit C

INVENTION DISCLOSURES

TOTAL _____

List all invention disclosures submitted to the Laboratory's Office of Intellectual Property & Industrial Partnership that were either directly derived from this LDRD or from any follow-on efforts. Provide the total number above.

PROJECT REVIEWS

TOTAL _____

List all formal review presentations that pertain to this work. Include the name of the reviewing body and date of review, title of presentation, and names of presenters. Do not include the mid-year LDRD program reviews. Provide the total number above.

STUDENTS AND RESEARCH ASSOCIATES

TOTAL _____

Provide names of all graduate students and Research Associates supported during the duration of this LDRD and give the number of months that they were supported. Provide the total number above combined as full time equivalents, rounded to the nearest month.

NEW HIRES

TOTAL _____

Provide names of any new staff that were hired as a direct result of this LDRD. Provide the total number above.

FOLLOW ON FUNDING

TOTAL _____

List all requests for funding including any that have been rejected, and those still pending decisions but not any that are in preparation. Give the title of the project, the Principal Investigator, date of submission, the name of the agency, action taken, amount funded or requested per year, and the duration. Provide the total number above.